CENTRO INTERNACIONAL DE ESTUDOS
DE DOUTORAMENTO E AVANZADOS
DA USC (CIEDUS)

DOCTORAL THESIS

# NANOCARRIERS FOR THE ORAL ADMINISTRATION OF THERAPEUTIC MACROMOLECULES

Irene Santalices Ramos

**INTERNATIONAL DOCTORAL SCHOOL**

**DOCTORAL PROGRAM IN DRUG RESEARCH AND DEVELOPMENT**

SANTIAGO DE COMPOSTELA

2018

USC
UNIVERSIDADE
DE SANTIAGO
DE COMPOSTELA

CENTRO INTERNACIONAL DE ESTUDOS
DE DOUTORAMENTO E AVANZADOS
DA USC (CIEDUS)

TESIS DE DOCTORADO

# NANOTRANSPORTADORES PARA LA ADMINISTRACIÓN ORAL DE MACROMOLÉCULAS TERAPÉUTICAS

Irene Santalices Ramos

**ESCUELA DE DOCTORADO INTERNACIONAL**

**PROGRAMA DE DOCTORADO EN I + D DE MEDICAMENTOS**

SANTIAGO DE COMPOSTELA

2018

USC
UNIVERSIDADE
DE SANTIAGO
DE COMPOSTELA

# AUTHORIZATION OF THE THESIS SUPERVISORS

**Nanocarriers for the oral administration of therapeutic macromolecules**

**Prof. María José Alonso Fernández**, Full Professor of the Department of Pharmacology, Pharmacy and Pharmaceutical Technology at the University of Santiago de Compostela

**Prof. Dolores Torres López**, Professor of the Department of Pharmacology, Pharmacy and Pharmaceutical Technology at the University of Santiago de Compostela

REPORT:

*That the present thesis, corresponds to the work carried out by Ms. Irene Santalices Ramos, under our supervision, and that we authorize its presentation considering it gathers the necessary requirements of article 34 of the USC Doctoral Studies regulation, and that as supervisors of this thesis, it does not incur in the abstention causes established by the law 40/2015.*

Santiago de Compostela, September 18th 2018

Sgd.: **María José Alonso Fernández**

Sgd.: **Dolores Torres López**

USC
UNIVERSIDADE
DE SANTIAGO
DE COMPOSTELA

# AUTORIZACIÓN DEL DIRECTOR / TUTOR DE LA TESIS

**Nanotransportadores para la administración oral de macromoléculas terapéuticas**

**Dña. María José Alonso Fernández**, Catedrática del Departamento de Farmacología, Farmacia y Tecnología Farmacéutica de la Universidad de Santiago de Compostela

**Dña. Dolores Torres López**, Prof. Titular del Departamento de Farmacología, Farmacia y Tecnología Farmacéutica de la Universidad de Santiago de Compostela

INFORMAN:

*Que la presente tesis, corresponde con el trabajo realizado por Dña.* ***Irene Santalices Ramos****, bajo nuestra dirección, y autorizamos su presentación, considerando que reúne los requisitos exigidos en el Reglamento de Estudios de Doctorado de la USC, y que como directoras de ésta no incurre en las causas de abstención establecidas en Ley 40/2015.*

*En Santiago de Compostela, a 18 de Septiembre de 2018*

Fdo.: **María José Alonso Fernández**

Fdo.: **Dolores Torres López**

USC
UNIVERSIDADE
DE SANTIAGO
DE COMPOSTELA

# PhD CANDIDATE STATMENT

**Nanocarriers for the oral administration of therapeutic macromolecules**

Ms. Irene Santalices Ramos

*I submit my Doctoral thesis, following the procedure according to the Regulation, stating that:*

1) *This thesis gathers the results corresponding to my work.*
2) *When applicable, explicit mention is given to the collaborations the work may have had.*
3) *The present document is the final version submitted for its defense and coincides with the document sent in electronic format.*
4) *I confirm that this thesis does not incur in any plagiarism of any other authors or documents submitted by me for obtaining other degrees.*

*Santiago de Compostela, September 18th 2018*

Sgd.: **Irene Santalices Ramos**

USC
UNIVERSIDADE
DE SANTIAGO
DE COMPOSTELA

# DECLARACIÓN DEL AUTOR DE LA TESIS

**Nanotransportadores para la administración oral de macromoléculas terapéuticas**

Dña. Irene Santalices Ramos

*Presento mi tesis, siguiendo el procedimiento adecuado al Reglamento, y declaro que:*

1) *La tesis abarca los resultados de la elaboración de mi trabajo.*
2) *En su caso, en la tesis se hace referencia a las colaboraciones que tuvo este trabajo.*
3) *La tesis es la versión definitiva presentada para su defensa y coincide con la versión enviada en formato electrónico.*
4) *Confirmo que la tesis no incurre en ningún tipo de plagio de otros autores ni de trabajos presentados por mí para la obtención de otros títulos.*

*En Santiago de Compostela, a 18 de Septiembre de 2018*

Fdo.: **Irene Santalices Ramos**

USC
UNIVERSIDADE
DE SANTIAGO
DE COMPOSTELA

## Conflict of interest

I declare that that there are no competing interests with the subject matter or materials discussed in this thesis.

Sgd.: **Irene Santalices Ramos**



USC
UNIVERSIDADE
DE SANTIAGO
DE COMPOSTELA

*A mi familia*

*A la vida…*

USC
UNIVERSIDADE
DE SANTIAGO
DE COMPOSTELA

*"La ciencia, muchacho, está hecha de errores, pero de errores útiles de cometer, pues poco a poco, conducen a la verdad"*

Julio Verne

*"Caminante, no hay camino, se hace camino al andar"*

Antonio Machado

*"Nunca choveu que non escampara"*

Proverbio gallego

USC
UNIVERSIDADE
DE SANTIAGO
DE COMPOSTELA




# Acknowledgements

USC
UNIVERSIDADE
DE SANTIAGO
DE COMPOSTELA

**Acknowledgements**

No podría empezar esta tesis sin antes daros las gracias a todos los que me habéis acompañado, guiado, aguantado y apoyado a lo largo de esta etapa. Sin duda sois parte responsable de que haya conseguido llegar hasta aquí, GRACIAS, no lo habría logrado sin vosotros.

Gracias a María José y a Loli, mis directoras de tesis. Gracias por vuestra disponibilidad y compromiso, por haber sido un ejemplo a seguir, por orientarme y confiar en mí para la realización de este trabajo. Gracias por acogerme en vuestro grupo y haberme ayudado a crecer tanto personalmente como profesionalmente.

Gracias a la Universidad de Santiago, y especialmente al CIMUS, por poner a mi disposición las instalaciones y soporte técnico necesario para desarrollar esta tesis. A la Xunta de Galicia y al programa de Formación de Profesorado Universitario del Gobierno de España por haberme concedido sendas becas de investigación para la realización de este trabajo. Gracias a todas las entidades financieras de los proyectos en los que he participado por el apoyo económico.

Obrigada Bruno, por me teres dado a oportunidade de fazer uma estadia no teu grupo de investigação. Obrigada pela tua dedicação, orientação e por me fazeres sentir parte do grupo. Obrigada a todos os membros do teu grupo fantástico, por me terem acolhido tão bem e por me terem feito sentir como em casa. Obrigada especialmente à Francisca por me ter mostrado o mundo das células, desconhecido para mim até então, e por ter trabalhado lado a lado comigo. Obrigada Mafalda e Inês por todas as gargalhadas partilhadas e Patrick pelos teus sábios conselhos. Obrigada a todos por todos os momentos partilhados, sois fantásticos.

Thanks to all the TransInt consortium, for giving me the opportunity to develop this thesis within this project and learn from plenty of experts in the field. Special thanks to Sanofi for providing the peptides used in this work. To Pep, Macarena, Meritxell Teixidó and Ernest Giralt, from IRB (Spain) for all the analytical support. To Ana, Neha and Véronique Préat, from Université Catholique de Louvain (Belgium), for your collaboration with cell studies. To Erick Tedesco, Federico Benetti, from European Center for the Sustainable Impact of Nanotechnology (Italy), and Ilaria Marigo, from Veneto Institute of Oncology (Italy), for your involvement in cytotoxicity and biodistribution studies. To Elena, Tania, Walid and Caitriona O'Driscoll, from University of Cork (Ireland), for having done your best with the lymphatic studies. Thanks, David, Juan, Jose, Diego, Javi, Sulay Tovar and Carlos Diéguez, from University of Santiago de Compostela, for all the efforts you devoted in the in vivo work. This thesis could not have happened without all of your collaborations.

Gracias a los profesores del Departamento de Farmacología, Farmacia y Tecnología Farmacéutica. En especial gracias a Noemi y Marcos, por compartir su experiencia y apoyarme a lo largo de estos años. Gracias Carlos Vázquez, del Departamento de Química Física por su ayuda con las medidas técnicas de MALS y AFM. Gracias a Mari, Miguel y Clara Álvarez, del Departamento de Fisiología, por su la realización de los estudios de bioactividad en células. Gracias a Vicky, Manolo y Mar Arroyo, de la Universidad de Castilla La Mancha, por su implicación en los estudios de mucodifusión.

**Acknowledgements**

Gracias a Puri, Sagrario y Esmorís por toda su ayuda con los temas burocráticos. Gracias María, Vanesa, Patricia por vuestra disponibilidad y cercanía. Gracias Rafiña y Balbi por aturar todas mis neuras y por toda vuestra ayuda, que ha sido fundamental para sacar las cosas adelante. Gracias a mis confidentes más veteranas por acogerme con los brazos abiertos. Gracias Desi por todo tu apoyo y por hacerme sentir comprendida en momentos de crisis. Gracias Belén por capear todos los síntomas de mi TOC con humor y sonidos guturales que sólo tú imitas a la perfección.

Thanks to the big incredible *Nanochachos* family for allowing me to be a part of it. These years wouldn't have been the same without your support and advice. Thanks for all the things I have learnt from all of you and the experiences you have shared with me, both, inside and outside the lab. Gracias a todos los que habéis coincidido conmigo en algún momento de esta etapa. Gracias Marta Alonso, Erea, Raquel Segunda, Rosana, Carmen Segunda, Belén Álvarez, Ivana, Nataliya, Khair, Edi, Mireia, Vanessa, Ovidio, Francesco, Howl, Paul, Noelia, Paulina, Blanca, Silvia. Gracias Tania, Mariajo y Esther por vuestra simpatía y todas las risas compartidas. Gracias al labo de la segunda por formar parte de esto, Carla, Maruthi, Sheila y Chema. Gracias a los que seguís haciendo que esta gran familia siga creciendo Cecilia, Catarina, Ricardo, Lali, Cris, Surasa, Shubaash, Sakthi, Ana. Obrigada Sofía por tu iniciativa para planear actividades que no impliquen tener una pipeta en la mano y por ser una fuente de alegría constante. Gracias Andrea porque lo que une una review no lo separará el hombre. Gracias Iago por sembrar el orden dentro del caos (menos mal que estás tú arriba porque un fregadero limpio no tiene precio). Gracias a mis quintos por aguantar estoicamente mis gritos y manías, Ana Olivera, Bhanu, Sergio, Carmen Tercera y Germán.

Gracias en especial a

…todo el TransInt team, mis férreos compañeros de batalla. Adam, Ana, Niu, Lu, Diego, Miguel, Sonia, Enrique, Mati, Lena, Inma, Tamara y Elena (aunque lejos siempre ahí). Porque sin vosotros este trabajo no hubiera sido posible. Gracias por todos esos momentos juntos, desde crisis existenciales pendientes de la alarma para salir corriendo hasta nuestras jornadas multilingüe gracias a las cuales palabras como "tapiku tapiku", "u tnui tnui" y "gantznale gantznale" siempre formarán parte de nuestro vocabulario. Thanks Niu and Lu for being my support since the beginning and for sharing your amazing cultures with me. Gracias Mati por todo el trabajo mano a mano y por montar gabinetes anti-crisis siempre que fuese necesario. Thanks Lena, for being such a good person, because meeting you along this journey has been amazing. Thanks because since I met you I realized that the world is going to be controlled by Greeks. Thanks all of you because *we have a goal, we are a team, we are TransInt*.

Gracias a mis queridas veteranas Ana y Sara por dejarme formar parte de vuestra vida (aunque al principio a regañadientes). Gracias Ana por haber sido mi mentora desde el principio, y por enseñarme a mantener las manos calentitas para escribir en el ordenador. Obrigada Sariña, mi traductora personal, porque sin ti mis emails no serían lo mismo. Muchas gracias por nuestras noches de juegos de mesa y por insistir en que hay vida más allá del labo, buenas lecciones de vida me has enseñado. La quinta no es lo mismo sin vosotras. Obrigada Cadete por toda tu energía,

incansables planes y por enseñarme como se hace un *calamardo* en condiciones. Gracias Raquel por todo tu cariño y buenos consejos. Gracias a mis queridos veteranos, Jose Vicente y Jorge. Gracias Jei V por todos nuestros reconfortantes pucho-brakes luchando contra la flojera, y porque no se olvidará la vaca que algún día fue ternero. Obrigada Pinto, por esos momentos de desahogo (non ... pa…) que tanto echo de menos, y como no, por esos bailes inolvidables en Tarasca.

Gracias Belenciña, por acompañarme durante todo este largo camino que emprendimos a la vez ya no me acuerdo cuando… Gracias por enseñarme a luchar y a no rendirme. Gracias por esa risa tan característica que me alegra el día. Gracias por todo, bueno, a excepción de todas las veces que me he saltado la dieta por culpa de tus dulces caseros.

Gracias Inma, mi flor de loto. Gracias por ser como eres, porque *de normal* uno no se encuentra en la vida amigas como tú. Gracias por haber sido mi compañera de *bancada* y por enseñarme a invocar a la Virgen del Sagrario como sólo tú sabes. Recuerda que aunque Mama Lara cerrara (*adiós la luz*), siempre nos quedará nuestro proyecto Santos.

Gracias a mis *Astuveivis*, mi familia Santiaguesa, mis consejeros incondicionales, sin duda lo mejor que me llevo de toda esta etapa. Que os voy a contar que no sepáis… *la vida*… Gracias por todos los momentos que hemos compartido y por los que vendrán, que aún nos quedan muchas *vaques* que descubrir por el mundo y una granja-escuela que sacar adelante. Gracias por todo vuestro cariño y por ser como sois, no cambiéis nunca!

Gracias Joseito, porque os teus chistes malos (pero malos, malos) alégranme o día. Graciñas por encherme a neveira de comida ecolóxica e por todas esas cañas/clariñas cheas de consellos que me axudan a mante-la "cordura" (e ás plantas con vida). Gracias por recordarme o moito que berro e todo o que vallo para a que ti consideras a miña vocación frustrada.

Gracias Carmen, Carmencha, Carmiña. Gracias por aportarme esa tranquilidad que tanto me hace falta cuando colapso. Gracias por estar siempre disponible para escuchar mis batallitas, y si es acompañadas de un Ramón Bilbao y una estrella mejor que mejor. Gracias por hacerme comprender la importancia del minimalismo en los adornos navideños y de que si pones un reno rosa en tu vida el día te sonreirá.

Gracias Sonita, *bribona orcasureña* con melenas la viento. Gracias por estar ahí siempre (aunque siempre llegues tarde lo importante lo importante es que siempre llegas). Gracias por esos consejos recíprocos de personal shopers que, aunque casi nunca seguimos (me sigue espantando esa cazadora de flores), nos mantienen entretenidas. Gracias por todas las risas y las cañitas que me daban la vida después de un día duro.

Gracias Adri, pequeño saltamontes reivindicativo lleno de energía. Gracias por escuchar siempre mis penurias y llenarme de consejos sinceros (me gusten o no). Gracias por todas las cañas y conversaciones sobre el sentido de la vida que terminan con un *Señooooooor ten piedaaaaad* muy apropiado a las circunstancias. *Ay sí*… y gracias por todos tus *perfectos*!

**Acknowledgements**

Gracias Maca (Tamara para el resto de los humanos), la mejor compañera de "pupitre" que jamás pude imaginar y con la que todo puedo compartir. Gracias por ayudarme a mantener la quinta a raya y reciclada. Gracias por ser mi contrapunto, por hacerme pensar antes de actuar (*lenta, pero segura*) y ser mi remanso de paz cuando me altero. Gracias por estar siempre pendiente, las tardes-noches interminables en la quinta no hubieran sido lo mismo sin ti.

Gracias Ele, porque aunque la barca la hayamos dejado en la arena nos hemos subido juntas, y en vez de una pareja de cada especie la hemos llenado de queso, red vintage y películas/series insufribles para que no nos falte de nada (un par de alpacas y de unicornios sí hemos metido, tranquila, no hiperventiles). Gracias de verdad por estar ahí siempre, por ser mi confidente y sacarme siempre una carcajada con tus audios/videos-selfies. No hubiera podido llegar hasta aquí sin tu apoyo y ayuda.

Y como también hay vida fuera del labo…

Gracias a mi *Comarquita*, porque con vosotras emprendí mi camino en Santiago. Gracias por hacer tan llevaderas todas las horas de biblioteca y de academia alternándolas con horas en el COI-SEU y terrazas varias. Gracias por ser tan divertidas y diferentes. Gracias por el equipo que formamos: *Reinas arriba...*!

Gracias a todos los que habéis estado ahí desde el principio en mi Pontevedra de toda la vida. Gracias a todos los *7V*, a todos y cada uno de vosotros por estar siempre disponibles aunque sea en la distancia. Gracias por todos los momentos que hemos vivido juntos, por todos los Forcarei, peñas, el anual cocido-cocida, todas las tardes-noches en la Verdura que revitalizan cuerpo y mente... y bueno, voy a parar porque podría escribir una tesis sólo enumerando los momentos compartidos dignos de recordar. De *7V* yo siempre seré! Gracias a mis *Pontenude*, por ser geniales y compartir tantos momentos juntas aunque estemos desperdigadas. Gracias en especial a mis *Pontep** Patty, Euge y Cris, por animarme, aguantarme y apoyarme todo este tiempo. Es genial contar con gente como vosotras a mi lado.

Gracias César, por haber estado a mi lado durante todo este camino. Por apoyarme, resignarte a mis horarios intensivos y por consolarme en momentos de crisis aunque no entendieras nada de lo que te estaba contando. Gracias por todos nuestros *nosbue* y *nasbue*. Gracias por hacerme feliz, gracias por todo.

Y por último, pero no menos importante, gracias a toda mi familia, a los que están y a los que les hubiera encantado estar. Gracias *padremadre*, mis padres, mi mayor pilar, por apoyar en todo momento mis decisiones aun advirtiéndome de todas las piedras que iba a tener que sortear en el camino. Gracias por ser un ejemplo para mí en todos los sentidos. Gracias *hijo*, por ser mi compañero de desesperación, entenderme y aguantar mis arrebatos de genio (conste en acta que yo también aguanto lo mío) como sólo un hermano como tú podría hacer. Recuerda siempre que hay luz al final del túnel y que paso a paso la alcanzaremos. Gracias porque sin vosotros no sería nadie. Os quiero.

USC
UNIVERSIDADE
DE SANTIAGO
DE COMPOSTELA

USC
UNIVERSIDADE
DE SANTIAGO
DE COMPOSTELA




# Table of Contents

USC
UNIVERSIDADE
DE SANTIAGO
DE COMPOSTELA

# Table of Contents

**Abstract/Resumen** ..... **31**

**Resumen *in extenso*** ..... **37**

**Introduction** ..... **67**

**Chapter 1: Advances on the formulation of proteins using nanotechnologies based on lipidic materials** ..... **107**

**Background, Hypothesis and Objectives** ..... **155**

**Chapter 2: Key factors affecting the physicochemical properties of chitosan nanocapsules and their ability to associate insulin** ..... **165**

**Chapter 3: Influence of the surface properties of nanocapsules on their interaction with intestinal barriers** ..... **197**

**Chapter 4: A nanoemulsion/micelles mixed nanosystem for the oral administration of hydrophobically modified insulin** ..... **233**

**Overall discussion** ..... **299**

**Conclusions** ..... **327**

**List of abbreviations** ..... **331**

**Ethical consierations** ..... **339**

USC
UNIVERSIDADE
DE SANTIAGO
DE COMPOSTELA




# Abstract/Resumen

USC
UNIVERSIDADE
DE SANTIAGO
DE COMPOSTELA

## Abstract

The high specificity and potency of therapeutic proteins and peptides have increasingly attracted the attention of the pharmaceutical research in the last decades. However, even though around 240 therapeutic peptides and proteins have already been approved by the FDA, their efficient administration by the oral route remains generally unviable due to their biopharmaceutical limitations (e.g., instability, limited bioavailability, short half-life, immunogenicity…). A strategy to overcome these drawbacks has relied on the design of biocompatible lipid-based nanocarriers with the capacity to protect their peptide cargo from degradation and enhance its absorption. According to these trending research challenges, the main goal of this work has been the generation of knowledge that could potentially contribute to make feasible the oral administration of peptides using lipid-based nanocarriers. The specific objective has been to study how the composition and surface properties of a lipid-based nanocarrier influence their capacity to load hydrosoluble peptides and their ability to overcome the biological barriers associated to the oral modality of administration.

The first chapter, which contains part of a recently published review entitled "A*dvances on the formulation of proteins using nanotechnologies"*, provides an overview of the nanotechnologies mostly explored to date to produce lipid-based nanocarriers for protein/peptide delivery. The basic principles, as well as the advantages and disadvantages of the most relevant techniques are discussed. Additionally, the main factors involved in the drug association capacity of these nanosystems, along with the release profile of their cargo, are briefly analyzed.

The second chapter describes a systematic study intended to elucidate what are the critical formulation parameters that influence the physicochemical properties of chitosan nanocapsules and their capacity to associate hydrosoluble peptides, using insulin glulisine as a model drug. The selection of chitosan nanocapsules was based on previous work from our group showing their capacity to increase the absorption of the peptide salmon calcitonin. The results obtained within the range of formulation conditions investigated, showed the interference of the polymer shell layers on the association of insulin to the nanocapsules. Other formulation parameters, e.g., type of oil and type and concentration of surfactants had a minor effect on the physicochemical properties and loading capacity of the nanocapsules.

*Chapter 3* describes a systematic study aimed at investigating the influence of the nanocarriers' surface properties on their interaction with the intestinal barriers (colloidal stability, enzymatic degradation, and mucoadhesion/mucodiffusion properties). For this purpose, we selected a set of 9 lipid-based nanosystems comprising both, uncoated nanoemulsions and polymeric nanocapsules, which were obtained through the combination of different polymers (chitosan and polyarginine) and surfactants (poloxamer 188 and 407). Our results indicated that both, the polymer shell and the surfactants located at the oil/water interface may have either synergic or disruptive effects on the nanosystems' capacity to overcome the intestinal barriers. For example, while the presence of the non-ionic surfactant poloxamer 407 in the uncoated nanoemulsion contributed to its stabilization, and improved its mucodiffusion, its use together with either chitosan or polyarginine had a limited effect on the nanocapsules performance.

In *Chapter 4*, and taking into account the results previously obtained, the specific objective was to develop and fully characterize a new nanoemulsion aimed to the oral administration of peptides using as model cargo a hydrophobically-modified insulin. For this purpose, the components of the prototype were carefully selected attending to their intrinsic properties and their performance on the previous studies. The results showed that the nanoemulsion co-existed with a population of micelles (mixed system) and exhibited a 100 % of insulin association efficiency. In brief, this nanosystem showed a great stability and miscibility in bio-relevant media, acceptable mucodiffusive properties and ability to interact and enter the intestinal cells without remarkable cytotoxic effects. Finally, the promising behavior of the nanosystem in terms of overcoming the biological barriers of the intestinal tract was translated into a moderate hypoglycemic response (≈ 20−30 %) following intestinal administration to rats.

Overall, the knowledge disclosed in this thesis is expected to contribute to the rational design of delivery carriers intended to overcome the biological barriers associated to the oral administration of peptides.

## Resumen

La alta especificidad y potencia de péptidos y proteínas ha motivado que en las últimas décadas la investigación farmacéutica orientada al logro de su uso terapéutico haya experimentado un notable incremento. Sin embargo, aunque la FDA ha aprobado alrededor de 240 péptidos/proteínas terapéuticas, su administración eficaz por vía oral continua siendo un reto debido a sus limitaciones biofarmacéuticas (ej., inestabilidad, biodisponibilidad limitada, vida media reducida, inmunogenicidad...). El diseño de nanotransportadores lipídicos biocompatibles, con capacidad de asociar, proteger de la degradación y mejorar la absorción de este tipo de macromoléculas está siendo una estrategia ampliamente explorada para superar estos inconvenientes. Dentro de este contexto, el objetivo principal de este trabajo ha sido generar conocimiento que pueda contribuir a hacer factible la administración oral de péptidos utilizando para ello nanovehículos lipídicos. El objetivo específico ha sido estudiar cómo la composición y las propiedades superficiales de estos nanovehículos influyen en su capacidad para asociar péptidos hidrosolubles y en su habilidad para superar las barreras biológicas asociadas a la administración oral.

El primer capítulo, que contiene parte de una revisión recientemente publicada titulada "*Avances en la formulación de proteínas usando nanotecnologías*", proporciona una visión general de las nanotecnologías más exploradas hasta la fecha para producir nanovehículos lipídicos para la administración de proteínas/péptidos. En él se discuten los principios básicos, así como las ventajas y desventajas de las técnicas más relevantes. Además, se analizan brevemente los principales factores involucrados en la capacidad de asociación de péptidos de estos nanosistemas, junto con su perfil de liberación.

El segundo capítulo describe un estudio sistemático orientado a dilucidar cuáles son los parámetros críticos de formulación que influyen sobre las propiedades fisicoquímicas de nanocápsulas de quitosano y en su capacidad para asociar péptidos hidrosolubles, utilizando insulina glulisina como fármaco modelo. La selección de nanocápsulas de quitosano se basó en el trabajo previo de nuestro grupo que mostró su capacidad para aumentar la absorción de calcitonina de salmón por vía oral. Los resultados obtenidos dentro de las condiciones de formulación investigadas, mostraron la influencia negativa de las cubiertas poliméricas en la asociación de insulina a las nanocápsulas. Otros parámetros de formulación, como por ejemplo, el tipo de aceite y el tipo y concentración de tensoactivos utilizados, no tuvieron un efecto relevante sobre las propiedades fisicoquímicas y la capacidad de asociación de insulina de las nanocápsulas.

El *Capítulo 3* describe un estudio sistemático orientado a investigar la influencia de las propiedades superficiales de los nanovehículos en su interacción con las barreras intestinales (estabilidad coloidal, degradación enzimática y propiedades de mucoadhesión/mucodifusión). Con este propósito, seleccionamos un conjunto de 9 nanosistemas lipídicos, incluyendo tanto nanoemulsiones no recubiertas como nanocápsulas poliméricas, que se obtuvieron mediante la combinación de diferentes polímeros (quitosano y poliarginina) y tensoactivos (poloxámero 188 y 407). Los resultados indicaron que tanto la incorporación de la cubierta polimérica como la de los tensoactivos en la interfaz aceite/agua puede provocar efectos sinérgicos o antagónicos en la capacidad de los nanosistemas para superar las barreras intestinales. Por ejemplo, aunque la presencia del tensoactivo no iónico poloxámero 407 en la nanoemulsión no recubierta contribuyó a su estabilización y mejoró su mucodifusión, su uso junto con quitosano o poliarginina tuvo un efecto limitado sobre el comportamiento de las nanocápsulas.

Teniendo en cuenta los resultados previamente obtenidos, en el *Capítulo 4* el objetivo específico fue desarrollar y caracterizar una nueva nanoemulsión destinada a la administración oral de péptidos, utilizando como modelo una insulina modificada hidrofóbicamente. Los componentes del prototipo fueron cuidadosamente seleccionados atendiendo a sus propiedades intrínsecas y a su comportamiento en los estudios previos. Los resultados mostraron una eficacia de asociación de insulina del 100% debido a la coexistencia de la nanoemulsión con una población de micelas (sistema mixto). Asimismo, este nanosistema mostró una gran estabilidad y miscibilidad en medios biorrelevantes, propiedades mucodifusivas aceptables y capacidad para interaccionar y entrar en las células intestinales sin efectos citotóxicos relevantes. De hecho, la capacidad mostrada por el sistema para superar las anteriores barreras gastrointestinales, se tradujo en una respuesta hipoglucémica moderada (≈ 20-30%) tras ser administrado intestinalmente a ratas diabéticas.

Finalmente, esperamos que el conocimiento divulgado en esta tesis contribuya al diseño racional de nanotransportadores destinados a superar las barreras biológicas asociadas a la administración oral de péptidos.




**Resumen *in extenso***

USC
UNIVERSIDADE
DE SANTIAGO
DE COMPOSTELA

## 1. Introducción

En las últimas décadas se han llevado a cabo importantes esfuerzos dirigidos a comercializar proteínas y péptidos terapéuticos, moléculas de gran interés terapéutico por su elevada potencia y selectividad. Sin embargo, su explotación como fármacos está limitada por su inestabilidad, baja biodisponibilidad y, en algunos casos inmunogenicidad [1]. Además de estos inconvenientes, el limitado cumplimiento del paciente de los tratamientos parenterales comúnmente utilizados en la práctica clínica [2], y el rápido aclaramiento plasmático de estas macromoléculas, han potenciado el desarrollo de nuevos sistemas de liberación (ej., nanotransportadores) para conseguir una administración eficaz [3–5]. Entre todas las rutas alternativas exploradas, la vía oral ha atraído especial atención ya que es la preferida por los pacientes, especialmente en tratamientos crónicos [6]. Sin embargo, la administración oral de péptidos y proteínas es especialmente compleja, ya que son susceptibles de sufrir procesos degradativos a lo largo del tracto gastrointestinal (pH, fuerza iónica, enzimas) [7]. Además, la alta hidrofilia y peso molecular generalmente inherentes a las moléculas peptídicas, suele conducir a una limitada permeabilidad a través de la mucosa intestinal [2,8,9]. Con el objetivo de superar estas limitaciones, la inclusión de estas macromoléculas en nanovehículos basados en materiales biodegradables y biocompatibles ha surgido como una estrategia muy prometedora para mejorar su biodisponibilidad [10–15]. Entre ellos, los nanovehículos lipídicos destacan para lograr esta finalidad por su biocompatibilidad y propiedades estabilizantes y promotoras de la absorción [16,17]. Sin embargo, a pesar de todos los avances logrados en este campo, el uso de los nanosistemas para la administración oral de péptidos y proteínas sigue siendo, de modo general, un reto [17,18]. En este sentido, la investigación orientada a ampliar el conocimiento sobre el efecto que las propiedades fisicoquímicas y la composición de los nanovehículos ejercen en su interacción con el tracto intestinal, resulta especialmente valiosa con vistas a implementar la administración oral de péptidos en la práctica clínica.

Dentro de este marco, los objetivos principales de esta tesis se han dirigido a: *i)* estudiar la influencia de las propiedades fisicoquímicas de nanotransportadores lipídicos en su potencial uso para la administración oral de péptidos (ej., capacidad de carga, interacción con el tracto gastrointestinal…); y *ii)* diseñar y desarrollar un nuevo nanosistema lipídico destinado a lograr una administración oral de péptidos eficaz, utilizando insulina como fármaco modelo. Partiendo de la base de que la explotación de los nanosistemas lipídicos como plataformas para la administración de péptidos está limitada por la baja liposolubilidad de estas macromoléculas, se realizó en primer lugar un estudio sistemático destinado a identificar los factores clave que afectan a sus propiedades fisicoquímicas y

capacidad para asociar péptidos. Para ello, se seleccionaron nanocápsulas de quitosano (NCs QS) e insulina glulisina como modelo de nanosistema lipídico y de péptido hidrófilo respectivamente, con el fin de investigar el efecto de varios parámetros de formulación (ej., tipo y concentración de diferentes componentes) sobre las características finales del sistema.

En este contexto, las propiedades de superficie de los nanovehículos influyen mucho en su interacción con el medio circundante. Teniendo esto en cuenta, seleccionamos NCs de QS y NCs de poliarginina (PARG), previamente desarrolladas por nuestro grupo de investigación, y las correspondientes nanoemulsiones no recubiertas (NEs), para evaluar sistemáticamente el efecto de su composición superficial en su capacidad de superar barreras intestinales específicas. Concretamente, evaluamos nueve nanosistemas diferentes en relación a *i)* su estabilidad, tanto coloidal como química, en fluido intestinal simulado y *ii)* su interacción (adhesión y difusión) con el mucus. Como último paso, y aprovechando la información generada en los estudios previos, se diseñó un nuevo nanosistema lipídico destinado a la administración de péptidos orales mediante la selección y combinación de lípidos con diferentes materiales (ej., tensoactivos, sales biliares...) con propiedades estabilizantes, mucodifusivas y promotoras de la absorción. Como resultado de este diseño racional, se desarrolló un nanosistema mixto compuesto por una nanoemulsión y un sistema micelar y se evaluó su potencial como sistema de administración oral de insulina. Finalmente el nanosistema mixto se caracterizó en términos de *i)* estabilidad y miscibilidad en fluidos intestinales simulados con y sin enzimas, *ii)* propiedades de mucodifusión, *iii)* capacidad de interacción con las células intestinales, *iv)* biodistribución tras de su administración oral y *v)* potencial para ser utilizado para la administración oral de insulina en ratas sanas y diabéticas.

## 2. Resultados y discusión

### 2.1. Identificación de los factores determinantes de las propiedades fisicoquímicas de los nanosistemas lipídicos y su capacidad para asociar péptidos

Como se comentó anteriormente, el uso de nanosistemas lipídicos como plataformas de administración de péptidos está condicionado por la baja solubilidad de estas macromoléculas en este tipo de vehículos. Por esta razón, diseñamos un estudio sistemático dirigido a identificar los factores cruciales que afectan a las propiedades fisicoquímicas y a la capacidad de las NCs QS para asociar péptidos. Para elaborar estas NCs, seleccionamos los principales componentes del núcleo lipídico de unas NCs de protamina previamente desarrolladas en nuestro grupo [10], y lo recubrimos con QS como

cubierta polimérica [19]. En la *Figura 1* (*panel superior*) se ilustra una representación esquemática de la organización de los componentes seleccionados inicialmente para constituir las NCs QS. Como molécula peptídica se eligió la insulina glulisina, que difiere de la insulina humana en los aminoácidos presentes en las posiciones 3 y 29 de su cadena B (asparagina y lisina reemplazadas respectivamente por lisina y ácido glutámico). Este cambio en la composición de aminoácidos, que no debía afectar significativamente a su asociación con el nanovehículo, facilita la disociación de sus hexámeros en dímeros y monómeros, desencadenando así una acción rápida tras su inyección. El triglicérido caprílico/cáprico de cadena media Miglyol®812N, se seleccionó no sólo por sus propiedades promotoras de la absorción, sino también porque se esperaba que aportase protección a la insulina contra la degradación enzimática [20,21]. El estearato de polietilenglicol 40 (PEGest40) se seleccionó como tensoactivo principal bajo la premisa de que sus cadenas de PEG estarían orientadas hacia la fase acuosa externa, mejorando así la estabilidad del nanosistema frente a la degradación enzimática [22–26] y favoreciendo su mucodifusión [25,27–30]. El colato de sodio (CNa) se seleccionó como co-tensoactivo por a sus propiedades promotoras de la absorción [31,32] y por la probabilidad de formar pares iónicos hidrofóbicos con la insulina [33–36], lo que favorecería su retención en el núcleo lipídico. Finalmente, QS fue el polímero elegido para formar la cubierta de las NCs por su biocompatibilidad y sus conocidas propiedades mucoadhesivas [37–40].

Las propiedades fisicoquímicas y la eficacia de asociación de insulina a las NCs QS se presentan en la *Figura 1* (*panel inferior*). A pesar de que las NCs QS obtenidas presentaban propiedades fisicoquímicas apropiadas (tamaño hidrodinámico medio de 346 ± 13 nm, bajo índice de polidispersión (0.2) y potencial−ζ positivo de +34 ± 2 mV), la eficacia de la asociación de insulina (28 ± 6 %) fue mucho más baja de la esperada. De hecho, NCs de protamina formuladas en las mismas condiciones mostraron una eficacia de asociación del 62 ± 16 % [10]. Estos resultados pusieron de manifiesto de qué manera el tipo de recubrimiento polimérico puede condicionar la eficacia de asociación y a la vez señalaron la necesidad de optimizar cada nanosistema para la carga a la que está destinado.

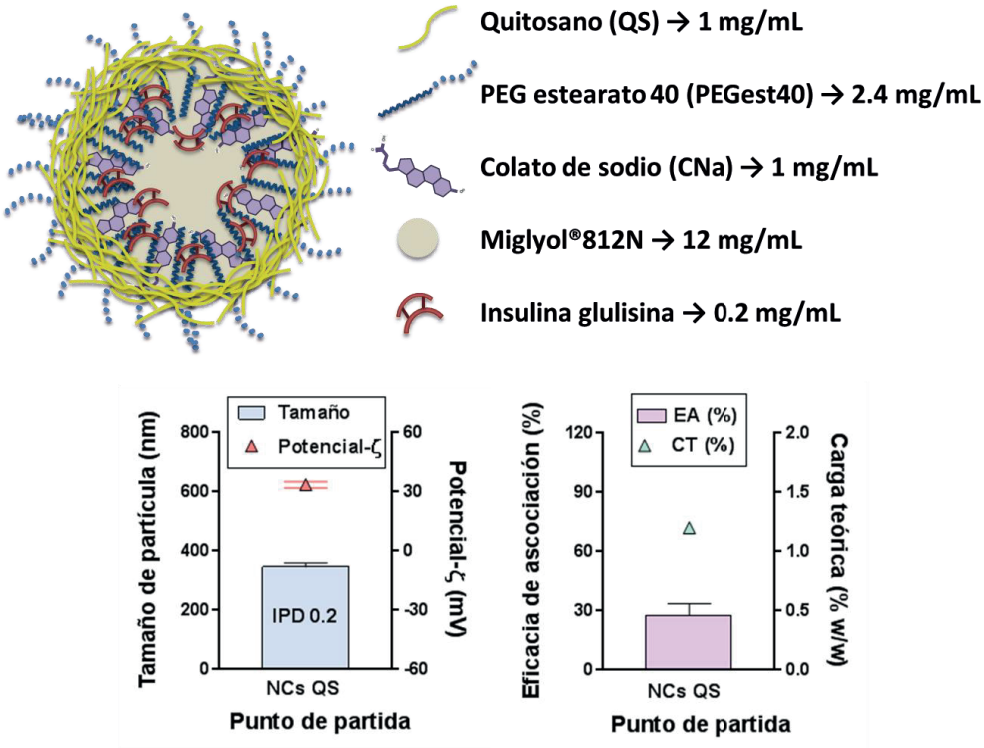



***Figura 1. Panel superior:*** *Representación esquemática y composición de las NCs QS utilizadas como punto de partida del cribado;* ***Panel inferior:*** *Caracterización fisicoquímica (tamaño, IDP y potencial–ζ), eficacia de la asociación de insulina (% EA) y carga teórica (% CT) de estas NCs QS (Media ± DE, n ≥ 3).*

Por consiguiente, se modificaron de forma sistemática varios parámetros de formulación, tales como el tipo y la concentración de diferentes componentes (ej., aceite, tensoactivo principal, sal biliar y polímero), así como la presencia de un recubrimiento adicional, para estudiar su influencia en las propiedades fisicoquímicas y la eficacia de asociación de insulina del prototipo seleccionado. La *Figura 2* resume las modificaciones llevadas a cabo con el nanosistema para desembocar finalmente en las NCs QS optimizadas (*Figura 2, panel inferior*).

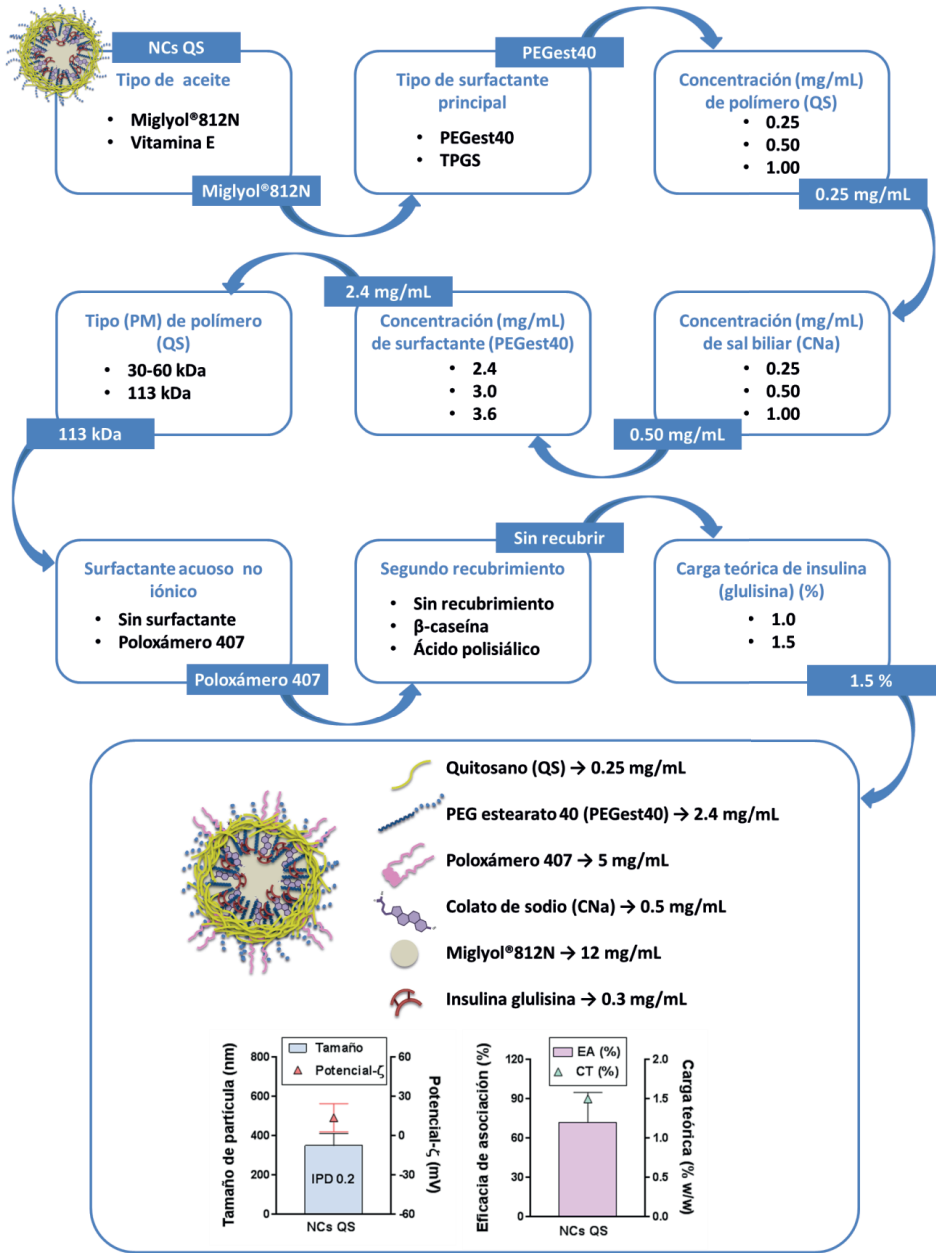



***Figura 2. Panel superior:*** *Representación esquemática del estudio sistemático llevado a cabo con el prototipo de NCs QS seleccionado, para identificar los factores críticos que afectan sus propiedades fisicoquímicas y la eficacia de la asociación de insulina.;* ***Panel inferior:*** *Representación esquemática, composición, caracterización físico-química (tamaño, IPD y potencial−ζ), eficacia de la asociación de insulina (% EA) y carga teórica (% CT) de las NCs optimizadas de QS (Media ± DE, n ≥ 3).*

La *Tabla 1* resume, de un modo cualitativo, los resultados que pudieron extraerse de esta evaluación. Si bien algunas de las variables estudiadas (ej., naturaleza y número de agentes tensoactivos), ejercieron un efecto menor tanto en las propiedades fisicoquímicas como en la asociación de la insulina, otros, como la composición de la cubierta polimérica, dieron lugar a un efecto drástico. En concreto, tanto el aumento de la concentración de QS como la presencia de una segunda cubierta polimérica, disminuyeron marcadamente la capacidad de las NCs QS para asociar insulina.

***Tabla 1.*** *Efecto de las diferentes condiciones estudiadas sobre el tamaño, índice de polidispersión (IPD), potencial-ζ (Pot−ζ) y eficacia de asociación de insulina (EA %) de las NCs QS elegidas como punto de partida en este cribado. Los símbolos indican de forma cualitativa la magnitud del correspondiente efecto: aumento (↑), disminución (↓) y prácticamente constante (≈).*

| Condición estudiada | Tamaño | IPD | Pot-ζ | EA % |
|---|---|---|---|---|
| **Tipo de aceite:** cambio de Miglyol®812N por DL−α−tocopherol | ↑↑ | ≈ | ↑ | ≈ |
| **Tipo de tensoactivo principal:** cambio de PEGst40 por TPGS | ≈ | ≈ | ≈ | ↓ |
| **Concentración de polímero:** aumento de la concentración de QS (0.25, 0.5 y 1 mg/mL) | ≈ | ≈ | ≈ | ↓↓ |
| **Concentración de sal biliar:** aumento de la concentración de CNa (0.25, 0.5 y 1 mg/mL) | ↓↓ | ↓ | ≈ | ≈ |
| **Concentración de tensoactivo principal:** aumento de la concentración de PEGst40 (2.4, 3.0 y 3.6 mg/mL) | ↑↑ | ↑↑ | ↓ | ↑↑ |
| **Tipo de polímero:** aumento del peso molecular del QS de 30−60 a 113 kDa | ↓ | ≈ | ↑↑ | ≈ |
| **Tensoactivo no iónico extra:** inclusión de poloxámero 407 | ≈ | ≈ | ↓ | ≈ |
| **Segunda cubierta extra:** inclusión de β−caseína/ácido polisiálico | ↑↑/≈ | ↑↑/↓ | ↓↓ | ↓↓ |
| **Carga teórica de péptido:** aumento de la carga teórica de insulina del 1 al 1.5 % | ≈ | ≈ | ≈ | ≈ |

En general, la formulación que presenta las mejores características es la preparada con las siguientes concentraciones: 0.25 mg/mL de QS, 12 mg/mL de Miglyol®812N, 2.4 mg/mL de PEGest40, 0.5 mg/mL de CNa, 5 mg/mL de poloxámero 407 y 0.3 mg/mL de insulina glulisina (1.5 % de carga teórica). Desafortunadamente, cuando se probó la estabilidad de estas NCs QS optimizadas en fluidos intestinales simulados (SIF y FaSSIF-V2), su tamaño disminuyó drásticamente (≈ 150 nm) y alrededor del 70-80 % de la insulina glulisina

asociada se liberó inmediatamente, lo que disminuyó su potencial para ser utilizados como nanovehículos orales.

Para complementar esta información, nuestro siguiente objetivo consistió en investigar la influencia de las propiedades de superficie de las nanocápsulas en su interacción con las barreras intestinales.

## 2.2. Influencia de las propiedades superficiales de las nanocápsulas en su interacción con las barreras intestinales

La versatilidad de las NCs poliméricas reside en la posibilidad de adaptar su núcleo lipídico a la naturaleza del fármaco y su cubierta polimérica a la vía de administración o tejido diana [41–45]. En esta línea, como mostramos anteriormente, se pueden emplear diferentes estrategias de formulación para mejorar la baja liposolubilidad de macromoléculas peptídicas en nanosistemas lipídicos. Además, una vez administradas oralmente, deben ser capaces de proteger al fármaco y superar las numerosas barreras fisiológicas que existen a lo largo del tracto gastrointestinal. En este sentido, las propiedades superficiales de los nanosistemas juegan un papel crucial en su interacción con el medio circundante. Teniendo esto en cuenta, seleccionamos composiciones específicas de NCs de QS y de PARG, desarrolladas por nuestro grupo de investigación [19,37,46], y sus correspondientes NEs como controles, para evaluar sistemáticamente el efecto de su composición superficial en su capacidad para superar barreras intestinales específicas. Preparamos nueve formulaciones, tanto NEs como NCs, (*Figura 3, panel inferior*), utilizando el procedimiento de desplazamiento de disolvente en dos pasos, previamente desarrollado en nuestro laboratorio (*Figura 3, panel superior*) [47]. Todos los nanosistemas constaban del mismo núcleo oleoso (Miglyol®812N y lecitina Epikuron®145V) y sus cubiertas estaban constituidas por polímeros catiónicos (QS y PARG), tensoactivos (poloxámero 188 (P188) y poloxámero 407 (P407) y la combinación de ambos. En total, se analizaron tres NEs y seis NCs diferentes en cuanto a *i)* su estabilidad, tanto coloidal como química, en fluido intestinal simulado y *ii)* su interacción (adhesión y difusión) en un modelo de mucus fisiológicamente relevante [48,49].

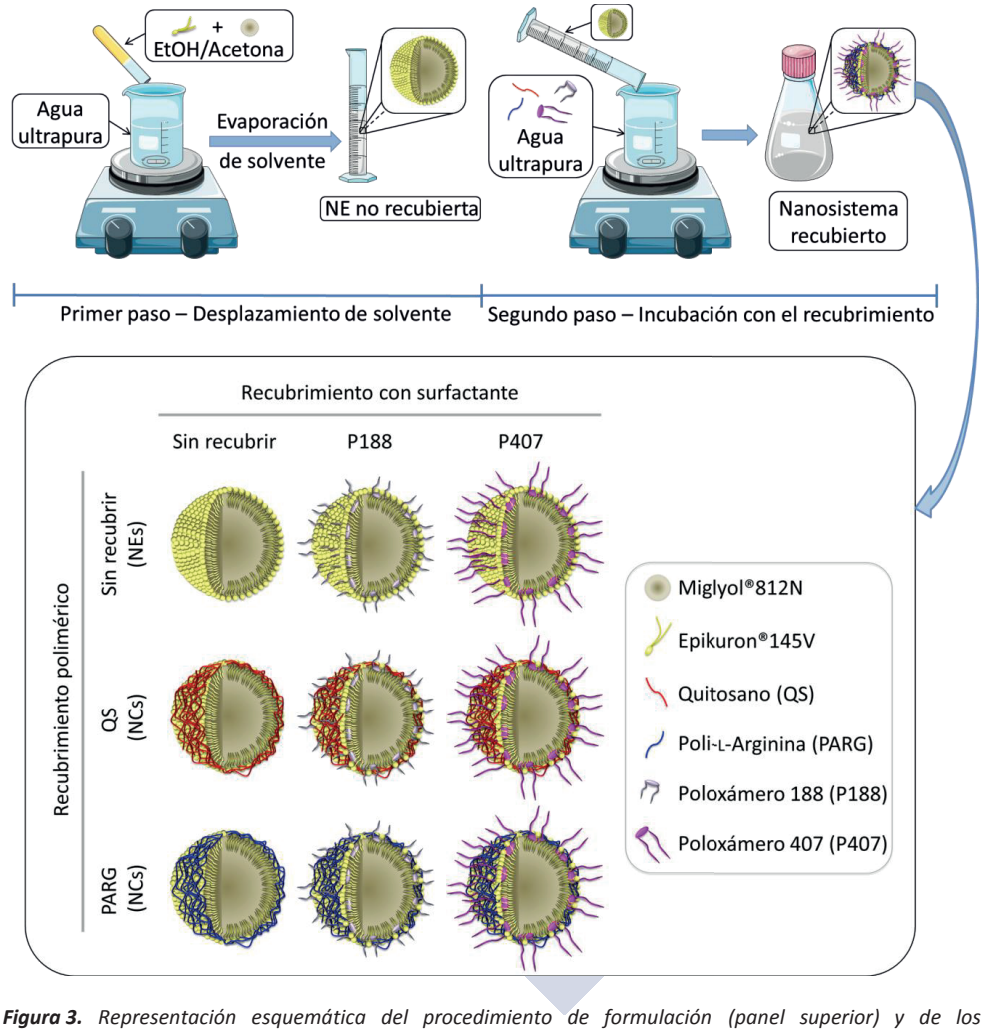



***Figura 3.*** *Representación esquemática del procedimiento de formulación (panel superior) y de los nanosistemas testados (panel inferior). Tanto el material como el equipamiento de laboratorio utilizados en esta figura han sido modificados del trabajo original (https://creativecommons.org/licenses/by/3.0/) obtenido de Servier Medical Art (http://smart.servier.com/).*

Los resultados mostrados en la *Tabla 2* indican la adecuada formación de la cubierta polimérica tras la incubación de las NEs con ambos polímeros (inversión de carga superficial), probablemente debido a la interacción electrostática entre el polímero catiónico (tanto QS como PARG) y la NE cargada negativamente [41,43]. Asimismo, la adsorción eficaz de los tensoactivos no iónicos en los nanosistemas debería conducir a una reducción en la magnitud de su potencial-ζ debido al desplazamiento del plano de cizalla hacia la fase acuosa [50]. En este sentido, los resultados señalaron una baja incorporación

del P188 a los nanosistemas independientemente de la composición de la cubierta, que fue posteriormente confirmada por la similar estabilidad, lipólisis e interacción con la mucina encontrados (*Tabla 2*) [43,51]. Por el contrario, los resultados de estabilidad y mucointeracción mostrados en la *Tabla 2* sugieren una mayor incorporación del P407 al núcleo oleoso de los nanosistemas, probablemente debido a su mayor lipofilia.

En cuanto a la estabilidad coloidal de los nanosistemas en SIF, mientras las NEs fueron estables en este medio, las NCs formuladas sin tensoactivos o con P188 mostraron una agregación inmediata. Por el contrario, las NCs con P407 fueron más estables, sobre todo las elaboradas con PARG. Mientras la estabilidad de las NEs y las NEs recubiertas con P188 se puede atribuir a las fuerzas electrostáticas repulsivas debido a su alto potencial-ζ en SIF ≈ −60 mV, la estabilidad mejorada de los nanosistemas recubiertos con P407 se deriva probablemente de la eficiente incorporación de este tensoactivo, que conduce a su estabilización estérica [26,52,53]. Se ha observado un comportamiento común en todos los sistemas tras su incubación en SIF con pancreatina. A pesar de que en ningún caso se produjo una agregación masiva, la carga superficial de todos los sistemas se volvió similar (≈ −15 ± 5 mV), probablemente debido a la formación de un recubrimiento estabilizante por parte de los enzimas presentes en el medio [54,55]. Por otro lado, los sistemas más resistentes a la degradación enzimática fueron aquellos formulados con P407. A continuación, un análisis preliminar (DLS) del papel de las propiedades superficiales de todos los prototipos en su interacción con la mucina [48] (*Tabla 2*) reveló una cierta interacción de todas las NEs con esta proteína (ausencia de agregación pero disminución de la magnitud del potencial-ζ). Como cabía esperar, las NCs QS y las NCs PARG mostraron una agregación dependiente de la concentración de mucina. De la misma manera, aunque la incorporación de P407 no puede prevenir completamente la interacción del sistema con las fibras de mucina (descenso en la magnitud de los potenciales-ζ), dicha interacción no dio lugar a su agregación.

***Tabla 2.*** *Propiedades fisicoquímicas y estabilidad de las nanoemulsiones (NEs), y nanocápsulas (NCs) de quitosano (QS) y poliarginina (PARG). Todos los sistemas presentan el mismo núcleo de Miglyol®812N/lecitina (n ≥ 3).*

| Cubierta polimérica | Cubierta de surfactante | Tamaño (nm) | IPD | Potencial−ζ (mV) | Estabilidad coloidal a 4 h en SIF | Lipolisis (% degradación a 2 h en SIF-1%-pancreatina) | Interacción con mucina (DLS) |
|---|---|---|---|---|---|---|---|
| -------- (NEs) | ----- | 179 ± 15 | 0.1 | −54 ± 1 | ✓ | 98 ± 2 | *Recubrimiento con mucina/ No agregación* |
| | **P188** | 172 ± 02 | 0.1 | −54 ± 3 | ✓ | 84 ± 1 | *Recubrimiento con mucina/ No agregación* |
| | **P407** | 174 ± 04 | 0.1 | −30 ± 3[a] | ✓ | 18 ± 2 | *Recubrimiento con mucina/ No agregación* |
| QS (NCs) | ----- | 380 ± 19 | 0.3 | +47 ± 3 | × | 82 ± 3 | Agregación dependiente de la concentración de mucina |
| | **P188** | 383 ± 18 | 0.3 | +49 ± 1 | × | 76 ± 7 | Agregación dependiente de la concentración de mucina |
| | **P407** | 327 ± 12[a] | 0.3 | +42 ± 2[b] | × | 56 ± 4 | *Recubrimiento con mucina/ No agregación* |
| PARG (NCs) | ----- | 188 ± 05 | 0.1 | +43 ± 1 | × | 86 ± 3 | Agregación dependiente de la concentración de mucina |
| | **P188** | 185 ± 03 | 0.1 | +45 ± 1 | × | 78 ± 6 | Agregación dependiente de la concentración de mucina |
| | **P407** | 183 ± 04 | 0.1 | +27 ± 2[a] | ✓ | 22 ± 6 | *Recubrimiento con mucina/ No agregación* |

*Para el análisis estadístico se aplicó un ANOVA de dos vías seguido por el test Fisher de la mínima diferencia significativa. [a]Significativamente diferente con respecto a la formulación sin tensoactivo no iónico y a la formulación con P188 (p ≤ 0.0001); [b]Significativamente diferente con respecto a la formulación sin tensoactivo no iónico (p ≤ 0.01) y a la formulación con P188 (p ≤ 0.001).*

Con el fin de interpretar el efecto de la composición de la cubierta de los nanosistemas en su interacción con la mucosa intestinal, se procedió a evaluar *i)* la interacción de los nanosistemas con un film de mucina inmovilizado en una placa con fondo de cristal, de modo semi-cuantitativo (*Figura 4, izquierda*) [56]; y *ii)* el coeficiente de difusión de los prototipos en mucus intestinal de cerdo usando "particle tracking analysis" (*Figura 4, derecha*) [57–59].

Aunque cuando se empleó mucina en placa, los resultados indicaron comportamientos mucoadhesivos claramente dependientes de la cubierta polimérica (*Figura 4, izquierda*), todas las formulaciones sin recubrir por tensoactivo (NE y NCs) mostraron una elevada retención en la matriz mucosa (*Figura 4, derecha*). Esta baja mucodifusión podría ser atribuida al carácter hidrofóbico de las NEs y la carga superficial positiva del QS y la PARG [24,60,61]. De acuerdo con resultados previos, no se encontró un efecto significativo de la adición de P188 sobre las propiedades mucoadhesivas y mucodifusivas de los tres nanosistemas. Esto sugiere que el recubrimiento con derivados de PEG de cadena 5−10 kDa, que normalmente resulta en una mejora en las propiedades mucodifusivas [58], no fue lo suficientemente denso para facilitar la mucodifusión de los nanosistemas [29,61]. Finalmente, a pesar de que la presencia de P407 redujo significativamente las propiedades mucoadhesivas de ambas NCs ($p \leq 0.05$) (*Figura 4, izquierda*), esta reducción no se tradujo en un aumento de la capacidad de mucodifusión en mucus (*Figura 4, derecha*). Esto podría deberse a la interferencia del QS y PARG en la formación de una cubierta densa y homogénea de P407 [29,61]. Por el contrario, en ausencia de cubierta polimérica (NE), el P407 podría unirse eficazmente a las nanogotículas oleosas favoreciendo la mucodifusión del sistema [29,60–62].

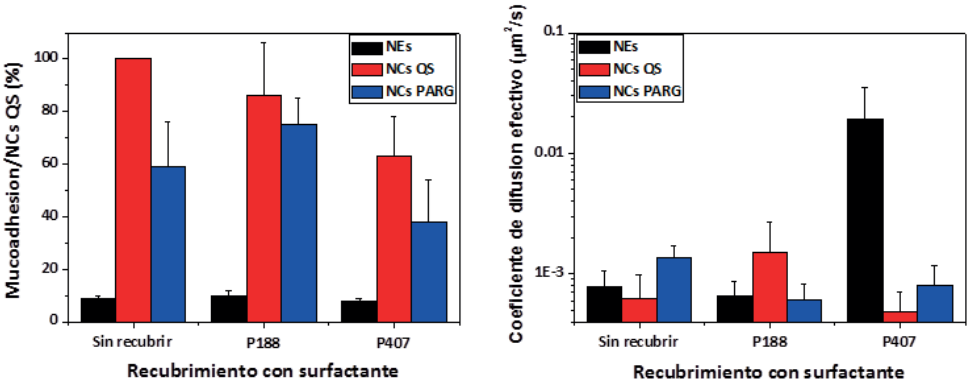



***Figura 4. Izquierda:*** *Mucoadhesión evaluada por microscopía de fluorescencia. Porcentaje de adhesión de los nanosistemas tras la incubación con un film de mucina, en comparación a las NCs QS sin recubrir por tensoactivo (considerado como 100 %) (Media ± DE, n ≥ 3).* ***Derecha:*** *Mucodifusión evaluada por "multiple particle tracking analysis". Coeficiente medio de difusión efectivo de las NEs (negro), NCs QS (rojo) y NCs PARG (azul) sin recubrir por tensoactivo, recubiertas con P188, y recubiertas con P407, calculado utilizando sus trayectorias en mucus intestinal porcino a 37 °C (Media ± DE; número de lotes analizados n = 3; n ≥ 1000 nanopartículas).*

En general, estos resultados nos indican que la interacción de los nanosistemas evaluados con las barreras biológicas depende en gran medida de su composición superficial, pudiendo verse comprometida la contribución de cada componente por la presencia de los otros. La incorporación de P407 puede resultar una estrategia adecuada para mejorar la capacidad del nanosistema para superar las numerosas barreras asociadas a la vía oral (ej., estabilidad coloidal, resistencia frente a la degradación enzimática e interacción/difusión en mucus intestinal). Sin embargo, cuando se hace uso de esta estrategia debe tenerse en consideración que la incorporación de este tensoactivo en la superficie de los nanosistemas puede interferir con otros componentes presentes en su cubierta (su uso en presencia de QS y PARG tuvo un efecto limitado en el comportamiento de la formulación).

## 2.3. Diseño racional, desarrollo y caracterización de un nuevo nanosistema lipídico para la administración oral de péptidos

El objetivo final de esta tesis se ha dirigido al desarrollo de un nuevo nanosistema lipídico capaz de superar las barreras asociadas a la administración oral. Por lo tanto, y teniendo en consideración el trabajo previo, donde los recubrimientos de QS y PARG en las NCs afectaron negativamente al potencial de las formulaciones para superar varias barreras intestinales, nos centramos en el diseño de una NE con poloxámero 407 en la superficie.

Para ello seleccionamos una insulina hidrofóbicamente modificada (HM-insulina), cuyos dominios hidrofóbicos (GRAVY ≈ -0.0333) y sus 8 aminoácidos positivamente cargados deberían favorecer su asociación con los núcleos lipídicos. El diseño del nanosistema se adecuó al cumplimiento de los siguientes criterios: *i)* preparación mediante una técnica sencilla y reproducible que permita obtener una población homogénea, *ii)* capacidad para asociar eficazmente insulina, *iii)* estabilidad y miscibilidad en fluidos intestinales simulados, *iv)* propiedades mucodifusivas, *v)* capacidad de interactuar con las células intestinales sin causar efectos citotóxicos, y *vi)* capacidad de producir una respuesta farmacológica adecuada tras su administración *in vivo*. Se seleccionaron Miglyol®812N (promotor de la absorción) como núcleo oleoso [20,21] y una sal sódica de fosfolípido PEGilado (MPEG-2000-DSPE) y poloxámero 407 como tensoactivos principales (propiedades estabilizantes y promotoras de la mucodifusión)[23–30]. Además, se seleccionó el taurocolato de sodio (TCS) como promotor de la absorción [31,32] con capacidad para formar pares iónicos hidrofóbicos con la HM-insulina [33–36]. Curiosamente, se encontró una fuerte interacción entre el MPEG-2000-DSPE y la HM−insulina, que finalmente dio lugar a un prototipo que consiste en una mezcla de NE y grupos micelares cargados con HM-insulina, cuya organización esquemática y caracterización se ilustran en la *Figura 5*.

La *Tabla 3* resume las propiedades fisicoquímicas, la eficacia de asociación de HM-insulina y la capacidad de mucodifusión del nanosistema mixto resultante (NE y micelas), así como los de sus especies por separado. Los resultados indicaron la obtención de un nanosistema mixto cargado con el 100 % de la HM-insulina, con un tamaño hidrodinámico medio de 219 ± 7 nm, bajo IPD (0.1) y potencial–ζ de -20 ± 1 mV, que también mostró propiedades de mucodifusión aceptables en mucus porcino (capacidad de difusión $D_m/D_a \approx 4.2 \times 10^{-2}$). La estrategia seguida para obtener una asociación alta de insulina se basó en: *i)* aumento de su hidrofobicidad (modificaciones hidrofóbicas y pH final ≈ 6.5 ± 0.2, cerca del punto isoeléctrico de la insulina (PI = 6.78)) para facilitar las interacciones hidrofóbicas entre los dominios hidrofóbicos de la HM-insulina y los diferentes componentes del nanosistema [15,63]; y *ii)* ajuste de su grado de ionización para facilitar su interacción electrostática con el TCS y el MPEG-2000-DSPE, cargados ambos negativamente [64]. Por otro lado, el sistema permaneció coloidalmente estable al menos durante 4 h en contacto con diferentes medios intestinales simulados (FaSSIF, SIF con y sin pancreatina al 1 %, FaSSIF-V2 y FeSSIF-V2 sin enzimas). La carga superficial negativa del sistema, junto con la presencia de derivados de PEG con PEG de PM por debajo de 10 kDa, en su superficie (P407 y MPEG-2000-DSPE), son probablemente responsables de la estabilización de la formulación en contacto con enzimas y lípidos intestinales [25,60], así como de favorecer su mucodifusión [25,27].

***Tabla 3.*** *Propiedades fisicoquímicas, eficacia de asociación (% EA) y capacidad de difusión ($D_m/D_a$)* en mucus porcino del nanosistema mixto cargado, de la nanoemulsión (NE) y de las micelas aisladas, conteniendo HM-insulina (Media ± DE, n ≥ 3).*

| Sistema cargado con HM-insulina | Tamaño (nm) | IPD | Potencial–ζ (mV) | EA (%) | Capacidad de difusión ($D_m/D_a$)* |
|---|---|---|---|---|---|
| **Sistema mixto (NE + micelas)** | 219 ± 7 | 0.1 | −20 ± 1 | ≈ 100 | $4.2 \times 10^{-2}$ |
| **NE** | 216 ± 3 | 0.1 | −19 ± 3 | 47 ± 11 | $1.0 \times 10^{-1}$ |
| **Micelas** | 184 ± 4 | 0.1 | −16 ± 3 | 56 ± 8 | $1.2 \times 10^{-1}$ |

**$D_m/D_a$ se calculó dividiendo el coeficiente medio de difusión efectiva en mucus ($D_m$) entre el coeficiente medio de difusión efectiva en agua ($D_a$).*

Para profundizar en la caracterización del nanosistema mixto, se determinó el tamaño de partícula y la forma de sus especies por separado mediante microscopía electrónica de transmisión (TEM), microscopía de fuerza atómica (AFM), dispersión de luz multiangular (MALS) y "*nanoparticle tracking analysis*" (NTA) (*Figura 5*). Los resultados indicaron que la interacción entre la HM-insulina y los fosfolípidos era lo suficientemente fuerte como para cambiar la configuración estructural de las micelas blancas y provocar la formación de una población homogénea de agrupaciones de micelas cargadas con HM-insulina.

USC UNIVERSIDADE DE SANTIAGO DE COMPOSTELA

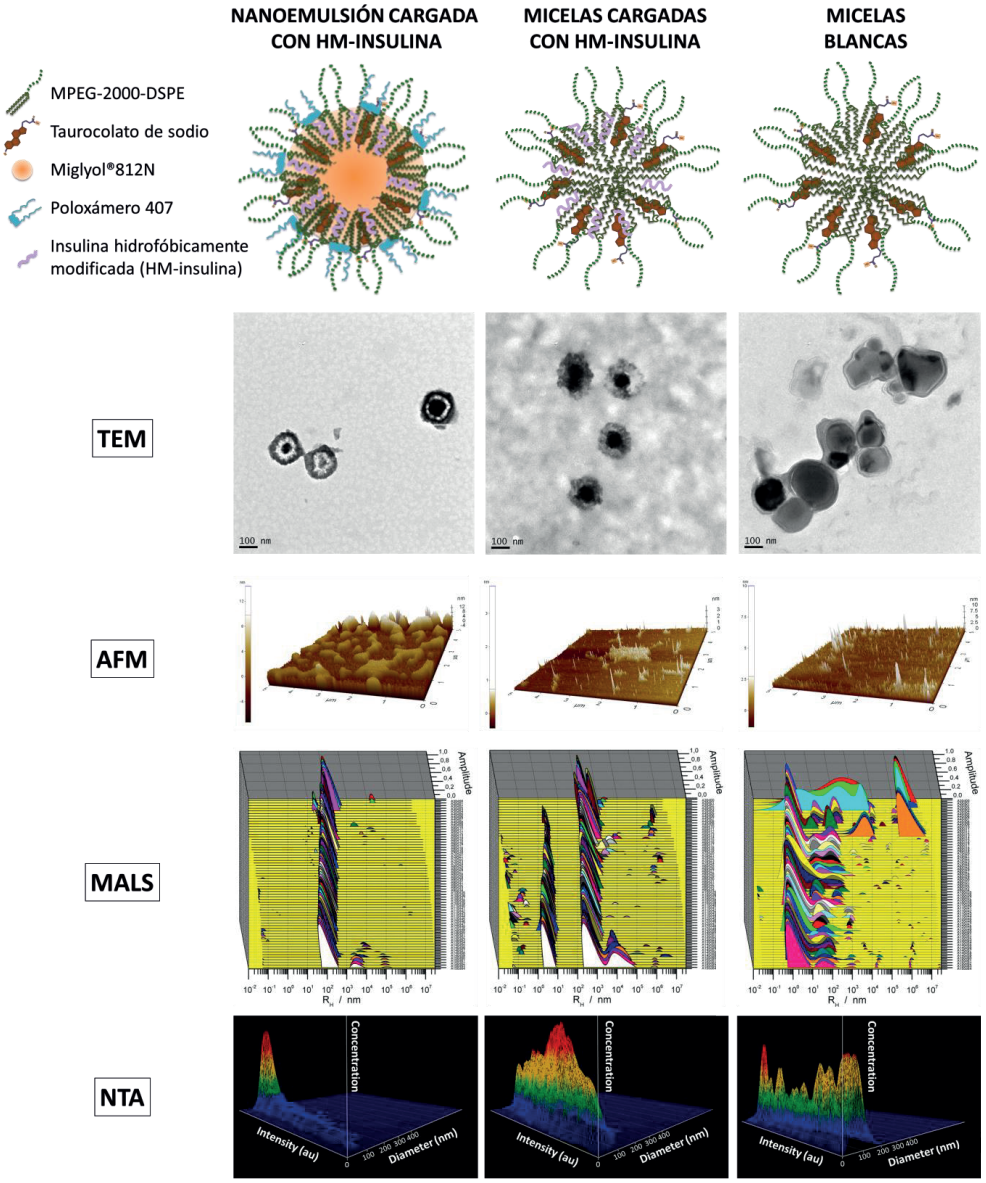



***Figura 5.*** *Representación esquemática y caracterización TEM, AFM, MALS y NTA de las especies separadas del nanosistema mixto: NE cargada con HM-insulina (izquierda), micelas cargadas con HM-insulina (centro) y también micelas blancas (derecha) como control comparativo.*

A continuación, evaluamos la interacción del nanosistema mixto cargado con HM-insulina (NE y micelas) con células intestinales. Para ello utilizamos diferentes líneas celulares: Caco-2, clon de Caco−2 de carcinoma de colon humano C2BBe1, y células HT29-MTX secretoras de mucus. A pesar de la capacidad de la línea celular Caco-2 para crecer en monocapas que reflejan algunas de características cruciales de la estructura del intestino humano (uniones estrechas y microvellosidades superficiales) [65–67], esta línea celular muestra una permeabilidad paracelular más restringida que la del intestino delgado humano (mayor presencia de uniones estrechas) [67–69] y carece de algunas características importantes, como la presencia de células caliciformes secretoras de mucus [70]. Por estas razones, también se evaluó la interacción del nanosistema mixto con el clon C2BBe1 (más similar morfológicamente que las células Caco-2, al borde del cepillo microvilliar exclusivamente localizado en el lado apical) y las células HT29-MTX secretoras de mucus (capa de mucus, microvellosidades más pequeñas y uniones estrechas menos restrictivas que las células Caco-2) [10,65,69,71].

En primer lugar, después de comprobar que el sistema permanecía estable en HBSS sin liberar la insulina asociada durante 4 h, se evaluó la citotoxicidad tanto del nanosistema mixto blanco como del cargado con HM-insulina en las tres líneas celulares mencionadas previamente utilizando diferentes técnicas (MTT, ATP, NRU y LDH). No se encontraron efectos citotóxicos relevantes tras 2 h de incubación con cualquiera de las líneas celulares analizadas. Sin embargo, sí se observó citotoxicidad dosis-dependiente tras 24 h de incubación, con ECs50 entre 2.0 y 2.3 mg/mL, valores bajos en comparación con otros sistemas nanométricos.

En segundo lugar, se analizó cuantitativamente mediante citometría de flujo (FACS) la interacción del nanosistema mixto cargado con HM-insulina con los monocultivos de Caco-2, clon C2BBe1, así como con el co-cultivo clon C2BBe1:HT29-MTX (9:1). Para este propósito, la HM-insulina se marcó covalentemente con FITC y se analizó la interacción tanto de HM-insulina libre como de HM-insulina incluida en el nanosistema. Los resultados de FACS mostraron un 100 % de células FITC positivas tras 3 h de incubación con todos los cultivos probados para ambos grupos, siendo esta interacción significativamente más alta que la observada para el control (células no tratadas).

Finalmente, también se analizó cualitativamente la interacción de ambos, la FITC-HM-insulina libre y el nanosistema mixto cargado con FITC-HM-insulina, con monocapas de Caco-2 tras 2 h de incubación usando microscopía confocal. Curiosamente, mientras casi la totalidad de la FITC-HM-insulina libre se detectó sólo en la superficie de la monocapa, el nanosistema mixto cargado con FITC-HM-insulina se encontró dentro de las células (*Figura 6*). Dado que los valores de TEER no se vieron afectados significativamente tras

estos experimentos, pudo descartarse que la internalización mejorada de los sistemas se debiese a un mayor transporte a través de la ruta paracelular. Estos resultados sugieren que la carga negativa y el PEG de la superficie del nanosistema mixto, potenciales responsables de minimizar su interacción con las proteínas del medio de cultivo celular, junto con las propiedades promotoras de la absorción de sus componentes, consiguieron mejorar su internalización en la monocapa de Caco-2 en comparación con la HM-insulina libre.

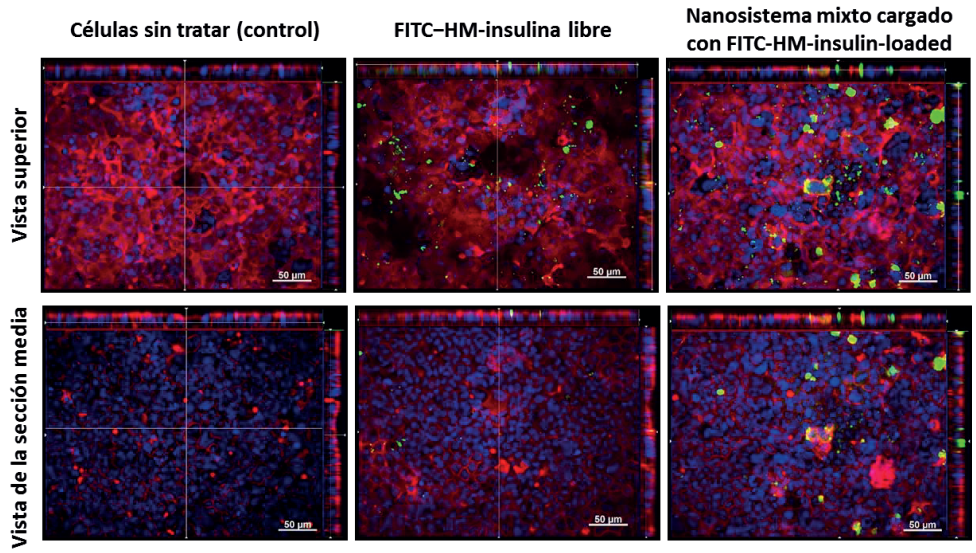



***Figura 6.*** *Imágenes de microscopía confocal (vistas superior y media a 25X) que representan la vista y-z, x-z y x-y de las monocapas de Caco-2 tras 2 h de incubación con FITC-HM-insulina libre (centro) y nanosistema mixto cargado con FITC-HM-insulina (NE + micelas) (derecha). Como control se usaron las monocapas sin tratar (izquierda). Las membranas celulares (rodamina-faloidina), los núcleos celulares (DAPI) y la HM-insulina (FITC) se visualizan en rojo, azul y verde, respectivamente.*

Una vez que el nanosistema mixto cargado con HM-insulina cumplió con los requisitos *in vitro* previos, comprobamos su eficacia hipoglucémica *in vivo* tanto en ratas sanas [32,72] como diabéticas [10,11,15,32].

En primer lugar, dado que los péptidos son macromoléculas lábiles susceptibles de resultar inactivadas como consecuencia del proceso de formulación [73], verificamos *i)* el efecto dosis-respuesta de la HM-insulina (no comercializada); y *ii)* si su bioactividad, una vez asociada al nanosistema mixto, se mantenía *in vivo* en ratas sanas. Las respuestas hipoglucémicas obtenidas tras la administración subcutánea (SC) del nanosistema mixto cargado con HM-insulina fueron comparables a las obtenidas con la dosis equivalente de una solución salina de HM-insulina (diferencias no significativas en términos de

disminución total de glucosa, cuantificada como área sobre la curva (AAC) al cabo de 8 h) (*Figura 7, derecha*). A pesar de que los valores globales obtenidos son similares, los perfiles que se observaron al administrar la dosis más baja de HM-insulina (1 UI / kg) fueron diferentes (*Figura 7, izquierda*). En el caso de los nanosistemas cargados con HM-insulina, una liberación lenta podría ser la responsable de una respuesta hipoglucémica más moderada y prolongada. La razón por la cual esta diferencia en los perfiles no se observó para la dosis alta de insulina necesita todavía ser dilucidada. Independientemente de esto, los resultados confirmaron que la estabilidad y bioactividad del péptido no se vieron comprometidas por el proceso de formulación. En cuanto a la evaluación de la relación dosis-respuesta, se observó un efecto más prolongado y estadísticamente superior con la dosis más alta probada (2 UI / kg) tanto para la insulina libre como para la asociada en el nanosistema mixto.

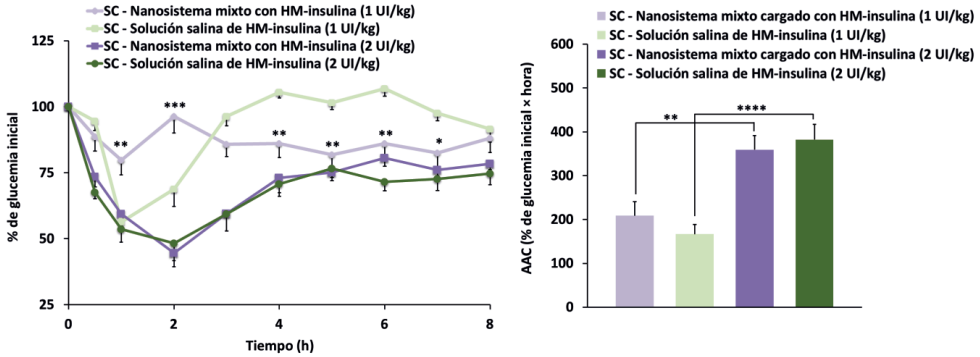



***Figura 7. Izquierda:*** *Efecto hipoglucémico normalizado (% de glucemia inicial) tras la administración subcutánea (SC) de una solución salina HM-insulina y de nanosistema mixto cargado con HM-insulina (Ne + micelas) a 1 (n = 8) y 2 UI/kg peso corporal (n = 13) a ratas sanas (media ± SEM) (Para el análisis estadístico se aplicó un ANOVA de dos vías seguido de un test Fisher de la mínima diferencia significativa: niveles de significación comparando el nanosistema mixto cargado con HM-insulina con la solución salina de HM-insulina a la misma concentración *p ≤ 0.05; **p ≤ 0.01; ***p ≤ 0.005).* ***Derecha:*** *Área sobre la curva a tiempo 8 h calculada estableciendo 120 % como límite superior (% de glucemia inicial × hora) (Media ± SEM) (Para el análisis estadístico se aplicó un ANOVA de una vía seguido de un test Fisher de la mínima diferencia significativa: niveles de significación **p ≤ 0.01; ****p ≤ 0.0001).*

Con respecto a la eficacia *in vivo* de esta formulación (100 UI/kg de peso corporal) en ratas sanas, se observó, al comparar con el nanosistema mixto blanco, un efecto hipoglucemiante leve, pero significativamente diferente (≈ 20 %, p ≤ 0.05) al cabo de 1 y 4 h de su administración intrayeyunal (IY) (*Figura 8, izquierda*). Sin embargo, no se encontraron diferencias significativas en la respuesta global, representada como AAC al cabo de 8 h (*Figura 8, derecha*).

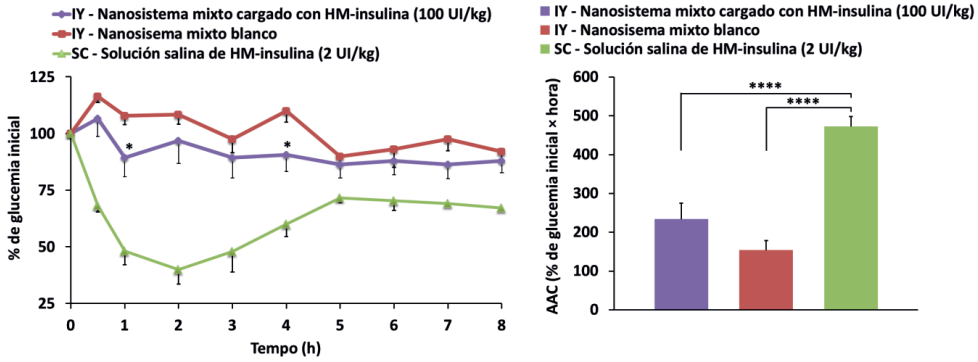



***Figura 8. Izquierda:*** *Efecto hipoglucémico normalizado (% de la glucemia inicial) tras la administración intrayeyunal (IY) del nanosistema mixto cargado con HM-insulina, dosis: 100 IU/kg (n = 8); sistema mixto blanco (n = 6) y administración subcutánea (SC) de una solución salina de HM-insulina, dosis: 2 IU/kg (n = 6) a ratas sanas (Media ± SEM) (Para el análisis estadístico se aplicó un ANOVA de dos vías seguido de un test Fisher de la mínima diferencia significativa: niveles de significación *p ≤ 0.05);* ***Derecha:*** *Área sobre la curva a tiempo 8 h calculada estableciendo 120 % como límite superior (% de glucemia inicial × hora) (Media ± SEM) (Para el análisis estadístico se aplicó un ANOVA de una vía seguido de un test Fisher de la mínima diferencia significativa: niveles de significación ****p ≤ 0.0001).*

Curiosamente, cuando se evaluó la eficacia de la formulación (100 UI/kg de peso corporal) por vía intraduodenal (ID) en un modelo de rata diabética, además de una respuesta hipoglucémica más alta en comparación con el nanosistema mixto blanco (≈ 30 %) al cabo de 1 ($p \leq 0.05$), 2, 4 y 5 ($p \leq 0.01$) h postadministración (*Figura 9, izquierda*), también se encontraron diferencias significativas ($p \leq 0.01$) en la respuesta global entre ambos grupos, representada como AAC después de 8 h (*Figura 9, derecha*).

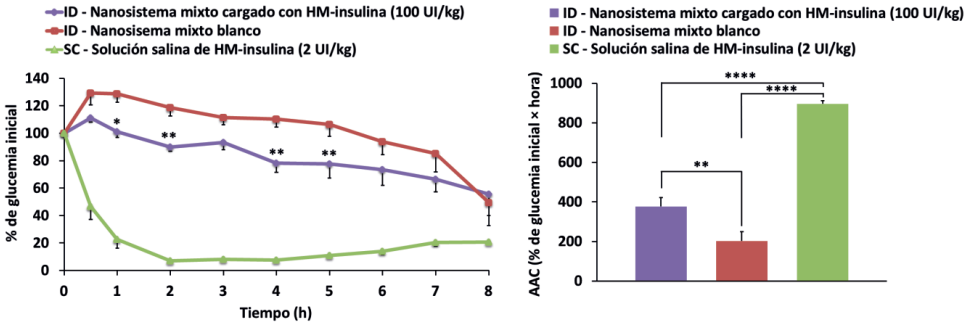



***Figure 9. Izquierda:*** *Efecto hipoglucémico normalizado (% de glucemia inicial) tras la administración intraduodenal (ID) del nanosistema mixto cargado con HM-insulina, dosis: 100 IU/kg (n = 8); sistema mixto blanco (n = 7) y administración subcutánea (SC) de una solución salina de HM-insulina, dosis: 2 IU/kg (n = 6) a ratas diabéticas (Media ± SEM) (Para el análisis estadístico se aplicó un ANOVA de dos vías seguido de un test Fisher de la mínima diferencia significativa: niveles de significación *p ≤ 0.05; **p ≤ 0.01);* ***Derecha:*** *Área sobre la curva a tiempo 8 h calculada estableciendo 130 % como límite superior (% de glucemia inicial × hora) (Media ± SEM) (Para el análisis estadístico se aplicaron un ANOVA de una vía seguido de un test Fisher de la mínima diferencia significativa: niveles de significación **p ≤ 0.01; ****p ≤ 0.0001).*

Se obtuvieron resultados de eficacia diferentes en función del modelo animal utilizado, lo que evidencia la necesidad de que la comunidad científica alcance un consenso en este sentido para permitir una comparación global de este parámetro. Por un lado, es posible utilizar modelos normoglucémicos de ratas para evitar *i)* la posible alteración del proceso de absorción causada por la anestesia y *ii)* la variabilidad en hiperglucemia provocada en las ratas diabéticas tras la administración de estreptozocina, causando también diferentes grados de deficiencia en las células−β- intrínsecamente dependiente del animal [10,15]. Sin embargo, a pesar del hecho de que el efecto de la insulina exógena podría verse obstaculizado en ratas normoglucémicas por el fenómeno de autorregulación (parada de la secreción de insulina endógena por las células−β) [74,75], se pueden encontrar mayores respuestas en la literatura cuando se usan determinados protocolos experimentales (ej., administración intraíleal, período prolongado de ayuno, anestesia, administración exógena de glucosa) [74–78]. Curiosamente, se encuentran resultados similares con administraciones intraduodenal/intrayeyunal (alta actividad enzimática y presencia de células M), tiempo de ayuno más cortos y evitando la anestesia [10,11,15,32]. Por otro lado, el modelo de rata diabética imita mejor las condiciones fisiológicas para evaluar las respuestas hipoglucémicas ya que presenta deficiencia de células−β y carece del fenómeno de autorregulación. Estas características hacen que estos animales sean más sensibles a la insulina [74,75], lo que explica la mayor eficacia que encontramos en el modelo diabético, y se correlaciona con el hecho de que la mayoría de las respuestas

hipoglucemiantes positivas publicadas hasta el momento se han logrado usando ratas anestesiadas o diabéticas [32,72].

Independientemente del valor positivo de los resultados *in vivo*, teniendo en cuenta las propiedades favorables mostradas *in vitro* (la preservación de la bioactividad de la insulina, buena estabilidad y miscibilidad en medios intestinales simulados, propiedades mucodifusivas, alta interacción celular sin efectos citotóxicos relevantes promoviendo la absorción celular de insulina y la interacción con el epitelio intestinal), se podría esperar una respuesta *in vivo* más robusta. A pesar de que los resultados sugieren que el nanosistema mixto fue capaz de proteger parcialmente de la degradación la insulina administrada por vía intraduodenal, desencadenando una respuesta hipoglucémica significativa, consideramos que la moderada eficacia *in vivo* que se obtuvo puede ser atribuible a que las condiciones *in vivo* son más drásticas, lo que probablemente restrinja el transporte de la insulina a la circulación sanguínea.

## 3. Conclusiones

Los resultados obtenidos en el trabajo experimental previamente expuesto nos han permitido llegar a las siguientes conclusiones:

1. La solubilidad limitada de péptidos y proteínas en nanosistemas lipídicos, así como sus propiedades fisicoquímicas pueden ser optimizados mediante la modificación de diferentes parámetros de formulación. Para el caso concreto de las nanocápsulas de quitosano cargadas con péptido, observamos que a pesar de que el tipo de tensoactivo no iónico tuvo un efecto mínimo tanto en las propiedades fisicoquímicas como en la asociación de insulina, otros factores como la concentración de polímero y la presencia de una segunda cubierta polimérica sí disminuyeron la carga de péptido en las nanocápsulas.

2. La interacción de los sistemas lipídicos con las múltiples barreras asociadas a la vía de administración oral es altamente dependiente de su composición superficial. En concreto, hemos demostrado que mientras la incorporación del tensoactivo no iónico poloxámero 188 en la superficie de los nanosistemas testados (nanoemulsión modelo, nanocápsulas de quitosano y de poliarginina) presentó efectos inapreciables sobre su comportamiento, la inclusión de poloxámero 407 mejoró tanto su estabilidad coloidal en fluidos intestinales simulados como su resistencia a la degradación enzimática. Asimismo, este tensoactivo resultó esencial a la hora de mejorar las propiedades de mucodifusión de las

nanoemulsiones, aunque este efecto no se pudo observar en el caso de las nanocápsulas poliméricas. Esto se atribuyó a la diferente incorporación del tensoactivo en los citados sistemas coloidales.

**3.** Utilizando como modelo de fármaco peptídico una insulina modificada hidrofóbicamente, se ha desarrollado y caracterizado un nuevo nanosistema lipídico destinado a la vía oral basado en un sistema mixto donde coexisten una nanoemulsión con una población de micelas. Este sistema mostró adecuadas propiedades fisicoquímicas (tamaño ≈ 219 ± 7 nm; PdI ≈ 0.1; potencial-ζ− ≈ −20 ± 1 mV) y una eficacia de asociación de insulina del 100 % preservando su bioactividad durante el proceso de formulación.

**3.1.** El nanosistema mixto cargado con insulina presentó adecuadas propiedades *in vitro*, tales como una adecuada miscibilidad y estabilidad en fluidos intestinales simulados, una mucodifusión aceptable en mucus porcino y una interacción/internalización significativa en varias líneas celulares modelo, sin efectos citotóxicos relevantes. Además, el sistema mixto en suspensión demostró ser estable durante al menos 3 meses en almacenamiento (4°C, temperatura ambiente ≈25 °C y 40 °C).

**3.2.** La biodistribución *in vivo* del nanosistema mixto cargado con insulina puso de manifiesto su potencial para interaccionar con el epitelio intestinal. Finalmente, tras su administración intraduodenal se observó una moderada pero significativa respuesta hipoglucémica en ratas diabéticas.

En conclusión, el trabajo descrito resalta la importancia del diseño racional de nanosistemas con el objetivo de cumplir los requerimientos necesarios para su uso como vehículos para administración oral. Asimismo, enfatiza el valor de caracterizar en profundidad los nanosistemas de acuerdo al fin con el que han sido diseñados. Finalmente, los resultados presentados también subrayan las dificultades de identificar parámetros de correlación *in vitro-in vivo* y la importancia de estandarizar protocolos experimentales para obtener resultados *in vitro* más predictivos.

## Referencias


[1] T.A.S. Aguirre, D. Teijeiro-Osorio, M. Rosa, I.S. Coulter, M.J. Alonso, D.J. Brayden, Current status of selected oral peptide technologies in advanced preclinical development and in clinical trials, Adv. Drug Deliv. Rev. 106 (2016) 223–241. doi:10.1016/j.addr.2016.02.004.

[2] S. Mitragotri, P.A. Burke, R. Langer, Overcoming the challenges in administering biopharmaceuticals: formulation and delivery strategies, Nat Rev Drug Discov. 13 (2014) 655–672. doi:10.1038/nrd4363.

[3] D.S. Pisal, M.P. Kosloski, S. V. Balu-Iyler, Delivery of therapeutic proteins, J. Pharm. Sci. 99 (2010) 2557–2575. doi:10.1002/jps.22054.

[4] C.F. Van Der Walle, O. Olejnik, An overview of the field of peptide and protein delivery, in: C.F. Van Der Walle (Ed.), Pept. Protein Deliv., First, Academic Press, 2011: pp. 1–22. doi:10.1016/b978-0-12-384935-9.10001-x.

[5] B.J. Bruno, G.D. Miller, C.S. Lim, Basics and recent advances in peptide and protein drug delivery, Ther. Deliv. 4 (2013) 1443–1467. doi:10.4155/tde.13.104.

[6] E. Arbit, The physiological rationale for oral insulin administration, Diabetes Technol. Ther. 6 (2004) 510–517. doi:10.1089/1520915041705929.

[7] A. Sood, R. Panchagnula, Peroral route: An opportunity for protein and peptide drug delivery, Chem. Rev. 101 (2001) 3275–3303. doi:10.1021/cr000700m.

[8] J. Wang, V. Yadav, A.L. Smart, S. Tajiri, A.W. Basit, Toward oral delivery of biopharmaceuticals: An assessment of the gastrointestinal stability of 17 peptide drugs, Mol. Pharm. 12 (2015) 966–973. doi:10.1021/mp500809f.

[9] M. Morishita, N.A. Peppas, Is the oral route possible for peptide and protein drug delivery?, Drug Discov. Today. 11 (2006) 905–910. doi:10.1016/j.drudis.2006.08.005.

[10] L.N. Thwala, A. Beloqui, N.S. Csaba, D. González-Touceda, S. Tovar, C. Dieguez, M.J. Alonso, V. Préat, The interaction of protamine nanocapsules with the intestinal epithelium: a mechanistic approach, J. Control. Release. 243 (2016) 109–120. doi:10.1016/j.jconrel.2016.10.002.

[11] Z. Niu, E. Samaridou, E. Jaumain, J. Coëne, G. Ullio, N. Shrestha, J. Garcia, M. Durán-Lobato, S. Tovar, M.J. Santander-Ortega, M.V. Lozano, M.M. Arroyo-Jimenez, R. Ramos-Membrive, I. Peñuelas, A. Mabondzo, V. Préat, M. Teixidó, E. Giralt, M.J. Alonso, PEG-PGA enveloped octaarginine-peptide nanocomplexes: an oral peptide delivery strategy, J. Control. Release. 276 (2018) 125–139. doi:10.1016/j.jconrel.2018.03.004.

[12] X. Li, S. Guo, C. Zhu, Q. Zhu, Y. Gan, J. Rantanen, U.L. Rahbek, L. Hovgaard, M. Yang, Intestinal mucosa permeability following oral insulin delivery using core shell corona nanolipoparticles, Biomaterials. 34 (2013) 9678–9687. doi:10.1016/j.biomaterials.2013.08.048.

[13] L. Inchaurraga, N. Martín-Arbella, V. Zabaleta, G. Quincoces, I. Peñuelas, J.M. Irache, In vivo study of the mucus-permeating properties of PEG-coated nanoparticles following oral administration, Eur. J. Pharm. Biopharm. 97 (2015) 280–289. doi:10.1016/j.ejpb.2014.12.021.

[14] W. Shan, X. Zhu, M. Liu, L. Li, J. Zhong, W. Sun, Z. Zhang, Y. Huang, Overcoming the diffusion barrier of mucus and absorption barrier of epithelium by self-Assembled nanoparticles for oral delivery of insulin, ACS Nano. 9 (2015) 2345–2356. doi:10.1021/acsnano.5b00028.

[15] Z. Niu, E. Tedesco, F. Benetti, A. Mabondzo, I.M. Montagner, I. Marigo, D. Gonzalez-Touceda, S. Tovar, C. Diéguez, M.J. Santander-Ortega, M.J. Alonso, Rational design of polyarginine nanocapsules

intended to help peptides overcoming intestinal barriers, J. Control. Release. 263 (2016) 4–17. doi:10.1016/j.jconrel.2017.02.024.

[16] T. Karamanidou, V. Bourganis, O. Kammona, C. Kiparissides, Lipid-based nanocarriers for the oral administration of biopharmaceutics, Nanomedicine. 11 (2016) 3009–3032. doi:10.2217/nnm-2016-0265.

[17] Z. Niu, I. Conejos-Sánchez, B.T. Griffin, C.M. O'Driscoll, M.J. Alonso, Lipid-based nanocarriers for oral peptide delivery, Adv. Drug Deliv. Rev. 106 (2016) 337–354. doi:10.1016/j.addr.2016.04.001.

[18] L. Rosenmayr-Templeton, The oral delivery of peptides and proteins: established versus recently patented approaches, Pharm. Pat. Anal. 2 (2013) 125–145. doi:10.4155/ppa.12.75.

[19] P. Calvo, C. Remuñán-López, J.L. Vila-Jato, M.J. Alonso, Development of positively charged colloidal drug carriers: chitosan-coated polyester nanocapsules and submicron-emulsions, Colloid Polym. Sci. 275 (1997) 46–53. doi:10.1007/s003960050050.

[20] K.A. Traul, A. Driedger, D.L. Ingle, D. Nakhasi, Review of the toxicologic properties of medium-chain triglycerides, Food Chem. Toxicol. 38 (2000) 79–98. doi:10.1016/S0278-6915(99)00106-4.

[21] B. Marten, M. Pfeuffer, J. Schrezenmeir, Medium-chain triglycerides, Int. Dairy J. 16 (2006) 1374–1382. doi:10.1016/j.idairyj.2006.06.015.

[22] M. Tobío, R. Gref, A. Sanchez, R. Langer, M.J. Alonso, Stealth PLA-PEG nanoparticles as protein carriers for nasal administration, Pharm. Res. 15 (1998) 270–275. doi:10.1023/A:1011922819926.

[23] M. Tobío, A. Sánchez, A. Vila, I. Soriano, C. Evora, J.. J. Vila-Jato, M.. M. Alonso, The role of PEG on the stability in digestive fluids and in vivo fate of PEG-PLA nanoparticles following oral administration, Colloids Surfaces B Biointerfaces. 18 (2000) 315–323. doi:10.1016/S0927-7765(99)00157-5.

[24] C. Prego, D. Torres, E. Fernandez-Megia, R. Novoa-Carballal, E. Quiñoá, M.J. Alonso, Chitosan-PEG nanocapsules as new carriers for oral peptide delivery: effect of chitosan pegylation degree, J. Control. Release. 111 (2006) 299–308. doi:10.1016/j.jconrel.2005.12.015.

[25] I. Santalices, D. Torres, M.V. Lozano, M.M. Arroyo-Jiménez, M.J. Alonso, M.J. Santander-Ortega, Influence of the surface properties of nanocapsules on their interaction with intestinal barriers, Submitt. to Eur. J. Pharm. Biopharm. (2018).

[26] M. Wulff-Pérez, J. de Vicente, A. Martín-Rodríguez, M.J. Gálvez-Ruiz, Controlling lipolysis through steric surfactants: new insights on the controlled degradation of submicron emulsions after oral and intravenous administration, Int. J. Pharm. 423 (2012) 161–166. doi:10.1016/j.ijpharm.2011.12.025.

[27] L.M. Ensign, R. Cone, J. Hanes, Oral drug delivery with polymeric nanoparticles: the gastrointestinal mucus barriers, Adv. Drug Deliv. Rev. 64 (2012) 557–570. doi:10.1016/j.addr.2011.12.009.

[28] A. Vila, H. Gill, O. McCallion, M.J. Alonso, Transport of PLA-PEG particles across the nasal mucosa: Effect of particle size and PEG coating density, J. Control. Release. 98 (2004) 231–244. doi:10.1016/j.jconrel.2004.04.026.

[29] Q. Xu, L.M. Ensign, N.J. Boylan, A. Schön, X. Gong, J.C. Yang, N.W. Lamb, S. Cai, T. Yu, E. Freire, J. Hanes, Impact of surface polyethylene glycol (PEG) density on biodegradable nanoparticle transport in mucus ex vivo and distribution in vivo, ACS Nano. 9 (2015) 9217–9227. doi:10.1021/acsnano.5b03876.

[30] D. Chen, D. Xia, X. Li, Q. Zhu, H. Yu, C. Zhu, Y. Gan, Comparative study of Pluronic® F127-modified liposomes and chitosan-modified liposomes for mucus penetration and oral absorption of

cyclosporine A in rats, Int. J. Pharm. 449 (2013) 1–9. doi:10.1016/j.ijpharm.2013.04.002.

[31] M. Niu, Y. Tan, P. Guan, L. Hovgaard, Y. Lu, J. Qi, R. Lian, X. Li, W. Wu, Enhanced oral absorption of insulin-loaded liposomes containing bile salts: A mechanistic study, Int. J. Pharm. 460 (2014) 119–130. doi:10.1016/j.ijpharm.2013.11.028.

[32] M. Niu, Y. Lu, L. Hovgaard, P. Guan, Y. Tan, R. Lian, J. Qi, W. Wu, Hypoglycemic activity and oral bioavailability of insulin-loaded liposomes containing bile salts in rats: The effect of cholate type, particle size and administered dose, Eur. J. Pharm. Biopharm. 81 (2012) 265–272. doi:10.1016/j.ejpb.2012.02.009.

[33] C. Chen, T. Fan, Y. Jin, Z. Zhou, Y. Yang, X. Zhu, Z. Zhang, Q. Zhang, Y. Huang, Orally delivered salmon calcitonin-loaded solid lipid nanoparticles prepared by micelle–double emulsion method via the combined use of different solid lipids, Nanomedicine. 8 (2013) 1085–1100. doi:10.2217/nnm.12.141.

[34] J. Liu, T. Gong, C. Wang, Z. Zhong, Z. Zhang, Solid lipid nanoparticles loaded with insulin by sodium cholate-phosphatidylcholine-based mixed micelles: preparation and characterization, Int. J. Pharm. 340 (2007) 153–162. doi:10.1016/j.ijpharm.2007.03.009.

[35] S. Sun, N. Liang, H. Piao, H. Yamamoto, Y. Kawashima, F. Cui, Insulin-S.O (sodium oleate) complex-loaded PLGA nanoparticles: Formulation, characterization and *in vivo* evaluation, J. Microencapsul. 27 (2010) 471–478. doi:10.3109/02652040903515490.

[36] S. Hu, M. Niu, F. Hu, Y. Lu, J. Qi, Z. Yin, W. Wu, Integrity and stability of oral liposomes containing bile salts studied in simulated and ex vivo gastrointestinal media, Int. J. Pharm. 441 (2013) 693–700. doi:10.1016/j.ijpharm.2012.10.025.

[37] C. Prego, D. Torres, M.J. Alonso, The potential of chitosan for the oral administration of peptides, Expert Opin. Drug Deliv. 2 (2005) 843–854. doi:10.1517/17425247.2.5.843.

[38] V. V. Khutoryanskiy, Advances in mucoadhesion and mucoadhesive polymers, Macromol. Biosci. 11 (2011) 748–764. doi:10.1002/mabi.201000388.

[39] M. Garcia-Fuentes, M.J. Alonso, Chitosan-based drug nanocarriers: where do we stand?, J. Control. Release. 161 (2012) 496–504. doi:10.1016/j.jconrel.2012.03.017.

[40] S. Roy, K. Pal, A. Anis, K. Pramanik, B. Prabhakar, Polymers in mucoadhesive drug-delivery systems: a brief note, Des. Monomers Polym. 12 (2009) 483–495. doi:10.1163/138577209X12478283327236.

[41] C. Prego, M. Fabre, D. Torres, M.J. Alonso, Efficacy and mechanism of action of chitosan nanocapsules for oral peptide delivery, Pharm. Res. 23 (2006) 549–556. doi:10.1007/s11095-006-9570-8.

[42] F.M. Goycoolea, A. Valle-Gallego, R. Stefani, B. Menchicchi, L. David, C. Rochas, M.J. Santander-Ortega, M.J. Alonso, Chitosan-based nanocapsules: physical characterization, stability in biological media and capsaicin encapsulation, Colloid Polym. Sci. 290 (2012) 1423–1434. doi:10.1007/s00396-012-2669-z.

[43] M.J. Santander-Ortega, M. V. Lozano-López, D. Bastos-González, J.M. Peula-García, J.L. Ortega-Vinuesa, Novel core-shell lipid-chitosan and lipid-poloxamer nanocapsules: Stability by hydration forces, Colloid Polym. Sci. 288 (2010) 159–172. doi:10.1007/s00396-009-2132-y.

[44] M.J. Santander-Ortega, J.M. Peula-García, F.M. Goycoolea, J.L. Ortega-Vinuesa, Chitosan nanocapsules: effect of chitosan molecular weight and acetylation degree on electrokinetic behaviour and colloidal stability, Colloids Surfaces B Biointerfaces. 82 (2011) 571–580. doi:10.1016/j.colsurfb.2010.10.019.

[45] D. Torrecilla, M. V. Lozano, E. Lallana, J.I. Neissa, R. Novoa-Carballal, A. Vidal, E. Fernandez-Megia, D. Torres, R. Riguera, M.J. Alonso, F. Dominguez, Anti-tumor efficacy of chitosan-g-poly(ethylene glycol) nanocapsules containing docetaxel: anti-TMEFF-2 functionalized nanocapsules vs. non-functionalized nanocapsules, Eur. J. Pharm. Biopharm. 83 (2013) 330–337. doi:10.1016/j.ejpb.2012.10.017.

[46] M. V. Lozano, G. Lollo, M. Alonso-Nocelo, J. Brea, A. Vidal, D. Torres, M.J. Alonso, Polyarginine nanocapsules: a new platform for intracellular drug delivery, J. Nanoparticle Res. 15 (2013) 15:1515. doi:10.1007/s11051-013-1515-7.

[47] C. Prego, M. García, D. Torres, M.J. Alonso, Transmucosal macromolecular drug delivery, J. Control. Release. 101 (2005) 151–162. doi:10.1016/j.jconrel.2004.07.030.

[48] S.K. Lai, Y.-Y. Wang, D. Wirtz, J. Hanes, Micro- and macrorheology of mucus, Adv. Drug Deliv. Rev. 61 (2009) 86–100. doi:10.1016/j.addr.2008.09.012.

[49] J. das Neves, M.F. Bahia, M.M. Amiji, B. Sarmento, Mucoadhesive nanomedicines: characterization and modulation of mucoadhesion at the nanoscale, Expert Opin. Drug Deliv. 8 (2011) 1085–1104. doi:10.1517/17425247.2011.586334.

[50] M.J. Santander-Ortega, A.B. Jódar-Reyes, N. Csaba, D. Bastos-González, J.L. Ortega-Vinuesa, Colloidal stability of Pluronic F68-coated PLGA nanoparticles: a variety of stabilisation mechanisms, J. Colloid Interface Sci. 302 (2006) 522–529. doi:10.1016/j.jcis.2006.07.031.

[51] L. Zhang, J.M. Chan, F.X. Gu, J.W. Rhee, A.Z. Wang, A.F. Radovic-Moreno, F. Alexis, R. Langer, O.C. Farokhzad, Self-assembled lipid-polymer hybrid nanoparticles: A robust drug delivery platform, ACS Nano. 2 (2008) 1696–1702. doi:10.1021/nn800275r.

[52] M.J. Santander-Ortega, N. Csaba, M.J. Alonso, J.L. Ortega-Vinuesa, D. Bastos-González, Stability and physicochemical characteristics of PLGA, PLGA: poloxamer and PLGA: poloxamine blend nanoparticles: a comparative study, Colloids Surfaces A Physicochem. Eng. Asp. 296 (2007) 132–140. doi:10.1016/j.colsurfa.2006.09.036.

[53] C. Olbrich, R.H. Müller, Enzymatic degradation of SLN-effect of surfactant and surfactant mixtures, Int. J. Pharm. 180 (1999) 31–39. doi:10.1016/S0378-5173(98)00404-9.

[54] M. García-Fuentes, D. Torres, M.J. Alonso, Design of lipid nanoparticles for the oral delivery of hydrophilic macromolecules, Colloids Surfaces B Biointerfaces. 27 (2002) 159–168. doi:10.1016/S0927-7765(02)00053-X.

[55] M. Tirado-Miranda, A. Schmitt, J. Callejas-Fernández, A. Fernández-Barbero, The aggregation behaviour of protein-coated particles: a light scattering study, Eur. Biophys. J. 32 (2003) 128–36. doi:10.1007/s00249-002-0275-6.

[56] A. Tachaprutinun, P. Pan-In, S. Wanichwecharungruang, Mucosa-plate for direct evaluation of mucoadhesion of drug carriers, Int. J. Pharm. 441 (2013) 801–808. doi:10.1016/j.ijpharm.2012.12.028.

[57] E. Zagato, K. Forier, T. Martens, K. Neyts, J. Demeester, S. De Smedt, K. Remaut, K. Braeckmans, Single-particle tracking for studying nanomaterial dynamics: applications and fundamentals in drug delivery, Nanomedicine. 9 (2014) 913–927. doi:10.2217/nnm.14.43.

[58] B.S. Schuster, L.M. Ensign, D.B. Allan, J.S. Suk, J. Hanes, Particle tracking in drug and gene delivery research: state-of-the-art applications and methods, Adv. Drug Deliv. Rev. 91 (2015) 70–91. doi:10.1016/j.addr.2015.03.017.

[59] J. Suh, M. Dawson, J. Hanes, Real-time multiple-particle tracking: Applications to drug and gene delivery, Adv. Drug Deliv. Rev. 57 (2005) 63–78. doi:10.1016/j.addr.2004.06.001.

[60] M. Plaza-Oliver, J. Fernández Sainz de Baranda, V. Rodríguez Robledo, L. Castro-Vázquez, J. Gonzalez-Fuentes, P. Marcos, M. V. Lozano, M.J. Santander-Ortega, M.M. Arroyo-Jimenez, Design of the interface of edible nanoemulsions to modulate the bioaccessibility of neuroprotective antioxidants, Int. J. Pharm. 490 (2015) 209–218. doi:10.1016/j.ijpharm.2015.05.031.

[61] M.J. Santander-Ortega, M. Plaza-Oliver, V. Rodríguez-Robledo, L. Castro-Vázquez, N. Villaseca-González, J. González-Fuentes, E.L. Cano, P. Marcos, M. V. Lozano, M.M. Arroyo-Jiménez, PEGylated nanoemulsions for oral delivery: role of the inner core on the final fate of the formulation, Langmuir. 33 (2017) 4269–4279. doi:10.1021/acs.langmuir.7b00351.

[62] Y.-Y. Wang, S.K. Lai, J.S. Suk, A. Pace, R. Cone, J. Hanes, Addressing the PEG mucoadhesivity paradox to engineer nanoparticles that "slip" through the human mucus barrier, Angew. Chemie - Int. Ed. 47 (2008) 9726–9729. doi:10.1002/anie.200803526.

[63] Z. Sezgin, N. Yüksel, T. Baykara, Preparation and characterization of polymeric micelles for solubilization of poorly soluble anticancer drugs, Eur. J. Pharm. Biopharm. 64 (2006) 261–268. doi:10.1016/j.ejpb.2006.06.003.

[64] L.N. Thwala, Protamine nanocapsules as carriers for oral peptide delivery, University of Santiagode de Compostela; University Catholique de Louvain, 2016.

[65] F. Araújo, B. Sarmento, Towards the characterization of an in vitro triple co-culture intestine cell model for permeability studies, Int. J. Pharm. 458 (2013) 128–134. doi:10.1016/j.ijpharm.2013.10.003.

[66] F. Araújo, C. Pereira, J. Costa, C. Barrias, P.L. Granja, B. Sarmento, In vitro M-like cells genesis through a tissue-engineered triple-culture intestinal model, J. Biomed. Mater. Res. - Part B Appl. Biomater. 104 (2016) 782–788. doi:10.1002/jbm.b.33508.

[67] F. Antunes, F. Andrade, F. Araújo, D. Ferreira, B. Sarmento, Establishment of a triple co-culture in vitro cell models to study intestinal absorption of peptide drugs, Eur. J. Pharm. Biopharm. 83 (2013) 427–435. doi:10.1016/j.ejpb.2012.10.003.

[68] C. Hilgendorf, H. Spahn-langguth, C.G. Regårdh, E. Lipka, Caco-2 versus Caco-2/HT29-MTX co-cultured cell lines: permeabilities via diffusion, inside- and outside-directed carrier-mediated transport, J. Pharm. Sci. 89 (2000) 63–75.

[69] I. Behrens, P. Stenberg, P. Artursson, T. Kissel, Transport of lipophilic drug molecules in a new mucus secreting cell culture model based on Ht-29 MTX cells, Pharm. Res. 18 (2001) 1138–1145.

[70] D. Yang, D. Liu, M. Qin, B. Chen, S. Song, W. Dai, H. Zhang, X. Wang, Y. Wang, B. He, X. Tang, Q. Zhang, Intestinal mucin induces more endocytosis but less transcytosis of nanoparticles across enterocytes by triggering nano-clustering and strengthening the retrograde pathway, ACS Appl. Mater. Interfaces. (2018) acsami.7b19153. doi:10.1021/acsami.7b19153.

[71] T. Lesuffleur, A. Barbat, E. Dussaulx, A. Zweibaum, Growth Adaptation to Methotrexate of HT-29 Human Colon Carcinoma Cells Is Associated with Their Ability to Differentiate into Columnar Absorptive and Mucus-secreting Cells, Cancer Res. 50 (1990) 6334–6343.

[72] N. Reix, A. Parat, E. Seyfritz, R. Van Der Werf, V. Epure, N. Ebel, L. Danicher, E. Marchioni, N. Jeandidier, M. Pinget, Y. Frère, S. Sigrist, In vitro uptake evaluation in Caco-2 cells and in vivo results in diabetic rats of insulin-loaded PLGA nanoparticles, Int. J. Pharm. 437 (2012) 213–220.

doi:10.1016/j.ijpharm.2012.08.024.

[73] M.C. Manning, G.J. Evans, R.W. Payne, Protein stability during bioprocessing, in: F. Jameel, S. Hershenson (Eds.), Formul. Process Dev. Strateg. Manuf. Biopharm., John Wiley & Sons, Inc., 2010: pp. 605–624. doi:10.1002/9780470595886.

[74] C. Damge, C. Michel, M. Aprahamian, P. Couvreur, New approach for oral administration of insulin with polyalkylcyanoacrylate nanocapsules as drug carrier, Diabetes. 37 (1988) 246–251. doi:10.2337/diab.37.2.246.

[75] C. Damge, C. Michel, M. Aprahamian, P. Couvreur, J.P. Devissaguet, Nanocapsules as carriers for oral peptide delivery, J. Control. Release. 13 (1990) 233–239. doi:10.1016/0168-3659(90)90013-J.

[76] L. Yin, J. Ding, C. He, L. Cui, C. Tang, C. Yin, Drug permeability and mucoadhesion properties of thiolated trimethyl chitosan nanoparticles in oral insulin delivery, Biomaterials. 30 (2009) 5691–5700. doi:10.1016/j.biomaterials.2009.06.055.

[77] C. Michel, M. Aprahamian, L. Defontaine, P. Couvreur, C. Damgé, The effect of site of administration in the gastrointestinal tract on the absorption of insulin from nanocapsules in diabetic rats, J. Pharm. Pharmacol. 43 (1991) 1–5. doi:10.1111/j.2042-7158.1991.tb05437.x.

[78] M. Morishita, T. Goto, K. Nakamura, A.M. Lowman, K. Takayama, N.A. Peppas, Novel oral insulin delivery systems based on complexation polymer hydrogels: Single and multiple administration studies in type 1 and 2 diabetic rats, J. Control. Release. 110 (2006) 587–594. doi:10.1016/j.jconrel.2005.10.029.

USC UNIVERSIDADE DE SANTIAGO DE COMPOSTELA




# Introduction

USC
UNIVERSIDADE
DE SANTIAGO
DE COMPOSTELA

## Table of contents

**1. The need of efficient peptide/protein delivery systems**

**2. Current status of peptide/protein-loaded nanotechnologies**

**3. Nanocarriers for oral protein/peptide delivery**

**4. The specific case of insulin**

4.1. The origin and variants of insulin currently available

4.2. Pharmacokinetics and pharmacodynamics of insulin

4.3. The need of an oral insulin

**5. Conclusions and perspectives**

USC UNIVERSIDADE DE SANTIAGO DE COMPOSTELA

USC
UNIVERSIDADE
DE SANTIAGO
DE COMPOSTELA

## 1. The need of efficient peptide/protein delivery systems

During the last decades, important efforts have been oriented to the commercialization of therapeutic proteins and peptides. Within this frame, the market has been growing exponentially, being proteins some of the top selling drugs in the last years, particularly antibodies [1,2]. *Figure 1* summarizes the main strengths, weaknesses, opportunities, and threats of naturally occurring peptides in their use as therapeutics [3]. Unfortunately, despite the well-known advantages of these drugs in terms of potency and selectivity, their exploitation as therapeutics is being limited by their instability, restricted bioavailability, short half-life, intrinsic immunogenicity (specially for high molecular weight proteins) and, in general, by the necessity of being administered by injection [1]. These draw-backs have stimulated research in the area of drug delivery and nanotechnology with the final goal of making the administration of these powerful drugs more efficient [4–6].

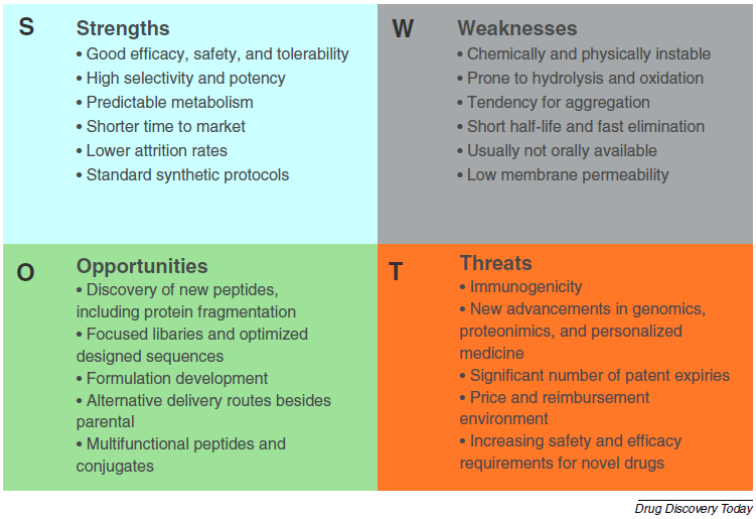



***Figure 1.*** *Main strengths, weaknesses, opportunities, and threats of naturally occurring peptides in their use as therapeutics. Image reused with permission from* [3].

The possibility of including peptides and proteins in nanovehicles that are able to protect and deliver them at the adequate site has generated increasing expectation during last decades (*Figure 2*) [7–9]. Liposomes were the first nanocarriers proposed for protein delivery in the early 70's [10,11]. Meanwhile, Speiser and co-workers investigated the possibility to encapsulate antigens into polyacrylic nanoparticles using micelle polymerization techniques [12]. A decade later, poly(alkyl cyanoacrylate) nanocapsules were proposed as carriers for the oral administration of insulin [13]. Finally, over the 90's Gasco et al. produced for the first time peptide-loaded solid lipid nanoparticles [14–16]

and our group pioneered the development of nanoparticles made of PLGA [17], PLA-PEG [18] and chitosan [19], as well as of nanocapsules made of chitosan [20–23], protamine [24–26] and polyarginine [27,28], for the delivery of proteins and antigens.

As illustrated in *Figure 2*, the interest around the use of all these nanocarriers for protein/peptide delivery has progressively increased in the past decades, being liposomes and polysaccharide-based nanoparticles the ones receiving the greatest attention. Noteworthy, the use of inorganic nanoparticles in the peptide/protein delivery field has grown-up during the past decade, as well. In particular, nanoparticles made of gold, iron oxide [29,30], calcium phosphate and silica likewise carbon nanotubes [31,32] have received a certain attention. However, overall, the tendency has been towards the use of biodegradable and biocompatible biomaterials that can form nanostructures based on friendly and easily scalable techniques. This tendency is expected to change the translational prospective of these delivery vehicles. Indeed, still nowadays and despite all the efforts devoted in this field, the development of efficacious and cost–effective nano-based protein products remains a challenge and this justifies the limited number of protein/peptide-based nanoparticulate products in the market or under clinical development [33–36]. The necessity for these nanomedicines to exhibit important quality attributes such as significant drug loading, maintenance of the loaded peptide/protein activity and controlled drug release, are just some examples of the bottlenecks to be overcame [37].

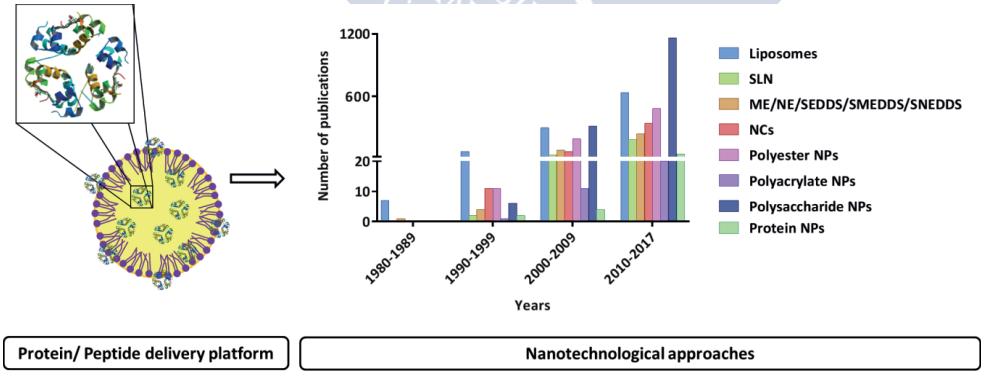



***Figure 2.*** *Trend of reported experimental works concerning nanocarriers for peptide/protein delivery from the 70's up to date. Data taken from Scopus (1971–2017) using protein/peptide delivery and the type of system as searching criteria. ME: microemulsion; NCs: nanocapsules; NE: nanoemulsion; NPs: nanoparticles; SEDDS: self-emulsified drug delivery system; SMEDDS: self-microemulsified drug delivery system; SNEDDS: self-nanoemulsified drug delivery system; SLN: solid lipid nanoparticles. Image reused with permission from* [38,39].

**X-ray structure of Human Recombinant insulin. Image from the RCSB PDB (www.rcsb.org) of PDB ID 5E7W.*

## 2. Current status of peptide/protein-loaded nanotechnologies

Although numerous attempts have been oriented towards making feasible the administration of proteins following a variety of modalities of administration (ocular, pulmonary, nasal, transdermal) [1,8,40–43], the most advanced developments are intended either for oral administration and local delivery to the intestinal cavity [44,45], or for systemic delivery upon oral [46,47] or parenteral administration [48].

With regard to the **parenteral modality of administration**, the use of nanodelivery carriers has been found to improve the biodistribution and half-life of proteins (e.g. growth factors and vaccines), thereby enhancing and prolonging their efficacy [48]. Among the nanocarriers investigated, liposomes are the ones that have made their way to the market, in particular in the area of vaccination. For example, Inflexal® V, which is in the market since 1997, is a 150 nm liposome formulation that contains influenza virus antigens [49]. Another liposomal marketed formulation is Mepact®, which contains the immune stimulant polypeptide drug mifamurtide, and was commercialized in Europe in 2009 for the treatment of non-metastasizing resectable osteosarcoma [50]. Also, a liposomal formulation containing HPV E6 + E7 peptides intended to the treatment of HPV-related cancers is currently in phase IIa clinical trials [34,51,52].

Other modalities of peptide/protein administration have also been explored so far with more limited success. For example, the **buccal administration**, offers the possibility of avoiding the first-pass effect, being also this environment almost free from the acidity and protease activity. However, its restrictive epithelium, low surface absorption area and the constant flow of saliva are detrimental to drug bioavailability [42]. In particular, insulin-loaded PEG-b-PLA nanoparticles embedded into a chitosan film were shown to increase the insulin permeation compared to pure insulin *ex vivo* administered [53,54]. Also, an insulin-loaded formulation consisting of phospholipid deformable vesicles with sodium deoxycholate, exhibited 15.6 % of relative pharmacological bioavailability (vs subcutaneous) when buccally administered to rabbits [55].

On the other hand, the **pulmonary modality of administration** has attracted particular attention due to the huge surface area and high vascularization of the pulmonary mucosa as well as to the highly permeable blood-alveolar barrier. Because of this, two insulin formulations have already been commercialized, one of them withdrawn from the market in a short time [56]. In view of this, some authors have considered that the encapsulation of peptides within nanocarriers may help to overcome the limitations of the simple powders or solutions that reached the market [42,43]. Nanocarriers such as liposomes and chitosan-based nanoparticles have been investigated for pulmonary delivery of different

drugs, such as insulin, calcitonin, leuprolide, enzymes, cytokines and cyclosporine A [57–62]. For example, Al-Qadi et al. demonstrated a pronounced hypoglycemic effect in normal rats after intratracheal administration of a powder consisting of chitosan nanoparticles encapsulated in mannitol [57]. Similarly, Trapani et al., developed heparin-loaded chitosan-based nanoparticles able to deliver the peptide to the lungs *in vivo* to treat thromboembolic disorders [63]. Finally, in this area it should be highlighted the development of a cyclosporine A liposomal formulation currently in phase II clinical trials. The inhalation of this formulation notably improved the pharmacokinetics of the peptide without showing any side effect [64,65].

Our group has devoted significant efforts to the **nasal administration** of peptides (i.e. insulin and calcitonin) [66–68] and protein antigens [69,70]. Compared to other types of epithelia, the nasal epithelium is rather porous and allows the transport of relatively large molecules. However, the nasal delivery of peptides/proteins is hampered by the efficient mucociliary clearance existing in the nasal cavity, which also results in a high physiological variability [43,71]. We pioneered the development of chitosan nanoparticles specifically designed for nasal insulin delivery [67]. We have also investigated the potential of an array of nanocarriers made of PLGA-PEG and also of chitosan for the delivery of antigens, i.e. tetanus toxoid and hepatitis B [21,69–71]. Interestingly, phase II clinical studies have been reached for HIV immunity with a formulation containing four different anti-HIV peptides (Vacc-4x) using the Endocine™ technology (Eurocine Vaccines). The intranasal administration of this formulation, which involves solid lipid nanoparticles containing mono-olein and oleic acid, has successfully induced dose-dependent T cell responses, as well as both, mucosal and systemic humoral responses [72,73].

Other modalities of administration, i.e. the **ocular and dermal/transdermal routes** have been explored as potential ways to deliver peptide/protein drugs with the help of nanotechnology. For example, cationic liposomes containing super oxide dismutase were used to treat UV-induced skin damages *in vivo*, showing an enhanced transport of the protein through the skin when liposomes were coupled with iontophoresis [74]. On the other hand, antibodies, growth factors, cyclosporine A and antibiotics are just some examples of proteins and peptides delivered to the eye, following different modalities of administration. For example, a cyclosporine A topical microemulsion formulation was marketed in 2003 with interesting outcomes for the treatment of dry eye [75]. Examples of preliminary preclinical developments include bevacizumab-loaded liposomes associated to the protein annexin A5 [76] and bevacizumab-loaded chitosan nanoparticles, which showed an enhanced anti-angiogenic effect after they were intravitreally injected in rats [77].

## 3. Nanocarriers for oral protein/peptide delivery

Among the explored routes for peptide delivery, the oral administration is specially complicated by the fact that peptides are susceptible to suffering degradation processes due to the wide range of pHs along the gastrointestinal tract (from pH 1 in the stomach to pH 8 in certain parts of the small intestine), such as oxidation, deamination and hydrolysis. Furthermore they are well-known substrates for intestinal peptidases, which potentially causes their pre-systemic degradation [78,79]. Additionally, the high hydrophilicity and molecular weight of most of peptides impede their diffusion across the intestinal epithelium [1,80,81] either by passive diffusion [82] or paracellular transport [83,84].

Among the approaches explored in the last decades to improve the oral bioavailability of peptides and proteins, apart from the chemical modification, there are the inclusion of absorption enhancers and/or enzyme inhibitors in the formulation and the use of nanovehicles. In particular, biodegradable and biocompatible lipid- and polymer-based nanocarriers engineered through the combination of different lipids, polymers, surfactants and other excipients have emerged as promising delivery platforms to enable the administration of these macromolecules [38,39,47,85]. *Figure 3* and *Figure 4* respectively illustrate a broad classification of the most investigated nanocarriers for oral peptide delivery and the trend of reported experimental works with *in vivo* results in this regard in the last 5 years. Within this frame, the general idea consists of protecting peptides and proteins from the aggressive environment which are going to be in contact with, through their efficient encapsulation or association to those nanocarriers. Additionally, they have to display proper mucoadhesion-mucodiffusion balance, control the peptide release at target sites and promote the peptide absorption [38,39]. In this regard, several properties have been identified as crucial to determine the appropriate fate and effect of the peptide-loaded nanosystems. Apart from the size, the particle surface properties (such as surface charge and hydrophobicity) have demonstrated to play a crucial role on the bioavailability of the loaded peptide, since they condition both, their interaction with the intestinal mucosa and the integrity of the encapsulated peptide [86–88]. For example, it has been proved that the incorporation of pegylated biomaterials to nanocarriers contributes to their stabilization (protection against enzymatic degradation and opsonization, and reduction of immunogenicity) and provides them with adequate mucodiffusion properties [88–90].

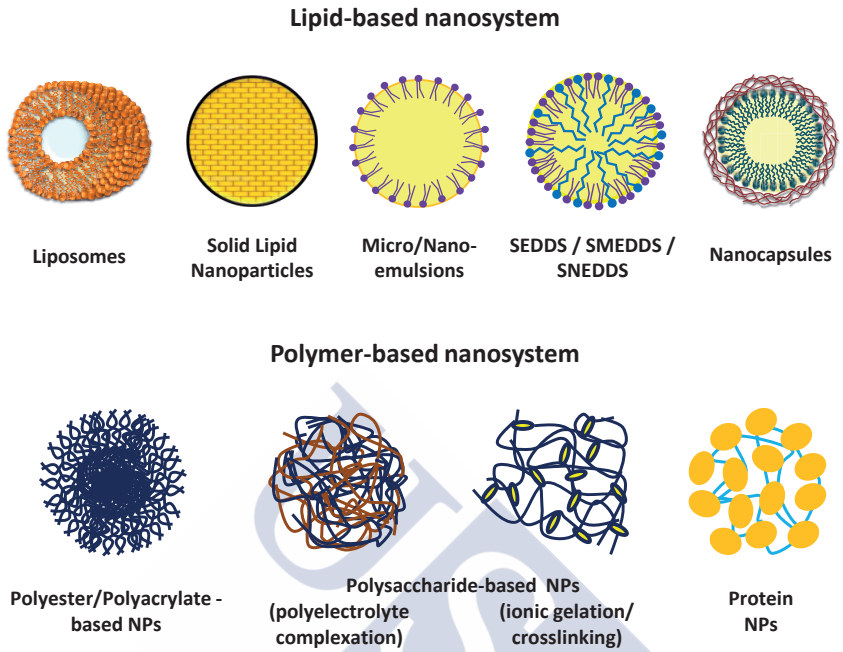



***Figure 3.*** *Illustration of the main lipid- and polymer-based nanosystems explored for oral protein/peptide delivery.* Adapted with permission from [38,39].

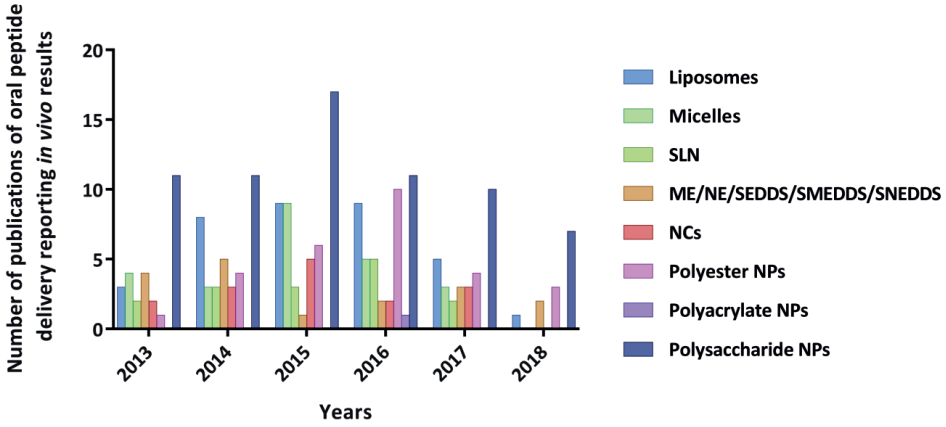



***Figure 4.*** *Trend of reported experimental works with in vivo results concerning nanocarriers for oral peptide/protein delivery in the last 5 years. Data taken from Scopus (2013–2018) using oral protein/peptide delivery, in vivo and the type of system as searching criteria. ME: microemulsion; NCs: nanocapsules; NE: nanoemulsion; NPs: nanoparticles; SEDDS: self-emulsified drug delivery system; SMEDDS: self-microemulsified drug delivery system; SNEDDS: self-nanoemulsified drug delivery system; SLN: solid lipid nanoparticles.*

So far there are only two marketed oral peptide formulations intended to achieve a systemic effect: Neoral® and DDAVP®. Neoral® is a microemulsion formulation containing the hydrophobic peptide cyclosporine A that was approved by the FDA in 1995 for the prophylactic treatment of organ rejection following organ transplant [91]. DDAVP®, approved by FDA in 1992, is a simple tablet formulation of desmopressin that has a very limited but sufficient bioavailability (0.1 %) [92]. The results of the clinical translation of the research efforts devoted in nanomedicine to facilitate the systemic delivery of peptide drugs are illustrated in *Table 1*. Within this frame, it is worth noting that a number of companies are currently working in advanced preclinical phases on nanoparticulate formulations for oral insulin delivery [93].

USC UNIVERSIDADE DE SANTIAGO DE COMPOSTELA

***Table 1.*** *Some selected examples of peptide delivery technologies currently in clinical trials for oral administration.*

| Peptide | Technology / Commercial name | Company / Partnership(s) | Status | Ref. |
|---|---|---|---|---|
| **Insulin** | GIPET® Technology (Gastrointestinal Permeation Enhancement Technology: absorption enhancers: medium chain fatty acids or derivatives) / tablet / capsule formulations | Novo Nordisk / Merrion Pharmaceuticals | Phase IIb | [94–96] |
| | NOD (Nanoparticle Oral Delivery: bioadhesive carbomer NPs with calcium phosphate core, PEG salts of fatty acids with an enteric coating (cellulose acetate phthalate)) / Nodlin™ | Shanghai Biolaxy Biomedical Science and Technology Co, Ltd. / NOD Pharmaceuticals, Inc | Phase I | [97,98] |
| | HDV–1 (Hepatic-Directed Vesicle insulin – Liver targeted liposomes: phospholipid bilayer vesicles with a proprietary hepatocyte-targeting molecule) / Enteric capsule | Diasome Pharma | Phase III | [99,100] |
| | Axcess™ Technology (GRAS aromatic alcohols as absorption enhancers and solubilizers / Capsulin™ (enteric capsule with dry powder) | Proxima Concepts Ltd / Diabetology Ltd | Phase IIb | [101–103] |
| | POD™ (Protein Oral Delivery – enzyme inhibitors, penetration enhancers) / ORMD–0801 (enteric capsule with oil powder) | Oramed Pharmaceuticals, Inc. | Phase IIb | [104,105] |
| | Oshadi ICP (proinsulin & C-peptide / silica-based NPs entrapped in a polysaccharide matrix) / Oil-based suspension | Oshadi Drug Administration Ltd | Phase II | [106] |
| | Alkylated PEG-insulin conjugate / Tregopil (IN–105 tablet form) | Biocon Ltd / Bristol-Myers Squibb | Phase II/III | [107,108] |

| Peptide | Technology / Commercial name | Company / Partnership(s) | Status | Ref. |
|---|---|---|---|---|
| **GLP1 analogs** | Axcess™ Technology (GRAS aromatic alcohols as absorption enhancers and solubilizers / Oral GLP-1 (enteric capsule with dry powder) | Proxima Concepts Ltd / Diabetology Ltd. | Phase I/IIa | [109] |
| | POD™ (Protein Oral Delivery – enzyme inhibitors, penetration enhancers) / ORMD-0901 (enteric capsule with oil powder) | Oramed Pharmaceuticals, Inc. | Phase Ib | [105] |
| | Eligen™ Technology (simple blending drug and penetration enhancers) | Emisphere Technologies Inc. / Novo Nordisk | Phase III | [110,111] |
| **Parathyroid hormone analog** | PEPTELLIGENCE® (protease inhibitor, absorption enhancer, enteric coating) / rhPTH(1-31)NH(2) enteric solid dosage form | Enteris BioPharma Inc. | Phase II | [112–114] |
| | POD™ (Protein Oral Delivery – enzyme inhibitors, penetration enhancers) / EB612 PTH 1-34 (enteric capsule with oil powder) | Entera Bio Ltd. / Oramed Pharmaceuticals, Inc. | Phase IIa | [115,116] |
| | POD™ (Protein Oral Delivery – enzyme inhibitors, penetration enhancers) / EB613 PTH 1-34 (enteric capsule with oil powder) | Entera Bio Ltd. / Oramed Pharmaceuticals, Inc. | Phase I/IIa | [115,117] |
| **Calcitonin** | Axcess™ Technology (GRAS aromatic alcohols as absorption enhancers and solubilizers / Capsitonin™ (enteric capsule with dry powder) | Proxima Concepts Ltd / Bone Medical Ltd. | Phase IIa | [103,118] |
| | PEPTELLIGENCE® (protease inhibitor, absorption enhancer, enteric coating) / TBRIA™- Oracal®: enteric solid dosage form | Enteris BioPharma Inc. / Tarsa Therapeutics Inc. | Phase II/III | [119–121] |

| Peptide | Technology / Commercial name | Company / Partnership(s) | Status | Ref. |
|---|---|---|---|---|
| **Kappa Opioid Agonist** | PEPTELLIGENCE® (protease inhibitor, absorption enhancer, enteric coating) / KORSUVA™ enteric solid dosage form | Enteris BioPharma Inc. / Cara Therapeutics | Phase IIb | [120,122, 123] |
| **Leuprolide** | PEPTELLIGENCE® (protease inhibitor, absorption enhancer, enteric coating) / OVAREST® enteric solid dosage form | Enteris BioPharma Inc. | Phase IIa | [120,124, 125] |
| **Octreotide** | TPE (Transient Permeability Enhancer: permeation enhancers) / Capsule containing oily suspension of solid hydrophilic microparticles | Chiasma Inc. | Phase III | [126,127] |

## 4. The specific case of insulin

### 4.1. The origin and variants of insulin currently available

Insulin was discovered in 1921-1922 by Frederick Grant Banting, Charles Best, James Collip and John James Rickard Macleod at the University of Toronto, being Banting and Macleod awarded with the Nobel Prize in Physiology or Medicine in 1923 [128]. Insulin derived from animals was used for the diabetes treatment during the first decades after being discovered. It was not until 1978, when Genetech Inc. produced synthetic "human" insulin by using recombinant DNA techniques, becoming insulin the first human protein biotechnologically manufactured. In the 80's, Eli Lilly started to commercialize synthetic human insulin (Humulin®) [129]. Human Insulin is a hormone (Mw 5.808 kDa) consisting of 51 amino acids divided into two polypeptide chains of 21 (A chain) and 30 (B chain) amino acids, which are bonded by disulfide bridges (*Figure 5*) [130].

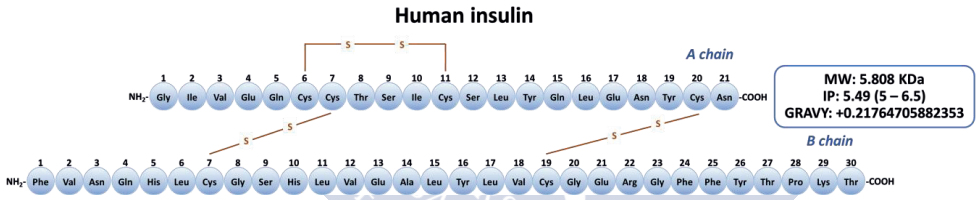



***Figure 5.*** *Amino acid sequence of human insulin.*

Numerous variants of insulin have been produced with the idea of modifying its pharmacokinetic profile *(Section 4.2.)*. Within the context of this thesis we have used insulin glulisine and a hydrophobically-modified insulin (HM-insulin), whose structure is illustrated in *Figure 6*. Insulin glulisine is a modified rapid acting insulin (change in two aminoacids) commercialized as Apidra®. This insulin differs from human insulin in the amino acids present at the positions 3 and 29 of its B chain, where asparagine and lysine were respectively replaced by lysine and glutamic acid. This change in the amino acid composition has been found to facilitate the dissociation of insulin hexamers into dimers and monomers, thereby eliciting a fast action upon injection. The HM-insulin is a variant still not commercialized that presents the following differences respect to the human insulin: i) the amino located at the positions 1 (glycine), 8 (threonine), 15 (glutamine), 18 and 21 (asparagines) of its A chain, were respectively replaced by arginine, histidine, glutamic acid, aspartic acid and glycine; ii) two arginine residues were added to the –COOH end of the B chain.

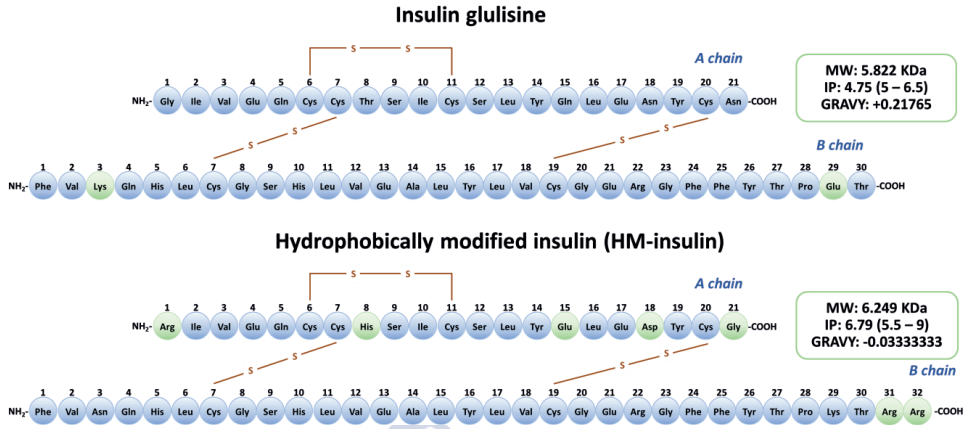



***Figure 6.*** *Amino acid sequence of insulin glulisine (upper panel) and the hydrophobically-modified insulin (lower panel). Differences respect to the human insulin are represented in green.*

## 4.2. Pharmacokinetics and pharmacodynamics of insulin

Insulin plays a crucial role in the blood glucose homeostasis. The glucose coming from the degradation of ingested carbohydrates raises the glucose on blood through its intestinal absorption. High blood glucose levels lead to the insulin secretion from the pancreas into the blood stream. Then, the secreted insulin binds to its cell surface receptors triggering the activation of several protein cascades through which, the uptake, use and storage of glucose from the target tissues (i.e., liver, muscles and adipose tissue) is promoted (*Figure 7*) [131].

Diabetes mellitus is a chronic metabolic disorder in which either the pancreas is not able to produce enough insulin (type 1 diabetes – autoimmune reaction against insulin-producing pancreatic β–cells) or the body cannot use it properly (type 2 diabetes – developing insulin resistance) (*Figure 7*). An imbalanced food metabolism is produced as a consequence of both phenomena, resulting in a hyperglycemia state (blood glucose accumulation), which causes damage and failure of several organs and tissues and triggers pathological conditions (i.e. nephropathy, neuropathy, retinopathy, blindness and cardiovascular complications) as time goes by.

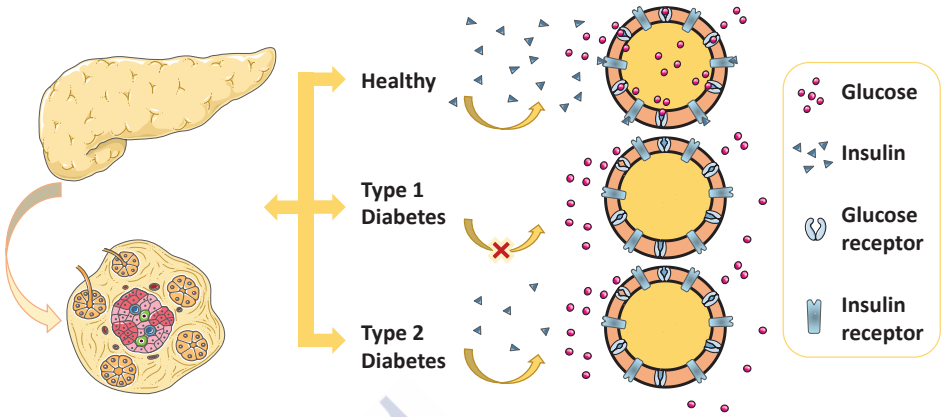



***Figure 7.*** *Schematic illustration of the physiological function of insulin on glucose uptake and metabolism.* ***A)*** *Healthy: after the binding of the released insulin to its receptor, protein activation cascades (including translocation of GLUT–2 to the plasma membrane), influx of glucose and synthesis of glycogen are induced;* ***B)*** *Type 1 Diabetes: there is no released insulin;* ***C)*** *Type 2 Diabetes: released insulin is not able to bind its receptors.* Pancreas, Islet of Langerhans and cells (*https://creativecommons.org/licenses/by/3.0/*) have been modified from the original work provided by Servier Medical Art (*http://smart.servier.com/*).

Currently, the main approach for treating both diabetes types consists of fighting the hyperglycemia symptoms, being the insulin replacement therapy the choice for the majority of patients with type 1 diabetes and a considerable percentage of type 2 patients [132]. This treatment consists almost entirely of the administration of different insulin formulations via subcutaneous injection. These marketed insulin formulations can be widely classified in the following four categories as a function of the time in which its maximum concentration in bloodstream is achieved and the duration of its action (*Figure 7*) [131–134]:

*i)* Rapid-acting insulin (Humalog®, Novolog® and Apidra®): is rapidly absorbed and displayed short action due to the fast dissociation of its hexamers into dimers and monomers.

*ii)* Regular or short-acting insulin (Humulin®R and Novolin®R): its action starts 2–3 post-injection and acts from 3 to 6 hours.

*iii)* Intermediate-acting insulin (Humulin N® and Lente insulins): the maximum insulin concentration in plasma is obtained from 4 to 12 hours post-injection and disappearing before 24 hours.

*iv)* Long-acting insulin (Ultralente insulins, Lantus® and Levemir®): are the analogs that attempt to mimic the human basal insulin secretion, obtaining a low level of insulin in the bloodstream throughout the day.

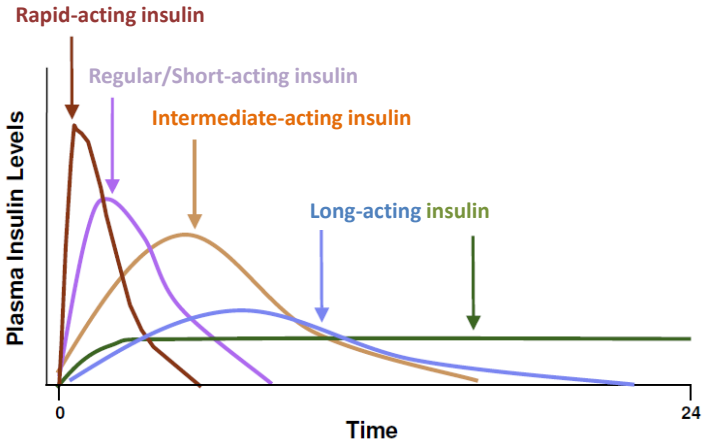



***Figure 7:*** *Plasma levels profiles of human insulin and analogues. Adapted with permission from* [134].

## 4.3. The need of an oral insulin

According to the International Diabetes Federation, 425 million people worldwide are diagnosed with diabetes and this number is expected to rise to 629 million by 2045 (*Figure 7*) [135]. As commented above, the current diabetes therapies are almost entirely based on the administration of subcutaneous insulin formulations [131–134]. However, the drawbacks associated with injections in chronic treatments, especially the discomfort for the patients, and thus their lack of compliance, make the alternative use of non-invasive routes a preferred objective in the recent decades [1].

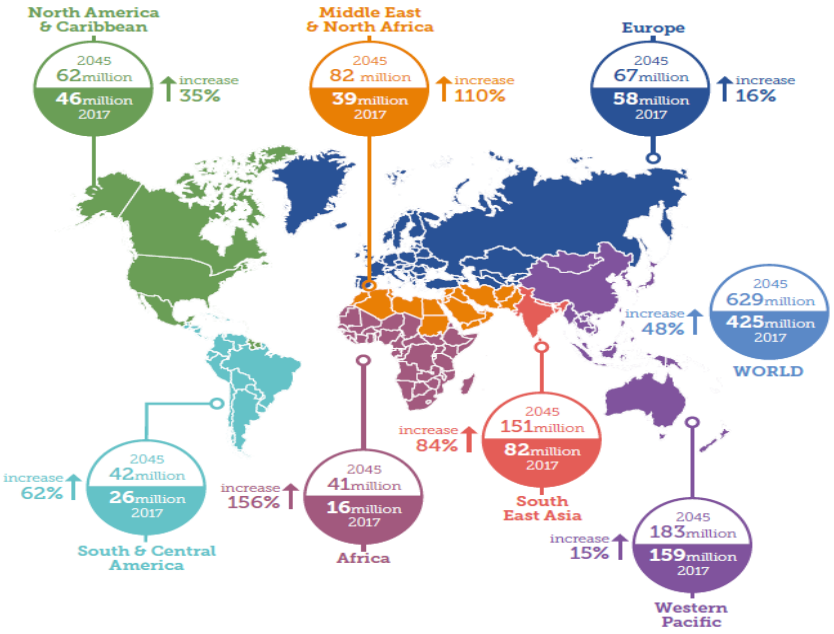



***Figure 7.*** *Number of people with diabetes worldwide and per region in 2017 and expected for 2045 (20–79 years). Reused with permission from* [135].

The alternative insulin administration route has been extensively researched since its discovery in 1921 [133,136]. Indeed, the first oral insulin pilot study in human was conducted in 1923 by G. A. Harrison [137]. Those results brought to light two important obstacles to overcome in order to make this challenge possible: the low bioavailability of insulin through this route and an enormous intra-subject variability. Since that time until now numerous technologies, some of which have reached the market, have been explored for its administration through different modalities of administration. For example, AFREZZA® (Technosphere® technology - Mannkind Corporation) [138–140] and Oral-Lyn™ (RapidMist™ technology - Generex Biotechnology Corporation) [141,142], are respectively commercialized in some countries as inhalable (dry powder) and buccal human insulin formulations. However, irrespective of the potential of other routes of administration, the oral route is particularly advantageous. First, because it is the one preferred by patients, and also because this modality of administration would mimic the pathway of the physiologically secreted insulin. Thus, the direct entrance of the insulin into the liver through the portal circulation, would avoid its previous distribution in the systemic circulation [143]. For this reason, insulin has been a molecule of choice for the validation of the utility of nanosystems for the oral delivery of peptides and proteins (*Table 1, Section 3*). To summarize the efforts oriented towards the development of an

oral insulin, we present in *Table 2* a summary of the work reported in the last 5 years with the highlight of the insulin bioavailability of its response. It is important to remark that the majority (approx. 90%) of the literature dealing with oral insulin delivery carriers do not report the results of the *in vivo* administration. This limited information raises the question about whether these previous reports consciously omit the *in vivo* work or lack of such information. Overall, the results presented in this table lead to a number of conclusions:

*i)* The differences in the followed *in vivo* experimental protocols make difficult the comparison among the different works. The majority of the studies were performed in diabetic rats, where the lack of auto-regulation phenomenon suppressing the secretion of endogenous insulin and the β−cell deficiency makes these animals more insulin-sensitive [13,144].

*ii)* Both, the pharmacodymanic (pharmacological availability (PA)) and pharmacokinectic (bioavailability (BA)) reported values are very variable, ranging PA from 0.3 to 18.2 % and BA from 0.4 to 33 %.

*iii)* The data reported do not generally provide a good understanding of these variable responses. This might be related on the one hand to the commonly used streptozocin model, which usually leads to different degrees of β−cell deficiency and, hence, very variable glycemic responses (PA) and, on the other hand to the difficulties associated to the *in vivo* quantification of insulin (BA). Also the non-expected correlation between the PK-PD responses, based on the insulin mechanism of action, could contribute to this variability.

Overall, despite all the efforts made until now and the progress achieved towards the clinical translation of this research (*Table 1*), the two main challenges found by Harris in 1923 (low bioavailability and high variability) continue still being the bottleneck limiting the efficient administration of insulin by oral route.

***Table 2.*** *Some selected examples of in vivo results involving nanocarriers for oral insulin administration published in the last 5 years (sorted from most to least recent).*

| DELIVERY SYSTEM | *IN VIVO* MODEL (animal specie, healthy / disease) | RESPONSE | | REF |
|---|---|---|---|---|
| | | ↓GLYCEMIA (others response specified when applicable) | BA or PA | |
| PEG-PGA enveloped octaargine nanocomplexes | Healthy rats | 20 % (5-7 h) | | [145] |
| Glycyl-glycine and alanyl-alanine conjugates of CS and TMCS NPs | Diabetic rats $_{anesthetized}$ | 35-50 % (7.5 h) | BA = 15.5-17.2 % | [146] |
| Deoxycholic acid-modified CS PGA NPs | Diabetic rats | 35-50 % (12 h) | BA = 7.2-15.9 % | [147] |
| PLGA-DSPE-PEG octaarginine NPs | Diabetic rats | 10-30 % (3 h) | BA = 2.6-6 % | [148] |
| PARG NCs | Healthy rats | 20-35 % (2-6 h) | PA = 0.7-2.1 % | [27] |
| PLGA-Gambogic acid nanoconjugates | Healthy rats | 40 -120 µIU/mL blood insulin (6-20h) | BA = 17-33 % | [149] |
| Polysialic-protamine/protamine NCs | Healthy rats | 10-20 % (1-3 h) | | [26] |
| Tween 61, CH, dicetyl phosphate, sodium cholate niosomes | Diabetic mice | 66-75 % (12 h) | | [150] |
| Vitamin B12-CS functionalized layer by layer calcium phosphate NPs | Healthy rats | 198-321 mg/dL blood insulin (12 h) | BA = 6.3-26.9 % | [151] |
| Transferring/PLGA-coated poly(ester amide) NPs | Diabetic mice | 5-40 % (4 h) | PA = 0.9-7.8 % | [152] |
| Carbopol 934, pectin, SCMC, EC mucoadhesive polymeric device | Healthy rats $_{anesthetized}$ | 25-68 % (5 h) | PA = 1.8-6.5 %; BA = 1.2-3.3 % | [153] |
| Bacterial cellulose-g-poly/acrylic acid hydrogel MPs | Diabetic rats | 40 % (5 h) | BA = 0.6-7.5 % | [154] |
| Dextran-PLGA diblock copolymer Nano-polymersomes | Diabetic rats | 75 % (9 h) | BA = 0.6-9.8 % | [155] |

| DELIVERY SYSTEM | *IN VIVO* MODEL (animal specie, healthy / disease) | RESPONSE | | REF |
|---|---|---|---|---|
| | | ↓GLYCEMIA (others response specified when applicable) | BA or PA | |
| TMCS, N-(2-hydroxypropyl) methacrylamide copolymer NPs | Diabetic rats | 40 % (4 h) | PA = 1.4-8.6 % | [156] |
| Lipoid S75, CS, lecithin NPs | Diabetic rats | 50-65 % (4h) | PA = 0.5-6.0 % | [157] |
| Carboxymethyl CS, CS nanogels | Diabetic rats | 68-80 % (5 h) | | [158] |
| Stearylated CPPs modified PLGA NPs | Healthy rats | 47-63 % (4-8h) | PA = 4.6-14.7 % / BA = 6-19.1 % | [159] |
| TMC coated PLGA–mPEG NPs | Diabetic rats | 26-44 % (4 h) | BA = 3.1-7.58 % | [160] |
| CPP-modified CS-PLGA-PVA NPs | Diabetic rats | 20-35 % (8 h) | | [161] |
| PLGA-PVA-lecithin SLN | Diabetic rats$_{anesthetized}$ | | BA = 1.7-8.3 % | [162] |
| Surfactin (bacterial lipopeptide) heteropolymers | Diabetic mice / Healthy Beagle dogs | 16-55 % (2-24 h) | PA = 6-12.5 % | [163] |
| CS-insulin reverse micelles | Diabetic rats | 30 % (3-12 h) | | [164] |
| CS-insulin reverse micelles suspension in W/O emulsion | Diabetic rats | 34-37 % (4-8 h) | | [165] |
| pHPMA derivatives coated Insulin-CPP NPs | Diabetic rats | 50 % (4-10 h) | PA = 2.6-6.6 % / BA = 1.5-3 % | [166] |
| PLGA-PEG- Concanavalin A NPs | Diabetic rats | 61 % (1-24 h) | | [167] |
| Poly-l-lysine – PEG-PVA-TPP NPs | Diabetic rats | 49 % (3-12 h) | BA = 3.8-7.1 % | [168] |
| Octaarginine and derivatives-insulin nanocomplex | Diabetic rats | 15-51 % (3 h) | | [169] |

| DELIVERY SYSTEM | *IN VIVO* MODEL (animal specie, healthy / disease) | RESPONSE | | REF |
|---|---|---|---|---|
| | | ↓GLYCEMIA (others response specified when applicable) | BA or PA | |
| CS-alginate NPs | Diabetic mice | 104-143 mg/dL blood insulin (7 h) | BA = 8.11 % | [170] |
| Sodium oleate-PLGA NPs in Eudragit® FS 30D microcapsules | Diabetic rats | 22-32 % (2-8 h) | | [171] |
| N-Arginine-CS and N-histidine-CS polyelectrolyte complexes | Diabetic rats | | PA = 1.1-5.4 % | [172] |
| Sterols, SPC, dipalmitoylphosphatidylglycerol liposomes | Healthy rats | 25-50 % (3-10 h) | | [173] |
| L-Valine- PLGA NPs | Diabetic rabbits | 55 % (12 h) | | [174] |
| TPGS-PEG-PLGA NPs | Diabetic rats | 51-60 % (6-12 h) | | [175] |
| PLGA- SPC-DSPE-PEG NPs/MPs | Diabetic rats | 50 % (12-24 h) | BA = 12.2 % | [176] |
| Diethylene triamine pentaacetic acid dianhydride, sodium bicarbonate, sodium dodecyl sulfate - Self-assembling bubble carrier | Diabetic rats | 30-50 % (6-10 h) | BA = 11-22 % | [177] |
| Vitamin B12, poloxamer 407, lecithin, glyceryl palmitostearate, Solutol HS 15 gel-core SLN | Diabetic rats $_{anesthetized}$ | 10-60 % (6-12 h) | PA = 3-9 % | [178] |
| TMCS-PLGA NPs | Diabetic rats | 14-35 % (10-12 h) | PA = 6-12 % | [179] |
| Deoxycholic acid conjugated PEG-polyhydroxybutyrate co-polymeric NPs | Diabetic rats | 60-75 % (12 h) | BA = 12 % | [180] |
| Alginate–dextran sulfate NPs | Diabetic rats | 43 % (3 h) | | [181] |
| CS-TPP/Mannitol NPs | Diabetic rats | 70 % (5 h) | | [182] |

| DELIVERY SYSTEM | *IN VIVO* MODEL (animal specie, healthy / disease) | RESPONSE | | REF |
|---|---|---|---|---|
| | | ↓GLYCEMIA (others response specified when applicable) | BA or PA | |
| CS/Thiomalyl CS-TPP NPs | Diabetic rats | 35 % (5 h) | PA = 1.5 % | [183] |
| Globell cell targeting peptide TMCS-TPP NPs dodecylamine-graft-g-PGA micelles | Diabetic rats | 30-49 % (3-4 h) | BA = 3-7 % | [184] |
| Folic Acid Functionalized PAA, PAH, PS, CH, stearylamine liposomes | Diabetic rats | 15-75 % (6 h) | PA = 2.5-19.2 % / BA = 3.1-19.3 % | [185] |
| Chondroitin sulfate-capped gold NPs | Diabetic rats | 32.1 % (1 h) | | [186] |
| Eudragit, paraffin, Span 60 MPs | Diabetic rats | 15-36 % (12 h) | | [187] |
| Insulin–SPC, mannitol, metoprolol capric acid triglycerid, glyceryl monocaprate, SNEDDS | Healthy rats | 10-38 % (3 h) | PA = 1.0-2.5 % / BA = 0.4 % | [188] |
| SPC-bile salts liposomes | Healthy rats | 2-7 µIU/mL blood insulin (1 h) | | [189] |
| CPPs-insulin solution mixture | Healthy mice $_{anesthetized}$ | 34 % (6 h) | PA = 1.8-18.2 % | [190] |
| CS/thiolated CS – insulin conjugates | Healthy rats | 10-140 µIU/L blood insulin (2 h) | BA = 0.6-15.3 % | [191] |
| Biotin-DSPE, SPC liposomes | Diabetic rats | 30-44 % (12h) | PA = 6.4-12.1 % / BA = 3.3-8.3 % | [192] |
| CS-PGA conjugated with ethylene glycol tetraacetic acid NPs | Diabetic rats | *Plasma levels. *Suppression of the rise of blood glucose (OGTT) | BA = 17.8 % | [193] |
| CS-PGA conjugated with ethylene glycol tetraacetic acid NPs | Diabetic rats | *Plasma levels and increase of rat insulin and glucagon; *Suppression of the rise of blood glucose (OGTT) | | [194] |
| FcRn-targeted PLA-PEG NPs | FcRn knockout mice | 10-50 % (10 h) | | [195] |

| DELIVERY SYSTEM | *IN VIVO* MODEL (animal specie, healthy / disease) | RESPONSE | | REF |
|---|---|---|---|---|
| | | ↓GLYCEMIA (others response specified when applicable) | BA or PA | |
| PEG-protamine crosslinked conjugate | Healthy rats | 71 % (10 h) | PA = 7.1 % | [196] |
| Poly-hydroxyethyl-aspartamide copolymers nanoaggregates | Healthy rats | 30 % (4 h) | | [197] |
| Eudragit-PEG300 / Eudragit-glycofurol NPs | Healthy rats | 25 % (2 h) | PA = 0.3-1.4 % | [198] |
| Octaarginine- Maleimide-PEG-PLGA NPs | Healthy rats $_{anesthetized}$ | 15-45 % (5-6) h | PA = 3-11.1 % / BA = 3-14 % | [199] |
| Antiacid-PLGA NPs | Diabetic/Healthy rats | 4.5 µIU/mL blood insulin (24 h) | | [200] |
| Pluronic F127 coated-CS-TPP NPs | Diabetic rats | 30-50 % (8-12h) | BA = 3.7-7.8 % | [201] |
| PLA-Pluronic P85 – PLA copolymer NPs | Diabetic mice | 60-85 % (2.5 h) | | [202] |
| CS-Eudragit-coated glutaraldehyde amphiphillic hollow carbon nanospheres | Diabetic rats | 33 % (4 h) | | [203] |
| CS-PGA conjugated with ethylene glycol tetraacetic acid NPs | Diabetic rats | 50 % (6-12 h) | BA = 21.3 % | [204] |

*BA: bioavailability; CH: cholesterol; CPPs: cell penetrating peptides; CS: chitosan; DSPE-PEG: 1,2-distearoyl-sn-glycero-3-phosphoethanol- amine-N-methoxy(polyethyleneglycol)-2000; EC: ethyl cellulose; MPs: microparticles; NCs: nanocapsules; NPs: nanoparticles; OGTT: oral glucose tolerance test; PA: pharmacological availability; PAH: poly(allyl amine) hydrochloride; PARG: polyarginine; PC: phosphatidylcholine; PEG: polyethyleneglycol; PGA: polyglutamic acid; pHPMA: N-(2-hydroxypropyl) methacrylamide copolymer; PLA: Poly(lactic acid); PLGA: Poly(lactic-co-glycolic acid); PVA: Polyvinyl alcohol; REF: reference; SCMC: sodium carboxymethylcellulose; SNEDDS: self-nanoemulsifying drug delivery systems; SLN: solid lipid nanoparticles; SPC: soybean phosphatidylcholine; TMCS: trimethyl CS; TPGS: d-α-tocopherol poly(ethylene glycol) 1000 succinate; TPP: tripolyphosphate; *Significant.*

## 5. Conclusions and perspectives

Overall, despite of the efforts made so far to develop nanocarriers for oral peptide delivery, more knowledge is still required in order to make significant progress in this field. Although several peptide-loaded nanoformulations are undergoing clinical trials, most of the studies reported so far have been based on trial and error approaches and minor emphasis has been put into a rational design. This is probably due to the still limited understanding of the interaction of nanocarriers with the biological barriers. This fact might be the reason of the variability and lack of reproducibility reported so far in *in vivo* studies. Overall, this information highlights the need of comprehensive techniques to evaluate the interaction of the formulations with the biological barriers in a systematic way.

Generally, the background literature suggests that, through the use of the nanotechnology and the combination of different excipients, the final goal of improving the delivery of macromolecules across the intestinal barrier is possible. The opportunity to materialize this background knowledge in a nanoformulation able to carefully accomplish the critical parameters for oral peptide delivery (such as adequate size, charge and surface properties, stability in biorelevant media, efficient peptide loading, good mucoadhesion/mucodiffusion balance, proper interaction with the target cells and adequate *in vivo* efficacy) has been the main basis for the idea behind this thesis work.

This brief introduction is complementary to the *Chapter 1* of this thesis entitled "*Advances on the formulation of proteins using nanotechnologies based on lipidic materials*", which is part of a recently published review [38]. Some of the information here disclosed has been either adapted or literally extracted from it with permission.

## References


[1] S. Mitragotri, P.A. Burke, R. Langer, Overcoming the challenges in administering biopharmaceuticals: formulation and delivery strategies, Nat Rev Drug Discov. 13 (2014) 655–672. doi:10.1038/nrd4363.

[2] J.M. Reichert, Antibodies to watch in 2017, MAbs. 9 (2017) 167–181. doi:10.1080/19420862.2016.1269580.

[3] K. Fosgerau, T. Hoffmann, Peptide therapeutics: Current status and future directions, Drug Discov. Today. 20 (2015) 122–128. doi:10.1016/j.drudis.2014.10.003.

[4] D.S. Pisal, M.P. Kosloski, S. V. Balu-Iyler, Delivery of therapeutic proteins, J. Pharm. Sci. 99 (2010) 2557–2575. doi:10.1002/jps.22054.

[5] C.F. Van Der Walle, O. Olejnik, An overview of the field of peptide and protein delivery, in: C.F. Van Der Walle (Ed.), Pept. Protein Deliv., First, Academic Press, 2011: pp. 1–22. doi:10.1016/b978-0-12-384935-9.10001-x.

[6] B.J. Bruno, G.D. Miller, C.S. Lim, Basics and recent advances in peptide and protein drug delivery, Ther. Deliv. 4 (2013) 1443–1467. doi:10.4155/tde.13.104.

[7] S.C. Yadav, A. Kumari, R. Yadav, Development of peptide and protein nanotherapeutics by nanoencapsulation and nanobioconjugation, Peptides. 32 (2011) 173–187. doi:10.1016/j.peptides.2010.10.003.

[8] F. Sousa, P. Castro, P. Fonte, P.J. Kennedy, M.T. Neves-Petersen, B. Sarmento, Nanoparticles for the delivery of therapeutic antibodies: Dogma or promising strategy?, Expert Opin. Drug Deliv. 00 (2017) 1–14. doi:10.1080/17425247.2017.1273345.

[9] K. Mg, Krenn V, F. Huebner, W. Wagner, Resch R, History and possible uses of nanomedicine based on nanoparticles and nanotechnological progress, J Nanomed Nanotechnol. 64172 (2015) 3362157–7439. doi:10.4172/2157-7439.1000336.

[10] G. Gregoriadis, P. Leathwood, B.E. Ryman, Enzyme entrapment in liposomes, FEBS Lett. 14 (1971) 95–99. doi:10.1016/0014-5793(71)80109-6.

[11] G. Gregoriadis, B.E. Ryman, Fate of protein containing liposomes injected into rats - An approach to the treatment of storage diseases, Eur. J. Biochem. 24 (1972) 485–491. doi:10.1111/j.1432-1033.1972.tb19710.x.

[12] G. Birrenbach, P.P. Speiser, Polymerized micelles and their use as adjuvants in immunology, J. Pharm. Sci. 65 (1976) 1763–1766. doi:10.1002/jps.2600651217.

[13] C. Damge, C. Michel, M. Aprahamian, P. Couvreur, New approach for oral administration of insulin with polyalkylcyanoacrylate nanocapsules as drug carrier, Diabetes. 37 (1988) 246–251. doi:10.2337/diab.37.2.246.

[14] S. Morel, M. Rosa Gasco, R. Cavalli, Incorporation in lipospheres of [D-Trp-6] LHRH, Int. J. Pharm. 105 (1994) R1–R3. doi:10.1016/0378-5173(94)90466-9.

[15] S. Morel, E. Ugazio, R. Cavalli, M.R. Gasco, Thymopentin in solid lipid nanoparticles, Int. J. Pharm. 132 (1996) 259–261.

[16] M.R. Gasco, Method for producing solid lipid microspheres having a narrow size distribution, US5250236, 1993.

[17] A. Sánchez, J. Vila-Jato, M.J. Alonso, Development of biodegradable microspheres and nanospheres

for the controlled release of cyclosporin A, Int. J. Pharm. 99 (1993) 263–273. doi:10.1016/0378-5173(93)90369-Q.

[18] P. Quellec, R. Gref, L. Perrin, E. Dellacherie, F. Sommer, J.M. Verbavatz, M.J. Alonso, Protein encapsulation within polyethylene glycol-coated nanospheres. I. Physicochemical characterization, J. Biomed. Mater. Res. 42 (1998) 45–54. doi:10.1002/(SICI)1097-4636(199810)42:1<45::AID-JBM7>3.0.CO;2-O.

[19] P. Calvo, C. Remuñán-López, J.L. Vila-Jato, M.J. Alonso, Novel hydrophilic chitosan-polyethylene oxide nanoparticles as protein carriers, J. Appl. Polym. Sci. 63 (1997) 125–132. doi:10.1002/(SICI)1097-4628(19970103)63:1<125::AID-APP13>3.0.CO;2-4.

[20] S. Vicente, B. Diaz-Freitas, M. Peleteiro, A. Sanchez, D.W. Pascual, A. Gonzalez-Fernandez, M.J. Alonso, A polymer/oil based nanovaccine as a single-dose immunization approach, PLoS One. 8 (2013) e62500. doi:10.1371/journal.pone.0062500.

[21] S. Vicente, M. Peleteiro, B. Díaz-Freitas, A. Sanchez, Á. González-Fernández, M.J. Alonso, Co-delivery of viral proteins and a TLR7 agonist from polysaccharide nanocapsules: a needle-free vaccination strategy, J. Control. Release. 172 (2013) 773–781. doi:10.1016/j.jconrel.2013.09.012.

[22] S. Vicente, M. Peleteiro, J.V. González-Aramundiz, B. Díaz-Freitas, S. Martínez-Pulgarín, J.I. Neissa, J.M. Escribano, A. Sanchez, Á. González-Fernández, M.J. Alonso, Highly versatile immunostimulating nanocapsules for specific immune potentiation, Nanomedicine (London). 9 (2014) 2273–2289. doi:10.2217/nnm.14.10.

[23] J. Crecente-Campo, S. Lorenzo-Abalde, A. Mora, J. Marzoa, N. Csaba, J. Blanco, Á. González-Fernández, M.J. Alonso, Bilayer polymeric nanocapsules: A formulation approach for a thermostable and adjuvanted E. coli antigen vaccine, J. Control. Release. 286 (2018) 20–32. doi:10.1016/j.jconrel.2018.07.018.

[24] J.V. González-Aramundiz, M. Peleteiro Olmedo, Á. González-Fernández, M.J. Alonso Fernández, N.S. Csaba, Protamine-based nanoparticles as new antigen delivery systems, Eur. J. Pharm. Biopharm. 97 (2015) 51–59. doi:10.1016/j.ejpb.2015.09.019.

[25] J.V. González-Aramundiz, E. Presas, I. Dalmau-Mena, S. Martínez-Pulgarín, C. Alonso, J.M. Escribano, M.J. Alonso, N.S. Csaba, Rational design of protamine nanocapsules as antigen delivery carriers, J. Control. Release. 245 (2017) 62–69. doi:10.1016/j.jconrel.2016.11.012.

[26] L.N. Thwala, A. Beloqui, N.S. Csaba, D. González-Touceda, S. Tovar, C. Dieguez, M.J. Alonso, V. Préat, The interaction of protamine nanocapsules with the intestinal epithelium: a mechanistic approach, J. Control. Release. 243 (2016) 109–120. doi:10.1016/j.jconrel.2016.10.002.

[27] Z. Niu, E. Tedesco, F. Benetti, A. Mabondzo, I.M. Montagner, I. Marigo, D. Gonzalez-Touceda, S. Tovar, C. Diéguez, M.J. Santander-Ortega, M.J. Alonso, Rational design of polyarginine nanocapsules intended to help peptides overcoming intestinal barriers, J. Control. Release. 263 (2016) 4–17. doi:10.1016/j.jconrel.2017.02.024.

[28] A. Gonzalez-Paredes, D. Torres, M.J. Alonso, Polyarginine nanocapsules: A versatile nanocarrier with potential in transmucosal drug delivery, Int. J. Pharm. 529 (2017) 474–485. doi:10.1016/j.ijpharm.2017.07.001.

[29] D. Heinemann, S. Kalies, M. Schomaker, W. Ertmer, H. Murua Escobar, H. Meyer, T. Ripken, Delivery of proteins to mammalian cells via gold nanoparticle mediated laser transfection, Nanotechnology. 25 (2014) 245101. doi:10.1088/0957-4484/25/24/245101.

[30] Q. Mu, F.M. Kievit, R.J. Kant, G. Lin, M. Jeon, M. Zhang, Anti-HER2/neu peptide-conjugated iron oxide nanoparticles for targeted delivery of paclitaxel to breast cancer cells, Naoscale. 7 (2015) 18010–18014. doi:10.1039/c5nr04867b.

[31] A. Antonucci, J. Kupis-Rozmyslowicz, A.A. Boghossian, Noncovalent protein and peptide functionalization of single-walled carbon nanotubes for biodelivery and optical sensing applications, ACS Appl. Mater. Interfaces. 9 (2017) 11321–11331. doi:10.1021/acsami.7b00810.

[32] B. Zeng, H. Shi, Y. Liu, A versatile pHresponsive platform for intracellular protein delivery using calcium phosphate nanoparticles, J. Mater. Chem. B. 3 (2015) 91159121. doi:10.1039/c5tb01760b.

[33] V. Weissig, T.K. Pettinger, N. Murdock, Nanopharmaceuticals (part 1): products on the market, Int. J. Nanomedicine. 9 (2014) 4357–4373. doi:10.2147/IJN.S46900.

[34] Nanomedicines Alliance, Nanomedicine drugs approved and in development, (2016). https://media.wix.com/ugd/310180_b313086a455a43d394eb370ba944af7c.pdf (accessed August 22, 2018).

[35] A. Hafner, J. Lovrić, G.P. Lakoš, I. Pepić, Nanotherapeutics in the EU: an overview on current state and future directions, Int. J. Nanomedicine. 9 (2014) 1005–1023. doi:10.2147/IJN.S55359.

[36] M. Yu, J. Wu, J. Shi, O.C. Farokhzad, Nanotechnology for protein delivery: overview and perspectives, J. Control. Release. 240 (2016) 24–37. doi:10.1016/j.jconrel.2015.10.012.

[37] N. Desai, Challenges in development of nanoparticle-based therapeutics, AAPS J. 14 (2012) 282–295. doi:10.1208/s12248-012-9339-4.

[38] I. Santalices, A. Gonella, D. Torres, M.J. Alonso, Advances on the formulation of proteins using nanotechnologies, J. Drug Deliv. Sci. Technol. 42 (2017) 155–180. doi:10.1016/j.jddst.2017.06.018.

[39] Z. Niu, I. Conejos-Sánchez, B.T. Griffin, C.M. O'Driscoll, M.J. Alonso, Lipid-based nanocarriers for oral peptide delivery, Adv. Drug Deliv. Rev. 106 (2016) 337–354. doi:10.1016/j.addr.2016.04.001.

[40] E. Samaridou, M.J. Alonso, Nose-to-brain peptide delivery – The potential of nanotechnology, Bioorg. Med. Chem. 26 (2018) 2888–2905. doi:10.1016/j.bmc.2017.11.001.

[41] M.R. Villegas, A. Baeza, M.V. Regí, Nanotechnological strategies for protein delivery, Molecules. 23 (2018) 1008. doi:10.3390/molecules23051008.

[42] J.O. Morales, K.R. Fathe, A. Brunaugh, S. Ferrati, S. Li, M. Montenegro-Nicolini, Z. Mousavikhamene, J.T. McConville, M.R. Prausnitz, H.D.C. Smyth, Challenges and future prospects for the delivery of biologics: oral mucosal, pulmonary, and transdermal routes, AAPS J. 19 (2017) 652–668. doi:10.1208/s12248-017-0054-z.

[43] L.N. Thwala, V. Préat, N.S. Csaba, Emerging delivery platforms for mucosal administration of biopharmaceuticals: a critical update on nasal, pulmonary and oral routes, Expert Opin. Drug Deliv. 14 (2017) 23–36. doi:10.1080/17425247.2016.1206074.

[44] A.L. Lewis, J. Richard, Challenges in the delivery of peptide drugs: an industry perspective, Ther. Deliv. 6 (2015) 149–163. doi:10.4155/tde.14.111.

[45] L.N. Hassani, A. Lewis, J. Richard, Oral peptide delivery: technology landscape & current status, OnDrugDelivery. 59 (2015) 12–17.

[46] E. Moroz, S. Matoori, J.C. Leroux, Oral delivery of macromolecular drugs: where we are after almost 100 years of attempts, Adv. Drug Deliv. Rev. 101 (2016) 108–121. doi:10.1016/j.addr.2016.01.010.

[47] T.A.S. Aguirre, D. Teijeiro-Osorio, M. Rosa, I.S. Coulter, M.J. Alonso, D.J. Brayden, Current status of

selected oral peptide technologies in advanced preclinical development and in clinical trials, Adv. Drug Deliv. Rev. 106 (2016) 223–241. doi:10.1016/j.addr.2016.02.004.

[48] A. Patel, K. Cholkar, A.K. Mitra, Recent developments in protein and peptide parenteral delivery approaches, Ther. Deliv. 5 (2014) 337–365. doi:10.4155/tde.14.5.

[49] C. Herzog, K. Hartmann, V. Künzi, O. Kürsteiner, R. Mischler, H. Lazar, R. Glück, Eleven years of Inflexal® V-a virosomal adjuvanted influenza vaccine, Vaccine. 27 (2009) 4381–4387. doi:10.1016/j.vaccine.2009.05.029.

[50] J.E. Frampton, P.M. Anderson, A.J. Chou, N.C. Federman, S. Ferrari, H.J. Kim, LoebD.M., K. Mori, Mifamurtide: a review of its use in the treatment of osteosarcoma, Pediatr. Drugs. 12 (2010) 141–153. doi:10.2165/11204910-000000000-00000.

[51] ClinicalTrials.gov, An Open-Label, Phase I, Escalating Dose Study to Evaluate the Safety, Tolerability, and Pharmacodynamics of PDS0101, (2014). https://clinicaltrials.gov/ct2/show/record/NCT02065973?term=PDS0101&rank=1 (accessed August 22, 2018).

[52] Pipeline - PDS Biotechnology, (n.d.). http://pdsbiotech.com/technology/pipeline/ (accessed September 9, 2018).

[53] C. Giovino, I. Ayensu, J. Tetteh, J.S. Boateng, Development and characterisation of chitosan films impregnated with insulin loaded PEG-b-PLA nanoparticles (NPs): a potential approach for buccal delivery of macromolecules, Int. J. Pharm. 428 (2012) 143–151. doi:10.1016/j.ijpharm.2012.02.035.

[54] C. Giovino, I. Ayensu, J. Tetteh, J.S. Boateng, An integrated buccal delivery system combining chitosan films impregnated with peptide loaded PEG-b-PLA nanoparticles, Colloids Surfaces B Biointerfaces. 112 (2013) 9–15. doi:10.1016/j.colsurfb.2013.07.019.

[55] T. Yang, X. Wang, X. Yan, Q. Zhang, Phospholipid Deformable Vesicles for Buccal Delivery of Insulin, Chem. Pharm. Bull. (Tokyo). 50 (2002) 749–753. doi:10.1248/cpb.50.749.

[56] J.-L. Sélam, Inhaled insulin: promises and concerns, J. Diabetes Sci. Technol. 2 (2008) 311–315. doi:10.1177/193229680800200225.

[57] S. Al-Qadi, A. Grenha, D. Carrión-Recio, B. Seijo, C. Remuñán-López, Microencapsulated chitosan nanoparticles for pulmonary protein delivery: In vivo evaluation of insulin-loaded formulations, J. Control. Release. 157 (2012) 383–390. doi:10.1016/j.jconrel.2011.08.008.

[58] H. Yamamoto, Y. Kuno, S. Sugimoto, H. Takeuchi, Y. Kawashima, Surface-modified PLGA nanosphere with chitosan improved pulmonary delivery of calcitonin by mucoadhesion and opening of the intercellular tight junctions, J. Control. Release. 102 (2005) 373–381. doi:10.1016/j.jconrel.2004.10.010.

[59] M. Kaipel, A. Wagner, E. Wassermann, K. Vorauer-Uhl, R. Kellner, H. Redl, H. Katinger, R. Ullrich, Increased biological half-life of aerosolized liposomal recombinant human Cu/Zn superoxide dismutase in pigs, J. Aerosol Med. Pulm. Drug Deliv. 21 (2008) 281–290. doi:10.1089/jamp.2007.0667.

[60] K.M. Skubitz, P.M. Anderson, Inhalational interleukin-2 liposomes for pulmonary metastases: a phase I clinical trial, Anticancer. Drugs. 11 (2000) 555–563. doi:10.1097/00001813-200008000-00006.

[61] B. Gilbert, C. Knight, F. Alvarez, J. Waldrep, J. Rodarte, V. Knite, W. Eschenbacher, Tolerance of volunteers to cyclosporine A-dilauroylphosphatidylcholine liposome aerosol, Am. J. Respir. Crit. Care

Med. 156 (1997) 1789–1793. doi:10.1164/ajrccm.156.6.9702101.

[62] A. Shahiwala, A. Misra, A preliminary pharmacokinetic study of liposomal leuprolide dry powder inhaler: a technical note, AAPS PharmSciTech. 6 (2005) E482–E486. doi:10.1208/pt060360.

[63] A. Trapani, S. Di Gioia, N. Ditaranto, N. Cioffi, F.M. Goycoolea, A. Carbone, M. Garcia-Fuentes, M. Conese, M.J. Alonso, Systemic heparin delivery by the pulmonary route using chitosan and glycol chitosan nanoparticles, Int. J. Pharm. 447 (2013) 115–123. doi:10.1016/j.ijpharm.2013.02.035.

[64] A.T. Iacono, B. a Johnson, W.F. Grgurich, J.G. Youssef, T.E. Corcoran, D. a Seiler, J.H. Dauber, G.C. Smaldone, A. Zeevi, S. a Yousem, J.J. Fung, G.J. Burckart, K.R. McCurry, B.P. Griffith, A randomized trial of inhaled cyclosporine in lung-transplant recipients, N. Engl. J. Med. 354 (2006) 141–150. doi:10.1056/NEJMoa043204.

[65] NCT01650545, Aerosol Liposomal Cyclosporine for Chronic Rejection in Lung Transplant Recipients, (2012). https://clinicaltrials.gov/ct2/show/study/NCT01650545 (accessed March 20, 2017).

[66] D. Teijeiro-Osorio, C. Remuñán-López, M.J. Alonso, New generation of hybrid poly/oligosaccharide nanoparticles as carriers for the nasal delivery of macromolecules, Biomacromolecules. 12 (2009) 243–249. doi:10.1021/bm800975j.

[67] R. Fernández-Urrusuno, P. Calvo, C. Remuñán-López, J.L. Vila-Jato, M.J. Alonso, Enhancement of nasal absorption of insulin using chitosan nanoparticles, Pharm. Res. 16 (1999) 1576–1581. doi:10.1023/A:1018908705446.

[68] C. Prego, D. Torres, M.J. Alonso, Chitosan nanocapsules: a new carrier for nasal peptide delivery, J. Drug Deliv. Sci. Technol. 16 (2006) 331–337. doi:10.1016/S1773-2247(06)50061-9.

[69] A. Vila, A. Sánchez, C. Évora, I. Soriano, O. McCallion, M.J. Alonso, PLA-PEG particles as nasal protein carriers: the influence of the particle size, Int. J. Pharm. 292 (2005) 43–52. doi:10.1016/j.ijpharm.2004.09.002.

[70] M. Tobío, R. Gref, A. Sanchez, R. Langer, M.J. Alonso, Stealth PLA-PEG nanoparticles as protein carriers for nasal administration, Pharm. Res. 15 (1998) 270–275. doi:10.1023/A:1011922819926.

[71] Y. Ozsoy, S. Gungor, E. Cevher, Nasal delivery of high molecular weight drugs, Molecules. 14 (2009) 3754–3779. doi:10.3390/molecules14093754.

[72] K. Brekke, A. Lind, C. Holm-Hansen, I.L. Haugen, B. Sørensen, M. Sommerfelt, D. Kvale, Intranasal administration of a therapeutic HIV vaccine (Vacc-4x) induces dose-dependent systemic and mucosal immune responses in a randomized controlled trial, PLoS One. 9 (2014) 1–9. doi:10.1371/journal.pone.0112556.

[73] ClinicalTrials.gov, Intranasal modified Vacc-4x Gag peptides with Endocine as adjuvant, (n.d.). https://clinicaltrials.gov/ct2/show/NCT01473810?term=nasal+and+peptide (accessed September 10, 2018).

[74] K. Kigasawa, M. Miyashita, K. Kajimoto, K. Kanamura, H. Harashima, K. Kogure, Efficient intradermal delivery of superoxide dismutase using a combination of liposomes and iontophoresis for protection against UV-induced skin damage, Biol. Pharm. Bull. 35 (2012) 781–785. doi:10.1248/bpb.35.781.

[75] P. Agarwal, I.D. Rupenthal, Modern approaches to the ocular delivery of cyclosporine A, Drug Discov. Today. 21 (2016) 977–988. doi:10.1016/j.drudis.2016.04.002.

[76] B.M. Davis, E.M. Normando, L. Guo, P. O'Shea, S.E. Moss, S. Somavarapu, M.F. Cordeiro, Topical delivery of avastin to the posterior segment of the eye in vivo using annexin A5-associated liposomes, Small. 10 (2014) 1575–1584. doi:10.1002/smll.201303433.

[77] Y. Lu, N. Zhou, X. Huang, J.-W. Cheng, F.-Q. Li, R.-L. Wei, J.-P. Cai, Effect of intravitreal injection of bevacizumab-chitosan nanoparticles on retina of diabetic rats, Int. J. Ophthalmol. 7 (2014) 1–7. doi:10.3980/j.issn.2222-3959.2014.01.01.

[78] A. Sood, R. Panchagnula, Peroral route: An opportunity for protein and peptide drug delivery, Chem. Rev. 101 (2001) 3275–3303. doi:10.1021/cr000700m.

[79] A.L. Smart, S. Gaisford, A.W. Basit, Oral peptide and protein delivery: intestinal obstacles and commercial prospects, Expert Opin. Drug Deliv. 11 (2014) 1323–1335. doi:10.1517/17425247.2014.917077.

[80] J. Wang, V. Yadav, A.L. Smart, S. Tajiri, A.W. Basit, Toward oral delivery of biopharmaceuticals: An assessment of the gastrointestinal stability of 17 peptide drugs, Mol. Pharm. 12 (2015) 966–973. doi:10.1021/mp500809f.

[81] M. Morishita, N.A. Peppas, Is the oral route possible for peptide and protein drug delivery?, Drug Discov. Today. 11 (2006) 905–910. doi:10.1016/j.drudis.2006.08.005.

[82] G. Camenisch, J. Alsenz, H. Van De Waterbeemd, G. Folkers, Estimation of permeability by passive diffusion through Caco-2 cell monolayers using the drugs' lipophilicity and molecular weight, Eur. J. Pharm. Sci. 6 (1998) 313–319. doi:10.1016/S0928-0987(97)10019-7.

[83] W. Rubas, M.E.M. Cromwell, Z. Shahrokh, J. Villagran, T.N. Nguyen, M. Wellton, T.H. Nguyen, R.J. Mrsny, Flux measurements across Caco-2 monolayers may predict transport in human large intestinal tissue, J. Pharm. Sci. 85 (1996) 165–169. doi:10.1021/js950267+.

[84] M. Bendayan, E. Ziv, D. Gingras, R. Ben-Sasson, H. Bar-On, M. Kidron, Biochemical and morpho-cytochemical evidence for the intestinal absorption of insulin in control and diabetic rats. Comparison between the effectiveness of duodenal and colon mucosa, Diabetologia. 37 (1994) 119–126. doi:10.1007/s001250050081.

[85] T. Karamanidou, V. Bourganis, O. Kammona, C. Kiparissides, Lipid-based nanocarriers for the oral administration of biopharmaceutics, Nanomedicine. 11 (2016) 3009–3032. doi:10.2217/nnm-2016-0265.

[86] L. Plapied, N. Duhem, A. des Rieux, V. Préat, Fate of polymeric nanocarriers for oral drug delivery, Curr. Opin. Colloid Interface Sci. 16 (2011) 228–237. doi:10.1016/j.cocis.2010.12.005.

[87] C. Damgé, C.P. Reis, P. Maincent, Nanoparticle strategies for the oral delivery of insulin., Expert Opin. Drug Deliv. 5 (2008) 45–68. doi:10.1517/17425247.5.1.45.

[88] I. Santalices, D. Torres, M.V. Lozano, M.M. Arroyo-Jiménez, M.J. Alonso, M.J. Santander-Ortega, Influence of the surface properties of nanocapsules on their interaction with intestinal barriers, Submitt. to Eur. J. Pharm. Biopharm. (2018).

[89] L. Inchaurraga, N. Martín-Arbella, V. Zabaleta, G. Quincoces, I. Peñuelas, J.M. Irache, In vivo study of the mucus-permeating properties of PEG-coated nanoparticles following oral administration, Eur. J. Pharm. Biopharm. 97 (2015) 280–289. doi:10.1016/j.ejpb.2014.12.021.

[90] L.M. Ensign, R. Cone, J. Hanes, Oral drug delivery with polymeric nanoparticles: the gastrointestinal mucus barriers, Adv. Drug Deliv. Rev. 64 (2012) 557–570. doi:10.1016/j.addr.2011.12.009.

[91] M.G. Choc, Bioavailability and pharmacokinetics of cyclosporine formulations: Neoral® vs Sandimmune®, Int. J. Dermatol. 36 (1997) 1–6. doi:10.1046/j.1365-4362.36.s1.2.x.

[92] A. Fjellestad-Paulsen, P. Höglund, S. Lundin, O. Paulsen, Pharmacokinetics of 1-deamino-8-D-arginine vasopressin after various routes of administration in healthy volunteers, Clin. Endocrinol. (Oxf). 38

(1993) 177–182. doi:10.1111/j.1365-2265.1993.tb00990.x.

[93] H.R. Lakkireddy, M. Urmann, M. Besenius, U. Werner, T. Haack, P. Brun, J. Alié, B. Illel, L. Hortala, R. Vogel, D. Bazile, Oral delivery of diabetes peptides — Comparing standard formulations incorporating functional excipients and nanotechnologies in the translational context, Adv. Drug Deliv. Rev. 106 (2016) 196–222. doi:10.1016/j.addr.2016.02.011.

[94] ClinicalTrials.gov, Trial to compare NNC0123-0000-0338 in a tablet formulation and insulin glargine in subjects with type 2 diabetes currently treated with oral antidiabetic therapy, (n.d.). https://clinicaltrials.gov/ct2/show/NCT02470039?term=gipet&rank=6 (accessed August 26, 2018).

[95] N. Nordisk, Novo Nordisk Trials, (n.d.). https://www.novonordisk-trials.com/es/studies?SearchTerm=gipet&Status=&AgeRanges=&Phases=&Conditions=&Pcode=&Language=es&Location_CountryInternal=0&Treatment=&IncludesCsrDoc=&SortField=Location_Distance&SortOrder=desc&page=0 (accessed August 26, 2018).

[96] Novo Nordisk, Sparkassen Kronjylland, (2013) 1–34.

[97] J. Li, Y. Wang, L. Han, X. Sun, H. Yu, Y. Yu, Time-action profile of an oral enteric insulin formulation in healthy Chinese volunteers, Clin. Ther. 34 (2012) 2333–2338. doi:10.1016/j.clinthera.2012.11.004.

[98] Adisinsight - Springer, Insulin oral - Shanghai Biolaxy, (n.d.). https://adisinsight.springer.com/drugs/800031298 (accessed August 31, 2018).

[99] W.B. Geho, H.C. Geho, J.R. Lau, T.J. Gana, Hepatic-directed vesicle insulin: a review of formulation development and preclinical evaluation, J. Diabetes Sci. Technol. 3 (2009) 1451–1459. doi:10.1177/193229680900300627.

[100] Diasome Pharmaceuticals Inc., Delivering medical breakthroughs for Diabetes & Obesity, (n.d.). http://diasome.com/pipeline/ (accessed January 17, 2018).

[101] Diabetology Ltd, Projects - Capsulin™, (n.d.). http://www.diabetology.co.uk/projects/capsulin/.

[102] S.D. Luzio, G. Dunseath, A. Lockett, T.P. Broke-Smith, R.R. New, D.R. Owens, The glucose lowering effect of an oral insulin (Capsulin) during an isoglycaemic clamp study in persons with type 2 diabetes, Diabetes, Obes. Metab. 12 (2010) 82–87. doi:10.1111/j.1463-1326.2009.01146.x.

[103] Proxima Concepts, Axcess™, (n.d.). http://www.proximaconcepts.com/axcess.htm (accessed August 31, 2018).

[104] R. Eldor, E. Arbit, A. Corcos, M. Kidron, Glucose-reducing effect of the ORMD-0801 oral insulin preparation in patients with uncontrolled type 1 diabetes: a pilot study, PLoS One. 8 (2013) e59524. doi:10.1371/journal.pone.0059524.

[105] Oramed Pharmaceuticals Inc., Pipeline, (n.d.). http://www.oramed.com/pipeline/ (accessed August 28, 2018).

[106] Efficacy safety and tolerability of multiple doses of Oshadi Icp (Oshadi oral insulin) in patients with type 1 diabetes mellitus - phase II clinical study, (2016). https://clinicaltrials.gov/ct2/show/NCT01973920 (accessed January 17, 2018).

[107] A. Khedkar, H. Iyer, A. Anand, M. Verma, S. Krishnamurthy, S. Savale, A. Atignal, A dose range finding study of novel oral insulin (IN-105) under fed conditions in type 2 diabetes mellitus subjects, Diabetes, Obes. Metab. 12 (2010) 659–664. doi:10.1111/j.1463-1326.2010.01213.x.

[108] ClinicalTrials.gov, Comparison of insulin Tregopil (IN-105) with insulin Aspart in type 2 diabetes mellitus patients, (n.d.).

[109] Diabetology Ltd, Projects - Oral GLP-1, (n.d.). http://www.diabetology.co.uk/projects/oral-glp-1/ (accessed August 28, 2018).

[110] Novo Nordisk, R&D Pipeline, (n.d.). https://www.novonordisk.com/rnd/rd-pipeline.html (accessed August 28, 2018).

[111] Emisphere Technologies, Current collaboration with Novo Nordisk to develop Oral GLP-1 Analogues and Oral Insulins for Type 2 Diabetes, (n.d.). https://www.emisphere.com/partnerships/#current-collaborations (accessed August 28, 2018).

[112] Enteris BioPharma, Peptelligence® - Oral drug delivery mechanism, (n.d.). https://enterisbiopharma.com/peptelligence/mechanism/ (accessed August 31, 2018).

[113] A. Sturmer, N. Mehta, J. Giacchi, T. Cagatay, R. Tavakkol, S. Mitta, L. Fitzpatrick, J. Wald, J. Trang, W. Stern, Pharmacokinetics of oral recombinant human parathyroid hormone [rhPTH(1-31)NH2] in postmenopausal women with osteoporosis, Clin. Pharmacokinet. 52 (2013) 995–1004. doi:10.1007/s40262-013-0083-4.

[114] K. Henriksen, J.R. Andersen, B.J. Riis, N. Mehta, R. Tavakkol, P. Alexandersen, I. Byrjalsen, I. Valter, B.S. Nedergaard, C.S. Teglbjærg, W. Stern, A. Sturmer, S. Mitta, A.J. Nino, L.A. Fitzpatrick, C. Christiansen, M.A. Karsdal, Evaluation of the efficacy, safety and pharmacokinetic profile of oral recombinant human parathyroid hormone [rhPTH(1-31)NH2] in postmenopausal women with osteoporosis, Bone. 53 (2013) 160–166. doi:10.1016/j.bone.2012.11.045.

[115] EnteraBio, Pipeline - Progress summary, (n.d.).

[116] EnteraBio, Pipeline - Hypoparathyroidism, (n.d.). https://www.enterabio.com/pipeline/hypoparathyroidism (accessed August 28, 2018).

[117] EnteraBio, Pipeline - Osteoporosis, (n.d.).

[118] BioSpace, Bone Medical Ltd phase II Capsitonin (oral calcitonin) interim clinical trial data in 36 patients positive, (n.d.). https://www.biospace.com/article/releases/bone-medical-ltd-phase-ii-capsitonin-oral-calcitonin-interim-clinical-trial-data-in-36-patients-positive-/ (accessed August 31, 2018).

[119] Tarsa Therapeutics, Tarsa's oral calcitonin - TBRIA™, (n.d.). http://tarsatherapeutics.com/products/tbria/ (accessed August 28, 2018).

[120] Enteris BioPharma, Pipeline, (n.d.). https://enterisbiopharma.com/pipeline/ (accessed August 28, 2018).

[121] N. Binkley, M. Bolognese, A. Sidorowicz-Bialynicka, T. Vally, R. Trout, C. Miller, C.E. Buben, J.P. Gilligan, D.S. Krause, A phase 3 trial of the efficacy and safety of oral recombinant calcitonin: The Oral Calcitonin in Postmenopausal Osteoporosis (ORACAL) trial, J. Bone Miner. Res. 27 (2012) 1821–1829. doi:10.1002/jbmr.1602.

[122] Enteris BioPharma, First patient dosed in trial of oral KORSUVA™, (n.d.). https://enterisbiopharma.com/first-patient-dosed-in-trial-of-oral-korsuva/ (accessed August 28, 2018).

[123] Cara Therapeutics, Pipeline & Technology - Kappa Opioid Receptor Agonists (KORAs), (n.d.).

[124] Enteris BioPharma, Ovarest®, (n.d.). https://enterisbiopharma.com/pipeline/ovarest/ (accessed August 28, 2018).

[125] Enteris BioPharma, Positive results in Ovarest® endometriosis trial, (n.d.).

[126] Chiasma, Clinical trials, (n.d.). http://www.chiasmapharma.com/clinical-trials (accessed August 28, 2018).

[127] Chiasma, Octreotide capsules, (n.d.). http://www.chiasmapharma.com/octreotide-capsules (accessed August 28, 2018).

[128] L. Rosenfeld, Insulin: discovery and controversy, Clin. Chem. 48 (2002) 2270–2288. doi:10.1126/science.211.4489.1404.

[129] Diabetes.co.uk, History of insulin - Discovery to modern day timeline, (n.d.). https://www.diabetes.co.uk/insulin/history-of-insulin.html (accessed August 24, 2018).

[130] M. Evans, P.M. Schumm-Draeger, J. Vora, a. B. King, A review of modern insulin analogue pharmacokinetic and pharmacodynamic profiles in type 2 diabetes: Improvements and limitations, Diabetes, Obes. Metab. 13 (2011) 677–684. doi:10.1111/j.1463-1326.2011.01395.x.

[131] C.M. Morello, Pharmacokinetics and pharmacodynamics of insulin analogs in special populations with type 2 diabetes mellitus, Int. J. Gen. Med. 4 (2011) 827–835. doi:10.2147/IJGM.S26889.

[132] M.J. Fowler, Diabetes Treatment: Insulin and Incretins, Clin. Diabetes. 28 (2010) 177–182. doi:10.2337/diaclin.28.4.177.

[133] a M. Gualandi-Signorini, G. Giorgi, Insulin formulations - a review., Eur. Rev. Med. Pharmacol. Sci. 5 (2001) 73–83.

[134] M. Valitutto, Common crossroads in diabetes management, Osteopath. Med. Prim. Care. 2 (2008) 4. doi:10.1186/1750-4732-2-4.

[135] I.D. Federation, IDF Diabetes Atlas, 8th ed., 2017.

[136] L. Heinemann, Y. Jacques, Oral Insulin and Buccal Insulin: A Critical Reappraisal, J. Diabetes Sci. Technol. 3 (2009) 568–584. doi:10.1177/193229680900300323.

[137] G.A. Harrison, Insulin in alcoholic solution by the mouth, Br. Med. J. 2 (1923) 1204–1205. doi:10.1136/bmj.2.3286.1204.

[138] FDA, FDA-approved diabetes medicines, (2014). https://www.fda.gov/ForPatients/Illness/Diabetes/ucm408682.htm (accessed January 17, 2018).

[139] Mannkind Corporation, Afrezza® (insulin human) inhalation powder, (n.d.). https://www.afrezza.com/ (accessed January 17, 2018).

[140] Mannkind Corporation, Technosphere® technology - Versatile drug delivery platform, (n.d.). http://www.mannkindcorp.com/Collateral/Documents/English-US/101LR-TechnosphereTechTeaser-01.19.11.pdf (accessed January 17, 2018).

[141] M. Bansal, S. Bansal, R. Kumria, The RapidMist™ system for buccal delivery of insulin, in: J. Das Neves, B. Sarmento (Eds.), Mucosal Deliv. Biopharm. Biol. Challenges Strateg., Springer, 2014: pp. 423–436. doi:10.1007/978-1-4614-9524-6.

[142] D. Fennell, Oral insulin conditionally approved by FDA, Diabetes Self Manag. (2009). https://www.diabetesselfmanagement.com/blog/oral-insulin-conditionally-approved-by-fda/ (accessed January 17, 2018).

[143] E. Arbit, The physiological rationale for oral insulin administration, Diabetes Technol. Ther. 6 (2004) 510–517. doi:10.1089/1520915041705929.

[144] C. Damge, C. Michel, M. Aprahamian, P. Couvreur, J.P. Devissaguet, Nanocapsules as carriers for oral peptide delivery, J. Control. Release. 13 (1990) 233–239. doi:10.1016/0168-3659(90)90013-J.

[145] Z. Niu, E. Samaridou, E. Jaumain, J. Coëne, G. Ullio, N. Shrestha, J. Garcia, M. Durán-Lobato, S. Tovar, M.J. Santander-Ortega, M.V. Lozano, M.M. Arroyo-Jimenez, R. Ramos-Membrive, I. Peñuelas, A. Mabondzo, V. Préat, M. Teixidó, E. Giralt, M.J. Alonso, PEG-PGA enveloped octaarginine-peptide nanocomplexes: an oral peptide delivery strategy, J. Control. Release. 276 (2018) 125–139. doi:10.1016/j.jconrel.2018.03.004.

[146] N. Jafary Omid, N. Bahari Javan, A.R. Dehpour, A. Partoazar, M. Rafiee Tehrani, F. Dorkoosh, In-vitro and in-vivo cytotoxicity and efficacy evaluation of novel glycyl-glycine and alanyl-alanine conjugates of chitosan and trimethyl chitosan nano-particles as carriers for oral insulin delivery, Int. J. Pharm. 535 (2018) 293–307. doi:10.1016/j.ijpharm.2017.11.020.

[147] W. Fan, D. Xia, Q. Zhu, X. Li, S. He, C. Zhu, S. Guo, L. Hovgaard, M. Yang, Y. Gan, Functional nanoparticles exploit the bile acid pathway to overcome multiple barriers of the intestinal epithelium for oral insulin delivery, Biomaterials. 151 (2018) 13–23. doi:10.1016/j.biomaterials.2017.10.022.

[148] J. Wu, Y. Zheng, M. Liu, W. Shan, Z. Zhang, Y. Huang, Biomimetic Viruslike and Charge Reversible Nanoparticles to Sequentially Overcome Mucus and Epithelial Barriers for Oral Insulin Delivery, ACS Appl. Mater. Interfaces. 10 (2018) 9916–9928. doi:10.1021/acsami.7b16524.

[149] R. Ganugula, M. Arora, M. Guada, P. Saini, M.N.V.R. Kumar, Noncompetitive active transport exploiting intestinal transferrin receptors for oral delivery of proteins by tunable nanoplatform, ACS Macro Lett. 6 (2017) 161–164. doi:10.1021/acsmacrolett.7b00035.

[150] A. Manosroi, T. Tangjai, C. Sutthiwanjampa, W. Manosroi, R.G. Werner, F. Götz, M. Sainakham, J. Manosroi, Hypoglycemic activity and stability enhancement of human insulin–tat mixture loaded in elastic anionic niosomes, 2016. doi:10.3109/10717544.2016.1157840.

[151] A. Verma, S. Sharma, P.K. Gupta, A. Singh, B.V. Teja, P. Dwivedi, G.K. Gupta, R. Trivedi, P.R. Mishra, Vitamin B12 functionalized layer by layer calcium phosphate nanoparticles: A mucoadhesive and pH responsive carrier for improved oral delivery of insulin, Acta Biomater. 31 (2016) 288–300. doi:10.1016/j.actbio.2015.12.017.

[152] X. Zhu, J. Wu, W. Shan, W. Tao, L. Zhao, J.M. Lim, M. D'Ortenzio, R. Karnik, Y. Huang, J. Shi, O.C. Farokhzad, Polymeric nanoparticles amenable to simultaneous installation of exterior targeting and interior therapeutic proteins, Angew. Chemie - Int. Ed. 55 (2016) 3309–3312. doi:10.1002/anie.201509183.

[153] V. Gupta, B.H. Hwang, N. Doshi, A. Banerjee, A.C. Anselmo, S. Mitragotri, Delivery of exenatide and insulin using mucoadhesive intestinal devices, Ann. Biomed. Eng. 44 (2016) 1993–2007. doi:10.1007/s10439-016-1558-x.

[154] N. Ahmad, M.C.I. Mohd Amin, I. Ismail, F. Buang, Enhancement of oral insulin bioavailability: *in vitro* and *in vivo* assessment of nanoporous stimuli-responsive hydrogel microparticles, Expert Opin. Drug Deliv. 13 (2016) 621–632. doi:10.1517/17425247.2016.1160889.

[155] M. Alibolandi, F. Alabdollah, F. Sadeghi, M. Mohammadi, K. Abnous, M. Ramezani, F. Hadizadeh, Dextran-b-poly (lactide-co-glycolide) polymersome for oral delivery of insulin: In vitro and in vivo evaluation, J. Control. Release. 227 (2016) 58–70. doi:10.1016/j.jconrel.2016.02.031.

[156] M. Liu, J. Zhang, X. Zhu, W. Shan, L. Li, J. Zhong, Z. Zhang, Y. Huang, Efficient mucus permeation and tight junction opening by dissociable "mucus-inert" agent coated trimethyl chitosan nanoparticles for oral insulin delivery, J. Control. Release. 222 (2016) 67–77. doi:10.1016/j.jconrel.2015.12.008.

[157] L. Liu, C. Zhou, X. Xia, Y. Liu, Self-assembled lecithin / chitosan nanoparticles for oral insulin delivery:

preparation and functional evaluation, Int. J. Nanomedicine. 11 (2016) 761–769. doi:10.2147/IJN.S96146.

[158] Y. Wang, W. Qu, S.H. Choi, FDA's regulatory science program for generic PLA/PLGA-based drug products, Am. Pharm. Rev. (2016).

[159] S. Zhu, S. Chen, Y. Gao, F. Guo, F. Li, B. Xie, J. Zhou, H. Zhong, Enhanced oral bioavailability of insulin using PLGA nanoparticles co-modified with cell-penetrating peptides and Engrailed secretion peptide (Sec), Drug Deliv. 23 (2016) 1980–1991. doi:10.3109/10717544.2015.1043472.

[160] C. Liu, W. Shan, M. Liu, X. Zhu, J. Xu, Y. Xu, Y. Huang, A novel ligand conjugated nanoparticles for oral insulin delivery, Drug Deliv. 23 (2016) 2015–2025. doi:10.3109/10717544.2015.1058433.

[161] F. Guo, M. Zhang, Y. Gao, S. Zhu, S. Chen, W. Liu, H. Zhong, J. Liu, Modified nanoparticles with cell-penetrating peptide and amphipathic chitosan derivative for enhanced oral colon absorption of insulin: preparation and evaluation, Drug Deliv. 23 (2016) 2003–2014. doi:10.3109/10717544.2015.1048489.

[162] M.J. Ansari, M.K. Anwer, S. Jamil, R. Al-Shdefat, B.E. Ali, M.M. Ahmad, M.N. Ansari, Enhanced oral bioavailability of insulin-loaded solid lipid nanoparticles: pharmacokinetic bioavailability of insulin-loaded solid lipid nanoparticles in diabetic rats, Drug Deliv. 23 (2016) 1972–1979. doi:10.3109/10717544.2015.1039666.

[163] L. Zhang, Z. Gao, X. Zhao, G. Qi, A natural lipopeptide of surfactin for oral delivery of insulin, Drug Deliv. 23 (2016) 2084–2093. doi:10.3109/10717544.2016.1153745.

[164] Z.I. Al-Kurdi, B.Z. Chowdhry, S.A. Leharne, M.M.H. Al Omari, A.A. Badwan, A.O. Jo, Low molecular weight chitosan–insulin polyelectrolyte complex: characterization and stability studies, Mar. Drugs. 13 (2015) 1765–1784. doi:10.3390/md13041765.

[165] N.A. Qinna, Q.G. Karwi, N. Al-Jbour, M.A. Al-Remawi, T.M. Alhussainy, K.A. Al-So'ud, M.M.H. Al Omari, A.A. Badwan, Influence of molecular weight and degree of deacetylation of low molecular weight chitosan on the bioactivity of oral insulin preparations, Mar. Drugs. 13 (2015) 1710–1725. doi:10.3390/md13041710.

[166] W. Shan, X. Zhu, M. Liu, L. Li, J. Zhong, W. Sun, Z. Zhang, Y. Huang, Overcoming the diffusion barrier of mucus and absorption barrier of epithelium by self-Assembled nanoparticles for oral delivery of insulin, ACS Nano. 9 (2015) 2345–2356. doi:10.1021/acsnano.5b00028.

[167] R. Sharma, U. Gupta, N.K. Garg, R.K. Tyagi, N.K. Jain, Surface engineered and ligand anchored nanobioconjugate: An effective therapeutic approach for oral insulin delivery in experimental diabetic rats, Colloids Surfaces B Biointerfaces. 127 (2015) 172–181. doi:10.1016/j.colsurfb.2015.01.035.

[168] K. Shi, Y. Fang, Q. Kan, J. Zhao, Y. Gan, Z. Liu, Surface functional modification of self-assembled insulin nanospheres for improving intestinal absorption, Int. J. Biol. Macromol. 74 (2015) 49–60. doi:10.1016/j.ijbiomac.2014.11.013.

[169] Y. Zhang, L. Li, M. Han, J. Hu, L. Zhang, D.J. McPhee, Amphiphilic lipopeptide-mediated transport of insulin and cell membrane penetration mechanism, Molecules. 20 (2015) 21569–21583. doi:10.3390/molecules201219771.

[170] P. Mukhopadhyay, S. Chakraborty, S. Bhattacharya, R. Mishra, P.P. Kundu, PH-sensitive chitosan/alginate core-shell nanoparticles for efficient and safe oral insulin delivery, Int. J. Biol. Macromol. 72 (2015) 640–648. doi:10.1016/j.ijbiomac.2014.08.040.

[171] S. Sun, N. Liang, H. Yamamoto, Y. Kawashima, F. Cui, P. Yan, pH-sensitive poly(lactide-co-glycolide) nanoparticle composite microcapsules for oral delivery of insulin, Int. J. Nanomedicine. 10 (2015) 3489–3498. doi:http://dx.doi.org/10.2147/IJN.S81715.

[172] S. Abbad, Z. Zhang, A.Y. Waddad, W.L.L. Munyendo, H. Lv, J. Zhou, Chitosan-modified cationic amino acid nanoparticles as a novel oral delivery system for insulin, J. Biomed. Nanotechnol. 11 (2015) 486–499. doi:10.1166/jbn.2015.1924.

[173] M. Cui, W. Wu, L. Hovgaard, Y. Lu, D. Chen, J. Qi, Liposomes containing cholesterol analogues of botanical origin as drug delivery systems to enhance the oral absorption of insulin, Int. J. Pharm. 489 (2015) 277–284. doi:10.1016/j.ijpharm.2015.05.006.

[174] A. Jain, S.K. Jain, l-Valine appended PLGA nanoparticles for oral insulin delivery, Acta Diabetol. 52 (2015) 663–676. doi:10.1007/s00592-015-0714-3.

[175] S. Malathi, P. Nandhakumar, V. Pandiyan, T.J. Webster, S. Balasubramanian, Novel PLGA-based nanoparticles for the oral delivery of insulin, Int. J. Nanomedicine. 10 (2015) 2207–2218. doi:10.2147/IJN.S67947.

[176] F. Yu, Y. Li, C.S. Liu, Q. Chen, G.H. Wang, W. Guo, X.E. Wu, D.H. Li, W.D. Wu, X.D. Chen, Enteric-coated capsules filled with mono-disperse micro-particles containing PLGA-lipid-PEG nanoparticles for oral delivery of insulin, Int. J. Pharm. 484 (2015) 181–191. doi:10.1016/j.ijpharm.2015.02.055.

[177] E.Y. Chuang, K.J. Lin, P.Y. Lin, H.L. Chen, S.P. Wey, F.L. Mi, H.C. Hsiao, C.T. Chen, H.W. Sung, Self-assembling bubble carriers for oral protein delivery, Biomaterials. 64 (2015) 115–124. doi:10.1016/j.biomaterials.2015.06.035.

[178] H. He, P. Wang, C. Cai, R. Yang, X. Tang, VB12-coated Gel-Core-SLN containing insulin: Another way to improve oral absorption, Int. J. Pharm. 493 (2015) 451–459. doi:10.1016/j.ijpharm.2015.08.004.

[179] J. Sheng, L. Han, J. Qin, G. Ru, R. Li, L. Wu, D. Cui, P. Yang, Y. He, J. Wang, N -Trimethyl Chitosan Chloride-Coated PLGA Nanoparticles Overcoming Multiple Barriers to Oral Insulin Absorption, ACS Appl. Mater. Interfaces. 7 (2015) 15430–15441. doi:10.1021/acsami.5b03555.

[180] K. Chaturvedi, K. Ganguly, A.R. Kulkarni, W.E. Rudzinski, L. Krauss, M.N. Nadagouda, T.M. Aminabhavi, Oral insulin delivery using deoxycholic acid conjugated PEGylated polyhydroxybutyrate co-polymeric nanoparticles, Nanomedicine. 10 (2015) 1569–1583. doi:10.2217/nnm.15.36.

[181] M.A. Lopes, B. Abrahim-Vieira, C. Oliveira, P. Fonte, A.M.T. Souza, T. Lira, J.A.D. Sequeira, C.R. Rodrigues, L.M. Cabral, B. Sarmento, R. Seiça, F. Veiga, A.J. Ribeiro, Probing insulin bioactivity in oral nanoparticles produced by ultrasonication-assisted emulsification/internal gelation, Int. J. Nanomedicine. 10 (2015) 5865–5880. doi:10.2147/IJN.S86313.

[182] M. Diop, N. Auberval, A. Viciglio, A. Langlois, W. Bietiger, C. Mura, C. Peronet, A. Bekel, D. Julien David, M. Zhao, M. Pinget, N. Jeandidier, C. Vauthier, E. Marchioni, Y. Frere, S. Sigrist, Design, characterisation, and bioefficiency of insulin-chitosan nanoparticles after stabilisation by freeze-drying or cross-linking, Int. J. Pharm. 491 (2015) 402–408. doi:10.1016/j.ijpharm.2015.05.065.

[183] M.R. Rekha, C.P. Sharma, Simultaneous effect of thiolation and carboxylation of chitosan particles towards mucoadhesive oral insulin delivery applications: An in vitro and in vivo evaluation, J. Biomed. Nanotechnol. 11 (2015) 165–176. doi:10.1166/jbn.2015.1904.

[184] P. Zhang, Y. Xu, X. Zhu, Y. Huang, Goblet cell targeting nanoparticle containing drug-loaded micelle cores for oral delivery of insulin, Int. J. Pharm. 496 (2015) 993–1005. doi:10.1016/j.ijpharm.2015.10.078.

[185] A.K. Agrawal, H. Harde, K. Thanki, S. Jain, Improved stability and antidiabetic potential of insulin containing folic acid functionalized polymer stabilized multilayered liposomes following oral administration, Biomacromolecules. 15 (2014) 350–360. doi:10.1021/bm401580k.

[186] H.J. Cho, J. Oh, M.K. Choo, J.I. Ha, Y. Park, H.J. Maeng, Chondroitin sulfate-capped gold nanoparticles for the oral delivery of insulin, Int. J. Biol. Macromol. 63 (2014) 15–20. doi:10.1016/j.ijbiomac.2013.10.026.

[187] M.A. Momoh, F.C. Kenechukwu, P.O. Nnamani, J.C. Umetiti, Influence of magnesium stearate on the physicochemical and pharmacodynamic characteristics of insulin-loaded Eudragit entrapped mucoadhesive microspheres, Drug Deliv. 22 (2015) 837–848. doi:10.3109/10717544.2014.898108.

[188] P. Li, A. Tan, C.A. Prestidge, H.M. Nielsen, A. Müllertz, Self-nanoemulsifying drug delivery systems for oral insulin delivery: In vitro and in vivo evaluations of enteric coating and drug loading, Int. J. Pharm. 477 (2014) 390–398. doi:10.1016/j.ijpharm.2014.10.039.

[189] M. Niu, Y. Tan, P. Guan, L. Hovgaard, Y. Lu, J. Qi, R. Lian, X. Li, W. Wu, Enhanced oral absorption of insulin-loaded liposomes containing bile salts: A mechanistic study, Int. J. Pharm. 460 (2014) 119–130. doi:10.1016/j.ijpharm.2013.11.028.

[190] E.J.B. Nielsen, S. Yoshida, N. Kamei, R. Iwamae, E.S. Khafagy, J. Olsen, U.L. Rahbek, B.L. Pedersen, K. Takayama, M. Takeda-Morishita, In vivo proof of concept of oral insulin delivery based on a co-administration strategy with the cell-penetrating peptide penetratin, J. Control. Release. 189 (2014) 19–24. doi:10.1016/j.jconrel.2014.06.022.

[191] G. Millotti, F. Laffleur, G. Perera, C. Vigl, K. Pickl, F. Sinner, A. Bernkop-SCHNÜ Rch, In vivo evaluation of thiolated chitosan tablets for oral insulin delivery, J. Pharm. Sci. 103 (2014) 3165–3170. doi:10.1002/jps.24102.

[192] X. Zhang, J. Qi, Y. Lu, W. He, X. Li, W. Wu, Biotinylated liposomes as potential carriers for the oral delivery of insulin, Nanomedicine Nanotechnology, Biol. Med. 10 (2014) 167–176. doi:10.1016/j.nano.2013.07.011.

[193] E.Y. Chuang, K.J. Lin, F.Y. Su, F.L. Mi, B. Maiti, C.T. Chen, S.P. Wey, T.C. Yen, J.H. Juang, H.W. Sung, Noninvasive imaging oral absorption of insulin delivered by nanoparticles and its stimulated glucose utilization in controlling postprandial hyperglycemia during OGTT in diabetic rats, J. Control. Release. 172 (2013) 513–522. doi:10.1016/j.jconrel.2013.05.006.

[194] E.Y. Chuang, G.T.H. Nguyen, F.Y. Su, K.J. Lin, C.T. Chen, F.L. Mi, T.C. Yen, J.H. Juang, H.W. Sung, Combination therapy via oral co-administration of insulin- and exendin-4-loaded nanoparticles to treat type 2 diabetic rats undergoing OGTT, Biomaterials. 34 (2013) 7994–8001. doi:10.1016/j.biomaterials.2013.07.021.

[195] E.M. Pridgen, F. Alexis, T.T. Kuo, E. Levy-Nissenbaum, R. Karnik, R.S. Blumberg, R. Langer, O.C. Farokhzad, Transepithelial transport of Fc-targeted nanoparticles by the neonatal Fc receptor for oral delivery, Sci. Transl. Med. 5 (2013). doi:10.1126/scitranslmed.3007049.

[196] H. He, J. Sheng, A.E. David, Y.M. Kwon, J. Zhang, Y. Huang, J. Wang, V.C. Yang, The use of low molecular weight protamine chemical chimera to enhance monomeric insulin intestinal absorption, Biomaterials. 34 (2013) 7733–7743. doi:10.1016/j.biomaterials.2013.06.047.

[197] M. Licciardi, G. Pitarresi, G. Cavallaro, G. Giammona, Nanoaggregates based on new poly-hydroxyethyl-aspartamide copolymers for oral insulin absorption, Mol. Pharm. 10 (2013) 1644–1654. doi:10.1021/mp300226d.

[198] A. Viehof, L. Javot, A. Béduneau, Y. Pellequer, A. Lamprecht, Oral insulin delivery in rats by nanoparticles prepared with non-toxic solvents, Int. J. Pharm. 443 (2013) 169–174. doi:10.1016/j.ijpharm.2013.01.017.

[199] X. Liu, C. Liu, W. Zhang, C. Xie, G. Wei, W. Lu, Oligoarginine-modified biodegradable nanoparticles improve the intestinal absorption of insulin, Int. J. Pharm. 448 (2013) 159–167. doi:10.1016/j.ijpharm.2013.03.033.

[200] G. Sharma, C.F. Van Der Walle, M.N.V. Ravi Kumar, Antacid co-encapsulated polyester nanoparticles for peroral delivery of insulin: Development, pharmacokinetics, biodistribution and pharmacodynamics, Int. J. Pharm. 440 (2013) 99–110. doi:10.1016/j.ijpharm.2011.12.038.

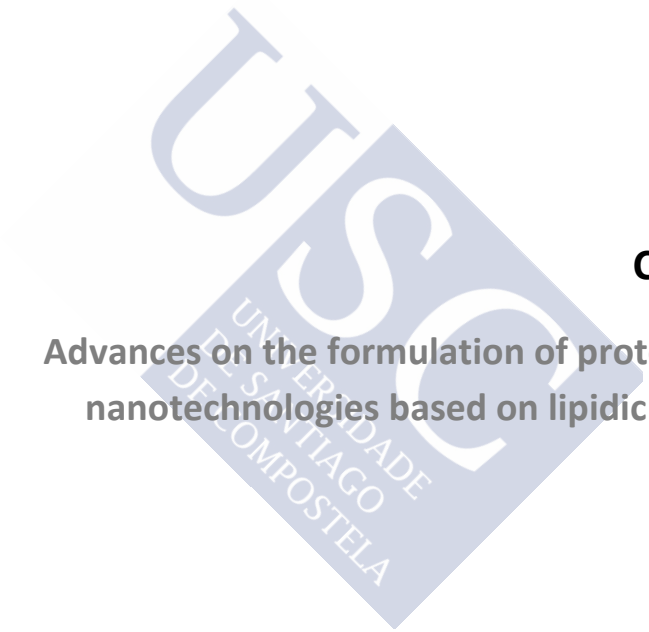
[201] X. Li, S. Guo, C. Zhu, Q. Zhu, Y. Gan, J. Rantanen, U.L. Rahbek, L. Hovgaard, M. Yang, Intestinal mucosa permeability following oral insulin delivery using core shell corona nanolipoparticles, Biomaterials. 34 (2013) 9678–9687. doi:10.1016/j.biomaterials.2013.08.048.

[202] X.Y. Xiong, Q.H. Li, Y.P. Li, L. Guo, Z.L. Li, Y.C. Gong, Colloids and Surfaces B : Biointerfaces Pluronic P85 / poly ( lactic acid ) vesicles as novel carrier for oral insulin delivery, Colloids Surfaces B Biointerfaces. 111 (2013) 282–288. doi:10.1016/j.colsurfb.2013.06.019.

[203] M. Ganeshkumar, T. Ponrasu, M. Sathishkumar, L. Suguna, Preparation of amphiphilic hollow carbon nanosphere loaded insulin for oral delivery, Colloids Surfaces B Biointerfaces. 103 (2013) 238–243. doi:10.1016/j.colsurfb.2012.10.043.

[204] E.Y. Chuang, K.J. Lin, F.Y. Su, H.L. Chen, B. Maiti, Y.C. Ho, T.C. Yen, N. Panda, H.W. Sung, Calcium depletion-mediated protease inhibition and apical-junctional- complex disassembly via an EGTA-conjugated carrier for oral insulin delivery, J. Control. Release. 169 (2013) 296–305. doi:10.1016/j.jconrel.2012.11.011.

USC UNIVERSIDADE DE SANTIAGO DE COMPOSTELA



# Chapter 1

## Advances on the formulation of proteins using nanotechnologies based on lipidic materials

USC
UNIVERSIDADE
DE SANTIAGO
DE COMPOSTELA

# Chapter 1

# Advances on the formulation of proteins using nanotechnologies based on lipidic materials

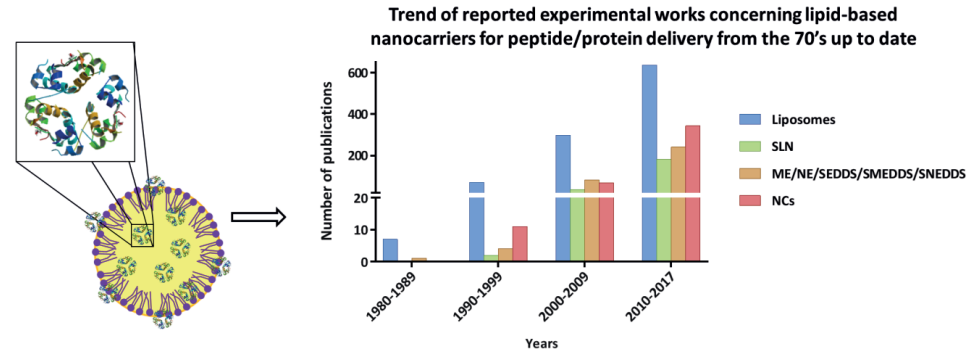
*This Chapter has been adapted/extracted from a recently published review entitled "Advances on the formulation of proteins using nanotechnologies"* [1].


## Abstract

Therapeutic proteins and peptides are very attractive from the pharmaceutical point of view due to their high potency and selectivity. Nonetheless, their instability and low bioavailability make their administration through non parenteral routes very difficult, a fact that hampers their efficient exploitation in therapeutics. Since the 70´s, significant amount of research in the area of drug delivery and nanotechnology has been done with the final goal of overcoming those hurdles. In particular, biodegradable and biocompatible lipid-based nanocarriers have emerged as promising delivery platforms to enable the administration of proteins and peptides. Here, we provide an overview of the nanotechnologies mostly explored to date to produce lipidic nanocarriers for protein/peptide delivery. The basic principles of the different techniques are discussed, and finally, the main factors involved in the drug association and release, are analyzed.

USC
UNIVERSIDADE
DE SANTIAGO
DE COMPOSTELA

## Graphical abstract




**Data taken from Scopus (1971–2017) using protein/peptide delivery and the type of system as searching criteria. ME: microemulsion; NCs: nanocapsules; NE: nanoemulsion; SEDDS: self-emulsified drug delivery system; SMEDDS: self-microemulsified drug delivery system; SNEDDS: self-nanoemulsified drug delivery system; SLN: solid lipid nanoparticles. Image adapted with permission from* [2].

**X-ray structure of Human Recombinant insulin. Image from the RCSB PDB (www.rcsb.org) of PDB ID 5E7W.*

UNIVERSIDADE DE SANTIAGO DE COMPOSTELA

USC
UNIVERSIDADE
DE SANTIAGO
DE COMPOSTELA

## Table of contents

**1. Introduction**

**2. Liposomes**

2.1. Preparation techniques

2.2. Characterization, peptide/protein loading, activity and release profile

**3. Solid lipid nanoparticles (SLN)**

3.1. Preparation techniques

3.2. Characterization, peptide/protein loading, activity and release profile

**4. Nanocapsules**

4.1. Preparation techniques

4.2. Characterization, peptide/protein loading, activity and release profile

**5. Microemulsions and Nanoemulsions**

5.1. Preparation techniques

5.2. Characterization, peptide/protein loading, activity and release profile

**6. Conclusions**

USC UNIVERSIDADE DE SANTIAGO DE COMPOSTELA

USC
UNIVERSIDADE
DE SANTIAGO
DE COMPOSTELA

## 1. Introduction

In the last decades, lipid-based nanocarriers (*Figure 1*) have emerged as potential nanocarriers for macromolecular delivery. This has been mainly due to the absorption enhancing properties of the lipids and the nanocarrier's ability to improve the drug stability. Furthermore, the biocompatible character of these biomaterials and the low cost of the production techniques have increased the interest in these nanocarriers [3]. Despite of this, the inclusion of hydrophilic macromolecules into these systems has been so far limited by their solubility. In order to improve their incorporation into these systems, many innovative strategies, which are summarized below, have been described as promising approaches for the formulation of peptide lipid-based delivery nanosystems (*Figure 2*).

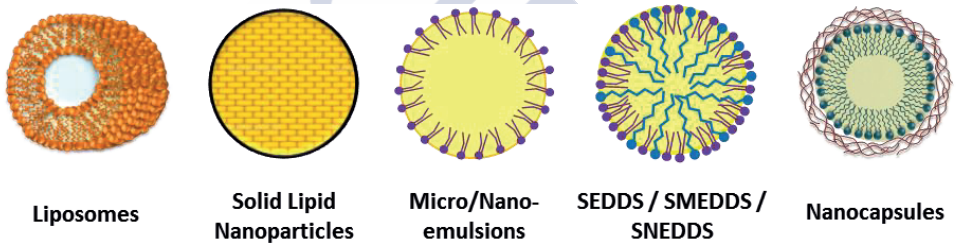



***Figure 1.*** *Illustration of the main lipid-based nanosystems explored for protein/peptide delivery. Adapted with permission from* [2].

**- Reverse micellization.** This strategy involves the use of amphiphilic molecules able to self-organize as reverse micelles exposing their hydrophobic chains to the exterior and their hydrophilic head groups to the inner part of the structure [4]. This inner cavity facilitates the incorporation of hydrophilic macromolecules prior to its inclusion in the final system [5].

**- Double emulsion method.** This technique consists on the formation of a W/O emulsion in which the hydrophilic drug is confined within its internal aqueous phase prior to its inclusion in the final system [6–8].

**- Hydrophobic ion paring.** This approach has been used to enhance the hydrophobicity of the drug, thereby improving its lipid solubility. It is based on the ionic complexation of a peptide/protein with a molecule, often an amphiphilic compound, with an opposite surface charge [9–11] or even with complex structures such as liposomes [12].

**- Hydrophobic – hydrophilic interactions.** This approach involves the dispersion of an aqueous solution of the hydrophilic drug into an amphiphilic compound, followed by the addition of the formed dispersion into the oily phase [13,14].

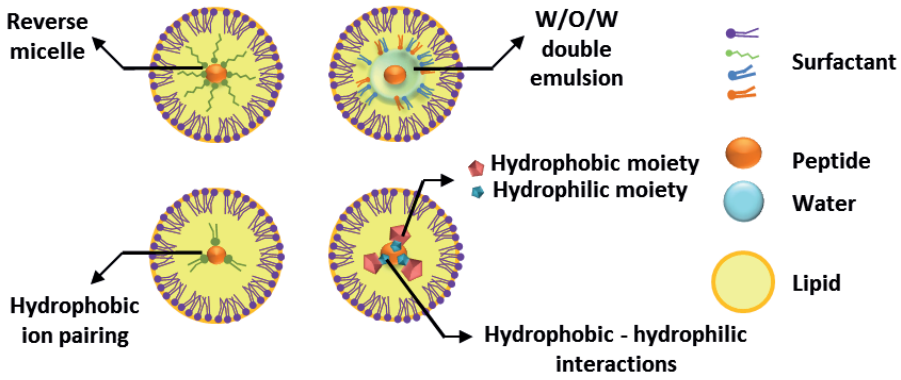



***Figure 2.*** *Illustration of the main strategies employed to improve the incorporation of hydrophilic macromolecules into lipid-based delivery nanosystems. Adapted with permission from* [2].

## 2. Liposomes

Since their discovery in 1964 [15,16], liposomes have been the most extensively drug delivery vehicles investigated. To date, 13 liposome-based products have been approved for human use by the FDA [2]. Briefly, liposomes are defined as vesicles with an aqueous core in the inner cavity, surrounded by one or more bilayers of amphiphilic phospholipids. Their sizes range from 20 nm (if unilamellar) up to microns (if multilamellar) [17]. Among the wide variety of lipids, those amphiphilic able to self-assembly, such as phospholipids, phosphatidylglycerol derivatives and both saturated and unsaturated fatty acids, are the most commonly used for producing liposomes [2]. Additionally, it is also possible the inclusion of polymers and surfactants into their structure [18–21]. Finally, the use of special lipids has led to the formation of nanostructures named as archeosomes (i.e., diether or tetraether lipids) [22] and niosomes (i.e., polyoxyethylene alkyl ethers) [23], which were supposed to facilitate the entrapment of peptides and proteins [24].

## 2.1. Preparation techniques

Overall, the technologies to prepare liposomes are relatively similar. The main difference among the variety of techniques described so far relies on the way of drying the lipids from the organic solvents and rehydrating them in aqueous media [25]. The main liposomes preparation methods used for protein/peptide association are those described below.

***i)*** **Film hydration**

This technique was introduced by Bangham and coworkers to produce liposomes by the first time (*Figure 3*) [15,16]. This technique involves the dissolution of the phospholipids in an organic solvent, followed by the solvent evaporation and the deposition of the phospholipids forming a lipid film. Then, an aqueous solution containing the protein is added over the lipidic film to hydrate it, usually with the help of sonication, thus leading to the formation of liposomes [26,27].

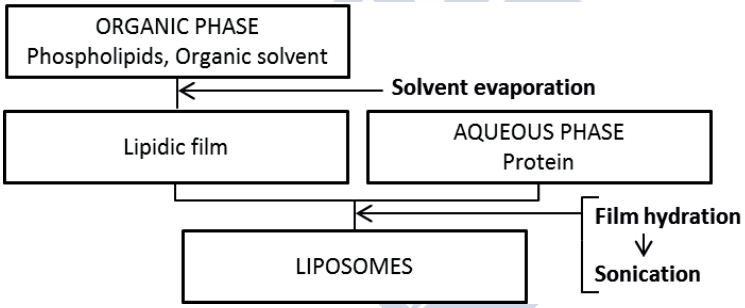



***Figure 3.*** *Schematic view of the film hydration technique to produce liposomes.*

***ii)*** **Reverse-phase evaporation**

This technique simply involves the formation of reverse micelles by mixing an organic solution of the phospholipids with a small volume of an aqueous phase containing the peptide/protein, usually using sonication. The evaporation of the solvent results in the formation of large unilamellar or multilamellar liposomes (*Figure 4*) [28].

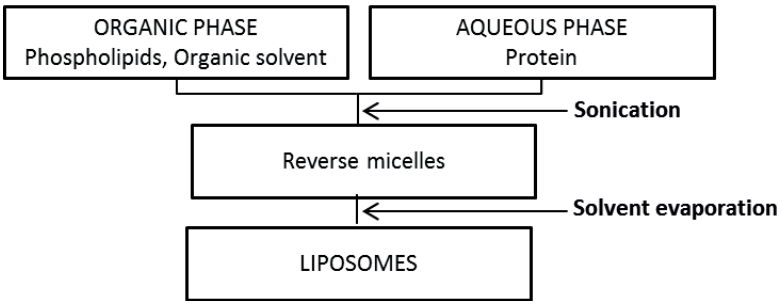



***Figure 4.*** *Schematic view of the reverse-phase evaporation technique to produce liposomes.*

## 2.2. Characterization, peptide/protein loading, activity and release profile

**- Particle size distribution:** generally, a homogenization step is necessary in order to obtain a narrow particle size distribution. The homogenization of the system can be achieved using extrusion [29,30], freeze-thawing [31,32], dehydration-rehydration [33,34], sonication or high pressure. Likewise, the ratio between the different components will influence the final liposomes particle size distribution.

**- Peptide/protein loading and activity:** liposomes have the ability to encapsulate hydrophilic (in the inner aqueous core), lipophilic (within the lipid bilayer) or amphiphilic drugs (partitioned between the lipid bilayer and the aqueous core) [35]. In general, the driving force for the encapsulation relies on the interaction between the protein/peptide and the lipids and also on the bilayer rigidity. For example, liposomes with insulin association efficiency (AE) values varying from 10 up to 90 % could be obtained by changing the phosphatidylcholine:phosphatidylethanol ratio [36]. To date, a variety of peptides and proteins have been efficiently entrapped into liposomes using the preparation methods disclosed in *Table 1*. Unfortunately, the loading capacity of the resulting formulations has not been described or has been low (< 1 %) [37]. Therefore, the loading capacity could be considered as a limitation of these delivery carriers.

Additionally, the loaded protein must remain active once encapsulated into the liposomes. The sources of peptide/protein instability differ depending on the production method considered, being the film hydration the less stressful for the integrity of the protein, even if sonication could affect its structure [38]. On the other hand, the reverse phase evaporation technique directly exposes the peptide/protein to organic solvents,

with the subsequent possibility of suffering denaturation [38,39]. Homogenization, extrusion and freeze thaw cycles can also cause protein denaturation/aggregation in both methods [38]. The integrity of the loaded peptide/protein has been studied using different methods, such as electrophoresis-based techniques (e.g. Western blot, SDS-PAGE, etc.), protein activity (particularly if the encapsulated protein is an enzyme) or directly through *in vivo* experiments [27,36,38,40].

**- Peptide/protein release:** the physicochemical properties of the phospholipids are known to determine the fluidity of the lipid bilayer and, as a consequence, influence the peptide/protein release profile. In this sense, a more sustained release is obtained when increasing the rigidity of the bilayer by the inclusion of cholesterol or long hydrophobic chains in the liposome [41]. Strategies to control the release of peptides/proteins from liposomes, such as the surface modification with polyethylene glycol (PEG) or other polymers, as well as their inclusion in other nanostructures, have been developed [37,42–45]. For example, a lower insulin release was showed after 4 h in simulated intestinal fluids from layer-by-layer coated liposomes (20 %) compared to those uncoated (60 %) [27].

In conclusion, both film hydration and reverse phase evaporation methods are suitable for encapsulating peptides/proteins in liposomes, allowing both, good association efficiencies and sustained release profiles. The bilayer rigidity and the electrostatic interactions between the peptide and the liposomes components are the main factors conditioning the loading capacity of liposomes. Regarding the release behavior, not only the rigidity of the phospholipidic bilayer has an important role in controlling the release, but also factors such as PEGylation, polymer association or their inclusion in other structures can help to obtain sustained release profiles.

***Table 1.*** *Examples of peptide/protein-loaded liposomes obtained by the different preparation methods: drug loading and release properties.*

| Preparation method | Peptide/ Protein | AE (%) | LC (%) | ≤1h burst/ cumulative release (time) – pH medium | Ref. |
|---|---|---|---|---|---|
| **Film hydration** | Insulin | 88 - 94 | n.a. | 10 - 40 % / 20 - 60 % (2 h) pH 1.2<br>10 - 35 % / 20 - 60 % (4 h) pH 6.8<br>10 - 30 % / 72-96 % (24 h) pH 7.4 | [27] |
| | | 10 - >90 | n.a. (4 mg / 50 mg lipid theor.) | n.a. | [36] |
| | sCT | 91 | n.a. | n.a. | [46] |
| | Leuprolide | 17 - 76 | n.a. | n.a. / 2 - 16 % (5 h) pH 1.2* / 7.4* | [47] |
| | BSA | 12 - 72 | 0.1 - 1 | 20 - 30 % (1 h) pH 7.5* | [37] |
| **Reverse-phase evaporation** | Insulin | 30 - 83 | n.a. | < 20 % / 50 - 95 % (30 h) pH 2*<br>10 – 30 % / 30 - 80 % (5 h) pH 7.4* | [45] |
| | Leuprolide | 33 - 47 | n.a. | No / 40 - 50 % (2 d) pH 7.4* | [48] |
| | | 66 - 72 | n.a. | n.a. | [49] |

*AE: association efficiency (100 x associated peptide mass / total peptide mass); BSA: bovine serum albumin; LC: loading capacity (100 x peptide mass / total formulation mass); n.a.: not applicable; Ref.: references; sCT: salmon calcitonin; theor.: theoretical; *Enzyme supplemented.*

## 3. Solid lipid nanoparticles (SLN)

SLN are nanoparticles made of solid lipids and stabilized by surfactants. These SLN, which were first described in the 90's [50,51], have the peculiarity of being in a solid form at both, room and body temperatures [52]. Among the wide variety of lipids, the long chain triglycerides, fatty acids and phospholipids are the most commonly used for producing SLN [2]. These lipids prevent SLN from rapid degradation, thereby facilitating the control of the drug release [52,53].

### 3.1. Preparation techniques

A variety of techniques summarized in *Table 2* have been proposed for the preparation of peptide-loaded SLN. The use of high pressure and temperature, the need of organic solvents, and/or the requirement of sophisticated equipment are the main parameters conditioning the choice of the technique to be used to prepare protein/peptide-loaded SLN.

***Table 2.*** *Main characteristics of the most commonly used preparation methods for SLN.*

| Technique | | Principle | Stress exposure | Organic solvents | Simplicity |
|---|---|---|---|---|---|
| **Microemulsi-fication / solidification** | | Precipitation of the lipidic phase of a ME by dispersing it in cold water | Low exposure to T > MP of the lipid | No necessarily | ++ |
| **HPH** | **Hot HPH** | Solidification of a NE previously homogenized under heating by cooling it down | High exposure to T > MP of the lipid; High pressure (100-200 bar) | No | + (special equipment) |
| | **Cold HPH** | Cavitation of a pre-suspension by homogenizing it at ≤RT | Low exposure to T > MP of the lipid; High pressure (100-200 bar) | No | + (special equipment) |
| **Double emulsion - solvent evaporation** | | Precipitation of the lipidic phase of a W/O/W emulsion after evaporating its solvent | No | Yes | ++ |
| **Nanopre-cipitation** | | Precipitation of a lipid blend by the diffusion of the solvent into an aqueous phase | No | Yes | ++ |
| **Supercritical fluid technology** | | Wide variety of methods based on supercritical fluid | Depending on the method and the SCF used (usually $CO_2$: $T_c$=31.1 °C; $p_c$=73.8 bar) | No necessarily | -- (special equipment) |

*HPH: high pressure homogenization; ME: microemulsion; MP: melting point; NE: nanoemulsion; $p_c$: critical pressure; SCF: supercritical fluid; RT: room temperature; $T_c$: critical temperature.*

***i)*** **Microemulsification/solidification**

This method, originally developed by Gasco and coworkers [51,54] involves two different steps (*Figure 5*). First, a W/O/W microemulsion containing the hydrophilic peptide in its internal aqueous phase is formed by adding an aqueous solution of the protein with the surfactant and co-surfactant(s) over a melted fatty acid/glyceride mixture (65 – 70 °C). This W/O microemulsion is then emulsified with a second aqueous phase containing surfactants. The second step consists on the dispersion of this W/O/W microemulsion in cold water (2 – 3 °C) under mild mechanical stirring [52,55]. The addition of this thermodynamically stable microemulsion to water leads to the precipitation of its lipidic phase forming small particles [11,54]. Alternatively to the double emulsion approach, a

primary O/W emulsion containing the hydrophilic peptide as hydrophobic ion pairing in the internal phase can be used [11].

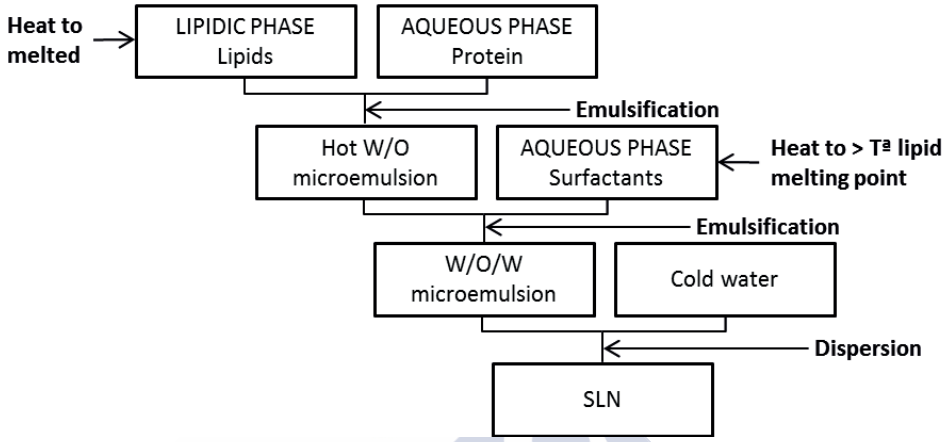



***Figure 5.*** *Schematic view of the W/O/W microemulsion-based technique to produce SLN.*

***ii)*** **High pressure homogenization (HPH)**

High pressure homogenization is a well-established technique for the preparation of SLN, which can operate either at hot or cold temperature.

**- Hot Homogenization.** The formation of SLN through this approach involves three different steps (*Figure 6*). Generally, this method is limited to the encapsulation of hydrophobic peptides/proteins. First, a lipidic phase containing the drug either solubilized or dispersed is melted and dispersed into an aqueous surfactant-containing phase at the same temperature using a high-shear mixing device. This hot pre-emulsion consisting of micrometric droplets is then homogenized under heating until the desirable O/W nanoemulsion is formed. SLN are obtained by simply leaving the system to cool down [56].

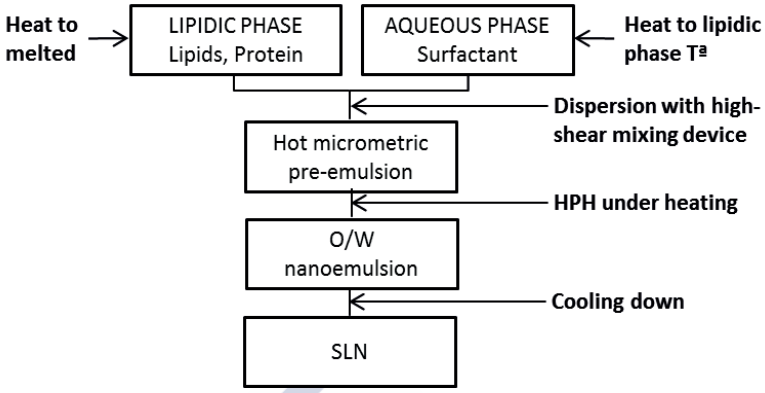



***Figure 6.*** *Schematic view of the hot high pressure homogenization (HPH) technique to produce SLN.*

**- Cold homogenization.** The cold homogenization process emerged as an alternative to the hot procedure to minimize the drug exposure to high temperatures (*Figure 7*). However, in this case it is still necessary to heat the lipids above their melting point in order to obtain a liquid phase in which the drug can be solubilized (if hydrophobic) or dispersed as an aqueous solution (if hydrophilic). Then, this melted blend is rapidly solidified, by cooling it down, using dry ice or liquid nitrogen. The obtained solid lipid matrix is then grinded in a powder mill until micrometric particles are formed. In a second step, these micrometric particles are dispersed into an emulsifier solution at or below room temperature to form a pre-suspension. Then, a final high speed homogenization process is carried out in order to break the micrometric particles into SLN [57].

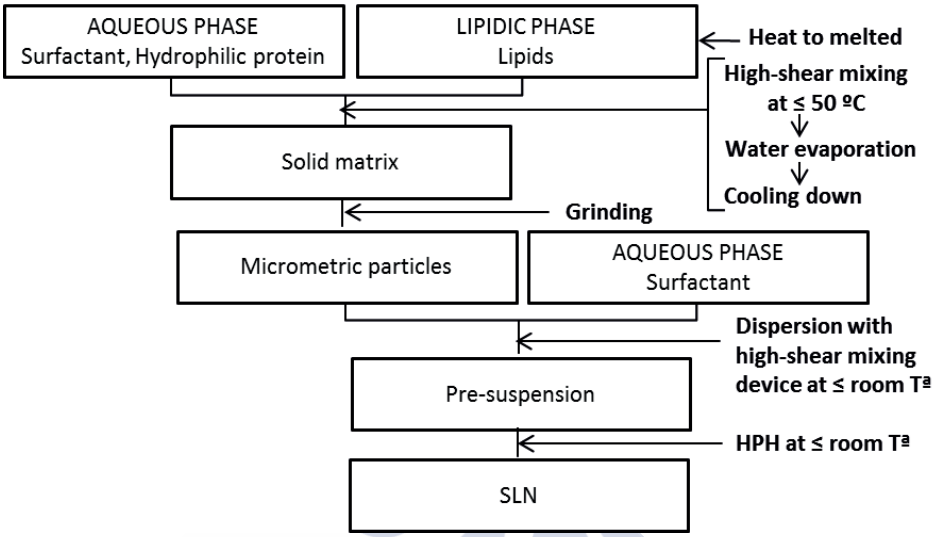



***Figure 7.*** *Schematic view of the cold high pressure homogenization (HPH) technique to produce SLN.*

***iii)*** **Double emulsion – solvent evaporation**

Sjöström and Bergenståhl were the first describing SLN prepared through its precipitation from O/W emulsions (*Figure 8*) [58]. To our knowledge, our group was the first adapting this method for the entrapment of hydrophilic protein/peptides by the incorporation of the double emulsion approach [59]. As a first step, an aqueous solution of the protein/peptide drug is emulsified using sonication into an organic phase consisting of lipids and a water-immiscible solvent. Then, this W/O emulsion is emulsified using sonication into an external aqueous phase containing surfactants, leading to the formation of a W/O/W double emulsion. Finally, the organic solvent is removed by evaporation, thereby inducing the precipitation of the lipids in the aqueous phase in the form of nanoparticles [6,7].

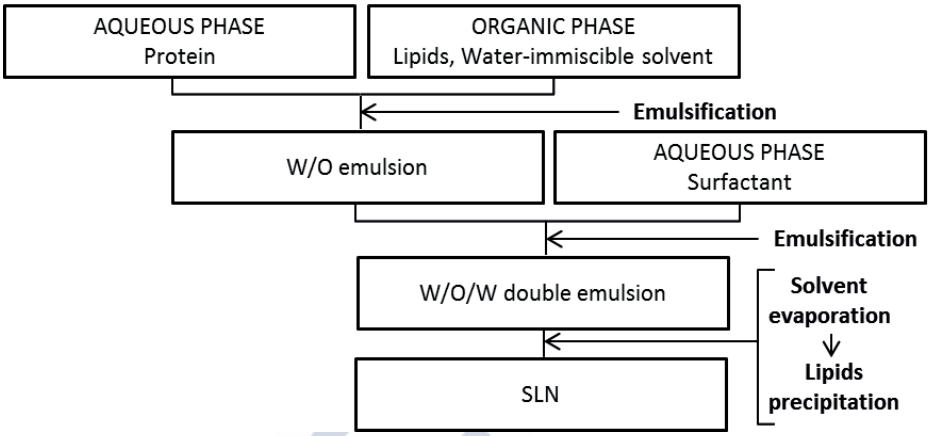



***Figure 8.*** *Schematic view of the double emulsion – solvent evaporation technique to produce SLN.*

***iv)*** **Nanoprecipitation**

This technique, illustrated in *Figure 9*, is based on the dispersion of a polar solvent containing the peptide/protein and the lipids in a water phase. Due to the immediate diffusion of the solvent the lipids precipitate entrapping the peptide/protein meanwhile. In principle, this technique is adapted for the encapsulation of hydrophobic peptides rather than hydrophilic proteins. However, there is also the possibility to co-dissolve a water-soluble peptide in a water/polar solvent mixture. In some instances the use of high temperature may help to co-dissolve the drug and lipids in the polar solvent [60,61].

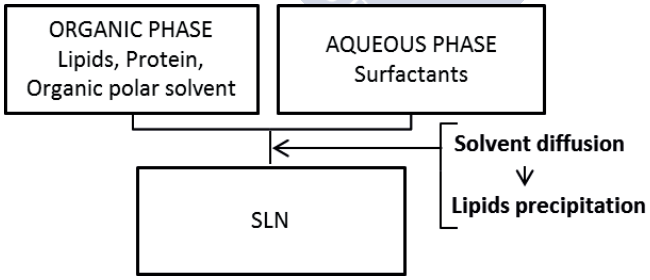



***Figure 9.*** *Schematic view of the nanoprecipitation technique to produce SLN.*

***v)* Supercritical fluid technology**

A new wide range of techniques based on the supercritical fluid technology have recently emerged to produce solvent-free lipid nano- and microcarriers. However, there is very limited information about protein encapsulation through these novel methods. The drug solubility in the supercritical fluid (usually $CO_2$) is the main parameter to be considered for choosing the most appropriate procedure [62].

## 3.2. Characterization, peptide/protein loading, activity and release profile

The physicochemical and pharmaceutical properties of SLN might be influenced by the type of fabrication technique and the formulation variables. An overall analysis of the characteristics of SLN is as follows.

**- Particle size distribution:** the final size of the SLN is generally influenced by the physicochemical properties (e.g. hydrophilicity, crystallization rate and crystal's shape) and concentration of the lipids in the organic phase. A high viscosity of the lipid phase may hamper its dispersion into the water phase leading to the formation of large particles. The final size is also affected by physical factors, such as the temperature, the homogenization pressure applied during the particle formation, and the number of cycles needed to obtain the formulation. Generally, low polidispersity indexes are obtained when using high stirring rates or high number of homogenization cycles [50,52,63,64].

**- Peptide/protein loading and activity:** in 1994,Morel et al. attempted for the first time to encapsulate peptides ([D-Trp-6] LHRH and thymopentin) into SLN [11,54] using the microemulsion based technique. Generally, the drug to be encapsulated in SLN is incorporated either directly in the lipidic phase (if hydrophobic) or using a W/O/W double emulsion approach by dissolving it in the internal aqueous phase (if hydrophilic). High AEs (79−98 %) and loading capacities (LCs) (6−13 %) were attained for hydrophobic peptides such as cyclosporine A using either the microemulsion-based technique [65] or the HPH methods [56]. However, for hydrophilic drugs, SLN have shown limited drug LC, being the solubility of the drug in the lipid matrix the main factor driving the AE [66]. To improve the incorporation of hydrophilic macromolecules into SLN a number of strategies highlighted in *Section 1* have been described. Among them, the double emulsion technique (W/O/W) including or not surfactants in the internal aqueous phase to form reverse micelles has been relatively successfully. This technique was first described by our group for the encapsulation of peptides into SLN, leading to the efficient association (90 %) of salmon

calcitonin (sCT) [6,7]. The addition of surfactants, i.e. bile salts, into the internal aqueous phase may lead to the formation of peptide-containing micelles. This approach has led to high AE and LC values for peptides such as sCT [67]. The inclusion of the positively charged sCT and insulin in negatively charged micelles was supposedly the factor favoring the retention of the peptide in the solid core. In fact, some authors showed that the increase of the bile salt concentration and its ratio with the oily phase surfactant had a clear impact on the insulin association efficiency (AE from 20 up to 99 %) [68].

When using the nanoprecipitation method, variables such as the temperature of the dispersed aqueous phase was found to influence the encapsulation of hydrophilic peptides, i.e. gonadorelin (50 % AE at 25 °C vs. 69 % at 0 °C). This improvement can be attributed to the rapid solidification of the lipid droplets at low temperature, which would facilitate the entrapment of the peptide [60].

As indicated, the protein/peptide stability is generally influenced by the presence of organic solvents (e.g. double emulsion/solvent evaporation or nanoprecipitation methods), high shear mechanical agitation and pressure (e.g. HPH method), high temperatures (e.g. microemulsification/solidification and HPH methods) or sonication processes (double emulsion/solvent evaporation method) [7,8,11,69]. The protein integrity and activity has been usually analyzed using the same techniques described for liposomes in the previous *Section 2.2.* (i.e., SDS-PAGE, capillary electrophoresis, enzymatic assays and *in vivo* studies) [6–8,11,57].

**- Peptide/protein release:** data indicated in *Table 3* highlight the high variability in the release profiles observed for different peptides/proteins entrapped in a variety of SLN [6,59,60]. Although in some works, no burst release was reported, normally there is a variable amount of peptide accumulated at the O/W interface during the production process that is released prematurely [52]. This burst effect and the subsequent release profile has been modulated following specific formulation approaches. In particular, the overall release profile is highly dependent on the SLN composition, since it is mainly governed by the peptide diffusion through the channels, originally present in the matrix, and enlarged in the course of the lipase-mediated lipids degradation [59]. These findings suggest that a selection of the lipidic components is important in order to modulate the protein/peptide release.

It is important to highlight the possibility of an interaction between the peptide/protein and the lipid components and their degradation products. For example, in a work

intended to encapsulate leuprolide acetate into SLN using the nanoprecipitation technique, the use of a hydrophobic ion pairing complex between leuprolide and sodium stearate led to a considerable reduction of the burst effect (1 h burst release: 10 % vs. 45 %). Following this initial fast release, the peptide was slowly released for up to 2 days [61]. In another example the sustained release of sCT (40−45 % in 6 h) from chitosan-coated SLN produced by the double emulsion-solvent evaporation method was attributed to the high affinity of the positively charged sCT for the negatively charged lipids (lecithin and tripalmitin) [6].

The incorporation of PEG into the lipid matrix has also been proposed as a strategy to modulate the release profile. For example, the release of insulin from SLNs produced by the supercritical fluid technology, could be controlled by incorporating 5 kDa PEG in the lipid mixture as a pore-forming agent [70]. Indeed, the total amount of insulin associated to PEG-containing SLNs was released in 3 days, whereas PEG-free SLNs needed 5 days to deliver their content.

From the results in literature up to date (*Table 3* shows some examples), we can conclude that the release of peptides from SLN is affected by the composition of the lipidic matrix (governing the degradation of the particles) and by the affinity of the peptide/protein towards the formulation components. Normally, the *in vitro* release of the proteins/peptides is prolonged for a few days, however, it could be expected that in an *in vivo* situation the process could be accelerated depending on the degradation rate of the lipidic matrix.

***Table 3.*** *Examples of peptide/protein-loaded SLN obtained through the different preparation methods: drug loading and release properties.*

| Preparation method | Specific strategy | Peptide/ Protein | AE (%) | LC (%) | ≤1h burst / cumulative release (time) – pH medium | Ref. |
|---|---|---|---|---|---|---|
| **Micro-emulsion-based technique** | **-** | CyA | n.a. | 6 - 13 | <4 % / <4 % (2 h) pH 7.4 | [65] |
| | **Double emulsion** | [D-Trp-6] LHRH | 90 | n.a. | <3 % / 10 % (8 h) pH 6.5 | [54] |
| | | Thymo-pentin | 2 | n.a. | <5 % / 10 % (6 h) pH 6.5 | [11] |
| | **Hydrophobic ion pairing** | Thymo-pentin | 5 | n.a. | <5 % / 10 % (6 h) pH 6.5 | |
| **Hot HPH** | **-** | CyA | 95 - 98 | 0.5 - 2 theor. | n.a. | [56] |
| | | | 96 | 1.9 | n.a. | [71] |
| **Cold HPH** | **-** | CyA | 79 - 94 | 0.5 - 2 theor. | n.a. | [56] |
| | | Lysozyme | 43 - 59 | 0.03 | n.a. | [57] |
| **Emulsion – solvent evaporation** | **Double emulsion** | sCT | 31->90 | n.a. | <30 % / <45 % (6 h) pH 4 | [6,7] |
| | **Double emulsion / Reverse micellization** | sCT | 88 - 95 | 5 - 11 | 60 - 100 % / 100 % (2 h) pH 6.8* | [67] |
| | | Insulin | 76-100 | 19 | 0 - 35 % / 60 - 90 % (6 d) pH 7.4 | [68] |
| **Nanopreci-pitation** | **-** | Gonado-relin | 50 - 69 | n.a. | <30 % / <80 % (14 d) pH 6.8 | [60] |
| | | Leupro-lide | 28 | 0.3 | <45 % / 100 % (2 d) pH 6.8 | [61] |
| | **Hydrophobic ion pairing** | Leupro-lide | 46 | 0.5 | <10 % / 100 % (2 d) pH 6.8 | |
| **Supercritical fluid technology** | **-** | Insulin | 20 - 80 | 1 - 4 | 0 - 17 % / 100 % (6 d) pH 7.4 | [70] |
| | | | 57 | 2.9 | <10 % / 100 % (4 d) pH 7.4 | [72] |
| | | rh-GH | 48 | 2.4 | <5 % / 100 % (4 d) pH 7.4 | |

*AE: association efficiency (100 x associated peptide mass / total peptide mass); CyA: cyclosporine A; [D-Trp-6] LHRH: agonist triptorelin - luteinizing hormone-releasing hormone; HPH: high pressure homogenization; LC: loading capacity (100 x peptide mass / total formulation mass); n.a.: not applicable; Ref.: references; rh-GH: recombinant human growth hormone; sCT: salmon calcitonin; theor.: theoretical; *Enzyme supplemented.*

## 4. Microemulsions and Nanoemulsions

Both, water-in-oil (W/O) and oil-in-water (O/W) microemulsions are usually considered as thermodynamically stable and isotropic systems, displaying sizes below 100 nm. The microemulsion formation has been described as a spontaneous process that occurs after mixing the oil and the water phases containing a certain amount of surfactants, in order to achieve a low interfacial tension between the two phases [73]. Nanoemulsions have also been described as colloidal dispersions that generally display sizes below 200 nm. In contrast with microemulsions, these systems are not isotropic. The nanoemulsion formation requires an external energy input in order to overcome their positive free energy and increase their contact area, leading to the formation of a kinetically stable colloidal dispersion [74]. A special type of emulsions is the one present in the self-emulsifying drug delivery systems (SEDDS) and the self-micro-emulsifying drug delivery systems (SMEDDS) which typically consist of mixtures of oil, surfactant and co-surfactants. Recently, many of these SMEDDS have been classified as self-nanoemulsifying systems (SNEDDS) [75]. Among the wide variety of lipids, the long and medium chain glycerides and fatty acids are the most commonly used for the preparation of self-emulsifying systems, microemulsions and nanoemulsions containing peptides [2]. Medium chain fatty acids are known to improve the peptide solubility and facilitate the emulsification process since their mixture with the aqueous phase is easier.

### 4.1. Preparation techniques

A wide variety of methods have been developed to produce micro/nanoemulsions. These techniques can be classified depending on the procedure used to supply energy to the system [76–78], being broadly categorized into the following two groups: i) High-energy processes, which imply the application of mechanical and intensive disruptive forces to the different phases of the system. Special devices are necessary in order to intermingle the oily and the aqueous phases, leading to the formation of nanodroplets (homogenization, microfluidization and ultrasonication) [79–81]; ii) Low-energy processes (spontaneous emulsification and phase inversion), which are based on the spontaneous formation of nanoemulsions either by changing the composition (i.e., ratio surfactant:oil:water, addition of salts, etc.) or the process conditions (i.e., temperature-time profile, stirring, addition speed, etc.) [78,82–85]. Among the wide variety of techniques, those based on the spontaneous emulsification are, so far, the most

commonly used for the association of peptides/proteins. This is mainly due to the fact that this method avoids the peptides/proteins being exposed to any temperature or pressure stress.

***i)* Spontaneous Emulsification**

Through this method, the nanoemulsion is spontaneously formed upon the mixture of the oily and the aqueous phases (*Figure 10*) [86,87]. The protein/peptide is included in one of them depending on its hydrophilicity or incorporated into the oily phase in a small amount of water. Both phases are immiscible in each other; however, one of the components present in one of them (i.e., an organic solvent, a surfactant) is partially miscible in both. Once the two phases are in contact, a non-equilibrium state is formed, causing the rapid shifting of the miscible component from its original phase into the other. This fact will lead to an increase in the oil-water interfacial area and turbulence, promoting the spontaneous formation of the nanoemulsion [88].

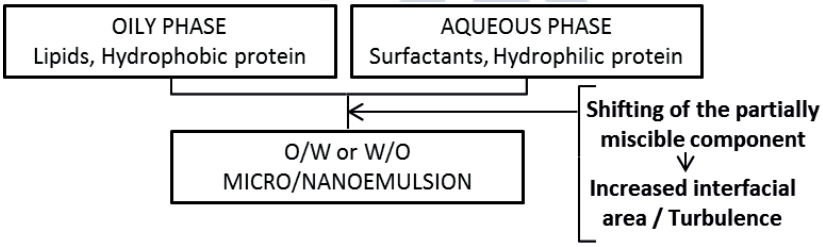



***Figure 10.*** *Schematic view of the spontaneous emulsification technique to produce nanoemulsions.*

## 4.2. Characterization, peptide/protein loading, activity and release profile

**- Particle size distribution:** by selecting appropriately the ingredients and the preparation method, emulsions showing a wide range of sizes, charges and physical properties can be obtained. The final size distribution of the emulsion can be modulated by optimizing its composition (concentration of the components, ratio surfactant:oil:water, interfacial tension, viscosity, emulsifier adsorption kinetics, etc.) and the operating conditions (temperature-time profile, stirring rate, pressure, amplitude of sonication and number of cycles, etc.) [89–92]. The use of ternary phase diagrams is an useful tool to predict the optimum conditions for the formation of the nanoemulsion [93,94].

**- Peptide/protein loading and activity:** the combination of the spontaneous emulsification technique with several specific strategies, such as, double emulsification, reverse micellization, hydrophobic ion paring or peptide-lipid/surfactant interaction (*Section 1*) has been effective for the loading of hydrophilic peptides (*Table 4*) such as insulin, with AEs higher than 85 % [5,14,95,96]. Among the factors influencing this association, it has been found that small variations in the final pH (from 6.5 to 6.8), may lead to sharp decreases in the AEs from 79 to 30 %. This result was attributed to the different ionization degree of both, the peptide and the polymer at the selected pHs, and their electrostatic and/or hydrophobic interactions [97]. Despite the good association efficiencies achieved, the loading capacity of these systems is usually lower than 1 % [9,98].

After system preparation, the loaded peptide/protein must be able to keep its activity. In fact, there are some operation conditions, i.e. the use of organic solvents and surfactants, which can lead to protein denaturation and/or aggregation. High shear agitations, temperatures or pressures can affect the integrity of the protein, as well [9,99,100]. In this regard, the use of ELISA assays has been reported as an efficient method to understand if the activity of the encapsulated protein is kept. However, in the specific case of micro- and nanoemulsions, direct *in vivo* evaluation of the formulation is the main approach reported to evaluate the efficacy of the loaded therapeutic agent [99,101].

**- Peptide/protein release:** only a few papers have been published dealing with the mechanism behind the release of the protein/peptide drugs from micro/nanoemulsions. In general, the release of the drug has been related to its partition between the emulsion and the surrounding medium and also to the alteration/degradation of the lipidic components. For example, when they are orally administrated, their contact with the gastrointestinal fluids can cause a phase inversion or separation of the emulsion phases, that may lead to a premature drug release [101,102]. The conversion of these liquid systems into solid forms through freeze drying, spray drying, melt granulation, melt extrusion or adsorption over solid carriers has been proposed as a way to overcome the colloidal instability of these systems [103]. Further improvements of this technology in order to optimize the delivery of hydrophilic drugs from self-emulsifying systems are still needed. However, for lipophilic peptides, some formulations, such as Neoral® (SMEDDS containing cyclosporine) have already been marketed [104].

***Table 4.*** *Examples of peptide/protein-loaded micro/nanoemulsions and SEDDS/SMEDDS/SNEDDS obtained through the spontaneous emulsification method: drug loading and release properties.*

| System | Specific strategy | Peptide/ Protein | AE (%) | LC (%) | ≤1h burst/ cumulative release (time) – pH medium | Ref. |
|---|---|---|---|---|---|---|
| **O/W** | - | sCT | > 90 | n.a. | n.a. | [100, 105] |
| | | Pliti-depsin | 95-98 | 0.54 | n.a. | [106] |
| **W/O** | - | TAT | 97 | 0.006 TAMRA-TAT | 90 % (1 h) pH 6.8* | [101] |
| | | rhPTH1-34 | 83 | n.a. (45 mg/mL) | 100 % (50 min) pH 8*<br>65 % / 80 % (2 h) pH 2* | [107] |
| | | Insulin + aprotinin | 97 | 0.1 (30 IU/g) | 0 % (1 h) pH 1.2* | [99] |
| | **Reverse micelles** | Insulin | > 85 | n.a. (2.2 % w/v theor.) | n.a. | [5] |
| | **Hydrophobic ion pairing** | Insulin | 30 - 79 (complex-ation) | n.a. | <10 % (1 h) pH 1.2* | [97] |
| **W/O/W** | **Double emulsion** | Insulin | 96 - 97 | n.a. (18 IU/g) | 0 - 80 % / 0 - 80 % (1.5 h) pH 7 | [95] |
| | | Insulin + aprotinin | 88 - 97 | 0.075 | 20 - 30 % / 20 - 30 % (2 h) pH 7 | [96] |
| | | sCT + aprotinin | n.a. | n.a. (400 IU/g theor.) | 90 % / 100 % (2 h) pH 6.4/1.2*<br>80 % / 80 % (2 h) pH 7.5* | [108] |
| **SMEDDS SNEDDS** | **Hydrophobic ion pairing** | Insulin | 64 - 71 | 0.3-1.1 | 15 % / 30 % (8 h) pH 7.4 | [98] |
| | | Leupro-relin | 59 (complex-ation) | 0.4 theor. complex | <20 % / 40 % of complex (30 h) pH 6.8 | [9] |
| | **Hydrophilic-hydrophobic interactions** | Insulin | 85 - 99 | n.a. | 1 % / 14 % (24 h) pH 7.4 | [14] |

*AE: association efficiency (100 x associated peptide mass / total peptide mass); LC: loading capacity (100 x peptide mass / total formulation mass); n.a.: not applicable; Ref.: references; rhPTH1-34: recombinant 1-34 N-terminal fragment of endogenous human parathyroid hormone; sCT: salmon calcitonin; TAMRA: tetramethylrhodamine; TAT: HIV transactivator of transcription; theor.: theoretical; *Enzyme supplemented.*

## 5. Nanocapsules

Nanocapsules are core-shell structured drug delivery carriers. They consist of an oily core which is stabilized by surfactants and it is surrounded by one or more polymer shells [109]. Both, core and outer shell layers, play a crucial role in the outcome of the formulation: whereas the core usually works as a drug reservoir, the polymer coating helps the associated drug to overcome biological barriers and modulate its release profile. Among the wide variety of lipids, the long chain fatty acids and the medium chain glycerides (mono-, di- and tri-), both showing penetration enhancer properties, are the most commonly used for producing nanocapsules [2].

### 5.1. Preparation techniques

The preparation of nanocapsules involves the emulsification of an oily phase into an aqueous phase. The polymer forming the shell can be incorporated into the organic phase or the aqueous phase [110,111]. Additionally, two different polymers can be incorporated one in each phase [112,113]. The shell is formed due to its precipitation at the interphase or to an ionic interaction between the oily core and the polymer. In a different situation, i.e. poly(alkylcyanoacrylates), the polymer shell is formed due to an interfacial polymerization process [114,115]. The main factors driving the choice of the appropriate nanocapsules production technique are the nature of the polymer as well as that of the peptide/protein to be encapsulated (*Table 5)*.

***Table 5.*** *Main characteristics of the most commonly used preparation methods for nanocapsules.*

| Technique | | Principle | Stress Exposure | Organic solvents | Simplicity |
|---|---|---|---|---|---|
| ***"In situ"* polymerization / Interfacial polymerization** | **Oily core nanocapsules** | Monomers polymerization "*in situ*" at the inter-face of an emulsion | Undesirable reactions drug-monomers / Vigorous stirring | Yes | + |
| | **Aqueous core nanocapsules** | | | No necessarily | |
| **Polymer precipitation/ deposition** | **Solvent displacement** | Solvent diffusion to the aqueous phase and polymer precipitation/deposition | Moderate stirring | Yes | ++ |
| | **Self-emulsification** | Surfactant shifting from the oily to the aqueous phase and polymer deposition | High surfactant concentration / Moderate stirring | No | ++ |

***i) "In situ" p*olymerization**

In this method, which is also named as interfacial polymerization, the polymer formation occurs "*in situ*" at the interface of an emulsion through a fast polymerization among reactive monomers. Due to their rapid and easy polymerization, alkylcyanoacrylates have been the monomers of choice for this purpose [116,117]. Unfortunately, the potential reaction between the drug and the reactive monomers during the process constitutes a limitation of this approach [118].

**- Interfacial polymerization in oily core nanocapsules**. In this case, the organic phase is composed by the peptide/protein, the oil, the monomers and an organic solvent. The solvent needs to be water-miscible in order to promote its diffusion towards the aqueous phase, allowing the spontaneous formation of nanometric oily droplets [119]. The organic phase is usually injected into the aqueous phase, which contains at least a hydrophilic surfactant. This process is usually performed under vigorous stirring, leading to the instantaneous formation of the nanocapsules (*Figure 11*). An additional final step to remove the organic solvents can be performed [115,117].

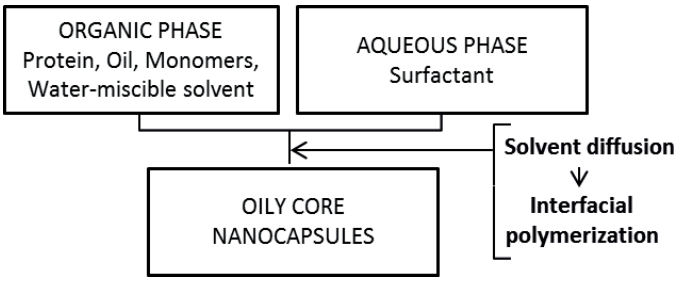



***Figure 11.*** *Schematic view of the interfacial polymerization technique to produce oily core nanocapsules.*

**- Interfacial polymerization in aqueous core nanocapsules**. In this method, the aqueous phase, which contains the protein/peptide, water and sometimes water-miscible solvent, is emulsified into an organic phase consisting of oil and a lipophilic surfactant using sonication or vigorous stirring. Once the W/O emulsion is formed, the monomers are added under mechanical stirring. This last step, triggers the polymerization at the W/O interface and leads to a final system consisting of aqueous core nanocapsules dispersed in oil (*Figure 12*) [120,121]. The nanocapsules are finally isolated by ultracentrifugation followed by their resuspension in water [122,123].

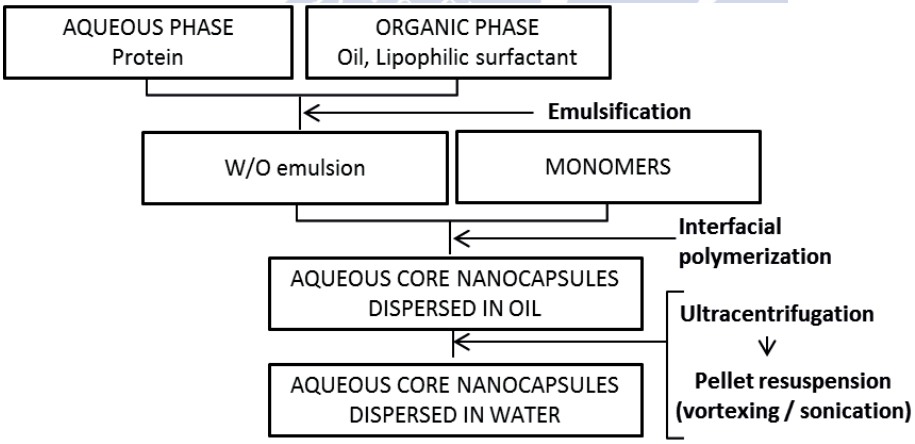



***Figure 12.*** *Schematic view of the interfacial polymerization technique to produce aqueous core nanocapsules.*

***ii)* Polymer precipitation/deposition**

Contrarily to the "*in situ*" polymerization, the use of preformed polymers allows a good control of the final polymer molecular weight, avoiding undesirable reactions between the drug and monomers. In this case, the polymer coating can be formed by either polymer precipitation or polymer deposition/interaction.

**- Polymer precipitation**. This technology was first reported by Fessi and coworkers [124,125]. This method involves the use of an organic polar phase containing a lipophilic surfactant, oil, and the polymer, and an aqueous phase, that may contain hydrophilic surfactants. The usual procedure can be summarized as follows (*Figure 13*): the organic phase is added dropwise over the aqueous phase under moderate stirring leading to the instantaneous diffusion of the water-miscible solvent from the lipophilic solution to the aqueous phase. As a consequence, the polymer precipitates at the interface of the formed oily droplets, stabilizing them. In a final step, solvents can be removed by evaporation under vacuum [110,112,125].

**- Polymer deposition/interaction**. Alternatively, nanocapsules can be produced using water soluble polymers according to a deposition/interaction technique. In this case, the polymer shell is formed due to its ionic interaction with the lipophilic components of the oily core. This interaction may occur during the solvent displacement process or after the incubation of the preformed nanoemulsion with the water-soluble polymer [105,111,126,127]. Additionally, the possibility of obtaining multi-layer nanocapsules has been reported. This layer by layer approach is based on the adsorption of different polymeric layers onto a colloidal template. The addition of each polymeric layer should invert the overall charge of the system in all the absorption steps [109]. Our group has reported the possibility of obtaining protein-loaded nanocapsules by triggering the polymer deposition by a **self-emulsification** method avoiding the use of organic solvents. The principle of this technique is the same described in *Section 4.1.* for the spontaneous formation of micro/nanoemulsions (*Figure 10*), including, additionally, a water-soluble polymer into the aqueous phase [128] or in a subsequent incubation step [129,130].

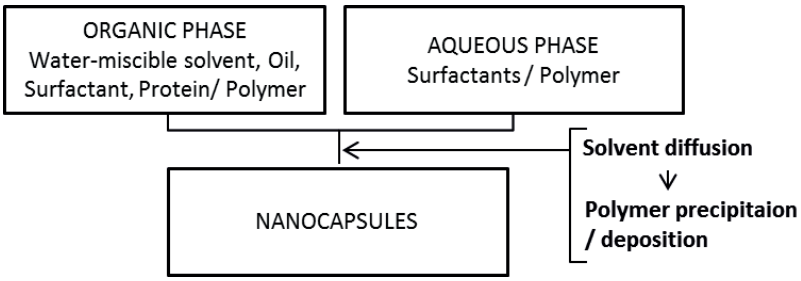



***Figure 13.*** *Schematic view of the solvent displacement - polymer precipitation/deposition technique to produce nanocapsules*

## 5.2. Characterization, peptide/protein loading, activity and release profile

**- Particle size distribution:** the main factors affecting the final particle size distribution of nanocapsules are the ratio and the mixing conditions between the two phases, as well as the physicochemical properties and concentration of the different components [100,110,111,131,132]. Overall, nanocapsules have been produced so far with a size between 30 and 400 nm.

**- Peptide/protein loading and activity:** Couvreur and coworkers were the first reporting the possibility of using nanocapsules as delivery vehicles for proteins [115]. Since their contribution through the encapsulation of insulin in poly(alkyl cyanoacrylate) nanocapsules, several authors have demonstrated the capability of nanocapsules to entrap different peptides/proteins (*Table 6*). Despite the high AEs attained, the LC values reported so far are below 2 %, which is usually due to the hard solubilization of hydrophilic peptides into the lipidic phase and their tendency to diffuse to the outer aqueous phase [122]. When nanocapsules are obtained by interfacial polymerization, the monomer concentration has been proved to be one of the main factors influencing the peptide association efficiency [133]. The pH of the peptide solution has also been shown to influence the AE of peptides to poly(alkyl cyanoacrylate) nanocapsules. This effect is attributed to the influence of the pH on the polymerization rate of the polymer [131].

Our group has also shown the possibility to attach proteins to preformed polymer nanocapsules. For example, we have efficiently associated the recombinant hepatitis B surface antigen (rHBsAg) onto preformed chitosan nanocapsules. In this situation the attachment of the protein was found to be dependent on both protein and nanocapsules

concentration and the mechanism of attachment was based on ionic/hydrophobic interactions [134–136].

Different formulation parameters could influence the peptide/protein structure. With "*in situ*" polymerization the drug could work as a monomer during the polymerization procedure, being denatured and losing its activity. However, ethanol can be used to preserve the peptide/protein structure [137]. Furthermore, in all the techniques described above for nanocapsules production, the presence of organic solvents and surfactants, as well as the vigorous stirring, could also affect the structure of the encapsulated peptide/protein [122,126,131]. Electrophoresis-based techniques (e.g. native SDS-PAGE), HPLC-based methods or circular dichroism have been reported to study the structural stability of nanoencapsulated peptides/proteins [122,131,137]. However, in the majority of the works, the activity of the encapsulated drug was evaluated after its *in vivo* administration [110,126,138].

**- Peptide/protein release:** the mechanism driving the release of peptides/proteins entrapped into nanocapsules has been defined as a combination of two main processes: the partition of the drug between the nanocarrier and the external release medium and the degradation of the polymer shell and the lipid core. Both processes can be affected by different factors, such as the pH of the release medium, the nature of the lipidic cores, the type and molecular weight of the polymer, as well as the thickness of the polymer shell [121,126,132,139]. BSA cumulative releases ranging from 35 % up to 90 % were reported for poly(butylcyanoacrylate) nanocapsules after 8 h in release media with different pHs (from 2.5 to 8.5) and different profiles were showed when poly(butylcyanoacrylate) of 4, 7 or 10 kDa was used. Likewise, the loading and the molecular weight confer the protein with different diffusion capacities and specific interactions with the components of the system. High loadings increase the protein gradient between the nanocapsule core and the outer phase, and proteins with high molecular weights diffuse more slowly through the polymeric wall [122]. On the other hand, when the protein is attached to the polymer shell, the mechanism of release is based on its disassociation [140] and this process is normally dependent on the pH and ionic strength of the release medium.

From the results in literature up to date, we can conclude that the solvent displacement technique is the most advantageous for encapsulating hydrophilic peptides in nanocapsules. Apart from its simplicity, and the possibility of controlling the exact

molecular weight of the polymer and avoiding undesirable cross-reactions, high association efficiencies can be attained.

***Table 6.*** *Examples of peptide/protein-loaded nanocapsules obtained by the different preparation methods: drug loading and release properties.*

| Preparation method | Peptide / Protein | AE (%) | LC (%) | ≤1h burst / cumulative release (time) – pH medium | Ref. |
|---|---|---|---|---|---|
| **Interfacial polymerization (Oily / Aqueous core)** | Insulin | 55 - 98 | n.a. | n.a. | [115,141, 142] |
| | | 90 | n.a. (0.45 mg/mL) | 10 % / 13 % (5 h) pH 7.4/1–2* 77 % / 80 % (5 h) pH 6-7* | [154, 160, 161] |
| | | 57 - 95 | n.a. | n.a. | [148, 162] |
| | | 100 | n.a. | n.a. | [146] |
| | Human calcitonin | 35 - 79 | n.a. (0.0067 - 0.67 mg/mL theor.) | 40 - 60 % (20 min) pH 7.4* | [147] |
| | Octreo-tide | 60 | n.a. | n.a. | [114] |
| | Insulin | 63 - 97 | n.a. | 25 - 50 % / 50 - 70 % (6 h) pH6.8 No / <5 % (2 h) pH 1.2 | [137, 138] |
| | | 12 - 52 | 0.6 - 1.8 | 35 - 90 % / 80-100 % (6h) pH 6.8 | [156, 165] |
| | OVA | 8 - 95 | n.a. | n.a. | [133] |
| | BSA | 90 | n.a. | n.a. | [149] |
| | | n.a. | 1 - 4 | 15 - 60 % / 60 - 90% (9 h) pH 7.4 15 - 50 % / 40 – 80 % (8 h) pH 2.5/5.5/7.2/8.5 | [122] |
| | D-Lys6-GnRH | 95 - 99 | n.a. | No / <11 % (5 d) pH 7.4 No / <5 % (6 h) pH 6.8*/1.2* <60 % / <60 % (4 h) pH 7.4* | [167, 168] |
| **Polymer precipitation** | CyA | 99 | n.a. | 75 % (5 min) pH 7.4 | [110] |

USC UNIVERSIDADE DE SANTIAGO DE COMPOSTELA

| Preparation method | Peptide / Protein | AE (%) | LC (%) | ≤1h burst / cumulative release (time) – pH medium | Ref. |
|---|---|---|---|---|---|
| Polymer deposition/ interaction | Insulin | 51 - 62 | 0.8 - 1 | 20 - 30 % / 20 - 40 % (6 h) pH 1.2/6.8/7.1<br>40 - 70 % / 65-80 % (2h) pH 6.8* | [111] |
| | | 99 | n.a. (0.5 mg/mL) | n.a. | [137] |
| | Elipsi-depsin | 46 - 54 | n.a. (0.25-1.6 mg/mL theor.) | n.a. / 10 % (4 h) pH 6.8 | [138] |
| | Pliti-depsin | 98 - 99 | 0.54 | 60 - 70 % / 60-70% (24 h) pH 7.4 | [106] |
| | sCT | 44 - 60 | n.a. | 10 – 20 % / 10-20 % (6 h) pH 4 | [123, 143, 144] |
| | rHBsAg | 55 - 83 | n.a | n.a | [134–136] |
| | CyA | 95 | 5 | n.a. | [129] |

*AE: association efficiency (100 x associated peptide mass / total peptide mass); BSA: bovine serum albumin; CyA: cyclosporine A; D-Lys6-GnRH: agonist gonadotropin releasing hormone; LC: loading capacity (100 x peptide mass / total formulation mass; n.a.: not applicable; OVA: ovalbumin; Ref.: references; rHBsAg: recombinant hepatitis B surface antigen; sCT: salmon calcitonin; theor.: theoretical; *Enzyme supplemented.*

## 6. Conclusions

All the above described technologies and related biomaterials have specific advantages and disadvantages. From the technological point of view, the use of solvent-free and energy-free approaches, which do not require chemical reactions, are obviously desirable. Lipid microemulsions, nanocapsules and polysaccharide-based nanoparticles are those nanosystems that can be produced according to the mild indicated techniques. However, a limitation of the lipid-based nanosystems is their limited loading capacity. Overall, the conclusion is that despite the important advances in the field, there is still a need to optimize the nanocarriers' properties for the desired peptidic drug through a rational design. In this regard, the capability of the nanocarrier to efficiently entrap, appropriately release and preserve the integrity of the protein/peptide loaded are so far the critical parameters to consider. Up until now, most nanocarriers have been limited in their composition and architectural design. The current design may need to imply the use of a combination of biomaterials conveniently organized within the nanosystems internal and

superficial structure. Hopefully, the use of these advanced nanocarriers as delivery platforms will allow in the early future the successful administration of a wide variety of potential therapeutic proteins/peptides.

## References

[1] I. Santalices, A. Gonella, D. Torres, M.J. Alonso, Advances on the formulation of proteins using nanotechnologies, J. Drug Deliv. Sci. Technol. 42 (2017) 155–180. doi:10.1016/j.jddst.2017.06.018.

[2] Z. Niu, I. Conejos-Sánchez, B.T. Griffin, C.M. O'Driscoll, M.J. Alonso, Lipid-based nanocarriers for oral peptide delivery, Adv. Drug Deliv. Rev. 106 (2016) 337–354. doi:10.1016/j.addr.2016.04.001.

[3] T. Karamanidou, V. Bourganis, O. Kammona, C. Kiparissides, Lipid-based nanocarriers for the oral administration of biopharmaceutics, Nanomedicine. 11 (2016) 3009–3032. doi:10.2217/nnm-2016-0265.

[4] P.L. Luisi, M. Giomini, M.P. Pileni, B.H. Robinson, Reverse micelles as hosts for proteins and small molecules, Biochim. Biophys. Acta (BBA)-Reviews Biomembr. 947 (1988) 209–246. doi:10.1016/0304-4157(88)90025-1.

[5] G. Sharma, K. Wilson, C.F. van der Walle, N. Sattar, J.R. Petrie, M.N.V. Ravi Kumar, Microemulsions for oral delivery of insulin: design, development and evaluation in streptozotocin induced diabetic rats, Eur. J. Pharm. Biopharm. 76 (2010) 159–169. doi:10.1016/j.ejpb.2010.07.002.

[6] M. Garcia-Fuentes, D. Torres, M.J. Alonso, New surface-modified lipid nanoparticles as delivery vehicles for salmon calcitonin, Int. J. Pharm. 296 (2005) 122–132. doi:10.1016/j.ijpharm.2004.12.030.

[7] M. Garcia-Fuentes, C. Prego, D. Torres, M.J. Alonso, A comparative study of the potential of solid triglyceride nanostructures coated with chitosan or poly(ethylene glycol) as carriers for oral calcitonin delivery, Eur. J. Pharm. Sci. 25 (2005) 133–143. doi:10.1016/j.ejps.2005.02.008.

[8] N. Zhang, Q. Ping, G. Huang, W. Xu, Y. Cheng, X. Han, Lectin-modified solid lipid nanoparticles as carriers for oral administration of insulin, Int. J. Pharm. 327 (2006) 153–159. doi:10.1016/j.ijpharm.2006.07.026.

[9] F. Hintzen, G. Perera, S. Hauptstein, C. Müller, F. Laffleur, A. Bernkop-Schnürch, In vivo evaluation of an oral self-microemulsifying drug delivery system (SMEDDS) for leuprorelin, Int. J. Pharm. 472 (2014) 20–26. doi:10.1016/j.ijpharm.2014.05.047.

[10] J.D. Meyer, M.C. Manning, Hydrophobic ion pairing: altering the solubility properties of biomolecules, Pharm. Res. 15 (1998) 188–193. doi:10.1023/A:1011998014474.

[11] S. Morel, E. Ugazio, R. Cavalli, M.R. Gasco, Thymopentin in solid lipid nanoparticles, Int. J. Pharm. 132 (1996) 259–261.

[12] G. Zhang, T. Wang, L. Gao, D. Quan, Oral delivery of oil-based formulation for a novel synthetic cationic peptide of GnRH (gonadotropin-releasing hormone) antagonist for prostate cancer treatment, Int. J. Pharm. 450 (2013) 138–144. doi:10.1016/j.ijpharm.2013.04.047.

[13] C. Zheng, M. Duan, H. Ma, H. Zhong, Zheng, Method for preparation of orally administrated insulin formulation, US 7018980 B2, 2006.

[14] E. Ma, H. Ma, Z. Liu, C. Zheng, M. Duan, In vitro and in vivo evaluation of a novel oral insulin formulation, Acta Pharmacol. Sin. 27 (2006) 1382–1388. doi:10.1111/j.1745-7245.2006.00424.x.

[15] A.D. Bangham, R.W. Horne, Negative staining of phospholipids and their structural modification by

surface-active agents as observed in the electron microscope, J. Mol. Biol. 8 (1964) 660–668. doi:10.1016/S0022-2836(64)80115-7.

[16] A.D. Bangham, M.M. Standish, J.C. Watkins, Diffusion of univalent ions across the lamellae of swollen phospholipids, J. Mol. Biol. 13 (1965) 238–252. doi:10.1016/S0022-2836(65)80093-6.

[17] D. Ibraheem, A. Elaissari, H. Fessi, Administration strategies for proteins and peptides, Int. J. Pharm. 477 (2014) 578–589. doi:10.1016/j.ijpharm.2014.10.059.

[18] E. Elizondo, E. Moreno, I. Cabrera, A. Córdoba, S. Sala, J. Veciana, N. Ventosa, Liposomes and other vesicular systems: structural characteristics, methods of preparation, and use in nanomedicine, 2011. doi:10.1016/B978-0-12-416020-0.00001-2.

[19] J. Swaminathan, C. Ehrhardt, Liposomal delivery of proteins and peptides, Expert Opin. Drug Deliv. 9 (2012) 1489–1503. doi:10.1517/17425247.2012.735658.

[20] F. Ahmed, D.E. Discher, Self-porating polymersomes of PEG-PLA and PEG-PCL: hydrolysis-triggered controlled release vesicles, J. Control. Release. 96 (2004) 37–53. doi:10.1016/j.jconrel.2003.12.021.

[21] B.M. Discher, Y.-Y. Won, D.S. Ege, J.C.-M. Lee, F.S. Bates, D.E. Discher, D.A. Hammer, Polymersomes: tough vesicles made from diblock copolymers, Science (80-. ). 284 (1999) 1143–1146. doi:10.1126/science.284.5417.1143.

[22] Z. Li, J. Chen, W. Sun, Y. Xu, Investigation of archaeosomes as carriers for oral delivery of peptides, Biochem. Biophys. Res. Commun. 394 (2010) 412–417. doi:10.1016/j.bbrc.2010.03.041.

[23] A. Pardakhty, J. Varshosaz, A. Rouholamini, In vitro study of polyoxyethylene alkyl ether niosomes for delivery of insulin, Int. J. Pharm. 328 (2007) 130–141. doi:10.1016/j.ijpharm.2006.08.002.

[24] A. Madni, M. Sarfraz, M. Rehman, M. Ahmad, N. Akhtar, S. Ahmad, N. Tahir, S. Ijaz, R. Al-Kassas, R. Löbenberg, Liposomal drug delivery: a versatile platform for challenging clinical applications, J. Pharm. Pharm. Sci. 17 (2014) 401–426. doi:10.18433/J3CP55.

[25] M.R. Mozafari, Liposomes : an overview of manufacturing techniques, Cell. Mol. Biol. Lett. 10 (2005) 711–719.

[26] A. Laouini, C. Jaafar-Maalej, I. Limayem-Blouza, S. Sfar, C. Charcosset, H. Fessi, Preparation, characterization and applications of liposomes: state of the art, J. Colloid Sci. Biotechnol. 1 (2012) 147–168. doi:10.1166/jcsb.2012.1020.

[27] A.K. Agrawal, H. Harde, K. Thanki, S. Jain, Improved stability and antidiabetic potential of insulin containing folic acid functionalized polymer stabilized multilayered liposomes following oral administration, Biomacromolecules. 15 (2014) 350–360. doi:10.1021/bm401580k.

[28] Y.P. Patil, S. Jadhav, Novel methods for liposome preparation, Chem. Phys. Lipids. 177 (2014) 8–18. doi:10.1016/j.chemphyslip.2013.10.011.

[29] A. Badiee, M.R. Jaafari, A. Khamesipour, Leishmania major: immune response in BALB/c mice immunized with stress-inducible protein 1 encapsulated in liposomes, Exp. Parasitol. 115 (2007) 127–134. doi:10.1016/j.exppara.2006.07.002.

[30] V.P. Torchilin, R. Rammohan, V. Weissig, T.S. Levchenko, TAT peptide on the surface of liposomes affords their efficient intracellular delivery even at low temperature and in the presence of metabolic inhibitors, Proc. Natl. Acad. Sci. U. S. A. 98 (2001) 8786–8791.

doi:10.1073/pnas.151247498.

[31] S. Murakami, T. Ono, S. Sakai, H. Ijima, K. Kawakami, Effect of diglucosamine on the entrapment of protein into liposomes, J. Liposome Res. 16 (2006) 103–112. doi:10.1080/08982100600680667.

[32] T. Goto, M. Morishita, K. Nishimura, M. Nakanishi, A. Kato, J. Ehara, K. Takayama, Novel mucosal insulin delivery systems based on fusogenic liposomes, Pharm. Res. 23 (2006) 384–391. doi:10.1007/s11095-005-9175-7.

[33] C. Kirby, G. Gregoriadis, Dehydration-rehydration vesicles: a simple method for high yield drug entrapment in liposomes, Nat. Biotechnol. 2 (1984) 979–984. doi:10.1038/nbt1184-979.

[34] M.A. García-Santana, J. Duconge, M.E. Sarmiento, M.E. Lanio-Ruíz, M. Becquer, L. Izquierdo, A. Acosta-Domínguez, Biodistribution of liposome-entrapped human gamma-globulin, Biopharnaceutics Drug Dispos. 27 (2006) 275–283. doi:10.1002/bdd.511.

[35] G. Gregoriadis, A.T. Florence, Liposomes in drug delivery, Drugs. 45 (1993) 15–28. doi:10.2165/00003495-199345010-00003.

[36] M.A. Kisel, L.N. Kulik, I.S. Tsybovsky, A.P. Vlasov, M.S. Vorob'yov, E.A. Kholodova, Z. V. Zabarovskaya, Liposomes with phosphatidylethanol as a carrier for oral delivery of insulin: studies in the rat, Int. J. Pharm. 216 (2001) 105–114. doi:10.1016/S0378-5173(01)00579-8.

[37] N. chitosan coated liposomes for oral protein drug delivery Kowapradit, JariyaMethylated N-(4-N, A. Apirakaramwong, T. Ngawhirunpat, T. Rojanarata, W. Sajomsang, P. Opanasopit, Methylated N-(4-N,N-dimethylaminobenzyl) chitosan coated liposomes for oral protein drug delivery, Eur. J. Pharm. Sci. 47 (2012) 359–366. doi:10.1016/j.ejps.2012.06.020.

[38] J. Colletier, B. Chaize, M. Winterhalter, D. Fournier, Protein encapsulation in liposomes: efficiency depends on interactions between protein and phospholipid bilayer, BMC Biotechnol. 2 (2002). doi:10.1186/1472-6750-2-9.

[39] J.S. Dua, A.C. Rana, A.K. Bhandari, Liposome: method of preparation and applications, Int. J. Pharm. Stud. Res. 3 (2012) 14–20.

[40] T. Wang, G.G.M. D'Souza, D. Bedi, O.A. Fagbohun, L. Prasanna Potturi, B. Papahadjopoulos-sternberg, V.A. Petrenko, V.P. Torchilin, Enhanced binding and killing of target tumor cells by drugloaded liposomes modified with tumor-specific phage fusion coat protein, Nanomedicine. 5 (2010) 563–574. doi:10.2217/nnm.10.30.

[41] M. Anderson, A. Omri, The effect of different lipid components on the in vitro stability and release kinetics of liposome formulations, Drug Deliv. 11 (2004) 33–39. doi:10.1080/10717540490265243.

[42] K. Iwanaga, S. Ono, K. Narioka, M. Kakemi, K. Morimoto, S. Yamashita, Y. Namba, O. Naoto, Application of surface-coated liposomes for oral delivery of peptide: effects of coating the liposome's surface on the GI transit of insulin, J. Pharm. Sci. 88 (1999) 248–252. doi:10.1021/js980235x.

[43] E.L.S. Carvalho, A. Grenha, C. Remuñán-López, M.J. Alonso, B. Seijo, Mucosal delivery of liposome-chitosan nanoparticle complexes, in: Methods Enzymol., Academic Press, 2009: pp. 289–312. doi:10.1016/S0076-6879(09)65015-1.

[44] V.J. Mohanraj, T.J. Barnes, C.A. Prestidge, Silica nanoparticle coated liposomes: a new type of hybrid

nanocapsule for proteins, Int. J. Pharm. 392 (2010) 285–293. doi:10.1016/j.ijpharm.2010.03.061.

[45] N. Zhang, Q.N. Ping, G.H. Huang, W.F. Xu, Investigation of lectin-modified insulin liposomes as carriers for oral administration, Int. J. Pharm. 294 (2005) 247–259. doi:10.1016/j.ijpharm.2005.01.018.

[46] A. Makhlof, S. Fujimoto, Y. Tozuka, H. Takeuchi, In vitro and in vivo evaluation of WGA-carbopol modified liposomes as carriers for oral peptide delivery, Eur. J. Pharm. Biopharm. 77 (2011) 216–224. doi:10.1016/j.ejpb.2010.12.008.

[47] M. Carafa, C. Marianecci, V. Annibaldi, A. Di Stefano, P. Sozio, E. Santucci, Novel O-palmitoylscleroglucan-coated liposomes as drug carriers: development, characterization and interaction with leuprolide, Int. J. Pharm. 325 (2006) 155–162. doi:10.1016/j.ijpharm.2006.06.040.

[48] N. Arulsudar, N. Subramanian, P. Mishra, K. Chuttani, R.K. Sharma, R.S.R. Murthy, Preparation, characterization, and biodistribution study of technetium-99m-labeled leuprolide acetate-loaded liposomes in ehrlich ascites tumor-bearing mice, AAPS J. 6 (2004) 45–56. doi:10.1208/ps060105.

[49] A. Shahiwala, A. Misra, A preliminary pharmacokinetic study of liposomal leuprolide dry powder inhaler: a technical note, AAPS PharmSciTech. 6 (2005) E482–E486. doi:10.1208/pt060360.

[50] C. Schwarz, W. Mehnert, J.S. Lucks, R.H. Müller, Solid lipid nanoparticles (SLN) for controlled drug delivery. I. Production, characterization and sterilization, J. Control. Release. 30 (1994) 83–96. doi:10.1016/0168-3659(94)90047-7.

[51] M.R. Gasco, Method for producing solid lipid microspheres having a narrow size distribution, US5250236, 1993.

[52] R.H. Müller, K. Mäder, S. Gohla, Solid lipid nanoparticles (SLN) for controlled drug delivery - a review of the state of the art, Eur. J. Pharm. Biopharm. 50 (2000) 161–177. doi:10.1016/S0939-6411(00)00087-4.

[53] V. Jannin, E. Dellera, S. Chevrier, Y. Chavant, C. Voutsinas, C. Bonferoni, F. Demarne, In vitro lipolysis tests on lipid nanoparticles: comparison between lipase/co-lipase and pancreatic extract, Drug Dev. Ind. Pharm. 41 (2015) 1582–1588. doi:10.3109/03639045.2014.972412.

[54] S. Morel, M. Rosa Gasco, R. Cavalli, Incorporation in lipospheres of [D-Trp-6] LHRH, Int. J. Pharm. 105 (1994) R1–R3. doi:10.1016/0378-5173(94)90466-9.

[55] S.M. Martins, B. Sarmento, D. Ferreira, E.B. Souto, Lipid-based colloidal carriers for peptide and protein delivery — Liposomes versus lipid nanoparticles, Int. J. Nanomedicine. 2 (2007) 595–607.

[56] L.J. Penkler, R.H. Müller, S.A. Runge, V. Ravelli, Pharmaceutical cyclosporin formulation with improved biopharmaceutical properties, improved physical quality and greater stability, and method for producing said formulation, US 6551619 B1, 2003.

[57] A.J. Almeida, S. Runge, R.H. Müller, Peptide-loaded solid lipid nanoparticles (SLN): influence of production parameters, Int. J. Pharm. 149 (1997) 255–265. doi:10.1016/S0378-5173(97)04885-0.

[58] B. Sjöström, B. Bergenståhl, Preparation of submicron drug particles in lecithin-stabilized o/w emulsions I. Model studies of the precipitation of cholesteryl acetate, Int. J. Pharm. 88 (1992) 53–62. doi:10.1016/0378-5173(93)90013-6.

[59] M. García-Fuentes, D. Torres, M.J. Alonso, Design of lipid nanoparticles for the oral delivery of

hydrophilic macromolecules, Colloids Surfaces B Biointerfaces. 27 (2002) 159–168. doi:10.1016/S0927-7765(02)00053-X.

[60] F.Q. Hu, Y. Hong, H. Yuan, Preparation and characterization of solid lipid nanoparticles containing peptide, Int. J. Pharm. 273 (2004) 29–35. doi:10.1016/j.ijpharm.2003.12.016.

[61] H. Yuan, S.-P. Jiang, Y.-Z. Du, J. Miao, X.-G. Zhang, F.-Q. Hu, Strategic approaches for improving entrapment of hydrophilic peptide drugs by lipid nanoparticles, Colloids Surfaces B Biointerfaces. 70 (2009) 248–253. doi:10.1016/j.colsurfb.2008.12.031.

[62] S.P. Sellers, G.S. Clark, R.E. Sievers, J.F. Carpenter, Dry powders of stable protein formulations from aqueous solutions prepared using supercritical CO2-assisted aerosolization, J. Pharm. Sci. 90 (2001) 785–797. doi:10.1002/jps.1032.

[63] S. Liedtke, S. Wissing, R.H. Müller, K. Mäder, Influence of high pressure homogenisation equipment on nanodispersions characteristics, Int. J. Pharm. 196 (2000) 183–185. doi:10.1016/S0378-5173(99)00417-2.

[64] W. Mehnert, M. Mäder, Solid lipid nanoparticles: production, characterization and applications, Adv. Drug Deliv. Rev. 47 (2001) 165–196. doi:10.1016/s0169-409x(01)00105-3.

[65] E. Ugazio, R. Cavalli, M.R. Gasco, Incorporation of cyclosporin A in solid lipid nanoparticles (SLN), Int. J. Pharm. 241 (2002) 341–344. doi:10.1016/S0378-5173(02)00268-5.

[66] M. Muchow, P. Maincent, R.H. Müller, Lipid nanoparticles with a solid matrix (SLN®, NLC®, LDC®) for oral drug delivery, Drug Dev. Ind. Pharm. 34 (2008) 1394–1405. doi:10.1080/03639040802130061.

[67] C. Chen, T. Fan, Y. Jin, Z. Zhou, Y. Yang, X. Zhu, Z. Zhang, Q. Zhang, Y. Huang, Orally delivered salmon calcitonin-loaded solid lipid nanoparticles prepared by micelle–double emulsion method via the combined use of different solid lipids, Nanomedicine. 8 (2013) 1085–1100. doi:10.2217/nnm.12.141.

[68] J. Liu, T. Gong, C. Wang, Z. Zhong, Z. Zhang, Solid lipid nanoparticles loaded with insulin by sodium cholate-phosphatidylcholine-based mixed micelles: preparation and characterization, Int. J. Pharm. 340 (2007) 153–162. doi:10.1016/j.ijpharm.2007.03.009.

[69] A.J. Almeida, E. Souto, Solid lipid nanoparticles as a drug delivery system for peptides and proteins, Adv. Drug Deliv. Rev. 59 (2007) 478–490. doi:10.1016/j.addr.2007.04.007.

[70] S. Salmaso, N. Elvassore, A. Bertucco, P. Caliceti, Production of solid lipid submicron particles for protein delivery using a novel supercritical gas-assisted melting atomization process, J. Pharm. Sci. 98 (2009) 640–650. doi:10.1002/jps.21434.

[71] R.H. Müller, S. Runge, V. Ravelli, W. Mehnert, A.F. Thünemann, E.B. Souto, Oral bioavailability of cyclosporine: solid lipid nanoparticles (SLN®) versus drug nanocrystals, Int. J. Pharm. 317 (2006) 82–89. doi:10.1016/j.ijpharm.2006.02.045.

[72] S. Salmaso, S. Bersani, N. Elvassore, A. Bertucco, P. Caliceti, Biopharmaceutical characterisation of insulin and recombinant human growth hormone loaded lipid submicron particles produced by supercritical gas micro-atomisation, Int. J. Pharm. 379 (2009) 51–58. doi:10.1016/j.ijpharm.2009.06.014.

[73] J.H. Schulman, W. Stoeckenius, L.M. Prince, Mechanism of formation and structure of micro emulsions by electron microscopy, J. Phys. Chem. 63 (1959) 1677–1680. doi:10.1021/j150580a027.

[74] D.J. McClements, Nanoemulsions versus microemulsions: terminology, differences, and similarities, Soft Matter. 8 (2012) 1719–1729. doi:10.1039/c2sm06903b.

[75] N. Anton, T.F. Vandamme, Nano-emulsions and micro-emulsions: Clarifications of the critical differences, Pharm. Res. 28 (2011) 978–985. doi:10.1007/s11095-010-0309-1.

[76] N. Anton, J.P. Benoit, P. Saulnier, Design and production of nanoparticles formulated from nano-emulsion templates - A review, J. Control. Release. 128 (2008) 185–199. doi:10.1016/j.jconrel.2008.02.007.

[77] D.J. McClements, Edible nanoemulsions: fabrication, properties, and functional performance, Soft Matter. 7 (2011) 2297–2316. doi:10.1039/C0SM00549E.

[78] D.J. McClements, Nanoemulsion-based oral delivery systems for lipophilic bioactive components: nutraceuticals and pharmaceuticals, Ther. Deliv. 4 (2013) 841–857. doi:10.4155/tde.13.46.

[79] B. Abismail, J.P. Canselier, A.M. Wilhelm, H. Delmas, C. Gourdon, Emulsification by ultrasound: drop size distribution and stability, Ultrason. Sonochem. 6 (1999) 75–83. doi:10.1016/S1350-4177(98)00027-3.

[80] J.M. Asua, Challenges for industrialization of miniemulsion polymerization, Prog. Polym. Sci. 39 (2014) 1797–1826. doi:10.1016/j.progpolymsci.2014.02.009.

[81] P. Walstra, Principles of emulsion formation, Chem. Eng. Sci. 48 (1993) 333–349. doi:10.1016/0009-2509(93)80021-H.

[82] K. Shinoda, H. Saito, The stability of O/W type emulsions as functions of temperature and the HLB of emulsifiers: the emulsification by PIT-method, J. Colloid Interface Sci. 30 (1969) 258–263. doi:10.1016/S0021-9797(69)80012-3.

[83] K. Shinoda, H. Saito, The effect of temperature on the phase equilibria and the types of dispersions of the ternary system composed of water, cyclohexane, and nonionic surfactant, J. Colloid Interface Sci. 26 (1968) 70–74. doi:10.1016/0021-9797(68)90273-7.

[84] J.C. Leroux, E. Allémann, E. Doelker, R. Gurny, New approach for the preparation of nanoparticles by an emulsification-diffusion method, Eur. J. Pharm. Biopharm. 41 (1995) 14–18.

[85] S. Magdassi, L. Spernath, Method for the preparation of nanoparticles from nenoemulsions, US 2011/0135734 A1, 2011.

[86] C.A. Miller, Spontaneous emulsification produced by diffusion - A review, Colloids and Surfaces. 29 (1988) 89–102. doi:10.1016/0166-6622(88)80173-2.

[87] N. Anton, T.F. Vandamme, The universality of low-energy nano-emulsification, Int. J. Pharm. 377 (2009) 142–147. doi:10.1016/j.ijpharm.2009.05.014.

[88] D.J. McClements, J. Rao, Food-grade nanoemulsions: formulation, fabrication, properties, performance, biological fate, and potential toxicity, Crit. Rev. Food Sci. Nutr. 51 (2011) 285–330. doi:10.1080/10408398.2011.559558.

[89] C. Qian, D.J. McClements, Formation of nanoemulsions stabilized by model food-grade emulsifiers using high-pressure homogenization: factors affecting particle size, Food Hydrocoll. 25 (2011) 1000–1008. doi:10.1016/j.foodhyd.2010.09.017.

[90] T.S.H. Leong, T.J. Wooster, S.E. Kentish, M. Ashokkumar, Minimising oil droplet size using ultrasonic

emulsification, Ultrason. Sonochem. 16 (2009) 721–727. doi:10.1016/j.ultsonch.2009.02.008.

[91] L. Lee, I.T. Norton, Comparing droplet breakup for a high-pressure valve homogeniser and a microfluidizer for the potential production of food-grade nanoemulsions, J. Food Eng. 114 (2013) 158–163. doi:10.1016/j.jfoodeng.2012.08.009.

[92] A.H. Saberi, Y. Fang, D.J. McClements, Fabrication of vitamin E-enriched nanoemulsions: factors affecting particle size using spontaneous emulsification, J. Colloid Interface Sci. 391 (2013) 95–102. doi:10.1016/j.jcis.2012.08.069.

[93] C.W. Pouton, C.J.H. Porter, Formulation of lipid-based delivery systems for oral administration: materials, methods and strategies, Adv. Drug Deliv. Rev. 60 (2008) 625–637. doi:10.1016/j.addr.2007.10.010.

[94] A.A. Date, N. Desai, R. Dixit, M. Nagarsenker, Self-nanoemulsifying drug delivery systems: formulation insights, applications and advances, Nanomedicine. 5 (2010) 1595–1616. doi:10.2217/nnm.10.126.

[95] A.S. Cunha, J.L. Grossiord, F. Puisieux, M. Seiller, Insulin in w/o/w multiple emulsions: preparation, characterization and determination of stability towards proteases in vitro, J Microencapsul. 14 (1997) 311–319. doi:10.3109/02652049709051135.

[96] A. Silva-Cunha, J.L. Grossiord, F. Puisieux, M. Seiller, W/O/W multiple emulsions of insulin containing a protease inhibitor and an absorption enhancer: preparation, characterization and determination of stability towards proteases in vitro, Int. J. Pharm. 158 (1997) 79–89. doi:10.1016/S0378-5173(97)00249-4.

[97] A. Elsayed, M. Al Remawi, N. Qinna, A. Farouk, A. Badwan, Formulation and characterization of an oily-based system for oral delivery of insulin, Eur. J. Pharm. Biopharm. 73 (2009) 269–279. doi:10.1016/j.ejpb.2009.06.004.

[98] T. Karamanidou, K. Karidi, V. Bourganis, K. Kontonikola, O. Kammona, C. Kiparissides, Effective incorporation of insulin in mucus permeating self-nanoemulsifying drug delivery systems, Eur. J. Pharm. Biopharm. 97 (2015) 223–229. doi:10.1016/j.ejpb.2015.04.013.

[99] T. Trenktrog, B.W. Müller, Preparation and characterization of a peptide containing w/o emulsion, Int. J. Pharm. 123 (1995) 199–207. doi:10.1016/0378-5173(95)00057-P.

[100] C. Prego, D. Torres, M.J. Alonso, Chitosan nanocapsules: a new carrier for nasal peptide delivery, J. Drug Deliv. Sci. Technol. 16 (2006) 331–337. doi:10.1016/S1773-2247(06)50061-9.

[101] D. Liu, T. Kobayashi, S. Russo, F. Li, S.E. Plevy, T.M. Gambling, J.L. Carson, R.J. Mumper, In vitro and in vivo evaluation of a water-in-oil microemulsion system for enhanced peptide intestinal delivery, AAPS J. 15 (2013) 288–298. doi:10.1208/s12248-012-9441-7.

[102] P.P. Constantinides, S.H. Yiv, Particle size determination of phase-inverted water-in-oil microemulsions under different dilution and storage conditions, Int. J. Pharm. 115 (1995) 225–234. doi:10.1016/0378-5173(94)00272-7.

[103] S. Gupta, R. Kesarla, A. Omri, Formulation strategies to improve the bioavailability of poorly absorbed drugs with special emphasis on self-emulsifying systems, ISRN Pharm. 2013 (2013) 1–16. doi:10.1155/2013/848043.

[104] T.A.S. Aguirre, D. Teijeiro-Osorio, M. Rosa, I.S. Coulter, M.J. Alonso, D.J. Brayden, Current status of selected oral peptide technologies in advanced preclinical development and in clinical trials, Adv. Drug Deliv. Rev. 106 (2016) 223–241. doi:10.1016/j.addr.2016.02.004.

[105] C. Prego, M. García, D. Torres, M.J. Alonso, Transmucosal macromolecular drug delivery, J. Control. Release. 101 (2005) 151–162. doi:10.1016/j.jconrel.2004.07.030.

[106] T. Gonzalo, G. Lollo, M. Garcia-Fuentes, D. Torres, J. Correa, R. Riguera, E. Fernandez-Megia, P. Calvo, P. Avilés, M.J. Guillén, M.J. Alonso, A new potential nano-oncological therapy based on polyamino acid nanocapsules, J. Control. Release. 169 (2013) 10–16. doi:10.1016/j.jconrel.2013.03.037.

[107] L. Guo, E. Ma, H. Zhao, Y. Long, C. Zheng, M. Duan, Preliminary evaluation of a novel oral delivery system for rhPTH1-34: in vitro and in vivo, Int. J. Pharm. 420 (2011) 172–179. doi:10.1016/j.ijpharm.2011.08.029.

[108] S.T. Dogru, S. Çalis, F. Öner, Oral multiple w/o/w emulsion formulation of a peptide salmon calcitonin: in vitro-in vivo evaluation, J. Clin. Pharm. Ther. 25 (2000) 435–443. doi:10.1046/j.1365-2710.2000.00306.x.

[109] S. Hirsjärvi, Y. Qiao, A. Royere, J. Bibette, J.P. Benoit, Layer-by-layer surface modification of lipid nanocapsules, Eur. J. Pharm. Biopharm. 76 (2010) 200–207. doi:10.1016/j.ejpb.2010.07.010.

[110] P. Calvo, A. Sánchez, J. Martínez, M.I. López, M. Calonge, J.C. Pastor, M.J. Alonso, Polyester nanocapsules as new topical ocular delivery systems for cyclosporin A, Pharm. Res. 13 (1996) 311–315. doi:10.1023/A:1016015803611.

[111] L.N. Thwala, A. Beloqui, N.S. Csaba, D. González-Touceda, S. Tovar, C. Dieguez, M.J. Alonso, V. Préat, The interaction of protamine nanocapsules with the intestinal epithelium: a mechanistic approach, J. Control. Release. 243 (2016) 109–120. doi:10.1016/j.jconrel.2016.10.002.

[112] P. Calvo, C. Remuñán-López, J.L. Vila-Jato, M.J. Alonso, Development of positively charged colloidal drug carriers: chitosan-coated polyester nanocapsules and submicron-emulsions, Colloid Polym. Sci. 275 (1997) 46–53. doi:10.1007/s003960050050.

[113] P. Calvo, J.L. Vila-Jato, M.J. Alonso, Evaluation of cationic polymer-coated nanocapsules as ocular drug carriers, Int. J. Pharm. 153 (1997) 41–50. doi:10.1016/S0378-5173(97)00083-5.

[114] C. Damgé, J. Vonderscher, P. Marbach, M. Pinget, Poly(alkyl cyanoacrylate) nanocapsules as a delivery system in the rat for octreotide, a long-acting somatostatin analogue, J. Pharm. Pharmacol. 49 (1997) 949–954. doi:10.1111/j.2042-7158.1997.tb06022.x.

[115] C. Damge, C. Michel, M. Aprahamian, P. Couvreur, New approach for oral administration of insulin with polyalkylcyanoacrylate nanocapsules as drug carrier, Diabetes. 37 (1988) 246–251. doi:10.2337/diab.37.2.246.

[116] C. Vauthier, K. Bouchemal, Methods for the preparation and manufacture of polymeric nanoparticles, Pharm. Res. 26 (2009) 1025–1058. doi:10.1007/s11095-008-9800-3.

[117] P. Couvreur, G. Barratt, E. Fattal, P. Legrand, C. Vauthier, Nanocapsule technology: a review, Crit. Rev. Ther. Drug Carr. Syst. 19 (2002) 99–134. doi:10.1615/CritRevTherDrugCarrierSyst.v19.i2.10.

[118] J.L. Grangier, M. Puygrenier, J.C. Gautier, P. Couvreur, Nanoparticles as carriers for growth hormone releasing factors, J. Control. Release. 15 (1991) 3–13. doi:10.1016/0168-3659(91)90098-X.

[119] M. Gallardo, G. Couarraze, B. Denizot, L. Treupel, P. Couvreur, F. Puisieux, Study of the mechanisms of formation of nanoparticles and nanocapsules of polyisobutyl-2-cyanoacrylate, Int. J. Pharm. 100 (1993) 55–64. doi:10.1016/0378-5173(93)90075-Q.

[120] S. Watnasirichaikul, T. Rades, I.G. Tucker, N.M. Davies, Effects of formulation variables on characteristics of poly(ethylcyanoacrylate) nanocapsules prepared from w/o microemulsions, Int. J. Pharm. 235 (2002) 237–246. doi:10.1016/S0378-5173(02)00002-9.

[121] S. Watnasirichaikul, T. Rades, I.G. Tucker, N.M. Davies, In-vitro release and oral bioactivity of insulin in diabetic rats using nanocapsules dispersed in biocompatible microemulsion, J. Pharm. Pharmacol. 54 (2002) 473–480. doi:10.1211/0022357021778736.

[122] S. Li, Y. He, C. Li, X. Liu, In vitro release of protein from poly(butylcyanoacrylate) nanocapsules with an aqueous core, Colloid Polym. Sci. 283 (2005) 480–485. doi:10.1007/s00396-004-1173-5.

[123] S. Watnasirichaikul, N.M. Davies, T. Rades, I.G. Tucker, Preparation of biodegradable insulin nanocapsules from biocompatible microemulsions, Pharm. Res. 17 (2000) 684–689. doi:10.1023/A:1007574030674.

[124] J.P. Devissaguet, H. Fessi, F. Puisieux, Process for the preparation of dispersible colloidal systems of a substance in the form of nanocapsules, 5049322, 1991.

[125] H. Fessi, F. Puisieux, J.P. Devissaguet, N. Ammoury, S. Benita, Nanocapsule formation by interfacial polymer deposition following solvent displacement, Int. J. Pharm. 55 (1989) R1–R4. doi:10.1016/0378-5173(89)90281-0.

[126] C. Prego, M. Fabre, D. Torres, M.J. Alonso, Efficacy and mechanism of action of chitosan nanocapsules for oral peptide delivery, Pharm. Res. 23 (2006) 549–556. doi:10.1007/s11095-006-9570-8.

[127] C. Prego, D. Torres, E. Fernandez-Megia, R. Novoa-Carballal, E. Quiñoá, M.J. Alonso, Chitosan-PEG nanocapsules as new carriers for oral peptide delivery: effect of chitosan pegylation degree, J. Control. Release. 111 (2006) 299–308. doi:10.1016/j.jconrel.2005.12.015.

[128] A. Cadete Pires, Hyaluronic acid nanocapsules for the intracellular delivery of anticancer drugs, University of Santiago de Compostela, University of Angers, 2016.

[129] P. Jakubiak, L.N. Thwala, A. Cadete-Pires, V. Préat, M.J. Alonso, A. Beloqui, N. Csaba, Solvent-free protamine nanocapsules as carriers for mucosal delivery of therapeutics, Eur. Polym. J. In Press (2017). doi:10.1016/j.eurpolymj.2017.03.049.

[130] A.H. Saberi, B. Zeeb, J. Weiss, D.J. McClements, Tuneable stability of nanoemulsions fabricated using spontaneous emulsification by biopolymer electrostatic deposition, J. Colloid Interface Sci. 455 (2015) 172–178. doi:10.1016/j.jcis.2015.05.037.

[131] F. Cournarie, M. Chéron, M. Besnard, C. Vauthier, Evidence for restrictive parameters in formulation of insulin-loaded nanocapsules, Eur. J. Pharm. Biopharm. 57 (2004) 171–179. doi:10.1016/S0939-6411(03)00191-7.

[132] C. Prego, D. Torres, M.J. Alonso, Chitosan nanocapsules as carriers for oral peptide delivery: effect of chitosan molecular weight and type of salt on the in vitro behaviour and in vivo effectiveness, J. Nanosci. Nanotechnol. 6 (2006) 2921–2928. doi:10.1166/jnn.2006.429.

[133] K. Krauel, N.M. Davies, S. Hook, T. Rades, Using different structure types of microemulsions for the preparation of poly(alkylcyanoacrylate) nanoparticles by interfacial polymerization, J. Control. Release. 106 (2005) 76–87. doi:10.1016/j.jconrel.2005.04.013.

[134] S. Vicente, B. Diaz-Freitas, M. Peleteiro, A. Sanchez, D.W. Pascual, A. Gonzalez-Fernandez, M.J. Alonso, A polymer/oil based nanovaccine as a single-dose immunization approach, PLoS One. 8 (2013) e62500. doi:10.1371/journal.pone.0062500.

[135] S. Vicente, M. Peleteiro, J.V. González-Aramundiz, B. Díaz-Freitas, S. Martínez-Pulgarín, J.I. Neissa, J.M. Escribano, A. Sanchez, Á. González-Fernández, M.J. Alonso, Highly versatile immunostimulating nanocapsules for specific immune potentiation, Nanomedicine (London). 9 (2014) 2273–2289. doi:10.2217/nnm.14.10.

[136] S. Vicente, M. Peleteiro, B. Díaz-Freitas, A. Sanchez, Á. González-Fernández, M.J. Alonso, Co-delivery of viral proteins and a TLR7 agonist from polysaccharide nanocapsules: a needle-free vaccination strategy, J. Control. Release. 172 (2013) 773–781. doi:10.1016/j.jconrel.2013.09.012.

[137] M. Aboubakar, F. Puisieux, P. Couvreur, M. Deyme, C. Vauthier, Study of the mechanism of insulin encapsulation in poly(isobutylcyanoacrylate) nanocapsules obtained by interfacial polymerization, J. Biomed. Mater. Res. 47 (1999) 568–576. doi:10.1002/(SICI)1097-4636(19991215)47:4<568::AID-JBM14>3.0.CO;2-X.

[138] G. Lollo, A. Gonzalez-Paredes, M. Garcia-Fuentes, P. Calvo, D. Torres, M.J. Alonso, Polyarginine nanocapsules as a potential oral peptide delivery carrier, J. Pharm. Sci. 106 (2017) 611–618. doi:10.1016/j.xphs.2016.09.029.

[139] A. Graf, T. Rades, S.M. Hook, Oral insulin delivery using nanoparticles based on microemulsions with different structure-types: optimisation and in vivo evaluation, Eur. J. Pharm. Sci. 37 (2009) 53–61. doi:10.1016/j.ejps.2008.12.017.

[140] C. Prego, P. Paolicelli, B. Díaz, S. Vicente, A. Sánchez, Á. González-Fernández, M.J. Alonso, Chitosan-based nanoparticles for improving immunization against hepatitis B infection, Vaccine. 28 (2010) 2607–2614. doi:10.1016/j.vaccine.2010.01.011.

[141] C. Michel, M. Aprahamian, L. Defontaine, P. Couvreur, C. Damgé, The effect of site of administration in the gastrointestinal tract on the absorption of insulin from nanocapsules in diabetic rats, J. Pharm. Pharmacol. 43 (1991) 1–5. doi:10.1111/j.2042-7158.1991.tb05437.x.

[142] C. Damge, C. Michel, M. Aprahamian, P. Couvreur, J.P. Devissaguet, Nanocapsules as carriers for oral peptide delivery, J. Control. Release. 13 (1990) 233–239. doi:10.1016/0168-3659(90)90013-J.

[143] M. Aboubakar, F. Puisieux, P. Couvreur, C. Vauthier, Physico-chemical characterization of insulin-loaded poly (isobutylcyanoacrylate) nanocapsules obtained by interfacial polymerization, Int. J. Pharm. 183 (1999) 63–66. doi:10.1016/S0378-5173(99)00045-9.

[144] M. Aboubakar, P. Couvreur, H. Pinto-Alphandary, B. Gouritin, B. Lacour, R. Farinotti, F. Puisieux, C. Vauthier, Insulin-loaded nanocapsules for oral administration: in vitro and in vivo investigation, Drug Dev. Res. 49 (2000) 109–117. doi:10.1002/(SICI)1098-2299(200002)49:2<109::AID-DDR4>3.0.CO;2-#.

[145] F. Cournarie, D. Auchere, D. Chevenne, B. Lacour, M. Seiller, C. Vauthier, Absorption and efficiency of insulin after oral administration of insulin-loaded nanocapsules in diabetic rats, Int. J. Pharm. 242 (2002) 325–328. doi:10.1016/S0378-5173(02)00175-8.

[146] H. Pinto-Alphandary, M. Aboubakar, D. Jaillard, P. Couvreur, C. Vauthier, Visualization of insulin-loaded nanocapsules: in vitro and in vivo studies after oral administration to rats, Pharm. Res. 20 (2003) 1071–1084. doi:10.1023/A:1024470508758.

[147] P.J. Lowe, C.S. Temple, Calcitonin and Insulin in Isobutylcyanoacrylate Nanocapsules: Protection Against Proteases and Effect on Intestinal Absorption in Rats, J. Pharm. Pharmacol. 46 (1994) 547–552. doi:10.1111/j.2042-7158.1994.tb03854.x.

[148] A. Graf, K.S. Jack, A.K. Whittaker, S.M. Hook, T. Rades, Protein delivery using nanoparticles based on microemulsions with different structure-types, Eur. J. Pharm. Sci. 33 (2008) 434–444. doi:10.1016/j.ejps.2008.01.013.

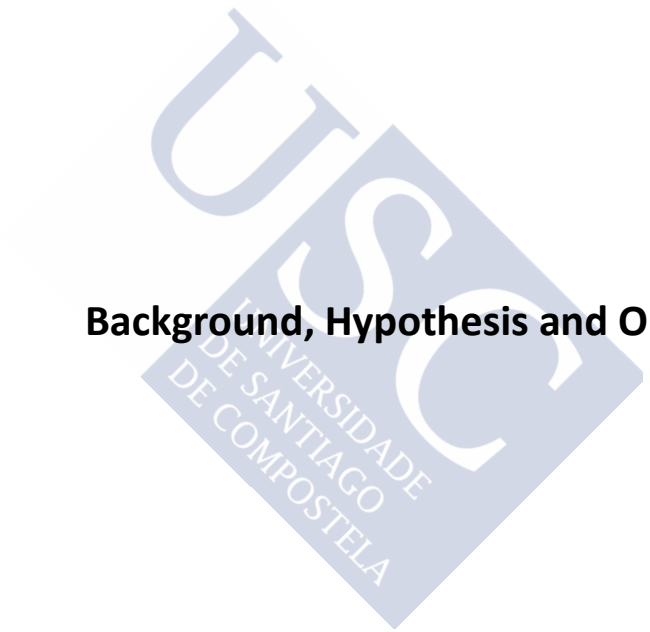
[149] N. Anton, P. Saulnier, C. Gaillard, E. Porcher, S. Vrignaud, J.P. Benoit, Aqueous-core lipid nanocapsules for encapsulating fragile hydrophilic and/or lipophilic molecules, Langmuir. 25 (2009) 11413–11419. doi:10.1021/la901565q.

[150] A.P. Kafka, B.J. McLeod, T. Rades, A. McDowell, Release and bioactivity of PACA nanoparticles containing D-Lys6-GnRH for brushtail possum fertility control, J. Control. Release. 149 (2011) 307–313. doi:10.1016/j.jconrel.2010.10.029.

[151] A.P. Kafka, T. Kleffmann, T. Rades, A. Mcdowell, Histidine residues in the peptide D-Lys6-GnRH: potential for copolymerization in polymeric nanoparticles, Mol. Pharm. 6 (2009) 1483–1491. doi:10.1021/mp900043e.

USC UNIVERSIDADE DE SANTIAGO DE COMPOSTELA

USC
UNIVERSIDADE
DE SANTIAGO
DE COMPOSTELA




# Background, Hypothesis and Objectives

USC
UNIVERSIDADE
DE SANTIAGO
DE COMPOSTELA

## Background

During the past decades, the idea of enhancing the oral bioavailability of peptides and proteins through their association with a variety of nanocarriers has been explored [1–3]. The accumulated knowledge has led to the conclusion that nanocarriers may help peptides/proteins to overcome the hurdles associated with the oral route of administration, such as, the harsh environment along the gastrointestinal tract (wide pH range 1.2−7.4 with high concentration of proteolytic enzymes) [4–6], the mucus layer covering up the intestinal epithelium (different thickness along the intestinal tract) [7,8], and the intestinal cells, which are poorly permeable to macromolecules [5,8,9]. Our group pioneered the development of a diversity of peptide/protein delivery platforms, some of which, i.e., PLA-PEG nanoparticles [10], lipid nanoparticles [11,12], chitosan nanoparticles [13,14], chitosan nanocapsules [15–18], polyarginine nanocapsules [9,19,20] and protamine nanocapsules [4] have been explored for the oral delivery of peptides and proteins. Overall, the results in terms of peptide/protein absorption *in vivo* (measured directly or indirectly through the pharmacological response) have been variable. In the case of PLA-PEG nanoparticles, we found for the first time that the PEGylation had a key role in their stability in intestinal fluids and in the absorption of the associated protein [10]. On the other hand, we observed that chitosan nanoparticles and nanocapsules could provide a significant absorption of salmon calcitonin, and a quite variable response when insulin was the loaded peptide [12,13,15–18]. Finally, polyarginine and protamine nanocapsules, resulted in a significant but moderate absorption of insulin [4,9].

In addition to the nanocapsules reported by our group, other authors have explored the potential of alternative lipid carriers based on the absorption enhancing properties of the lipids and the nanocarrier's ability to improve the drug stability. Several innovative strategies, such as reverse micellization [21–23], double emulsion method [12,24,25], hydrophobic ion paring [26–28] and hydrophobic – hydrophilic interactions [29,30], have been described in order to improve the peptide association, which is so far limited by their solubility, and exploit their potential as delivery platforms. Furthermore, the biocompatible character of these biomaterials and the low cost of the production techniques have increased the interest around these nanocarriers [1,2,31].

## Hypothesis

1. The identification of the key factors affecting the physicochemical properties of lipid-based nanosystems and their capacity to associate peptides will help to increase their limited peptide loading and improve their versatility as peptide delivery carriers.

2. The generation of knowledge about how the components (i.e., polymers, surfactants) and surface properties of a lipid–based nanocarrier can influence its fate and interaction with the intestinal tract will contribute to the rational design of nanocarriers intended to act as oral delivery platforms.

3. The rational design of a nanocarrier based on the selection and combination of lipids with different materials (i.e., polymers, surfactants, bile salts…) with stabilizing, mucodiffusive and permeation enhancing properties, and with the capacity to associate and deliver peptides, will result in a potential oral peptide delivery platform.

USC UNIVERSIDADE DE SANTIAGO DE COMPOSTELA

## Objectives

Based on the background knowledge and hypothesis above outlined, the main objectives of this thesis were first , to generate knowledge about how the composition and surface properties of a lipid-based nanocarrier may influence its capacity to load peptides and to overcome biological barriers associated to the oral modality of administration; and second, to rationally design and develop a new lipid-based nanosystem intended to efficiently deliver a hydrophobically modified insulin, by the oral route. Specifically, to address these objectives, from an experimental point of view, the following activities were undertaken:

### A) Identifying the key factors affecting the physicochemical properties of lipid-based nanosystems and their ability to associate peptides

1. Preparation, physicochemical characterization and determination of the peptide association efficiency of a lipid-based nanosystem by selecting chitosan nanocapsules as starting point prototype and insulin glulisine as a model peptide.

2. Study of the influence of the nanocapsules' composition (i.e., use of different concentrations of the main components and inclusion of surfactants/polymers) on their physicochemical properties and their ability to associate peptides.

The results corresponding to this objective are presented in *Chapter 2* entitled as *"Key factors affecting the physicochemical properties of chitosan nanocapsules and their ability to associate insulin"*.

### B) Generating knowledge about how the different surface properties of lipid-based nanosystems influence their interaction with the barriers existing at intestinal level

1. Preparation and physicochemical characterization of different lipid-based nanocarriers (nanocapsules and nanoemulsions) with a common oily core but different surfactants and polymers on the surface.

2. Study of the influence of nanocarrier's composition on their colloidal stability and resistance to degradation in simulated intestinal fluids.

3. Evaluation of the influence of the composition and physicochemical properties of the nanocarriers on their mucoadhesive and mucodiffusive behaviour.

The results corresponding to this objective are presented in *Chapter 3* entitled as *"Influence of the surface properties of nanocapsules on their interaction with intestinal barriers"*.

### C) Rational design, development and characterization of a peptide-loaded lipid-based nanocarrier

1. Rational development and physicochemical and morphological characterization of a new lipid-based nanocarrier with a narrow size distribution, with the capacity to efficiently load a hydrophobically modified insulin.

2. Study of the miscibility and stability of the nanosystem with different simulated biorelevant media with and without enzymes and under different storage conditions.

3. Evaluation of the *in vitro* cytotoxicity and interaction of the lipid-based nanosystem with the intestinal cells (Caco−2, C2BBe1 human colon carcinoma Caco−2 clone and mucus secreting HT29−MTX model cell lines).

4. Study of the biodistribution of the nanosystem after its oral administration to mice, and determination of the pharmacological effect of insulin associated to the nanosystem, following subcutaneous and intra-intestinal administration to healthy and diabetic rats.

The results corresponding to this objective are presented in *Chapter 4* entitled as *"A nanoemulsion/micelles mixed nanosystem for the oral administration of hydrophobically-modified insulin"*.

## References


[1] Z. Niu, I. Conejos-Sánchez, B.T. Griffin, C.M. O'Driscoll, M.J. Alonso, Lipid-based nanocarriers for oral peptide delivery, Adv. Drug Deliv. Rev. 106 (2016) 337–354. doi:10.1016/j.addr.2016.04.001.

[2] I. Santalices, A. Gonella, D. Torres, M.J. Alonso, Advances on the formulation of proteins using nanotechnologies, J. Drug Deliv. Sci. Technol. 42 (2017) 155–180. doi:10.1016/j.jddst.2017.06.018.

[3] T.A.S. Aguirre, D. Teijeiro-Osorio, M. Rosa, I.S. Coulter, M.J. Alonso, D.J. Brayden, Current status of selected oral peptide technologies in advanced preclinical development and in clinical trials, Adv. Drug Deliv. Rev. 106 (2016) 223–241. doi:10.1016/j.addr.2016.02.004.

[4] L.N. Thwala, A. Beloqui, N.S. Csaba, D. González-Touceda, S. Tovar, C. Dieguez, M.J. Alonso, V. Préat, The interaction of protamine nanocapsules with the intestinal epithelium: a mechanistic approach, J. Control. Release. 243 (2016) 109–120. doi:10.1016/j.jconrel.2016.10.002.

[5] Z. Niu, E. Samaridou, E. Jaumain, J. Coëne, G. Ullio, N. Shrestha, J. Garcia, M. Durán-Lobato, S. Tovar, M.J. Santander-Ortega, M.V. Lozano, M.M. Arroyo-Jimenez, R. Ramos-Membrive, I. Peñuelas, A. Mabondzo, V. Préat, M. Teixidó, E. Giralt, M.J. Alonso, PEG-PGA enveloped octaarginine-peptide nanocomplexes: an oral peptide delivery strategy, J. Control. Release. 276 (2018) 125–139. doi:10.1016/j.jconrel.2018.03.004.

[6] X. Li, S. Guo, C. Zhu, Q. Zhu, Y. Gan, J. Rantanen, U.L. Rahbek, L. Hovgaard, M. Yang, Intestinal mucosa permeability following oral insulin delivery using core shell corona nanolipoparticles, Biomaterials. 34 (2013) 9678–9687. doi:10.1016/j.biomaterials.2013.08.048.

[7] L. Inchaurraga, N. Martín-Arbella, V. Zabaleta, G. Quincoces, I. Peñuelas, J.M. Irache, In vivo study of the mucus-permeating properties of PEG-coated nanoparticles following oral administration, Eur. J. Pharm. Biopharm. 97 (2015) 280–289. doi:10.1016/j.ejpb.2014.12.021.

[8] W. Shan, X. Zhu, M. Liu, L. Li, J. Zhong, W. Sun, Z. Zhang, Y. Huang, Overcoming the diffusion barrier of mucus and absorption barrier of epithelium by self-Assembled nanoparticles for oral delivery of insulin, ACS Nano. 9 (2015) 2345–2356. doi:10.1021/acsnano.5b00028.

[9] Z. Niu, E. Tedesco, F. Benetti, A. Mabondzo, I.M. Montagner, I. Marigo, D. Gonzalez-Touceda, S. Tovar, C. Diéguez, M.J. Santander-Ortega, M.J. Alonso, Rational design of polyarginine nanocapsules intended to help peptides overcoming intestinal barriers, J. Control. Release. 263 (2016) 4–17. doi:10.1016/j.jconrel.2017.02.024.

[10] M. Tobío, A. Sánchez, A. Vila, I. Soriano, C. Evora, J.. J. Vila-Jato, M.. M. Alonso, The role of PEG on the stability in digestive fluids and in vivo fate of PEG-PLA nanoparticles following oral administration, Colloids Surfaces B Biointerfaces. 18 (2000) 315–323. doi:10.1016/S0927-7765(99)00157-5.

[11] M. García-Fuentes, D. Torres, M.J. Alonso, Design of lipid nanoparticles for the oral delivery of hydrophilic macromolecules, Colloids Surfaces B Biointerfaces. 27 (2002) 159–168. doi:10.1016/S0927-7765(02)00053-X.

[12] M. Garcia-Fuentes, C. Prego, D. Torres, M.J. Alonso, A comparative study of the potential of solid triglyceride nanostructures coated with chitosan or poly(ethylene glycol) as carriers for oral calcitonin delivery, Eur. J. Pharm. Sci. 25 (2005) 133–143. doi:10.1016/j.ejps.2005.02.008.

[13] E.L.S. Carvalho, A. Grenha, C. Remuñán-López, M.J. Alonso, B. Seijo, Mucosal delivery of liposome-

chitosan nanoparticle complexes, in: Methods Enzymol., Academic Press, 2009: pp. 289–312. doi:10.1016/S0076-6879(09)65015-1.

[14] M. Alonso-Sande, M. Cuña, C. Remuñán-López, D. Teijeiro-Osorio, J.L. Alonso-Lebrero, M.J. Alonso, Formation of new glucomannan - chitosan nanoparticles and study of their ability to associate and deliver proteins, Macromolecules. 39 (2006) 4152–4158. doi:10.1021/ma060230j.

[15] C. Prego, M. Fabre, D. Torres, M.J. Alonso, Efficacy and mechanism of action of chitosan nanocapsules for oral peptide delivery, Pharm. Res. 23 (2006) 549–556. doi:10.1007/s11095-006-9570-8.

[16] C. Prego, D. Torres, E. Fernandez-Megia, R. Novoa-Carballal, E. Quiñoá, M.J. Alonso, Chitosan-PEG nanocapsules as new carriers for oral peptide delivery: effect of chitosan pegylation degree, J. Control. Release. 111 (2006) 299–308. doi:10.1016/j.jconrel.2005.12.015.

[17] C. Prego, D. Torres, M.J. Alonso, Chitosan nanocapsules as carriers for oral peptide delivery: effect of chitosan molecular weight and type of salt on the in vitro behaviour and in vivo effectiveness, J. Nanosci. Nanotechnol. 6 (2006) 2921–2928. doi:10.1166/jnn.2006.429.

[18] C. Prego, M. García, D. Torres, M.J. Alonso, Transmucosal macromolecular drug delivery, J. Control. Release. 101 (2005) 151–162. doi:10.1016/j.jconrel.2004.07.030.

[19] A. Gonzalez-Paredes, D. Torres, M.J. Alonso, Polyarginine nanocapsules: A versatile nanocarrier with potential in transmucosal drug delivery, Int. J. Pharm. 529 (2017) 474–485. doi:10.1016/j.ijpharm.2017.07.001.

[20] G. Lollo, A. Gonzalez-Paredes, M. Garcia-Fuentes, P. Calvo, D. Torres, M.J. Alonso, Polyarginine nanocapsules as a potential oral peptide delivery carrier, J. Pharm. Sci. 106 (2017) 611–618. doi:10.1016/j.xphs.2016.09.029.

[21] P.L. Luisi, M. Giomini, M.P. Pileni, B.H. Robinson, Reverse micelles as hosts for proteins and small molecules, Biochim. Biophys. Acta (BBA)-Reviews Biomembr. 947 (1988) 209–246. doi:10.1016/0304-4157(88)90025-1.

[22] G. Sharma, K. Wilson, C.F. van der Walle, N. Sattar, J.R. Petrie, M.N.V. Ravi Kumar, Microemulsions for oral delivery of insulin: design, development and evaluation in streptozotocin induced diabetic rats, Eur. J. Pharm. Biopharm. 76 (2010) 159–169. doi:10.1016/j.ejpb.2010.07.002.

[23] C. Chen, T. Fan, Y. Jin, Z. Zhou, Y. Yang, X. Zhu, Z. Zhang, Q. Zhang, Y. Huang, Orally delivered salmon calcitonin-loaded solid lipid nanoparticles prepared by micelle–double emulsion method via the combined use of different solid lipids, Nanomedicine. 8 (2013) 1085–1100. doi:10.2217/nnm.12.141.

[24] M. Garcia-Fuentes, D. Torres, M.J. Alonso, New surface-modified lipid nanoparticles as delivery vehicles for salmon calcitonin, Int. J. Pharm. 296 (2005) 122–132. doi:10.1016/j.ijpharm.2004.12.030.

[25] N. Zhang, Q. Ping, G. Huang, W. Xu, Y. Cheng, X. Han, Lectin-modified solid lipid nanoparticles as carriers for oral administration of insulin, Int. J. Pharm. 327 (2006) 153–159. doi:10.1016/j.ijpharm.2006.07.026.

[26] F. Hintzen, G. Perera, S. Hauptstein, C. Müller, F. Laffleur, A. Bernkop-Schnürch, In vivo evaluation of an oral self-microemulsifying drug delivery system (SMEDDS) for leuprorelin, Int. J. Pharm. 472 (2014) 20–26. doi:10.1016/j.ijpharm.2014.05.047.

[27] J.D. Meyer, M.C. Manning, Hydrophobic ion pairing: altering the solubility properties of

biomolecules, Pharm. Res. 15 (1998) 188–193. doi:10.1023/A:1011998014474.

[28] S. Morel, E. Ugazio, R. Cavalli, M.R. Gasco, Thymopentin in solid lipid nanoparticles, Int. J. Pharm. 132 (1996) 259–261.

[29] C. Zheng, M. Duan, H. Ma, H. Zhong, Zheng, Method for preparation of orally administrated insulin formulation, US 7018980 B2, 2006.

[30] E. Ma, H. Ma, Z. Liu, C. Zheng, M. Duan, In vitro and in vivo evaluation of a novel oral insulin formulation, Acta Pharmacol. Sin. 27 (2006) 1382–1388. doi:10.1111/j.1745-7245.2006.00424.x.

[31] T. Karamanidou, V. Bourganis, O. Kammona, C. Kiparissides, Lipid-based nanocarriers for the oral administration of biopharmaceutics, Nanomedicine. 11 (2016) 3009–3032. doi:10.2217/nnm-2016-0265.

USC UNIVERSIDADE DE SANTIAGO DE COMPOSTELA

USC
UNIVERSIDADE
DE SANTIAGO
DE COMPOSTELA

# Chapter 2

## Key factors affecting the physicochemical properties of chitosan nanocapsules and their ability to associate insulin

USC
UNIVERSIDADE
DE SANTIAGO
DE COMPOSTELA

# Chapter 2

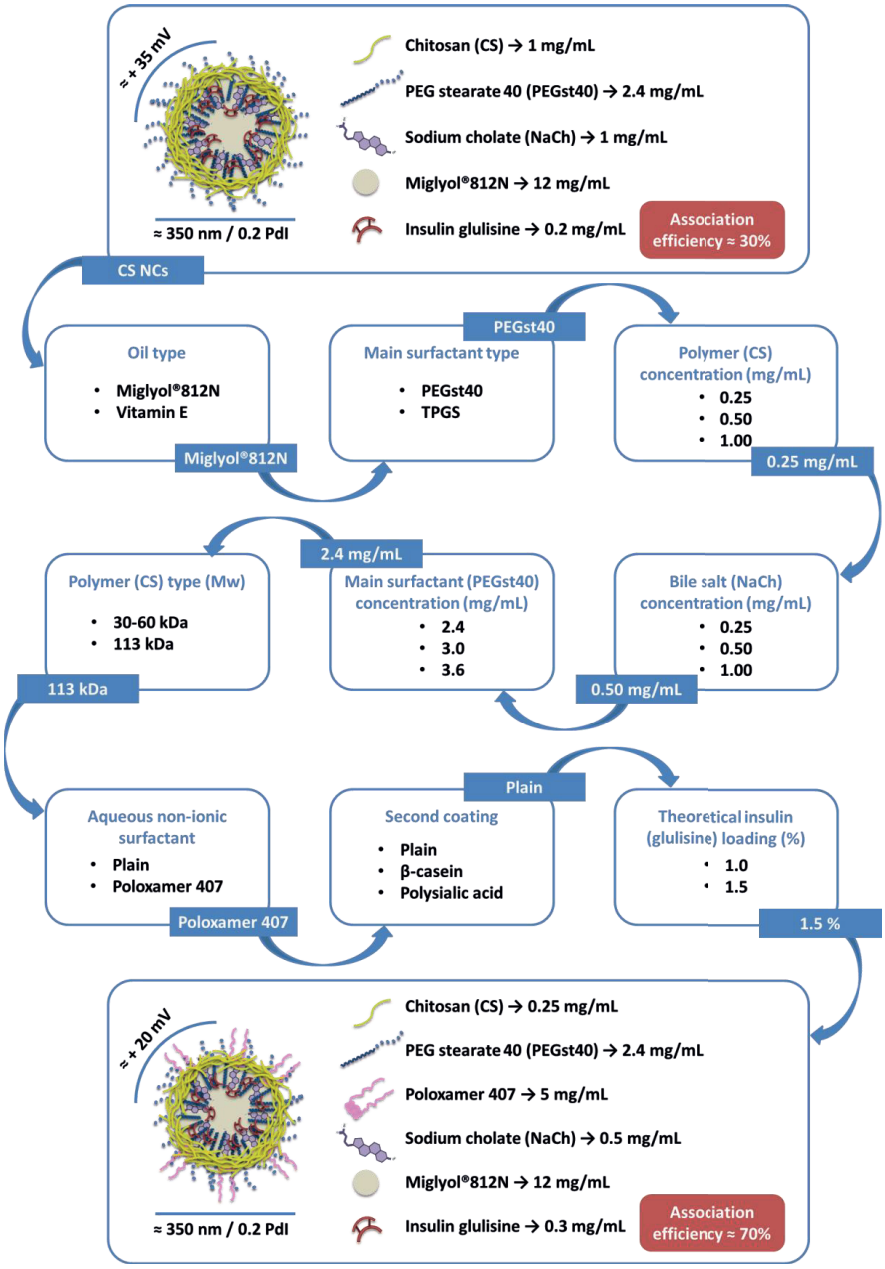
## Key factors affecting the physicochemical properties of chitosan nanocapsules and their ability to associate insulin


### Abstract

Our laboratory has reported the utility of chitosan nanocapsules as oral delivery vehicles for the cationic peptide, salmon calcitonin. Despite these positive results the association of insulin to these nanocarriers has been found to be limited by its acidic nature and limited solubility in lipids. Based on this, the objective of this work was to further explore the possibilities to associate a modified rapid acting insulin (change in two aminoacids), named as insulin glulisine, and to analyze the physicochemical properties of the said nanocarriers that are expected to determine their fate following oral administration. The results showed that some of the investigated parameters, such as the type of surfactant or oil had minor effects on both the physicochemical properties and insulin association efficiency of these chitosan nanocapsules Other factors, such as the increase in chitosan concentration and the presence of a second coating shell, had a negative effect on the insulin association efficiency. Overall, the information here disclosed helps to identify the crucial factors to tune the physicochemical properties of lipid-based nanocarriers and/or their ability to associate peptides.

USC
UNIVERSIDADE
DE SANTIAGO
DE COMPOSTELA

## Graphical abstract



USC
UNIVERSIDADE
DE SANTIAGO
DE COMPOSTELA

## Table of contents

**1. Introduction**

**2. Materials and methods**

2.1. Materials

2.2. Preparation of insulin-loaded chitosan nanocapsules

2.3. Physicochemical properties of insulin-loaded chitosan nanocapsules (DLS)

2.4. Insulin association efficiency (AE %)

2.5. Stability and insulin release of chitosan nanocapsules in bio-relevant media: SIF and FaSSIF−V2

**3. Results and discussion**

3.1. Effect of the oil type used as nanocapsules core: Miglyol®812N vs DL−α−tocopherol (vitamin E)

3.2. Effect of the PEG-surfactant type: PEG stearate 40 vs D−α−tocopheryl PEG 1000 succinate (TPGS)

3.3. Effect of the concentration of the chitosan polymer: 0.25 vs 0.5 vs 1 mg/mL

3.4. Effect of the bile salt (Na cholate) concentration: 0.25 vs 0.5 vs 1 mg/mL

3.5. Effect of the PEG stearate 40 concentration: 2.4 vs 3.0 vs 3.6 mg/mL

3.6. Effect of the chitosan molecular weight

3.7. Effect of the inclusion of the non-ionic surfactant poloxamer 407

3.8. Effect of the inclusion of a second coating: plain vs β−casein-coated vs polysialic acid (PSA)-coated chitosan nanocapsules

3.9. Effect of the theoretical insulin glulisine) loading: 1 vs 1.5 %

3.10. Stability and insulin release of chitosan nanocapsules in bio-relevant media: SIF and FaSSIF−V2

**4. Conclusions**

USC
UNIVERSIDADE
DE SANTIAGO
DE COMPOSTELA

## 1. Introduction

During the past decades, the idea of enhancing the oral bioavailability of peptides and proteins through their association to nanocarriers has been extensively explored [1–3]. This strategy has proved to help the peptides/proteins to overcome the hurdles associated with the oral route of administration (i.e., harsh gastrointestinal environment [4], mucus layer [5–8], poor macromolecular permeability of intestinal cells, [9–11]). Within this frame and taking advantage of the absorption enhancing properties of lipids, biodegradable and biocompatible lipid-based nanocarriers have been widely investigated as macromolecular delivery platforms able to improve the drug stability in harsh conditions. Specifically, our group has already reported promising results (good pharmacodynamics and mucoadhesive properties) following the administration of salmon calcitonin loaded in chitosan (CS) nanocapsules (NCs) [12–14]. Likewise, we showed that polyarginine and protamine NCs could improve the oral delivery of insulin and a modified version of it, insulin glulisine [15,16]. However, so far the association of insulin to CS NCs has been found to be very limited. For these reasons, we considered that a better understanding of the critical formulation parameters affecting the physicochemical properties and the association of peptides to this kind of nanocarriers would be helpful to further increase the peptide loading capacity of lipid-based nanosystems.

Bearing in mind the previous background information, we selected the main core components of previously reported protamine NCs [16] and CS as polymeric shell [17] to screen the factors affecting the physicochemical properties and peptide association efficiency of the forming CS NCs using insulin glulisine. For that purpose, several formulation parameters, such as the type and concentration of different components (e.g., oil, main surfactant, bile salt and polymer), as well as the presence of an extra coating, were modified in a systematic way using the selected CS NCs as starting point.

## 2. Materials and Methods

### 2.1. Materials

Insulin glulisine (Mw 5.822 kDa, IP ≈ 4.75) was kindly provided by Sanofi (Paris, France). Sodium cholate (NaCh) of pharmaceutical grade was purchased from New Zealand Pharmaceuticals (Palmerston North, New Zealand). Pharmaceutical grade polyethylene glycol stearate 40 (PEGst40), D−α−tocopheryl polyethylene glycol 1000 succinate (TPGS)

and poloxamer 407 (Kolliphor® P 407) were purchased from Croda Europe Ltd. (Snaith, UK), Antares Health Products Inc. (Batavia, USA) and BASF (Ludwigshafen, Germany) respectively. Caprylic/capric triglyceride (Miglyol®812N) and DL−α−tocopherol (vitamin E) were purchased from Cremer, Oleo Division (Witten, Germany) and Calbiochem (Merk KGaA, Germany) respectively. Chitosan (CS) with 113 kDa Mw and deacetylation degree 70−90 % and CS with 30−60 kDa Mw and deacetylation degree 80−90 % were purchased from FMC Biopolymer/Novamatrix (Sandvika, Norway) and Heppe Medical Chitosan GmbH ($HMC^+$) (Saale, Germany) respectively. β−casein and polysialic acid (PSA) were purchased from Sigma Aldrich (St. Louis, USA) and Nacalai Tesque Inc. (Tokyo, Japan) respectively. Triton™ X−100 for molecular biology was obtained from Sigma Aldrich (St. Louis, USA). Organic solvents used were of HPLC grade and all other products used were of high purity or reagent grade.

## 2.2. Preparation of insulin-loaded chitosan nanocapsules

Insulin-loaded chitosan nanocapsules (CS NCs) used as starting point in this screening were prepared by the solvent displacement technique, as previously described our group [17]. Briefly, polyethylene glycol stearate 40 (PEGst40) (12 mg) and Miglyol®812N (59 mg) were dissolved in 4.875 mL ethanol. Fifty µL of an aqueous solution of sodium cholate (NaCh) (100 mg/mL) were then added to this lipidic phase followed by the addition of 1 mg insulin glulisine dissolved in 100 µL 0.01 M HCl. This organic phase was vortexed (VELP Scientifica, Usmate, Italy) and then immediately poured over 10 mL of an aqueous solution of CS (0.0125 % w/v) under magnetic stirring at 900 rpm, causing the instantaneous diffusion of the ethanol towards the aqueous phase, leading to the rapid formation of CS NCs. Finally, ethanol was removed and CS NCs were concentrated up to a final volume of 5 mL by evaporation under vacuum (Rotavapor Heidolph Hei−VAP Advantage, Schwabach, Germany). The rest of the CS NCs used in this screening were prepared by the same method but modifying the corresponding parameter later specified.

## 2.3. Physicochemical properties of insulin-loaded chitosan nanocapsules (DLS)

The mean particle size and polydispersity index (PdI) of the nanocarriers were measured by dynamic light scattering using a Zetasizer® (NanoZS, ZEN 3600, Malvern Instruments, Worcestershire, UK) after diluting isolated CS NCs with ultrapure water 33 times. The ζ−potentials were measured by laser-Doppler anemometry after diluting isolated CS NCs

33 times in 1 mM KCl (Zetasizer®, NanoZS, ZEN 3600, Malvern Instruments, Worcestershire, UK). Analysis was done at least in triplicate. To isolate CS NCs, 1 mL of the non-isolated CS NCs was ultracentrifuged at 82656 g for 1 h at 15 °C (Beckman Coulter, Optima L−90K, 70.1 Ti rotor, Brea, USA) obtaining a cream consisting of the isolated-CS NCs, both fractions was collected and diluted with ultrapure water up to 1 mL to maintain the same concentrations as before.

## 2.4. Insulin association efficiency (AE %)

The percentage of insulin associated to the nanosystem was directly determined after extracting the peptide from isolated CS NCs by their complete disruption. To isolate CS NCs, 1 mL of the non-isolated CS NCs was ultracentrifuged at 82,656 g for 1 h at 15 °C (Beckman Coulter, Optima L−90K, 70.1 Ti rotor, Brea, USA) obtaining a cream consisting of the isolated-CS NCs and an undernatant containing the free material. Then, both fractions were collected and diluted with ultrapure water up to 1 mL to maintain the same concentrations as before. Afterwards, for digestion, the insulin-loaded CS NCs were vortexed together with a combination of acetonitrile, Triton™ X−100 and 0.045 % (v/v) TFA using a 2:1:1:16 proportion until obtaining a clear solution. Reverse phase high performance liquid chromatography (Agilent, HPLC 1100 Series, USA) with a C18 column as stationary phase (Superspher® 100 RP−18 endcapped, 4 µm, packed into a LiChroCART® 125 × 4 mm, Merk KGaA, Germany) at 35 °C, coupled with a UV detector set at 214.8 nm was used in a isocratic mode for the insulin quantification. For this purpose, 10 µL of each sample at 25 °C were injected in duplicate and the flow rate was set to 1 mL/min (20 min run/sample). Phosphoric acid and sodium perchlorate buffers (pH 2.3) were mixed with acetonitrile at ratios 93:7 (mobile phase A) and 43:57 (mobile phase B) respectively and used as mobile phases (44 % mobile phase A:56 % mobile phase B).

The AE (%) of insulin was calculated according to the following equation (*Eq. 1*):

$$AE\ (\%) = \frac{Insulin\ in\ the\ disrupted\ nanocarrier}{Total\ insulin}\ X\ 100$$

Where *Insulin in the disrupted* nanocarrier is the insulin concentration determined by HPLC after treating the nanosystem for its disruption, and *Total insulin* is the theoretical total insulin concentration in the formulation. Analysis was done at least in duplicate.

The theoretical insulin loading was calculated according to the following equation (*Eq. 2*):

$$Theoretical\ loading\ (\%) = \frac{Total\ insulin}{Total\ formulation\ components}\ X\ 100$$

Where *Total insulin* is the theoretical total insulin concentration in the formulation, and *Total formulation components* corresponds to the theoretical concentration of all the components forming the NCs.

## 2.5. Stability and insulin release of chitosan nanocapsules in bio-relevant media: SIF and FaSSIF–V2

The colloidal stability of the insulin-loaded nanocapsules was evaluated by analyzing its particle size by DLS (Zetasizer® NanoZS, ZEN 3600, Malvern Instruments, Worcestershire, UK) during a-4 hours incubation period under moderate horizontal shaking (300 rpm, Heidolph Instruments GmbH & Co. KG, Schwabach, Germany) at 37 °C with two different simulated gastrointestinal media (1:33.33 dilution of the original formulation. Final concentration of formulations was 0.6135 mg/mL), whose composition is detailed in *Table 1* [18,19]. PdI, and derived count rate were also monitored (data not shown). To verify that the effect of each media was not interfering in the analysis, blank controls of each medium alone were also carried out. This study was done at least in three different batches in triplicate.

The amount of insulin released from the NCs upon their contact with SIF was also evaluated. For this purpose, the CS NCs were diluted three times in this medium and samples were immediately ultracentrifuged at 18,001 g for 30 min at 15 °C (Beckman Coulter, Optima L−90K, 70.1 Ti rotor, Brea, USA). As a result, two different fractions were obtained: a cream consisting of the isolated-CS NCs and an undernatant containing the insulin released from the nanocapsules. Finally, the insulin present in both fractions was determined by HPLC as described in *Section 2.4.*. This study was done at least in three different batches in triplicate.

***Table 1.*** *SIF and FaSSIF−V2 media composition.*

| Composition | SIF | FaSSIF−V2 |
|---|---|---|
| Sodium hydroxide | 15.4 mM | 34.8 mM |
| Monobasic potassium phosphate | 50 mM | |
| Sodium taurocholate | | 3 mM |
| Lecithin | | 0.2 mM |
| Maleic acid | | 19.12 mM |
| Sodium chloride | | 68.62 mM |
| pH | 6.8 | 6.5 |

### 2.6. Statistical analysis

GraphPad Prism 7 program (California, USA) was used to perform the statistical analysis. Where applicable, data were compared using either the t test (when comparing two groups) or the one-way ANOVA followed by a Fisher's LSD test (when comparing three groups), considering p-values lower than 0.05 as statistically significant.

## 3. Results and Discussion

A schematic representation of the organization of the rationally and initially selected components of CS NCs is illustrated in *Figure 1 (upper panel)*. A rapid acting insulin named as insulin glulisine was selected for this study. This insulin differs from human insulin in the amino acids present at the positions 3 and 29 of its B chain, where asparagine and lysine were respectively replaced by lysine and glutamic acid. This change in the amino acid composition has been found to facilitate the dissociation of insulin hexamers into dimers and monomers, thereby eliciting a fast action upon injection. From the formulation point of view, this change was not supposed to significantly affect its association to the nanocarrier. Based on its isoelectric point (≈ 4.75), insulin was dissolved in HCl 0.01 M (pH ≈ 2) in order to promote its interaction with the negatively charged sodium cholate incorporated in the formulation, as indicated below. Miglyol®812N, a medium chain caprylic/capric triglyceride was selected to constitute the lipid core of the NCs not only because of its permeation enhancing properties, but also because its potential contribution to the protection of the loaded peptide against the degradation [20,21]. PEGst40 was selected as a surfactant to disperse the oily phase into the external aqueous

phase under the premise that its PEG moieties would be oriented towards the external aqueous phase, thereby enhancing the stability of the nanosystem against the enzymatic degradation [12,22–25] as well as promoting its mucodiffusion [24,26–29]. Sodium cholate (NaCh) was selected as co-surfactant apart from its penetration enhancing properties [30,31], because it was expected to form hydrophobic ionic pairs [32–35] with insulin, thereby enhancing its retention in the lipid core. Finally, CS was selected as polymeric shell due to its biocompatibility and well-known mucoadhesive properties [36–39].

Physicochemical properties and insulin association efficiency of the resulting CS NCs are also showed in *Figure 1 (lower panel)*. Despite the obtained CS NCs presented appropriate physicochemical properties (hydrodynamic mean size of 346 ± 13 nm, low polydispersity index (0.2) and positive ζ–potential of +34 ± 2 mV), the insulin association efficiency value (28 ± 6 %) was much lower than the one reported for protamine NCs (62 ± 16 %) [16]. These results, brought to light the importance of the type of polymer coating on this characteristic and the need of optimizing each nanosystem for the cargo it is intended to. Accordingly, we studied the influence of several formulation parameters using these CS NCs as starting point and trying to end up in a formulation with appropriate properties.

USC UNIVERSIDADE DE SANTIAGO DE COMPOSTELA

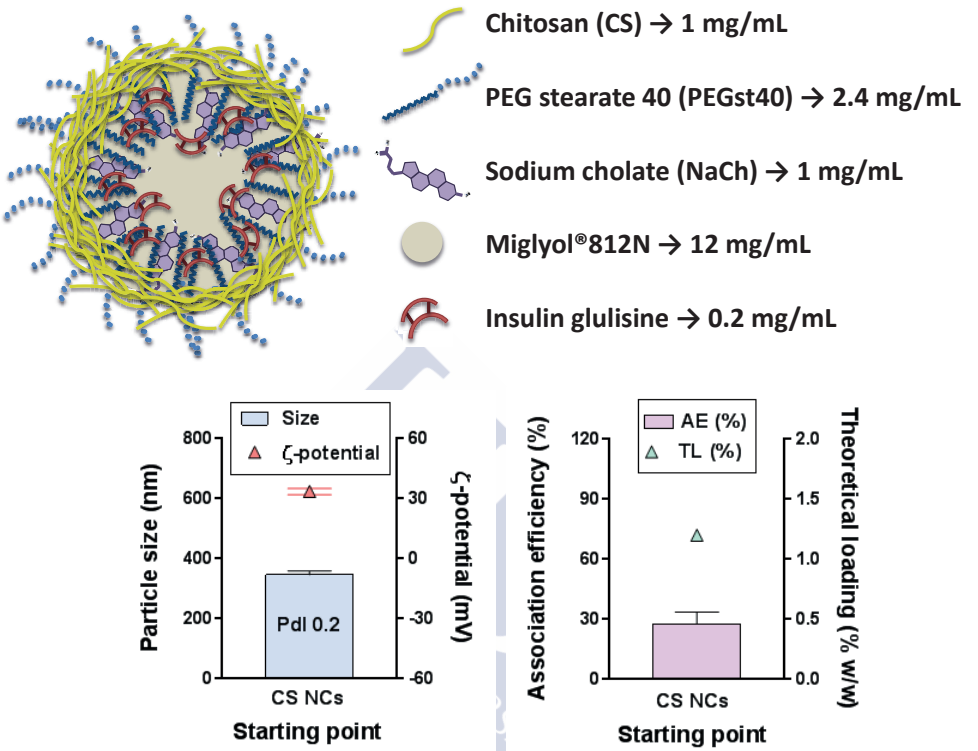



***Figure 1. Top:*** *Schematic representation and composition of the CS NCs used as screening starting point;* ***Bottom:*** *Physicochemical characterization (size, PdI and ζ-potential), insulin association efficiency (% AE) and theoretical loading (% TL) of these CS NCs (Mean ± SD, n ≥ 3).*

### 3.1. Effect of the oil type used as nanocapsules core: Miglyol®812N vs DL–α–tocopherol (vitamin E)

First, the effect of substituting Miglyol®812N for DL–α–tocopherol was evaluated. DL–α–tocopherol is the most biologically active form of the vitamin E, and it was selected in this screening due to their intrinsic antioxidant and anti-inflammatory properties, having been already proved its ability to partially correct the defective monocytic chemotactic function and motility observed in diabetes, which usually complicates infections in these patients [40,41]. For this purpose, and being type of oil (Miglyol®812N vs DL–α–tocopherol) the variable under study, we fixed the following concentrations to prepare the CS NCs: 1 mg/mL of CS, 12 mg/mL of oil, 2.4 mg/mL of PEGst40, 1 mg/mL of

NaCh and 0.2 mg/mL of insulin glulisine (1.2 % theoretical loading). As shown in *Figure 2*, the insulin association efficiency observed for both formulations was similar (≈ 27 %), however, the size and ζ−potential were significantly higher ($p \leq 0.01$, ≈ 180 nm and ≈ 12 mV increment) when vitamin E (≈ 525 ± 65 nm, ≈ 46 ± 4 mV) was used instead of Miglyol®812N (≈ 346 ± 13 nm, ≈ 34 ± 2 mV). This could be attributed to the higher viscosity of the vitamin E respect to Miglyol®812N, which probably hampered the diffusion of the organic solvent towards the aqueous phase during the formation process of the NCs, thus leading to the formation of less in number, but bigger, oily droplets. Attending to these physicochemical properties, Miglyol®812N was selected as oily core for the following studies.

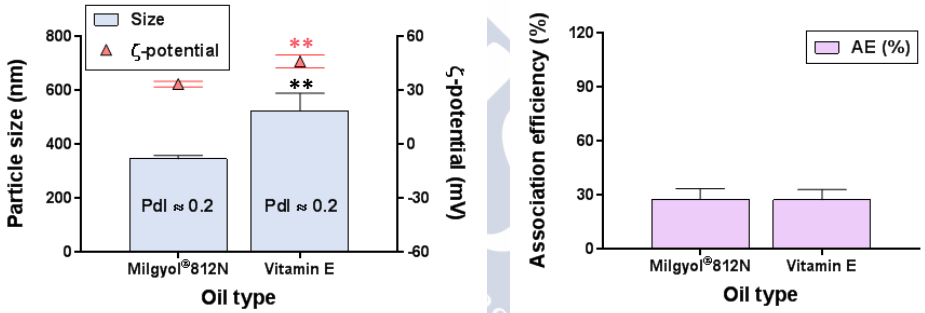



***Figure 2.*** *Influence of the oil type used as nanocapsules core: Miglyol®812N vs DL−α−tocopherol (vitamin E) on the physicochemical properties* ***(left)*** *and insulin association efficiency* ***(right)*** *of CS NCs (Mean ± SD, n ≥ 3) (t test was applied for the statistical analysis; significance levels **p ≤ 0.01). Constant formulation parameters: 1 mg/mL of CS, 12 mg/mL of oil, 2.4 mg/mL of PEGst40, 1 mg/mL of NaCh and 0.2 mg/mL of insulin glulisine (1.2 % theoretical loading).*

## 3.2. Effect of the main surfactant type: PEG stearate 40 vs D−α−tocopheryl PEG 1000 succinate (TPGS)

The effect of main surfactant type was evaluated by comparing the formulation with PEGst40 (HLB ≈ 17, Mw ≈ 2 kDa) and TPGS (HLB ≈ 13, Mw ≈ 1.5 kDa). Both emulsifiers were selected due to their permeation enhancing properties and also because their PEG moieties were expected to enhance the stability of the nanosystem against the enzymatic degradation [12,22–25] as well as promote its mucodiffusion [24,26–29]. Additionally, since TPGS is a polyethylene glycol 1000 ester of the D−α−tocopheryl succinate, it was supposed to hold the interesting properties described for vitamin E in the previous

section. For this purpose, and being the type of surfactant (PEGst40 vs TPGS) the variable under study, we fixed the following concentrations to prepare the CS NCs: 1 mg/mL of CS, 12 mg/mL of Miglyol®812N, 2.4 mg/mL of surfactant, 1 mg/mL of NaCh and 0.2 mg/mL of insulin glulisine (1.2 % theoretical loading). In this case, probably due to the high similarity of both surfactants, non-significant differences were observed in terms of physicochemical properties (size, ζ–potential and PdI) (*Figure 3*). However, since a slight but significant improvement of the insulin association efficiency ($p \leq 0.05$) was observed in the NCs formulated with PEGst40, this surfactant was selected for the subsequent studies.

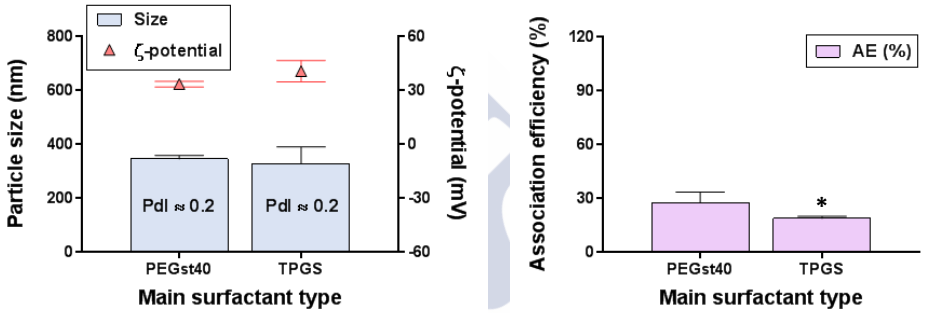



***Figure 3.*** *Influence of the main surfactant type: PEG stearate 40 vs D–α–tocopheryl PEG 1000 succinate (TPGS) on the physicochemical properties* ***(left)*** *and insulin association efficiency* ***(right)*** *of CS NCs (Mean ± SD, n ≥ 3) (t test was applied for the statistical analysis; significance levels *p ≤ 0.05). Constant formulation parameters: 1 mg/mL of CS, 12 mg/mL of Miglyol®812N, 2.4 mg/mL of surfactant, 1 mg/mL of NaCh and 0.2 mg/mL of insulin glulisine (1.2 % theoretical loading).*

## 3.3. Effect of the concentration of the CS polymer: 0.25 vs 0.5 vs 1 mg/mL

The fact that, under the same formulation conditions, the cationic polymer protamine led to a much greater association (62 ± 16 %) [16] than CS (28 ± 6 %) (*Section 2.3*), led us to the hypothesis that CS molecules have such a high affinity for the oil/water interface that they compete with insulin molecules, which are positively charged for being dissolved in HCl 0.01 M (pH ≈ 2 <insulin isoelectric point ≈ 4.75), in their interaction with the acidic lipid components. On the other hand, we also considered the possibility of having an excess of CS that led to the presence of free CS in the formulation that may have interacted with the insulin preventing its association to the nanosystem. For these reasons, we investigated the influence of the CS concentration: 1, 0.5 and 0.25 mg/mL, in the insulin association efficiency, by keeping constant the following parameters:

12 mg/mL of Miglyol®812N, 2.4 mg/mL of PEGst40, 1 mg/mL of NaCh and 0.2 mg/mL of insulin glulisine (1.2 % theoretical loading). As expected, the results showed that insulin association efficiency was inversely proportional to the CS concentration (*Figure 4*), and interestingly, non-significant differences were found among the physicochemical properties of the NCs formulated with the three CS concentrations tested, which suggested that 0.25 mg/mL of CS was concentration enough to form a polymer shell around the oily cores. In view of the results obtained we selected 0.25 mg/mL CS as a fixed parameter for subsequent experiments.

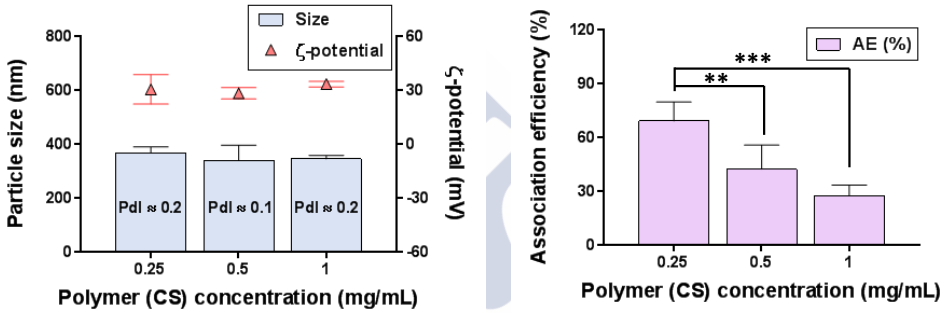



***Figure 4.*** *Influence of the concentration of the CS polymer coating: 0.25 vs 0.5 vs 1 mg/mL on the physicochemical properties* ***(left)*** *and insulin association efficiency* ***(right)*** *of CS NCs (Mean ± SD, n ≥ 3) (One-way ANOVA followed by a Fisher's LSD test were applied for the statistical analysis; significance levels **p ≤ 0.01; ***p ≤ 0.001). Constant formulation parameters: 12 mg/mL of Miglyol®812N, 2.4 mg/mL of PEGst40, 1 mg/mL of NaCh and 0.2 mg/mL of insulin glulisine (1.2 % theoretical loading).*

### 3.4. Effect of the NaCh bile salt concentration: 0.25 vs 0.5 vs 1 mg/mL

As indicated, we introduced NaCh in this formulation apart from its penetration enhancing properties [30,31], because it was supposed to favor the retention of the peptide in the lipid core improving its association efficiency through the formation of hydrophobic ionic pairs [32–35]. For this purpose, and being the concentration of NaCh (1, 0.5 and 0.25 mg/mL) the variable under study, we fixed the following concentrations to prepare the CS NCs: 0.25 mg/mL of CS, 12 mg/mL of Miglyol®812N, 2.4 mg/mL of PEGst40 and 0.2 mg/mL of insulin glulisine (1.2−1.3 % theoretical loading). The results in *Figure 5* indicate that the concentration of NaCh bile salt influenced the physicochemical properties of the NCs, however, it did not affect the insulin association efficiency. Indeed, CS NCs prepared with 0.5 and 1 mg/mL of NaCh showed a smaller size (≈ 350 nm) and

polydispersity index (≈ 0.2) than those formulated with 0.25 mg/mL of NaCh (≈ 486 nm, 0.3 PdI), probably due to the surfactant properties of this bile salt. Therefore, the formulation with 0.5 mg/mL NaCh was selected for the subsequent studies.

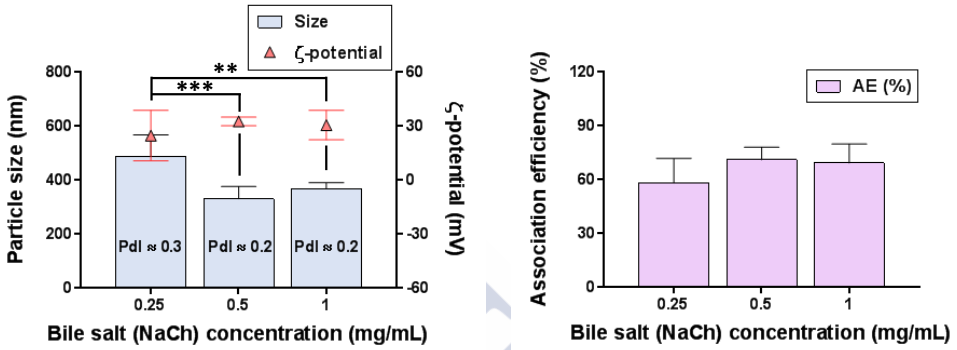



***Figure 5.*** *Influence of the concentration of the NaCh bile salt: 0.25 vs 0.5 vs 1 mg/mL on the physicochemical properties* ***(left)*** *and insulin association efficiency* ***(right)*** *of CS NCs (Mean ± SD, n ≥ 3) (One-way ANOVA followed by a Fisher's LSD test were applied for the statistical analysis; significance levels **p ≤ 0.01; ***p ≤ 0.001). Constant formulation parameters: 0.25 mg/mL of CS, 12 mg/mL of Miglyol®812N, 2.4 mg/mL of PEGst40 and 0.2 mg/mL of insulin glulisine (1.2–1.3 % theoretical loading).*

## 3.5. Effect of the PEGst40 main surfactant concentration: 2.4 vs 3.0 vs 3.6 mg/mL

In the same line, different concentrations of the main surfactant (2.4, 3.0 and 3.6 mg/mL), PEGst40 (HLB ≈ 17, Mw ≈ 2 kDa), were screened. The PEG moieties of this surfactant are expected to be oriented towards the external aqueous phase, therefore enhancing the stability of the nanosystem against the enzymatic degradation [12,22–25], as well as promoting its mucodiffusion [24,26–29]. For this purpose, and being the concentration of PEGst40 (2.4, 3 and 3.6 mg/mL) the variable under study, we fixed the following concentrations to prepare the CS NCs: 0.25 mg/mL of CS, 12 mg/mL of Miglyol®812N, 0.5 mg/mL of NaCh and 0.2 mg/mL of insulin glulisine (1.2–1.3 % theoretical loading). The results in *Figure 6* indicate that the size, PdI and insulin association efficiency progressively increased with the use of higher PEGst40 concentrations. The size increase could be attributed to the presence of an excess of PEGst40, thus triggering a higher incorporation of this surfactant into the NCs, and/or the formation of a second population of colloidal micelle-like structures (clusters), which would interact with the insulin. In fact, knowing that insulin can interact with NaCh, we could speculate about the potential formation of

mixed micelles consisting of PEGst40 and NaCh containing insulin. Indeed, the concentration of this surfactant is much higher than its critical micelle concentration (≈ 0.11 mg/mL) [42]. On the other hand, ζ-potential was significantly reduced when the highest concentration of PEGst40 was used; probably do to the higher amount of PEG chains available to shield the positive charge of CS on the surface of the NCs. In view of these results CS NCs with 2.4 mg/mL of PEGst40 were chosen for the next studies.

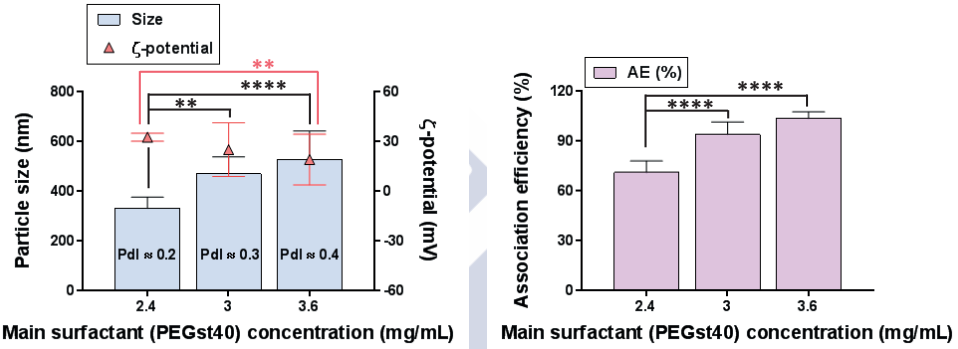



***Figure 6.*** *Influence of the concentration of PEGst40 used as main surfactant: 2.4 vs 3 vs 3.6 mg/mL on the physicochemical properties* ***(left)*** *and insulin association efficiency* ***(right)*** *of CS NCs (Mean ± SD, n ≥ 3) (One-way ANOVA followed by a Fisher's LSD test were applied for the statistical analysis; significance levels **p ≤ 0.01; ****p ≤ 0.0001). Constant formulation parameters: 0.25 mg/mL of CS, 12 mg/mL of Miglyol®812N, 0.5 mg/mL of NaCh and 0.2 mg/mL of insulin glulisine (1.2−1.3 % theoretical loading).*

## 3.6. Effect of the chitosan molecular weight: 113 vs 30-60 kDa

As previously mentioned, CS with a ≈ 113 kDa Mw, and a deacetylation degree ≈ 70−90 % was initially selected in the screening. In order to investigate the effect of CS Mw on the physicochemical properties and insulin association efficiency of these NCs, we chose CS with a Mw of 30−60 kDa and a similar deacetylation degree (80−90 %). For this purpose, and being the Mw of CS (113 vs 30−60 kDa) the variable under study, we fixed the following concentrations to prepare the CS NCs: 0.25 mg/mL of CS, 12 mg/mL of Miglyol®812N, 2.4 mg/mL of PEGst40, 0.5 mg/mL of NaCh and 0.2 mg/mL of insulin glulisine (1.3 % theoretical loading). As shown in *Figure 7*, CS NCs could be formed using either type of CS, although a slight size increment ($p \leq 0.01$) and a drastic reduction in the zeta potential values (from +33 ± 2 mV to +1 ± 5 mV) were observed when using the low Mw CS. Irrespective of these changes, non-significant differences were observed in terms

of insulin association efficiency, which varied from 71 ± 7 % to 82 ± 5 % for the low Mw CS. According to the DLVO theory, which states that the total potential of interaction ($V_T$) between two approaching particles can be expressed as $V_T = V_A + V_R$, where $V_A$ is the attractive potential of interaction due to the Van der Waals forces and $V_R$ is the repulsive electrostatic potential that depends on the ζ−potential magnitude [43], higher ζ−potentials would confer the nanosystem with higher colloidal stability. Accordingly, NCs with low Mw CS were potentially more unstable tha those with high Mw CS due to their neutral character, which was the reason behind the choice of higher CS Mw NCs CS to perform the subsequent studies.

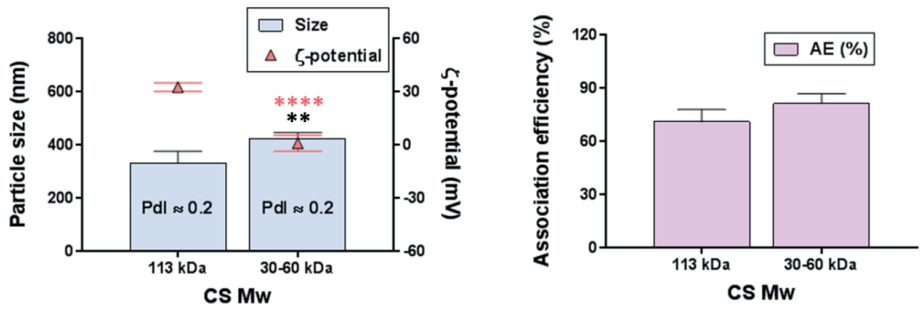



***Figure 7.*** *Influence of the CS molecular weight: 113 vs 30–60 kDa Mw on the physicochemical properties* ***(left)*** *and insulin association efficiency* ***(right)*** *of CS NCs (Mean ± SD, n ≥ 3) (t test was applied for the statistical analysis; significance levels **p ≤ 0.01; ****p ≤ 0.0001). Constant formulation parameters: 0.25 mg/mL of CS, 12 mg/mL of Miglyol®812N, 2.4 mg/mL of PEGst40, 0.5 mg/mL of NaCh and 0.2 mg/mL of insulin glulisine (1.3 % theoretical loading).*

### 3.7. Effect of inclusion of the non-ionic surfactant poloxamer 407

Since it has been reported that the surfactant poloxamer 407 may enhance the stability of nanosystems in enzyme-rich intestinal media [12,22–25] as well as promote their mucodiffusion [24,26–29], we incorporated it (5 mg/mL) in the CS NCs formulation that was found to be optimal in the screening while keeping constant the following parameters: 0.25 mg/mL of CS, 12 mg/mL of Miglyol®812N, 2.4 mg/mL of PEGst40, 0.5 mg/mL of NaCh and 0.2 mg/mL of insulin glulisine (1−1.3 % theoretical loading). This non-ionic surfactant is formed by polyethylene oxide (PEO) and propylene oxide (PPO) units organized in a $PEO_n$–$PPO_m$–$PEO_n$ architecture, with two hydrophilic side arms with 100 × PEO monomers and a central hydrophobic block formed by 65 × PPO monomers

(Mw ≈ 12 kDa; HLB ≈ 22). The number of monomers in the hydrophilic side arms may influence the protective steric layer of the nanostructures [44,45] since PEG moieties will be oriented towards the external aqueous phase, whereas the central hydrophobic block is expected to determine the interfacial adsorption of the surfactant as well as its ability to compete with other components present at the oil/water interface [46–48]. As depicted in *Figure 8*, the incorporation of this non-ionic surfactant on the CS NCs surface did not significantly affect the size and PdI of the NCs, however, it led to a displacement of the shear plane (where the ζ–potential is defined) towards the aqueous phase, and, hence, to a significant reduction on the ζ–potential magnitude ($p \leq 0.0001$) [45]. Due to the expected positive contribution of this surfactant in terms of stability [12,23–25] and mucodiffusion [28,48,49], and since its incorporation in the nanosystem did not significantly affect to its insulin association efficiency, CS NCs containing poloxamer 407 were selected for subsequent studies.

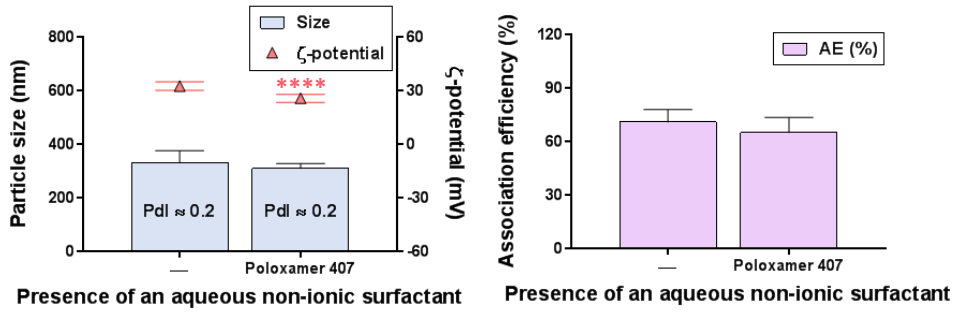



***Figure 8.*** *Influence of the inclusion of an extra non-ionic surfactant on the CS NCs surface: plain vs poloxamer 407-containing CS NCs on the physicochemical properties* ***(left)*** *and insulin association efficiency* ***(right)*** *of CS NCs (Mean ± SD, n ≥ 3) (t test was applied for the statistical analysis; significance levels ****p ≤ 0.0001). Constant formulation parameters: 0.25 mg/mL of CS, 12 mg/mL of Miglyol®812N, 2.4 mg/mL of PEGst40, 0.5 mg/mL of NaCh and 0.2 mg/mL of insulin glulisine (1–1.3 % theoretical loading).*

## 3.8. Effect of the inclusion of a second coating: plain vs β–casein-coated vs polysialic acid (PSA)-coated chitosan nanocapsules

Since it has been reported the additional value of incorporating a second coating on the surface of this kind of NCs [16,50], we wanted to explore the possibility of adding an extra shell to the formulation here screened. For that purpose, we rationally selected two different biomaterials: β–casein and polysialic acid (PSA). On the one hand, casein (cow's

milk protein) is a biodegradable and FDA GRAS (Generally Recognized as Safe) biomaterial with a non-toxic profile that has been approved for human use [51,52]. Caseins presents both hydrophilic and hydrophobic domains that also confers this material with surfactant properties [53,54] and interestingly, its role as protective agent and absorption enhancer has been reported for oral delivery of insulin [55]. On the other hand, it has been reported that PSA, a non-toxic and biodegradable polysaccharide, was able to improve the stability of both peptides and lipid-based nanocarriers by hampering their interaction with enzymes [16,56–59]. For this purpose, and being the presence of a second coating (plain vs β−casein-coated vs PSA-coated CS NCs) the variable under study, we fixed the following concentrations to prepare the CS NCs: 0.25 mg/mL of the second polymer, 0.25 mg/mL of CS, 12 mg/mL of Miglyol®812N, 2.4 mg/mL of PEGst40, 0.5 mg/mL of NaCh, 5 mg/mL of poloxamer 407 and 0.2 mg/mL of insulin glulisine (1 % theoretical loading). The significant reduction of the ζ−potential magnitude ($p \leq 0.0001$) observed when either PSA or β-casein were incorporated into the CS NCs (CS NCs ≈ +26 ± 2 mV; β-casein-coated CS NCs ≈ +2 ± 5 mV; PSA-coated CS NCs ≈ −3 ± 4 mV) (*Figure 9, left*), confirmed the formation of the extra coating. Unfortunately, as depicted in *Figure 9, right*, the second polymer coating led to an important reduction of the insulin association efficiency ($p \leq 0.0001$), which led us to discard these formulations. The fact that a precipitate containing 60−80 % of the insulin was obtained when isolating these formulations, led us to hypothesize that the second polymer layer could have promoted the detachment of the first CS layer from the oily core rather than being deposited onto it. This detachment would agree with the reduction of the zeta potential of the nanocarrier and the disassociation of insulin.

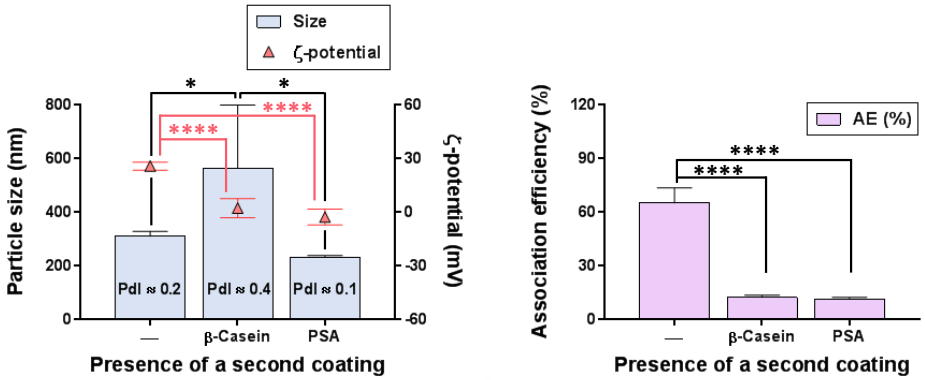



***Figure 9.*** *Influence of the inclusion of a second coating on the CS NCs surface: plain vs β-casein-coated vs PSA-coated CS NCs on the physicochemical properties* ***(left)*** *and insulin association efficiency* ***(right)*** *of CS NCs (Mean ± SD, n ≥ 3) (One-way ANOVA followed by a Fisher's LSD test were applied for the statistical analysis; significance levels *p ≤ 0.05; ****p ≤ 0.0001). Constant formulation parameters: 0.25 mg/mL of the second polymer, 0.25 mg/mL of CS, 12 mg/mL of Miglyol®812N, 2.4 mg/mL of PEGst40, 0.5 mg/mL of NaCh, 5 mg/mL of poloxamer 407 and 0.2 mg/mL of insulin glulisine (1 % theoretical loading).*

## 3.9. Effect of the theoretical insulin glulisine loading

Once we selected a prototype (0.25 mg/mL of CS, 12 mg/mL of Miglyol®812N, 2.4 mg/mL of PEGst40, 0.5 mg/mL of NaCh and 5 mg/mL of poloxamer 407) with acceptable physicochemical properties and insulin association efficiency, we tried to increase its insulin loading. For that purpose we added, during the formulation process, two different amounts of insulin glulisine: 1 mg (1 % theoretical loading) and 1.5 mg (1.5 % theoretical loading) by keeping constant the volume of HCl 0.01 in which it was dissolved (100 µL). As shown in *Figure 10*, both the physicochemical properties and insulin association efficiency were similar in both cases. Therefore, using the highest theoretical insulin loading it was possible to increase the final insulin loading of the nanosystem from approximately 0.65 % to 1.1 %.

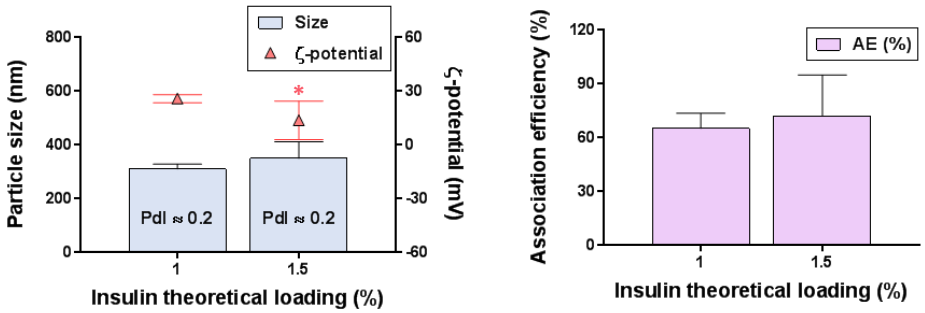



***Figure 10.*** *Influence of the theoretical insulin glulisine loading: 1 mg (1 % theoretical loading) vs 1.5 mg (1.5 % theoretical loading) on the physicochemical properties* ***(left)*** *and insulin association efficiency* ***(right)*** *of CS NCs (Mean ± SD, n ≥ 3) (t test was applied for the statistical analysis; significance levels *p ≤ 0.05). Constant formulation parameters: 0.25 mg/mL of CS, 12 mg/mL of Miglyol®812N, 2.4 mg/mL of PEGst40, 0.5 mg/mL of NaCh, 5 mg/mL of poloxamer 407 and 100 µL of HCl 0.01 M to dissolve the insulin glulisine.*

As a summary, the estimated influence of the formulation variables investigated in this screening process is illustrated in *Table 2*. Overall, the formulation that exhibits the best characteristics is the one composed of 0.25 mg/mL of CS, 12 mg/mL of Miglyol®812N, 2.4 mg/mL of PEGst40, 0.5 mg/mL of NaCh, 5 mg/mL of poloxamer 407 and 0.3 mg/mL of insulin glulisine (1.5 % theoretical loading).

***Table 2.*** *Effect of the different factors under study on the size, PdI, ζ–potential (ζ–Pot.) and insulin association efficiency (AE %) of the CS NCs used as starting point. Symbols show in a qualitative way the magnitude of the corresponding effect: increment (↑), reduction (↓) and almost constant (≈).*

| Factor under study | Size | PdI | ζ–Pot. | AE % |
|---|---|---|---|---|
| **Oil type:** change from Miglyol®812N to DL–α–tocopherol | ↑↑ | ≈ | ↑ | ≈ |
| **Main surfactant type:** change from PEGst40 to TPGS | ≈ | ≈ | ≈ | ↓ |
| **Polymer concentration:** increasing CS concentration (0.25, 0.5 and 1 mg/mL) | ≈ | ≈ | ≈ | ↓↓ |
| **Bile salt concentration:** increasing NaCh concentration (0.25, 0.5 and 1 mg/mL) | ↓↓ | ↓ | ≈ | ≈ |
| **Main surfactant concentration:** increasing PEGst40 concentration (2.4, 3.0 and 3.6 mg/mL) | ↑↑ | ↑↑ | ↓ | ↑↑ |
| **Polymer type:** increasing CS Mw from 30–60 to 113 kDa | ↓ | ≈ | ↑↑ | ≈ |
| **Extra non-ionic surfactant:** inclusion of poloxamer 407 | ≈ | ≈ | ↓ | ≈ |
| **Extra second coating:** inclusion of β–casein/polysialic acid as second polymer coating | ↑↑/≈ | ↑↑/↓ | ↓↓ | ↓↓ |
| **Peptide theoretical loading:** increasing theoretical insulin loading from 1 to 1.5 % | ≈ | ≈ | ≈ | ≈ |

## 3.10. Stability and insulin release of CS NCs in bio-relevant media: SIF and FaSSIF–V2

The ability of the CS nanocapsules selected in the previous screening to maintain their physicochemical properties upon exposure to intestinal fluids was thought to be critical to assess its capacity to overcome the oral biological barriers. For this purpose, the colloidal stability of the insulin-loaded CS NCs was monitored by DLS (size, PdI and derived count rate) during 4 hours contact with two simulated intestinal fluids (SIF and FaSSIF–V2, composition detailed in *Table 1*) at 37 °C. Unfortunately, results showed the unstable behaviour of these CS NCs in simulated intestinal fluids (*Figure 11*), since the system drastically decreased its size (≈ 150 nm). The reduction of the size could be due to the detachment of the polymer and surfactant from the surface of the nanocapsules in the presence of the medium with high ionic content [60,61].

On the other hand, *in vitro* release studies showed that 70-80 % of the associated insulin was released upon contact with simulated intestinal fluids. Therefore, these results suggest a disassembling of the structure in highly diluted conditions and in presence of high ionic forces. Whether such a process should be expected *in vivo* remains to be elucidated.

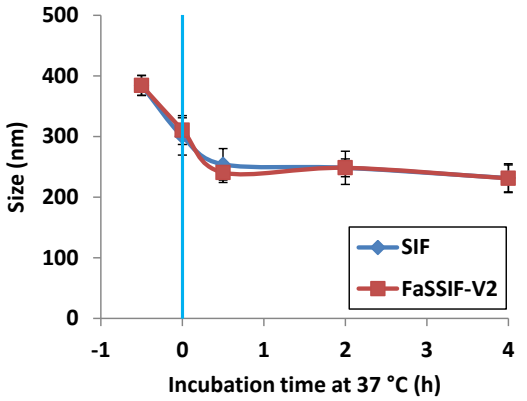



***Figure 11.*** *Colloidal stability profile of the finally selected insulin-loaded CS NCs after its incubation in two simulated bio-relevant media (SIF and FaSSIF–V2) at 37 °C.* Size represented at t = −0.5, corresponds to the size of the CS NCs in water (Mean ± SD, n ≥ 3).

## 4. Conclusions

Overall, we have shown a variety of factors that influence the physicochemical properties and ability of CS NCs to associate insulin. While some of the studied variables, such as the type of the main surfactant and the inclusion of an extra non-ionic surfactant in the formulation, had minor effects on both, the physicochemical properties and insulin association, others, e.g., the composition of the polymer shell, had a drastic effect. Among the latest, it should be pointed out the negative effect of both, the increase of the concentration of polymer and the presence of a second coating shell on the ability of the CS NCs to associate insulin. The results of this work led us to deeper investigate the "*Influence of the surface properties of nanocapsules on their interaction with the intestinal barriers*", being the results of this study developed in the *Chapter 3* of this thesis.

## References

[1] Z. Niu, I. Conejos-Sánchez, B.T. Griffin, C.M. O'Driscoll, M.J. Alonso, Lipid-based nanocarriers for oral peptide delivery, Adv. Drug Deliv. Rev. 106 (2016) 337–354. doi:10.1016/j.addr.2016.04.001.

[2] I. Santalices, A. Gonella, D. Torres, M.J. Alonso, Advances on the formulation of proteins using nanotechnologies, J. Drug Deliv. Sci. Technol. 42 (2017) 155–180. doi:10.1016/j.jddst.2017.06.018.

[3] T.A.S. Aguirre, D. Teijeiro-Osorio, M. Rosa, I.S. Coulter, M.J. Alonso, D.J. Brayden, Current status of selected oral peptide technologies in advanced preclinical development and in clinical trials, Adv. Drug Deliv. Rev. 106 (2016) 223–241. doi:10.1016/j.addr.2016.02.004.

[4] A. Sood, R. Panchagnula, Peroral route: An opportunity for protein and peptide drug delivery, Chem. Rev. 101 (2001) 3275–3303. doi:10.1021/cr000700m.

[5] S. Mitragotri, P.A. Burke, R. Langer, Overcoming the challenges in administering biopharmaceuticals: formulation and delivery strategies, Nat Rev Drug Discov. 13 (2014) 655–672. doi:10.1038/nrd4363.

[6] M. Morishita, N.A. Peppas, Is the oral route possible for peptide and protein drug delivery?, Drug Discov. Today. 11 (2006) 905–910. doi:10.1016/j.drudis.2006.08.005.

[7] J. Wang, V. Yadav, A.L. Smart, S. Tajiri, A.W. Basit, Toward oral delivery of biopharmaceuticals: An assessment of the gastrointestinal stability of 17 peptide drugs, Mol. Pharm. 12 (2015) 966–973. doi:10.1021/mp500809f.

[8] C. Atuma, V. Strugala, A. Allen, L. Holm, The adherent gastrointestinal mucus gel layer: thickness and physical state in vivo, Am. J. Physiol. Gastrointest. Liver Physiol. 280 (2001) G922–G929. http://www.ncbi.nlm.nih.gov/pubmed/11292601.

[9] G. Camenisch, J. Alsenz, H. Van De Waterbeemd, G. Folkers, Estimation of permeability by passive diffusion through Caco-2 cell monolayers using the drugs' lipophilicity and molecular weight, Eur. J. Pharm. Sci. 6 (1998) 313–319. doi:10.1016/S0928-0987(97)10019-7.

[10] W. Rubas, M.E.M. Cromwell, Z. Shahrokh, J. Villagran, T.N. Nguyen, M. Wellton, T.H. Nguyen, R.J. Mrsny, Flux measurements across Caco-2 monolayers may predict transport in human large intestinal tissue, J. Pharm. Sci. 85 (1996) 165–169. doi:10.1021/js950267+.

[11] M. Bendayan, E. Ziv, D. Gingras, R. Ben-Sasson, H. Bar-On, M. Kidron, Biochemical and morpho-cytochemical evidence for the intestinal absorption of insulin in control and diabetic rats. Comparison between the effectiveness of duodenal and colon mucosa, Diabetologia. 37 (1994) 119–126. doi:10.1007/s001250050081.

[12] C. Prego, D. Torres, E. Fernandez-Megia, R. Novoa-Carballal, E. Quiñoá, M.J. Alonso, Chitosan-PEG nanocapsules as new carriers for oral peptide delivery: effect of chitosan pegylation degree, J. Control. Release. 111 (2006) 299–308. doi:10.1016/j.jconrel.2005.12.015.

[13] C. Prego, D. Torres, M.J. Alonso, Chitosan nanocapsules as carriers for oral peptide delivery: effect of chitosan molecular weight and type of salt on the in vitro behaviour and in vivo effectiveness, J. Nanosci. Nanotechnol. 6 (2006) 2921–2928. doi:10.1166/jnn.2006.429.

[14] C. Prego, M. Fabre, D. Torres, M.J. Alonso, Efficacy and mechanism of action of chitosan nanocapsules for oral peptide delivery, Pharm. Res. 23 (2006) 549–556. doi:10.1007/s11095-006-

9570-8.

[15] Z. Niu, E. Tedesco, F. Benetti, A. Mabondzo, I.M. Montagner, I. Marigo, D. Gonzalez-Touceda, S. Tovar, C. Diéguez, M.J. Santander-Ortega, M.J. Alonso, Rational design of polyarginine nanocapsules intended to help peptides overcoming intestinal barriers, J. Control. Release. 263 (2016) 4–17. doi:10.1016/j.jconrel.2017.02.024.

[16] L.N. Thwala, A. Beloqui, N.S. Csaba, D. González-Touceda, S. Tovar, C. Dieguez, M.J. Alonso, V. Préat, The interaction of protamine nanocapsules with the intestinal epithelium: a mechanistic approach, J. Control. Release. 243 (2016) 109–120. doi:10.1016/j.jconrel.2016.10.002.

[17] P. Calvo, C. Remuñán-López, J.L. Vila-Jato, M.J. Alonso, Development of positively charged colloidal drug carriers: chitosan-coated polyester nanocapsules and submicron-emulsions, Colloid Polym. Sci. 275 (1997) 46–53. doi:10.1007/s003960050050.

[18] E. Jantratid, N. Janssen, C. Reppas, J.B. Dressman, Dissolution media simulating conditions in the proximal human gastrointestinal tract: An update, Pharm. Res. 25 (2008) 1663–1676. doi:10.1007/s11095-008-9569-4.

[19] E. Roger, F. Lagarce, J.P. Benoit, The gastrointestinal stability of lipid nanocapsules, Int. J. Pharm. 379 (2009) 260–265. doi:10.1016/j.ijpharm.2009.05.069.

[20] K.A. Traul, A. Driedger, D.L. Ingle, D. Nakhasi, Review of the toxicologic properties of medium-chain triglycerides, Food Chem. Toxicol. 38 (2000) 79–98. doi:10.1016/S0278-6915(99)00106-4.

[21] B. Marten, M. Pfeuffer, J. Schrezenmeir, Medium-chain triglycerides, Int. Dairy J. 16 (2006) 1374–1382. doi:10.1016/j.idairyj.2006.06.015.

[22] M. Tobío, R. Gref, A. Sanchez, R. Langer, M.J. Alonso, Stealth PLA-PEG nanoparticles as protein carriers for nasal administration, Pharm. Res. 15 (1998) 270–275. doi:10.1023/A:1011922819926.

[23] M. Tobío, A. Sánchez, A. Vila, I. Soriano, C. Evora, J.. J. Vila-Jato, M.. M. Alonso, The role of PEG on the stability in digestive fluids and in vivo fate of PEG-PLA nanoparticles following oral administration, Colloids Surfaces B Biointerfaces. 18 (2000) 315–323. doi:10.1016/S0927-7765(99)00157-5.

[24] I. Santalices, D. Torres, M.V. Lozano, M.M. Arroyo-Jiménez, M.J. Alonso, M.J. Santander-Ortega, Influence of the surface properties of nanocapsules on their interaction with intestinal barriers, Submitt. to Eur. J. Pharm. Biopharm. (2018).

[25] M. Wulff-Pérez, J. de Vicente, A. Martín-Rodríguez, M.J. Gálvez-Ruiz, Controlling lipolysis through steric surfactants: new insights on the controlled degradation of submicron emulsions after oral and intravenous administration, Int. J. Pharm. 423 (2012) 161–166. doi:10.1016/j.ijpharm.2011.12.025.

[26] L.M. Ensign, R. Cone, J. Hanes, Oral drug delivery with polymeric nanoparticles: the gastrointestinal mucus barriers, Adv. Drug Deliv. Rev. 64 (2012) 557–570. doi:10.1016/j.addr.2011.12.009.

[27] A. Vila, H. Gill, O. McCallion, M.J. Alonso, Transport of PLA-PEG particles across the nasal mucosa: Effect of particle size and PEG coating density, J. Control. Release. 98 (2004) 231–244. doi:10.1016/j.jconrel.2004.04.026.

[28] Q. Xu, L.M. Ensign, N.J. Boylan, A. Schön, X. Gong, J.C. Yang, N.W. Lamb, S. Cai, T. Yu, E. Freire, J. Hanes, Impact of surface polyethylene glycol (PEG) density on biodegradable nanoparticle transport

in mucus ex vivo and distribution in vivo, ACS Nano. 9 (2015) 9217–9227. doi:10.1021/acsnano.5b03876.

[29] D. Chen, D. Xia, X. Li, Q. Zhu, H. Yu, C. Zhu, Y. Gan, Comparative study of Pluronic® F127-modified liposomes and chitosan-modified liposomes for mucus penetration and oral absorption of cyclosporine A in rats, Int. J. Pharm. 449 (2013) 1–9. doi:10.1016/j.ijpharm.2013.04.002.

[30] M. Niu, Y. Tan, P. Guan, L. Hovgaard, Y. Lu, J. Qi, R. Lian, X. Li, W. Wu, Enhanced oral absorption of insulin-loaded liposomes containing bile salts: A mechanistic study, Int. J. Pharm. 460 (2014) 119–130. doi:10.1016/j.ijpharm.2013.11.028.

[31] M. Niu, Y. Lu, L. Hovgaard, P. Guan, Y. Tan, R. Lian, J. Qi, W. Wu, Hypoglycemic activity and oral bioavailability of insulin-loaded liposomes containing bile salts in rats: The effect of cholate type, particle size and administered dose, Eur. J. Pharm. Biopharm. 81 (2012) 265–272. doi:10.1016/j.ejpb.2012.02.009.

[32] C. Chen, T. Fan, Y. Jin, Z. Zhou, Y. Yang, X. Zhu, Z. Zhang, Q. Zhang, Y. Huang, Orally delivered salmon calcitonin-loaded solid lipid nanoparticles prepared by micelle–double emulsion method via the combined use of different solid lipids, Nanomedicine. 8 (2013) 1085–1100. doi:10.2217/nnm.12.141.

[33] J. Liu, T. Gong, C. Wang, Z. Zhong, Z. Zhang, Solid lipid nanoparticles loaded with insulin by sodium cholate-phosphatidylcholine-based mixed micelles: preparation and characterization, Int. J. Pharm. 340 (2007) 153–162. doi:10.1016/j.ijpharm.2007.03.009.

[34] S. Sun, N. Liang, H. Piao, H. Yamamoto, Y. Kawashima, F. Cui, Insulin-S.O (sodium oleate) complex-loaded PLGA nanoparticles: Formulation, characterization and *in vivo* evaluation, J. Microencapsul. 27 (2010) 471–478. doi:10.3109/02652040903515490.

[35] S. Hu, M. Niu, F. Hu, Y. Lu, J. Qi, Z. Yin, W. Wu, Integrity and stability of oral liposomes containing bile salts studied in simulated and ex vivo gastrointestinal media, Int. J. Pharm. 441 (2013) 693–700. doi:10.1016/j.ijpharm.2012.10.025.

[36] C. Prego, D. Torres, M.J. Alonso, The potential of chitosan for the oral administration of peptides, Expert Opin. Drug Deliv. 2 (2005) 843–854. doi:10.1517/17425247.2.5.843.

[37] V. V. Khutoryanskiy, Advances in mucoadhesion and mucoadhesive polymers, Macromol. Biosci. 11 (2011) 748–764. doi:10.1002/mabi.201000388.

[38] M. Garcia-Fuentes, M.J. Alonso, Chitosan-based drug nanocarriers: where do we stand?, J. Control. Release. 161 (2012) 496–504. doi:10.1016/j.jconrel.2012.03.017.

[39] S. Roy, K. Pal, A. Anis, K. Pramanik, B. Prabhakar, Polymers in mucoadhesive drug-delivery systems: a brief note, Des. Monomers Polym. 12 (2009) 483–495. doi:10.1163/138577209X12478283327236.

[40] H.R. Hill, N.H. Augustine, M.L. Rallison, J.I. Santos, Defective monocyte chemotactic responses in diabetes-mellitus, J. Clin. Immunol. 3 (1983) 70–77.

[41] R.P. Tengerdy, Vitamin E, immune response, and disease resistance, Ann. N. Y. Acad. Sci. 570 (1989) 335–344. doi:10.1111/j.1749-6632.1989.tb14932.x.

[42] W.B. Satkowski, S.K. Huang, R.L. Liss, Polyoxyethylene esters of fatty acids, in: M.J. Schick (Ed.), Nonion. Surfactants, M. Dekker, Inc., 1967: pp. 142–174.

[43] J.A. Bernate, Vector chromatography of suspendedparticles in 1D-periodic systems, ProQuest LLC,

2012.

[44] M.J. Santander-Ortega, M. V. Lozano-López, D. Bastos-González, J.M. Peula-García, J.L. Ortega-Vinuesa, Novel core-shell lipid-chitosan and lipid-poloxamer nanocapsules: Stability by hydration forces, Colloid Polym. Sci. 288 (2010) 159–172. doi:10.1007/s00396-009-2132-y.

[45] M.J. Santander-Ortega, A.B. Jódar-Reyes, N. Csaba, D. Bastos-González, J.L. Ortega-Vinuesa, Colloidal stability of Pluronic F68-coated PLGA nanoparticles: a variety of stabilisation mechanisms, J. Colloid Interface Sci. 302 (2006) 522–529. doi:10.1016/j.jcis.2006.07.031.

[46] A. Torcello-Gómez, J. Maldonado-Valderrama, J. de Vicente, M.A. Cabrerizo-Vílchez, M.J. Gálvez-Ruiz, A. Martín-Rodríguez, Investigating the effect of surfactants on lipase interfacial behaviour in the presence of bile salts, Food Hydrocoll. 25 (2011) 809–816. doi:10.1016/j.foodhyd.2010.09.007.

[47] M. Plaza-Oliver, J. Fernández Sainz de Baranda, V. Rodríguez Robledo, L. Castro-Vázquez, J. Gonzalez-Fuentes, P. Marcos, M. V. Lozano, M.J. Santander-Ortega, M.M. Arroyo-Jimenez, Design of the interface of edible nanoemulsions to modulate the bioaccessibility of neuroprotective antioxidants, Int. J. Pharm. 490 (2015) 209–218. doi:10.1016/j.ijpharm.2015.05.031.

[48] M.J. Santander-Ortega, M. Plaza-Oliver, V. Rodríguez-Robledo, L. Castro-Vázquez, N. Villaseca-González, J. González-Fuentes, E.L. Cano, P. Marcos, M. V. Lozano, M.M. Arroyo-Jiménez, PEGylated nanoemulsions for oral delivery: role of the inner core on the final fate of the formulation, Langmuir. 33 (2017) 4269–4279. doi:10.1021/acs.langmuir.7b00351.

[49] B.S. Schuster, L.M. Ensign, D.B. Allan, J.S. Suk, J. Hanes, Particle tracking in drug and gene delivery research: state-of-the-art applications and methods, Adv. Drug Deliv. Rev. 91 (2015) 70–91. doi:10.1016/j.addr.2015.03.017.

[50] A. Gonzalez-Paredes, D. Torres, M.J. Alonso, Polyarginine nanocapsules: A versatile nanocarrier with potential in transmucosal drug delivery, Int. J. Pharm. 529 (2017) 474–485. doi:10.1016/j.ijpharm.2017.07.001.

[51] A.O. Elzoghby, W.S. Abo El-Fotoh, N.A. Elgindy, Casein-based formulations as promising controlled release drug delivery systems, J. Control. Release. 153 (2011) 206–216. doi:10.1016/j.jconrel.2011.02.010.

[52] FDA, Inactive ingredient search for approved drug products, (2018). https://www.accessdata.fda.gov/scripts/cder/iig/index.cfm?event=BasicSearch.page (accessed June 12, 2018).

[53] D.G. Dalgleish, Casein Micelles as Colloids: Surface Structures and Stabilities, J. Dairy Sci. 81 (1998) 3013–3018. doi:10.3168/jds.S0022-0302(98)75865-5.

[54] Y.D. Livney, Milk proteins as vehicles for bioactives, Curr. Opin. Colloid Interface Sci. 15 (2010) 73–83. doi:10.1016/j.cocis.2009.11.002.

[55] T. Morçöl, P. Nagappan, L. Nerenbaum, A. Mitchell, S.J.D. Bell, Calcium phosphate-PEG-insulin-casein (CAPIC) particles as oral delivery systems for insulin, Int. J. Pharm. 277 (2004) 91–97. doi:10.1016/j.ijpharm.2003.07.015.

[56] T. Yin, L. Yang, Y. Liu, X. Zhou, J. Sun, J. Liu, Sialic acid (SA)-modified selenium nanoparticles coated with a high blood-brain barrier permeability peptide-B6 peptide for potential use in Alzheimer's

disease, Acta Biomater. 25 (2015) 172–183. doi:10.1016/j.actbio.2015.06.035.

[57] T. Zhang, Z. She, Z. Huang, J. Li, X. Luo, Y. Deng, Application of sialic acid/polysialic acid in the drug delivery systems, Asian J. Pharm. Sci. 9 (2014) 75–81. doi:http://dx.doi.org/10.1016/j.ajps.2014.03.001.

[58] G. Gregoriadis, S. Jain, I. Papaioannou, P. Laing, Improving the therapeutic efficacy of peptides and proteins : A role for polysialic acids, 300 (2005) 125–130. doi:10.1016/j.ijpharm.2005.06.007.

[59] R.A. Bader, P.R. Wardwell, Polysialic acid: overcoming the hurdles of drug delivery, Ther. Deliv. 5 (2014) 235–237. doi:10.4155/tde.13.153.

[60] M. Zengshuan, H.H. Yeoh, L.Y. Lim, Formulation pH modulates the interaction of insulin with chitosan nanoparticles, J. Pharm. Sci. 91 (2002) 1396–1404. doi:10.1002/jps.10149.

[61] H. Jonassen, A.L. Kjøniksen, M. Hiorth, Effects of ionic strength on the size and compactness of chitosan nanoparticles, Colloid Polym. Sci. 290 (2012) 919–929. doi:10.1007/s00396-012-2604-3.

USC UNIVERSIDADE DE SANTIAGO DE COMPOSTELA

# Chapter 3

## Influence of the surface properties of nanocapsules on their interaction with intestinal barriers

USC
UNIVERSIDADE
DE SANTIAGO
DE COMPOSTELA

# Chapter 3

## Influence of the surface properties of nanocapsules on their interaction with intestinal barriers

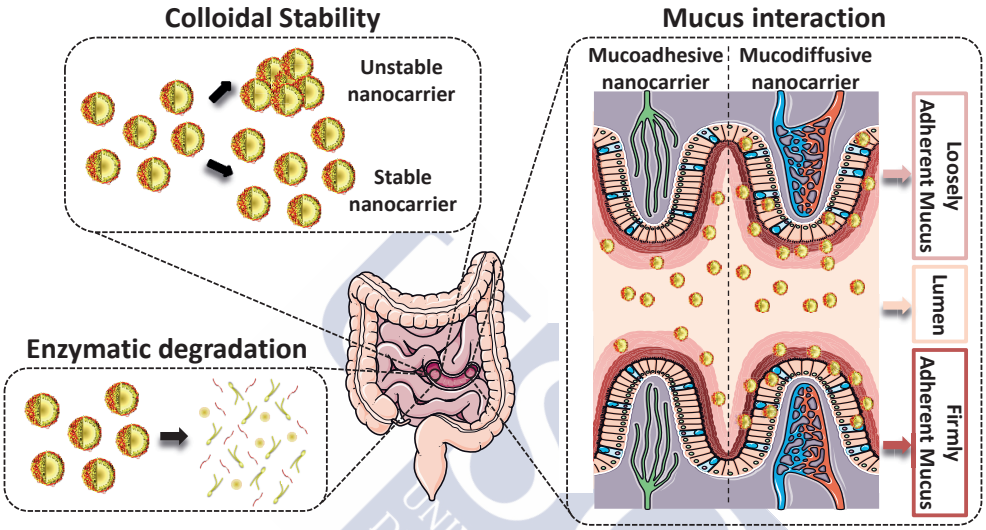
*This work was done in collaboration with the Universidad de Castilla-La Mancha (Spain).*


### Abstract

Despite the convenience of the oral route for drug administration, the existence of different physiological barriers associated with the intestinal tract greatly lowers the bioavailability of many active compounds. We have previously suggested the potential polymeric nanocapsules, consisting of an oily core surrounded by a polymer shell, as oral drug delivery carriers. Here we present a systematic study of the influence of the surface properties of these nanocapsules on their interaction with the intestinal barriers. Two different surfactants, Pluronic®F68 (PF68) and F127 (PF127), and two polymeric shells, chitosan (CS) and polyarginine (PARG) were chosen for the formulation of the nanocapsules. We analyzed nine different combinations of these polymers and surfactants, and studied the effect of each specific combination on their colloidal stability, enzymatic degradation, and mucoadhesion/mucodiffusion. Our results indicate that both, the polymer shell and the surfactants located at the oil/water interface, influence the interaction of the nanocapsules with the intestinal barriers. More interestingly, according to our observations, the shell components of the nanosystems may have either synergic or disruptive effects on their capacity to overcome the intestinal barriers.

USC
UNIVERSIDADE
DE SANTIAGO
DE COMPOSTELA

## Graphical abstract




Small intestine and intestinal villi (*https://creativecommons.org/licenses/by/3.0/*) have been modified from the original work provided by Servier Medical Art (*http://smart.servier.com/*).

USC
UNIVERSIDADE
DE SANTIAGO
DE COMPOSTELA

## Table of contents

**1. Introduction**

**2. Materials and methods**

2.1. Materials

2.2. Preparation of nanoemulsions and nanocapsules

2.3. Characterization of the physicochemical properties and DiD encapsulation efficiency of the nanosystems

2.4. Colloidal stability in simulated intestinal fluid (SIF)

2.5. Lipolysis assay

2.6. Mucoadhesion studies

2.6.1. Dynamic light scattering

2.6.2. Fluorescence microscopy

2.7. Mucodiffusion studies

2.7.1. Particle Tracking Analysis using porcine mucus

2.7.2. Capillary in porcine mucus

2.8. Statistical analysis

**3. Results and discussion**

3.1. Physicochemical characterization of nanoemulsions and nanocapsules

3.2. Stability of nanoemulsions and nanocapsules in simulated intestinal fluid

3.3. Lipolysis of the oily core of nanoemulsions and nanocapsules

3.4. Mucoadhesion of nanoemulsions and nanocapsules

3.4.1. Dynamic light scattering

3.4.2. Fluorescence microscopy

3.5. Mucodiffusion of nanoemulsions and nanocapsules

3.5.1. Particle Tracking Analysis using porcine mucus

3.5.2. Capillary in porcine mucus

**4. Conclusions**

USC
UNIVERSIDADE
DE SANTIAGO
DE COMPOSTELA

## 1. Introduction

The oral route is one of the most accepted routes for the administration of drugs, especially in the case of chronic treatments. Despite having an adequate patient compliance, this route of administration has several well-known physiological barriers that hamper the administration of many drugs. When administrated orally, the drugs must overcome several hurdles, such as their potential degradation by the intestinal enzymes, their instability in the presence of high ionic forces at different pHs, and their difficulty to pass through the intestinal mucosa [1,2]. The existence of all these physiological barriers influences particularly the bioavailability of certain active substances (e.g. peptides and proteins) after oral administration and, hence, their potential therapeutic effect [3–6].

Some of the strategies proposed to improve the oral bioavailability of peptides and proteins refer to the incorporation into their formulation of absorption enhancers or enzyme inhibitors [7–14]. This variety of formulation strategies has opened new avenues for the increasing number of peptidic drugs in industry pipelines [15,16]. However, despite the improved bioavailability of some drugs when associated with nanocarriers [17], advances in this area have been hampered by the limited knowledge about the effect of the physicochemical properties and composition of the nanocarriers in their interaction with the intestinal tract [13,18].

The high concentration of electrolytes and enzymes in the intestinal environment is a major obstacle for the maintenance of the integrity of the nanocarriers and of their associated active compounds, since they can undergo degradation even before reaching the intestinal epithelium. In this scenario, the role of pancreatin, a combination of amylases, lipases and proteases enzymes, is particularly relevant [19–21]. Consequently, to understand the influence that the properties and composition of these nanocarriers have on their interaction with these enzymes is crucial to further advance in this field.

Additionally, the intestinal epithelium is covered by a mucus layer whose biological function is to keep the epithelium lubricated and protected from pathogens and exogenous substances [22]. The mucus layer, with a thickness that varies along the intestinal tract [23,24], consists of a first layer firmly attached to the cellular epithelium and a second layer that is constantly being replaced [25–27]. This is why, mucoadhesive colloidal systems, specially designed to interact with the intestinal mucus [28–30], may become immobilized in the superficial mucus layer, and eventually removed [26,31,32].

Therefore, the nanocarriers intended for oral drug delivery must exhibit an adequate mucoadhesive/mucodiffusive balance.

Based on this information, the objective of this work was to evaluate the effect of the surface composition on the capacity of different oily-based nanocarriers (nanoemulsions and nanocapsules) to overcome specific barriers associated to the oral modality of administration. The basis for the selection of the nanocarriers rely of previous activity from our group showing the potential of chitosan (CS) nanocapsules (NCs) and polyarginine (PARG) NCs for the oral administration of salmon and insulin, respectively [33–39]. These nanocarriers are composed of an oily core and a polymeric shell, which is the main determinant for the interaction with the surrounding medium. Overall, the behaviour of nine nanosystems (schematized in *Figure 1*) containing different surfactants and polymer shells was investigated. A nanoemulsion (NE) consisting of Miglyol®812N and Epikuron®145V lecithin was used as reference in order to study the effect of the Pluronic® surfactant F68 and F127 , as well as that of the cationic polymers CS and PARG. In total, 3 different NEs and 6 different NCs were systematically analyzed for their capacity to overcome specific intestinal barriers. Namely, we evaluated the nanosystems for *i)* their stability, both colloidal and chemical, in simulated intestinal fluid and *ii)* their interaction (adhesion and diffusion) with mucus, while mimicking the physiological conditions [27,40].

## 2. Materials and methods

### 2.1. Materials

For the preparation of nanosystems, the neutral oil Miglyol®812N, a triglyceride formed from medium-chain fatty acids (capric and caprilic acids) was kindly donated by Cremer Oleo Division (Germany); soybean lecithin (Epikuron®145V), used as surfactant in the oily phase, was supplied by Cargill (Spain); poloxamer 188 (Pluronic®F68–PF68) and poloxamer 407 (Pluronic®F127–PF127), used as surfactants in the aqueous phases, were supplied by Sigma-Aldrich (Spain). *Table 1* shows the chemical structure and main characteristics of both poloxamers. According to the HLB values, PF68 is more hydrophilic than PF127. The polysaccharide chitosan (deacetylation degree: 75−90 %; Mw ≈ 113 kDa) and the polyamino acid poly-L−arginine (Mw ≈ 5−15 kDa), selected as cationic polymers, were purchased from FMC Biopolymer (USA) under the commercial name of Protasan Cl 113 and Sigma-Aldrich (Spain) respectively. When necessary, the lipophilic tracer DiD (DiIC18(5) oil (1,1'−dioctadecyl-3,3,3',3'−tetramethylindodicarbocyanine

perchlorate)) used as fluorescent dye ($\lambda_{ex} \approx 644$ nm, $\lambda_{em} \approx 665$ nm) was supplied by Invitrogen (Belgium).

***Table 1.*** *Chemical structure and main characteristics of Pluronic®F68 and Pluronic®F127. PEO: polyethylene oxide unit; PPO: propylene oxide unit. Mw: molecular weight. HLB: hydrophilia-lipophilia balance.*

| | $HO(CH_2CH_2O)_n(CHCH_2O)_m(CH_2CH_2O)_nH$ (CH₃ on CHCH₂O) | |
|---|---|---|
| | Pluronic®F68 | Pluronic®F127 |
| n (PEO) | 75 | 100 |
| m (PPO) | 30 | 65 |
| Mw (kDa) | 8.4 | 12.6 |
| HLB | 29 | 22 |

For the stability studies, pancreatin from porcine pancreas (4 × USP) was supplied by Sigma-Aldrich (Spain). For the mucoadhesion studies, partially purify mucin type III from porcine stomach and poly-D−lysine hydrobromide were purchased from Sigma-Aldrich (Spain). Glass bottom dishes (35 mm dish with 14 mm glass diameter, uncoated) were purchased from MatTek Corporation (USA). For mucodiffusion studies square borosilicate capillaries (0.6 square internal diameter (mm) × 0.12 wall (mm)) were purchased from VitroCom (USA).

## 2.2. Preparation of nanoemulsions and nanocapsules

For this study, nine different formulations were prepared (*Figure 1, lower panel*), according to the two steps procedure previously described by our group (*Figure 1, upper panel*) [41]. First, we prepared the primary NE by the solvent displacement technique [37–40,42]. Briefly, an organic phase consisting of 20 mg of lecithin dissolved at 37 °C in 0.25 mL of ethanol, 62.5 µL of Miglyol®812N, and acetone to a total volume of 5 mL, and then poured onto 10 mL of ultrapure water under constant magnetic stirring (500 rpm). The mixture turned milky immediately due to the formation of the NE. After stirring for 10 minutes, the solvents were evaporated under vacuum to a final volume of 4 mL. When necessary, in a second step, this primary NE was coated with the correspondent surfactants (PF68 and PF127) and polymers (CS and PARG) by simple incubation in the aqueous solutions of these components or simply diluted with ultrapure water to obtain the different NEs-surfactant and NCs [33,43] having always the same concentration of the common components present in the core. More specifically, 4 mL of the primary NE were

incubated under magnetic stirring for 10 minutes with 1 mL of aqueous solution containing or not, the corresponding polymer (CS – 5 mg/mL or PARG – 2.5 mg/mL) or/and the surfactant (PF68 or PF127 – both of them 25 mg/mL), which led to the formation of the final nanosystems. Concentration of coating materials was chosen according to previously reported works [39,41,44].

When a fluorescent marker was needed, DiD was incorporated to the oily core by substitution of 80 µL of ethanol by the same volume of an ethanol DiD solution (2.5 mg/mL).

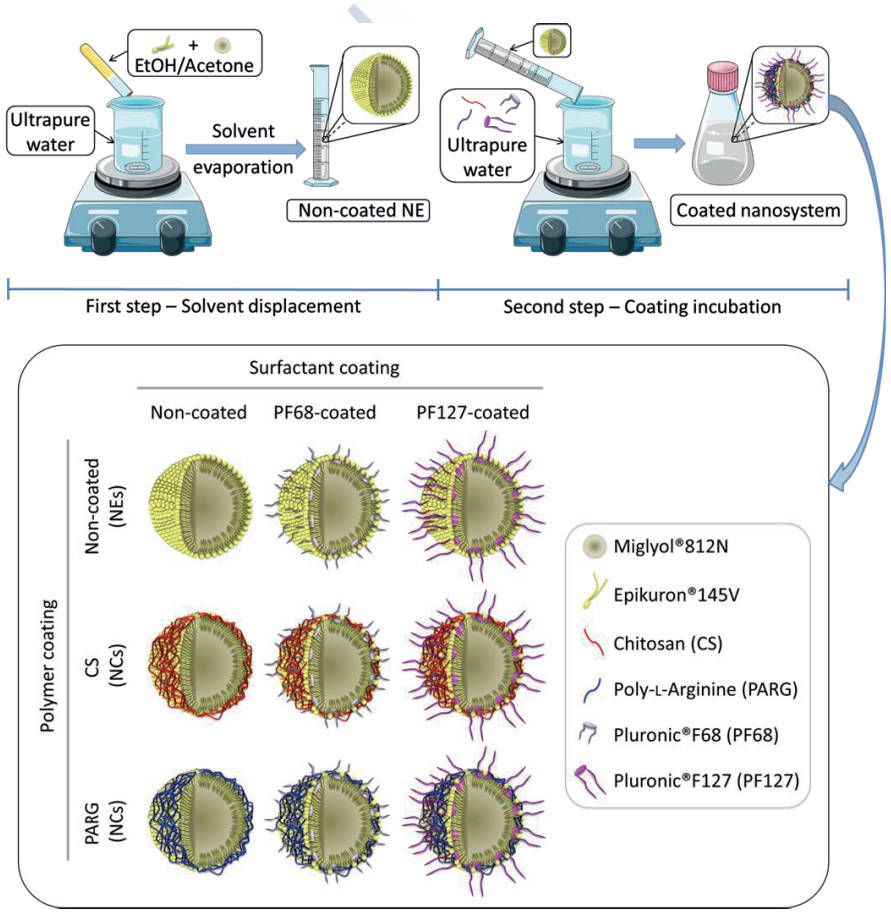



***Figure 1.*** *Schematic representation of the formulation procedure* ***(upper panel)*** *and the nanosystems tested* ***(lower panel).*** *Laboratory material and equipment (https://creativecommons.org/licenses/by/3.0/) have been modified from the original work provided by Servier Medical Art (http://smart.servier.com/).*

## 2.3. Characterization of the physicochemical properties and DiD encapsulation efficiency of the nanosystems

Size and polydispersity index were analyzed by photon correlation spectroscopy, and ζ−potential was determined by laser Doppler anemometry using a Malvern Zeta-sizer device (NanoZS, ZEN 3600, Malvern Instruments, Worcestershire, UK). To obtain DLS measurements, nanosystems were appropriately diluted (30 µL of nanosystems + 970 µL of dilution medium) in ultrapure water to determine their size, and in a low ionic strength saline medium to determine their ζ−potential ($n \geq 3$).

The encapsulation efficiency of DiD in the systems was determined upon separation of the NE or NCs from the free components in the aqueous medium. The analysis was done directly. Briefly, 1 mL of the non-isolated formulations was ultracentrifuged (Beckman Coulter, Optima L−90K, Brea, USA) at 112,202.7 g for 1 h at 15 °C. After the isolation the cream fractions were collected and resuspended with ultrapure water up to their initial volume. Then, the encapsulated DiD was extracted from the isolated systems by the following procedure: *i)* 100 µL of the isolated system was vortexed with 100 µL of acetonitrile for 1 min; *ii)* 100 µL of Triton™ X−100 were incorporated to the previous mixture and vortexed for 1 min; *iii)* Finally, samples were diluted with extra-acetonitrile, and the fluorescence emitted by the broken isolated nanosystems was analyzed using an EnVision Multilabel plate reader 2104−0010A ($\lambda_{ex}$ = 644 nm, $\lambda_{em}$ = 665 nm) in order to determine the amount of DiD associated to them. In addition, 1 mL of non-isolated systems were degraded following the same procedure and the total DiD concentration was determined in the same way as control. The encapsulation efficiency of DiD in the systems was expressed as percentage, and calculated dividing the amount of DiD determined in the isolated nanosystems by the total amount of DiD incorporated to them initially. The analysis was done in triplicate.

## 2.4. Colloidal stability in simulated intestinal fluid (SIF)

In order to evaluate the colloidal stability, size and changes in the ζ−potential were determined using a Malvern Zeta-sizer device (NanoZS, ZEN 3600, Malvern Instruments, Worcestershire, UK). In short, 30 µL of the systems were incubated with 970 µL of the corresponding medium under horizontal shaking at 37 °C, and for the size evaluation, samples were analyzed at 0, 0.5, 1, 2, and 4 hours. Colloidal stability was studied in plain (without enzymes) and in normal SIF (USP XXIX). The SIF (1 % w/v pancreatin) medium was

centrifuged 5 minutes at 5000 g at 5 °C using a Universal 32 R, Hettich Zentrifugen (Hettich Instruments) in order to eliminate the pancreatin aggregates, prior to the incubation of the nanocarriers. In addition, to check the changes in the surface charge of the systems, the same procedure was done and the ζ–potential determined after 1 hour of incubation.

## 2.5. Lipolysis assay

The potential effect of the nanosystems surface on their chemical degradation by the intestinal enzymes was evaluated using an acid-base titration. The lipases present in the medium degrade the triglycerides of the oily core and generate two fatty acids and one monoglyceride. The release of these fatty acids causes a decrease in the pH of the medium. Therefore, the titration of these fatty acids with NaOH will allow the quantification of the amount of triglycerides degraded by the enzymes after the incubation of the nanosystems with 1 % pancreatin SIF. The degradation of the NE without surfactants after 5 hours of incubation in SIF was set as 100 % degradation. For this study, a titrator TitroLine® alpha Plus (Scott Instruments, Germany) was used to evaluate the release of fatty acids using NaOH 0.01 N.

To perform the titration, on the one hand, 1 mL of formulation was mixed with 4 mL of SIF and its pH was adjusted to 6.8 with NaOH 0.01 N; on the other hand, a solution of 2 % (w/v) pancreatin in SIF was prepared under magnetic stirring and then centrifuged 5 minutes at 5000 g at 5 °C using a Universal 32 R, Hettich Zentrifugen (Hettich Instruments, Germany). After the centrifugation, the pH of 5 mL of undernatant was adjusted to 6.8 with NaOH 0.01 N. Then, these 5 mL were mixed with the 5 mL containing the system previously mixed with SIF, to a final pancreatin concentration of 1 %. The titration was done at 37 °C under continuous magnetic stirring.

## 2.6. Mucoadhesion studies

### 2.6.1. Dynamic light scattering

This method, based on a modification of a previously described technique [45], was designed as a fast bench screening assay to study the affinity of the systems for mucin, which is the main component of the mucus [27]. The study involved the analysis of the nanosystems size (expressed as the aggregation ratio $Size_{MUCIN}/Size_{SIF}$) and ζ–potential upon exposure to non-supplemented SIF diluted in water (1/25) containing increasing

concentrations of mucin ($1 \times 10^{-4}$ to $1 \times 10^{-1}$ % (w/v)). For this study, a Malvern Zeta-sizer device (NanoZS, ZEN 3600, Malvern Instruments, Worcestershire, UK) was used.

### 2.6.2. Fluorescence microscopy

This method, a modification of the method already published by Tachaprutinun et al. [46], allows the evaluation of the nanosystems interaction with a mucin film, as a complementary assay to determine the mucoadhesion of the prototypes as a function of their shell composition. This technique is based on the determination of the fluorescent-labeled nanosystems retention after their incubation with a mucin layer. Briefly, two series of glass bottom dishes were pretreated either with poly-D−lysine (to promote the adsorption of the mucin to the glass dish) or with a 25 mg/mL solution of PF127 (as negative control). Then 200 µL of a 5 % (w/v) mucin solution in diluted plain SIF (1/25) was added. After 8 hours of incubation, the excess of mucin or PF127 was removed by washing the glass bottom 5 times with ultrapure water, and letting it dry. Through this procedure, a superficial layer of mucin, bounded by electrostatic interactions to the poly-D−lysine, was created. Then, 200 µL of the different isolated DiD-loaded nanosystems were incubated onto the glass bottom during 2 hours. Finally, the non-muco-interactive nanosystem was eliminated by washing the glass bottom 3 times with ultrapure water. Photos of the glass dishes were taken with a 20X objective and the fluorescence intensity was determined ($\lambda_{ex} \approx 644$ nm, $\lambda_{em} \approx 665$ nm) using a microscope Leica AF6000 (Leica Microsystems, Germany). As the potential mucoadhesive properties of CS [38,47–49] are well known, we considered the fluorescence emitted by the CS NCs without surfactants as a reference to define the 100 % of mucoadhesion and allow the comparison of the mucoadhesive properties of the different systems through the semi-quantitative analysis of their corresponding retained particles.

## 2.7. Mucodiffusion studies

### 2.7.1. Particle Tracking Analysis using porcine mucus

As model of the human intestinal mucosa, we used fresh porcine intestinal mucus obtained from the local slaughterhouse. NEs and NCs were fluorescently labeled by incorporating the lipophilic tracer DiD to the oil core during the formulation process. Briefly, 5 µL of nanosystem previously diluted in PBS 2 mM were mixed with 100 µL of

mucus. Volumes of 10 µL of each sample were placed between a microscope slide and a cover glass in a chamber created by the placement of a 120 µm thick, double-sided adhesive sticker between slide and cover (Sigma). The Nikon microscope (Izasa Scientific, Spain) equipped with an Andor Zyla 4.2 camera and a PLAN APO 100X 1.4 oil-immersion objective was always focused at 12−16 µm above the cover glass. For each sample, more than 20 movies of 800 frames were recorded at a frame rate of 100 fps, obtaining more than 100 trajectories per movie. The diffusion coefficient of each particle was obtained off-line from the fitting of the mean square displacement ⟨MSD⟩ as a function of the time according to the following equation: $\langle MSD \rangle = 4D_e\tau^{\alpha}$ (*Eq. 1*), where $D_e$ is the effective diffusion coefficient, α the anomalous exponent that gives information about the nature of the diffusion mode of the nanoparticle in mucus and τ, the time scale, which is the time over which particles are allow to move before calculating their displacement trajectories. The time scale was fixed at 1 second for these experiments (100 frames/s) [50–52].

The same procedure was performed using an aqueous solution of DiD at the sample concentration, and the results were analyzed to ensure that the signal observed did not originated from the released DiD.

### 2.7.2. Capillary in porcine mucus

To learn about the mucodiffusion of the systems from a macroscopic point of view, we adapted a capillary technique described elsewhere [53,54]. Briefly, borosilicate capillaries were filled at one end with intestinal porcine mucus obtained from the local slaughterhouse while the DiD-labeled formulations were slowly injected at the opposite end. After the formulation came in contact with the porcine mucus, the diffusion of the nanosystems was studied using a fluorescence microscope Leica AF6000 (Leica Microsystems, Germany) by measuring at $\lambda_{ex} \approx 644$ nm and $\lambda_{em} \approx 665$ nm. The capillaries were maintained in a vertical position during the measurement.

By fitting of the fluorescence decay versus the distance, it was possible to calculate the mean penetration capacity of the systems through porcine mucus ($X_{1/2}$) using the following equation: $I_F = A + I_0 e^{-x/k}$ (*Eq. 2*), where $I_F$ is the normalized fluorescence, *A* is the basal normalized fluorescence, $I_0$ the fluorescence at $X = 0$ (mucus/nanosystems interface), *X* is the distance from the mucus/nanoparticles interface towards the mucus, and *k* is a decay constant that obeys: $k = \frac{X_{1/2}}{\ln 2}$ (*Eq. 3*), being $X_{1/2}$ the penetration capacity,

which means the thickness (μm) of intestinal porcine mucus that allows the transport of 50 % of the nanosystems.

### 2.7. Statistical analysis

GraphPad Prism 7 program (California, USA) was used to perform the statistical analysis. Where applicable and after confirming the data adjustment to normality through a Shapiro-Wilk normality test, they were compared using the two-way ANOVA followed by a Fisher's LSD test, considering p-values lower than 0.05 as statistically significant.

## 3. Results and discussion

In this study, we analyzed nine different nanosystems in the form of nanoemulsions or nanocapsules, all of them having the same oily core but different shell composition. The shell was made of polymers (CS and PARG), surfactants (PF68 and PF127) and a combination of them. Specifically, we studied the effect of each specific combination on the colloidal stability, enzymatic degradation and mucoadhesion/mucodiffusion of these colloidal systems.

### 3.1. Physicochemical characterization of nanoemulsions and nanocapsules

The versatility of the core-shell polymeric NCs relies on the possibility to adapt the composition of the oily core to the nature of the cargo, and that of the polymeric shell to the administration route or target tissue [35,43,55–57]. Bearing this in mind, the first studies focused on the analysis of the effect of the polymer and the surfactant coating on the physicochemical properties of the systems. As shown in *Table 2*, the incorporation of either CS or PARG led to the charge inversion of the nanostructures, while their hydrodynamic mean sizes remained in the nanometric range with a low polydispersity index. These results indicated the efficient formation of a polymeric shell after the incubation of the NE with either polymer, most probably due to the attractive electrostatic interaction between the cationic polymer (either CS or PARG) and the negatively charged NE [35,39,55].

Regarding the influence of the non-ionic surfactant on the physicochemical properties of the three different nanosystems, the results in *Table 2* indicate that the addition of PF68 did not lead to a significant modification of their initial size and ζ–potential values. However, the incorporation of PF127 to the nanosystems led to different behaviors depending on their composition. An important decrease on the ζ–potential magnitude was observed in plain NE and PARG NCs when PF127 was incorporated, however, this reduction less marked in the case of CS NCs (*Table 2*). The different behaviour observed for both surfactants can be attributed to their different molecular structures (see *Table 1*). Although both Pluronics® share the same $PEO_n$–$PPO_m$–$PEO_n$ architecture, PF68 presents two hydrophilic side arms with 75 × PEO monomers and a central hydrophobic block formed by 29 × PPO monomers (HLB ≈ 29), while PF127 has 100 × PEO units in its hydrophilic side arms and 65 × PPO units in the central hydrophobic block (HLB ≈ 22). The number of monomers in the hydrophilic side arms may influence the protective steric layer of the nanostructures [55,58], whereas the central hydrophobic block is expected to determine the interfacial adsorption of the surfactant as well as its ability to compete with other components present at the oil/water interface [44,59,60]. In theory, the presence of non-ionic surfactants on the nanosystems surface should lead to a displacement of the shear plane (where the ζ–potential is defined) towards the aqueous phase, and, hence, to a reduction on the ζ–potential magnitude [58]. Bearing this in mind, our results would indicate a low incorporation of PF68 to the nanostructure irrespective of the shell composition, since its incorporation did not produce any significant change in the ζ–potential [32,55,61]. In contrast, the significant ζ–potential reduction in magnitude for both, NE and PARG NCs, when PF127 was used instead of PF68, could be an indication of its greater incorporation onto the oily core due to its higher lipophilicity. In the case of CS NCs, the lower but still significant reduction on the ζ–potential suggests a low incorporation of PF127.

***Table 2.*** *Physicochemical properties of nanoemulsions (NEs), chitosan (CS) and polyarginine (PARG) nanocapsules (NCs). All systems share the same Miglyol®812N/lecithin core (n ≥ 3).*

| Polymeric Coating | Surfactant Coating | Final formulation pH | Size (nm) | PdI | ζ–Potential (mV) |
|---|---|---|---|---|---|
| -------- (NEs) | ----- | 5.3 ± 0.1 | 179 ± 15 | 0.1 | −54 ± 1 |
| | **PF68** | 5.1 ± 0.1 | 172 ± 02 | 0.1 | −54 ± 3 |
| | **PF127** | 5.2 ± 0.1 | 174 ± 04 | 0.1 | −30 ± 3[a] |
| **CS (NCs)** | ----- | 4.8 ± 0.2 | 380 ± 19 | 0.3 | +47 ± 3 |
| | **PF68** | 4.7 ± 0.1 | 383 ± 18 | 0.3 | +49 ± 1 |
| | **PF127** | 4.8 ± 0.1 | 327 ± 12[a] | 0.3 | +42 ± 2[b] |
| **PARG (NCs)** | ----- | 4.3 ± 0.1 | 188 ± 05 | 0.1 | +43 ± 1 |
| | **PF68** | 4.3 ± 0.1 | 185 ± 03 | 0.1 | +45 ± 1 |
| | **PF127** | 4.4 ± 0.1 | 183 ± 04 | 0.1 | +27 ± 2[a] |

*Two-way ANOVA followed by a Fisher's LSD test were applied for the statistical analysis ($p < 0.05$). [a]Significantly different compared to both, the formulation without non-ionic surfactant and to the formulation with PF68 ($p \leq 0.0001$); [b]Significantly different compared to the formulation without non-ionic surfactant ($p \leq 0.01$) and to the formulation with PF68 ($p \leq 0.001$).*

## 3.2. Stability of nanoemulsions and nanocapsules in simulated intestinal fluid

We evaluated the role of the nanosystem surface composition on both, colloidal stability and resistance to the enzymatic degradation upon incubation in simulated intestinal fluid (SIF) USP XXIX. Given the complex composition of the intestinal medium, and in order to achieve a better understanding of the effect of each nanosystem surface component on the colloidal behaviour of the formulations, we first studied the size evolution of the systems in SIF supplemented or not with 1 % pancreatin.

As depicted in *Figure 2 (upper panel)*, CS and PARG NCs formulated without surfactants or with PF68 showed an immediate aggregation (CS NCs ≥ 1 µm and PARG NCs ≈ 750 nm) upon incubation in SIF without enzymes. These results correlate with the similar physicochemical properties showed by the non-coated and PF68-containing systems (no significant differences, *Table 2*), and agree with our hypothesis of a low incorporation of PF68 to the oil/water interface. On the contrary, the NCs formulated with PF127 were more stable. As expected, this effect was more noticeable in the case of PARG NCs than in the case of CS NCs, probably due to the lower incorporation of the surfactant onto the CS NCs.

Once the effect of the electrolytes present in the intestinal fluids has been established, we found important to understand the role of the intestinal enzymes in the colloidal stability of the systems. For this purpose, the previous stability assay was performed on normal SIF (supplemented with 1 % of pancreatin). As shown in *Figure 2 (lower panel)*, all systems presented a certain modification in size, which could be attributed to the enzymes adsorption [33,62,63]. The absence of a massive aggregation observed in this case might be a consequence of the formation of an stabilizing coating of the particles by the enzymes present in the medium [64].

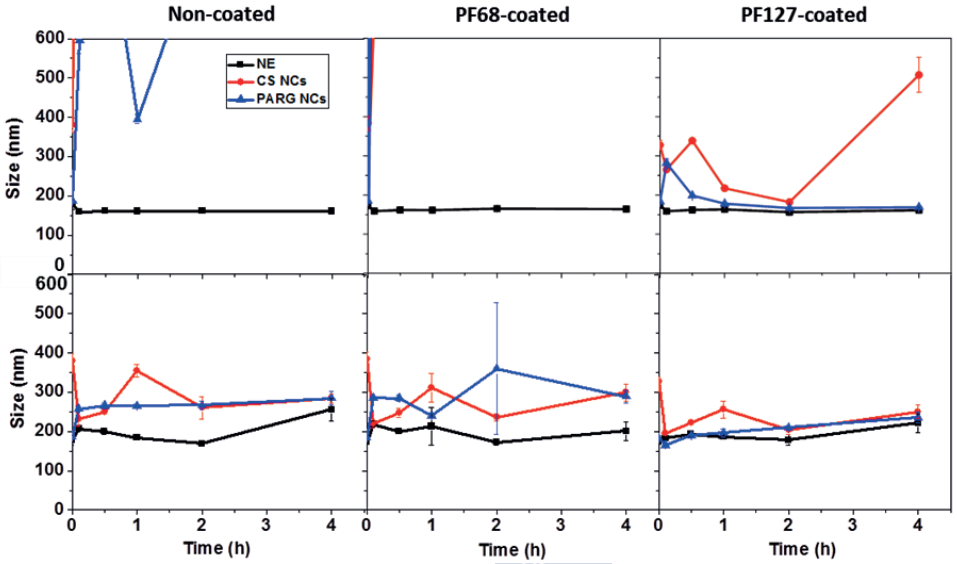



***Figure 2.*** *Colloidal stability in simulated intestinal fluid. Hydrodynamic mean size of the NEs (black), CS NCs (red) and PARG NCs (blue) incubated either in SIF without enzymes (top) or in 1 % pancreatin supplemented SIF (bottom) (Error bars mean standard deviation; n ≥ 3).*

The DLVO theory states that the total potential of interaction ($V_T$) between two approaching particles can be expressed as $V_T = V_A + V_R$, where $V_A$ is the attractive potential of interaction due to the Van der Waals forces and $V_R$ is the repulsive electrostatic potential that depends on the ζ–potential magnitude [65]. Bearing this in mind, the evolution of the ζ–potential values upon incubation of the nanosystems in SIF with and without pancreatin was monitored (*Figure 3*) in order to elucidate if the stability profile of the nanosystems was driven by either electrostatic interactions or steric hindrances. In the absence of enzymes, it was found that NEs incubated in SIF suffered a minor reduction of

their ζ–potential. Therefore, while the high negative ζ–potential observed in the case of non-coated and FP68-coated NEs (≈ −60 mV) could be responsible for their stability in plain SIF, in the case of the PF127-coated NE, whose ζ–potential was much lower in magnitude (≈ −23 mV), its stability would be mainly attributable to a steric stabilization provided by the PF127-coating, as previously reported [21,66,67]. In contrast, both types of NCs experienced a significant decrease in their ζ–potential in plain SIF, which was attributed to the reduced ionization of the–$NH_3^+$ groups ($pK_a$ ≈ 8) in this medium (pH 6.8), as compared to the one in the original pH of these formulations (≈ 4.5, *Table 2*) [55]. The ζ–potential decrease observed in the case of the NCs (≤ +15 mV, p ≤ 0.0001) may result in a reduction of $V_R$ (repulsive electrostatic potential) and, hence, in the instability in plain SIF of the non-sterically stabilized particles (*Figure 2*) [55,60,66]. Also, it could be assumed that the incorporation of PF127 to PARG NCs was high enough to lead to the steric stabilization of the nanosystem [33,62,63]. Finally, a generic observation is that upon incubation in SIF with pancreatin the surface charge of all systems becomes similar (≈ −15 ± 5 mV), a fact that could be due to their interaction with enzymes present in the medium and the formation of a stabilizing enzyme coating.

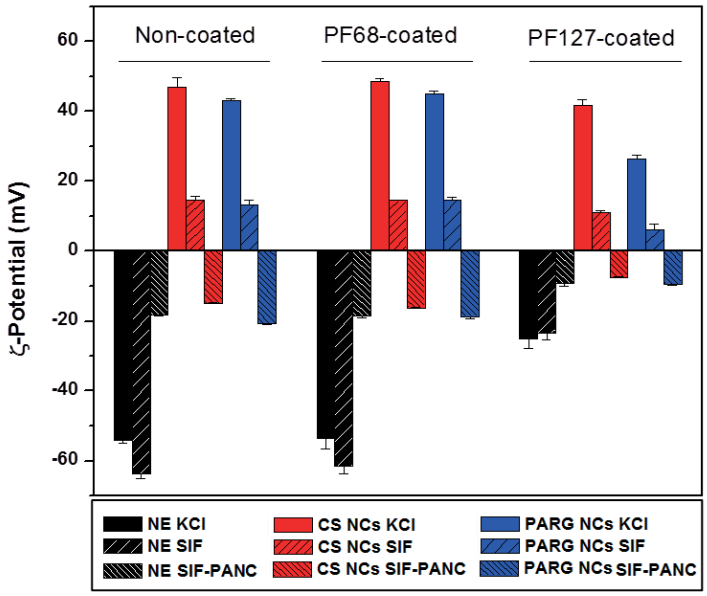



***Figure 3.*** *Surface charge of the nanosystem in different media. ζ–potential (mV) of the NEs (black), CS NCs (red) and PARG NCs (blue) measured either in KCl 1 mM (closed bars), SIF without enzymes (sparse dashed bars) or 1 % pancreatin supplemented SIF (dashed bars) (Error bars mean standard deviation; n ≥ 3).*

### 3.3. Lipolysis of the oily core of nanoemulsions and nanocapsules

Another important aspect to consider is the potential protection that the different polymer/surfactant coatings confer to the nanosystems against enzimatic degradation. *Figure 4* shows the percentage of oily core degradation of the different systems when incubated in normal SIF in the presence of pancreatic lipase [19]. The degradation kinetics was qualitatively similar for the 9 tested systems showing an initial fast degradation (during the first 20 minutes), followed by a plateau for the rest of the experiment.

As expected, due to the important exposure to the enzymes of the oily core of the NE prepared without non-ionic surfactants, this was the formulation that presented the highest degradation by pancreatic enzymes (70 % in 20 minutes), being its area under the curve significantly higher than those corresponding to CS NCs ($p \leq 0.0001$) and PARG NCs ($p \leq 0.001$). This was mainly attributed to the interaction of the pancreatic lipase with the oily droplets [19,60,68], being this degradation slightly reduced by the CS and PARG coatings. We have speculated that this limited protective effect of the polymeric shell could be attributed to the presence of amylases, enzymes with the capacity of degrading CS through the α(1,4) glycosidic bond cleavage [69–71], and peptidases, enzymes capable of degrading PARG backbone through the peptide bond [68,72].

Our group has previously shown that PF68 can efficiently protect nanoparticles made of polylactic-co-glycolic acid (PLGA) from enzymatic degradation in SIF [58,72]. As depicted in *Figure 4*, the incorporation of PF68 did significantly slow down the degradation of the NE (70 % of degradation in 40 minutes) ($p \leq 0.0001$) and of the NCs (70 % of degradation in 60 minutes) ($p \leq 0.01$ for CS NCs and $p \leq 0.001$ for PARG NCs), although it did not prevent totally the action of the pancreatic lipase

The most resistant systems against enzymatic degradation were those formulated with PF127. While both, NE and PARG NCs, presented a maximum degradation of about 20 % after 2 hours of incubation in SIF; the percentage of degradation of CS NCs was close to 60 %. As discussed above, the surfactant protection effect depends on its capacity to be efficiently adsorbed and retained onto the nanosystems upon their incubation with enzymes. Considering the ζ−potential values from *Table 2* and the low degradation observed for NE and PARG NCs, it seems that PF127 was efficiently incorporated to the oil/water interface of both formulations. In addition, the low degradation observed in this case suggests that the surfactant was not displaced from the oil/water interface by the macromolecules present in SIF [21,59,67,73]. Accordingly, the significantly higher

degradation observed for CS NCs ($p \leq 0.0001$ compared to both NE and PARG NCs) could be mainly attributed to a lower incorporation of PF127, but not to a displacement of the surfactant from the oil/water interface after incubation in SIF [21,73].

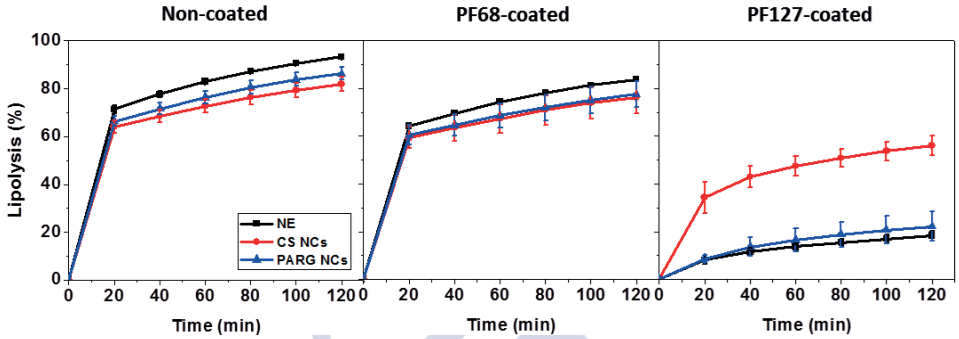



***Figure 4.*** *Lipolysis in simulated intestinal fluid. Percentage of lipolysis of the NEs (black), CS NCs (red) and PARG NCs (blue) incubated in SIF. Degradation of the non-coated NE after 5 hours of incubation in SIF was set as 100 % of degradation (Error bars mean standard deviation; n ≥ 3).*

## 3.4. Mucoadhesion of nanoemulsions and nanocapsules

### 3.4.1. Dynamic light scattering

To be successful, in addition to overcoming the harsh intestinal environment, nanomedicines should diffuse across the intestinal mucosa and reach the intestinal epithelium [27,31]. Bearing this in mind, the role of the surface properties of our prototypes on their interaction with mucin was first analyzed according to a simple DLS-based procedure [27]. The analysis of the $Size_{MUCIN}/Size_{SIF}$ and the ζ–potential of the different systems in the presence of increasing amounts of mucin in SIF allowed us to classify the nanosystem-mucin interaction as follows: *i)* strong interactions with mucin fibers will probably lead to the entrapment of the nanosystems within mucin meshes, thus triggering an increment in the size of particles/oily droplets (aggregation) meanwhile their ζ–potential will tend to values closer to the mucin charge; *ii)* the formation of an homogeneous mucin coating around the nanosystems might be suspected when their size remain invariable while variations in their ζ–potential, tending to the mucin charge, are observed ; *iii)* muco-inert nanosystems will not experience variations in either size or ζ–potential when incubating with mucin fibers.

As shown in *Figure 5*, NE formulated without poloxamer presented a constant size for all mucin concentrations while the corresponding NCs suffered a mucin concentration-dependent aggregation induced by the interaction with mucin [64]. Parallel analysis of ζ–potential as function of the mucin concentration complemented the information obtained by size analysis. These results revealed that, despite the constant size displayed by the NE, the decrease in its ζ–potential magnitude with the mucin concentration towards those values observed for the pure mucin solution is a clear indicative of the interaction of the system with the mucin fibers.

In agreement with the results described above, formulations containing PF68 behaved like the formulations without surfactant. This is consistent with our hypothesis that the incorporation of this surfactant onto the oil/water interface is low, and it has a tendency to be displaced by other macromolecules with more affinity for this interface. Contrary to what was observed with PF68, PF127 formulations displayed a negligible size modification, but their ζ–potential was also dependent on the mucin concentration. These results indicate that PF127 cannot totally prevent the colloidal system from interacting with the mucin fibers. However, this interaction did not translate to an aggregation of the nanosystems.

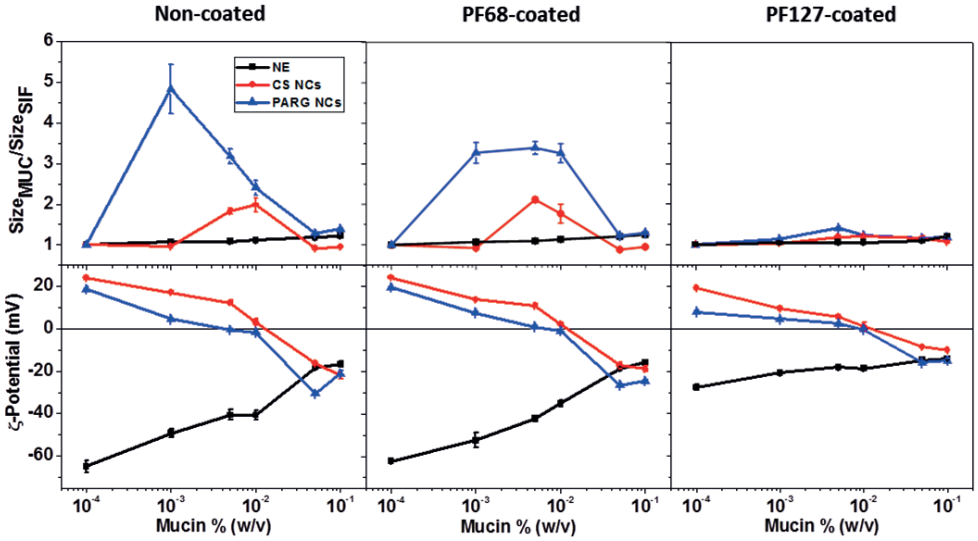



***Figure 5.*** *Mucoadhesion assessed by the dynamic light scattering approach. Hydrodynamic mean size increase, expressed as $Size_{Mucin}/Size_{SIF}$ ratio (top), and ζ–potential modification (bottom) of the NEs (black), CS NCs (red) and PARG NCs (blue) incubated in mucin solutions in diluted SIF (1/25) without enzymes with a concentration ranging from 1 x $10^{-4}$ to 1 x $10^{-1}$ % (w/v) (Error bars mean standard deviation; n ≥ 3).*

### 3.4.2. Fluorescence microscopy

In order to understand better the effect that the shell composition of the systems has on their interaction with the intestinal mucosa, we studied the interaction of the nanosystems with a film of mucin immobilized on a glass bottom dish [46]. We incubated each system 2 hours with the mucin film and performed a semi-quantitative analysis of the retained particles by fluorescent microscopy. For this purpose, the systems used in this assay were formulated with the fluorescent dye DiD in their oil core (all the systems presented an encapsulation efficiency $\geq$ 80 %; data not shown).

Based in the well-known mucoadhesive properties of CS [35,38,41,47–49,74], the fluorescence intensity measured for de CS NCs formulated without Pluronics® was set as 100 %. As shown in *Figure 6*, in the absence of poloxamer, the mucoadhesive behaviour was found to be clearly dependent on the polymeric shell. In the case of the NEs, a negligible amount of particles were retained on the film mucin. This result suggest that despite the mucin-NE interaction observed by dynamic light scattering, this interaction is weak enough for the particles to avoid being adsorbed to the mucin film. Both polymers, CS and PARG, substantially increase the mucoadhesion of the systems ($p \leq 0.0001$ compare to the NE). As expected, CS NCs, referred as 100 % mucoadhesion, showed the highest retention on the films, while PARG NCs had less affinity for the mucin ($\approx$ 60 %; $p \leq 0.0005$ compared to CS NCs).

No significant effect was found on the mucoadhesive properties of the three nanosystems after the addition of PF68. This result agrees with the hypothetical low incorporation of this surfactant onto the oil/water interface. In contrast, the presence of PF127 significantly decreased these mucoadhesive properties for both NCs ($p \leq 0.05$), being the mucoadhesion displayed by the CS NCs significantly higher than that of PARG NCs ($p \leq 0.05$). This agrees with the more efficient incorporation of PF127 expected for the NE and the PARG NCs, than for the CS NCs. The effect of PF127 may be attributed to the more intense interaction of this Pluronic® with the oil droplets [44,60], which ended up in a more efficient coating against the interaction with the physiological macromolecules, such as mucin [44,60,61].

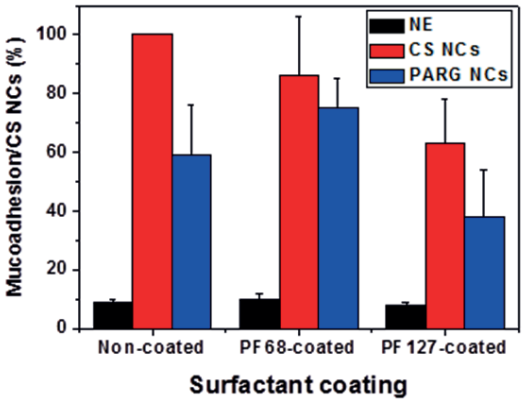



***Figure 6.*** *Mucoadhesion assessed by the fluorescence microscopy approach. Adhesion percentage upon incubation with a mucin film of the NEs (black), CS NCs (red) and PARG NCs (blue) compared to the non-coated CS NCs (set as 100 %) (Error bars mean standard deviation; n ≥ 3).*

## 3.5. Mucodiffusion of nanoemulsions and nanocapsules

Once the nanosystems are captured by the intestinal mucus the next step is their diffusion across the mucus blanket that covers the intestinal epithelium. The nanosystems must be mucodiffusive enough to avoid being removed together with the loosely adherent mucus by the mucus clearance process and to reach and pass through the tightly bound mucus to finally be able to interact with the intestinal cells [26]. This diffusion was the focus of the last set of experiments, the analysis of the mucodiffusion capacity of the systems as a function of their specific surface composition. This analysis was performed from both microscopic and macroscopic points of view using intestinal porcine mucus as mucus model [75].

### 3.5.1. Particle Tracking Analysis using porcine mucus

Particle tracking was selected as the experimental technique used to evaluate the diffusion coefficient of the prototypes in intestinal mucus from a microscopic point of view. With this technique, the fitting of the mean square displacement of the particles ⟨MDS⟩ as a function of the time using the following equation: $\langle MSD \rangle = 4D_e\tau^{\alpha}$ (*Eq. 1*), allowed the calculation of the effective diffusion coefficient ($D_e$) of each individual particle, being α an indicative value about the nature of the diffusion mode of the

nanoparticles in mucus and τ (time scale) the time over which particles were allowed to move before calculating their displacement trajectories (1 second, 100 frames/s) [50–52].

*Figure* 7 shows the distribution of the effective diffusion coefficient ($D_e$) of each individual particle of the nanosystems in both, intestinal porcine mucus and PBS calculated as a time scale of 1 second. Prototypes formulated without non-ionic surfactants displayed a clear reduction on their mobility once incubated in mucus. This is in line with our previous results that showed that all these systems displayed, to some extent, a clear interaction with mucin. Incorporation of PF68 to the prototypes did not have a clear effect on their diffusion capacity in mucus. Finally, the inclusion of PF127 was found to have a different effect depending on the prototype. While for CS and PARG NCs, this surfactant did not display a clear modification of their diffusion capacity, the NE showed a remarkable displacement of the particles population towards higher diffusion values in mucus.

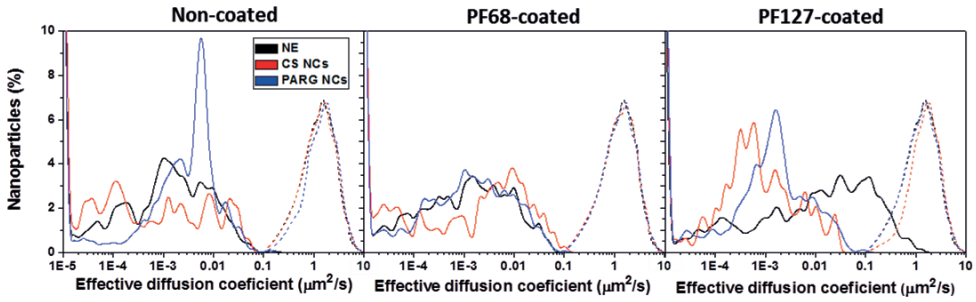



***Figure 7.*** *Mucodiffusion assessed by multiple particle tracking analysis. Histogram of the effective diffusion coefficient ($D_e$) of the different nanosystems tested in intestinal porcine mucus (continuous line) and in PBS (dotted line) calculated at a time scale of 1 second. Non-coated (left), PF68-coated (middle) and PF127-coated (right) NEs (black), CS NCs (red) and PARG NCs (blue) (number of batches analyzed n = 3; n ≥ 1000 nanoparticles).*

All these data were analyzed in depth by calculation of the mean effective diffusion coefficient (mean of the $D_e$ of each individual particle) of each prototype (*Figure 8*) [50,51]. No significant differences ($p \leq 0.05$) were found in the mean effective diffusion coefficient displayed by the non-coated formulations, resulting all of them (NE and NCs) highly retained in the mucus matrix. These results could be attributed to the hydrophobic character of the NE and the positive surface charge of CS and PARG. Both characteristics are expected to promote the interaction of the formulation with the mucin fibers present in the intestinal porcine mucus [34,35,38,41,44,60].

The incorporation of PF68 resulted in a similar behavior for the three nanosystems, with no significant differences being observed among them and with the non-coated formulations ($p \leq 0.05$). This could be attributed to the low association of this surfactant to the nanosystems, as highlighted before. In fact, the adsorption of PEG derivatives with a PEG−Mw in the 5−10 kDa range, normally results in an enhancement of the mucodiffusion properties [51]. However, to achieve this goal, it is necessary to create a homogeneous and dense enough coating [44,76]. If the coating is not thick enough, it may lead to the entrapment of the nanostructure in the mucin mesh of the mucus [44,76].

The use of PF127 led to a remarkable improvement in the mucodiffusion capacity of the NE ($p \leq 0.0001$), with a mean diffusion coefficient of $1.9 \times 10^{-2}$ $\mu m^2/sec$. These results are indicative of a better coating of the NE by this non-ionic surfactant [44,76]. However, this significant improvement was not observed in the case of the NCs, where it seems, that it was not possible to obtain a dense and homogeneous coating due to the presence of the CS or PARG polymers. As previously mentioned, the mucodiffusion capacity of the colloidal systems is strongly dependent on the coating density of the nanosystem, meaning that if the non-ionic surfactant coating is not perfectly homogeneous, it can result in a retention of the nanosystem in the mucus mesh [44,76].

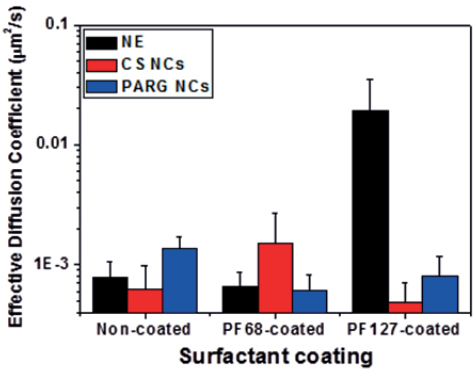



***Figure 8.*** *Mucodiffusion assessed by multiple particle tracking analysis. Mean effective diffusion coefficient of the non-coated, PF68-coated, and PF127-coated NEs (black), CS NCs (red) and PARG NCs (blue) calculated from their trajectories in porcine intestinal mucus at 37 °C at a time scale of 1 second (Error bars mean standard deviation; number of batches analyzed n = 3; n ≥ 1000 nanoparticles).*

### 3.5.2. Capillary in porcine mucus

The previously discussed mucodiffusion microscopic assay was complemented by a macroscopic analysis, where the penetration profile of each nanosystem across a capillary filled with porcine intestinal mucus was also determined. The results in *Figure 9* show the mean penetration capacity ($X_{1/2}$), which means the thickness (µm) of intestinal porcine mucus that allows the transport of 50 % of the nanosystems. Overall, the results followed the same trend found using particle tracking analysis (*Figure 8*), although some slight differences were observed. This distinct behavior could be attributable to the different concentration of nanosystem used in both procedures, being either not diluted for the capillary technique or 100-fold diluted for particle tracking analysis. These results showed that in the absence of poloxamer PARG NCs displayed the highest mucodiffusive properties ($p \leq 0.0001$), being the slighter cationic character of the PARG NCs ($p \leq 0.05$) probably the reason behind the lower retention of these NCs in the intestinal porcine mucus mesh ($p \leq 0.0001$) [26]. In agreement with the conclusions extracted from the nanoparticle tracking analysis, the low incorporation of PF68 in both NE and NCs did not result in an improved mucodiffusion of these nanosystems. In the same line, results showed the non-effective incorporation of PF127 in presence of CS and PARG and highlighted the important effect of PF127 on the mucodiffusion of the nanoemulsions [44,51,76].

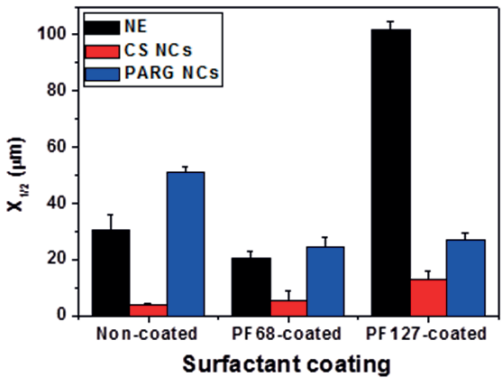



***Figure 9.*** *Mucodiffusion assessed by the capillary approach. Mean penetration capacity ($X_{1/2}$) of the non-coated, PF68-coated and PF127-coated NEs (black), CS NCs (red) and PARG NCs (blue) according to their penetration profile through a capillary filled with porcine mucus at 37 °C (Error bars mean standard deviation; n ≥ 3).*

Overall, these data suggest that the use of PF127 may be a strategy to improve the capacity of a nanosystem to overcome the multiple barriers associated to the oral modality of administration, i.e. colloidal stability, resistance against enzymatic degradation and intestinal mucus interaction/diffusion. However, when using this approach, one must take into account that the incorporation of this surfactant onto the surface of the nanosystem may interfere with other constituents present in the nanosystems shell.

## 4. Conclusions

Our results show that the interaction of nanosystems with biological barriers is dependent on their surface composition and that the contribution of each component can be affected by the presence of other components. Specifically, while the presence of PF127 alone contributes deeply to the stability of the formulation, and its capacity to diffuse across intestinal mucus, its use in the presence of CS or PARG had a limited effect on the formulation performance. In brief, these results highlight the need of a specifically engineered rational design of the nanocarriers in order for them to fulfill the adequate requirements for their performance as oral drug delivery vehicles. Ultimately, these data also emphasize the value of a proper characterization of the nanocarriers in line with their expected biological behavior.

## References

[1] M. Koziolek, M. Grimm, F. Schneider, P. Jedamzik, M. Sager, J.-P. Kühn, W. Siegmund, W. Weitschies, Navigating the human gastrointestinal tract for oral drug delivery: uncharted waters and new frontiers, Adv. Drug Deliv. Rev. 101 (2016) 75–88. doi:10.1016/j.addr.2016.03.009.

[2] A.L. Smart, S. Gaisford, A.W. Basit, Oral peptide and protein delivery: intestinal obstacles and commercial prospects, Expert Opin. Drug Deliv. 11 (2014) 1323–1335. doi:10.1517/17425247.2014.917077.

[3] M. Morishita, N.A. Peppas, Is the oral route possible for peptide and protein drug delivery?, Drug Discov. Today. 11 (2006) 905–910. doi:10.1016/j.drudis.2006.08.005.

[4] K. Park, I.C. Kwon, K. Park, Oral protein delivery: Current status and future prospect, React. Funct. Polym. 71 (2011) 280–287. doi:10.1016/j.reactfunctpolym.2010.10.002.

[5] E. Moroz, S. Matoori, J.-C. Leroux, Oral delivery of macromolecular drugs: where we are after almost 100 years of attempts, Adv. Drug Deliv. Rev. 101 (2016) 108–121. doi:10.1016/j.addr.2016.01.010.

[6] S.R. Hwang, Y. Byun, Advances in oral macromolecular drug delivery, Expert Opin. Drug Deliv. 11 (2014) 1955–1967. doi:10.1517/17425247.2014.945420.

[7] S. Maher, R.J. Mrsny, D.J. Brayden, Intestinal permeation enhancers for oral peptide delivery, Adv. Drug Deliv. Rev. 106 (2016) 277–319. doi:10.1016/j.addr.2016.06.005.

[8] B.F. Choonara, Y.E. Choonara, P. Kumar, D. Bijukumar, L.C. du Toit, V. Pillay, A review of advanced oral drug delivery technologies facilitating the protection and absorption of protein and peptide molecules, Biotechnol. Adv. 32 (2014) 1269–1282. doi:10.1016/j.biotechadv.2014.07.006.

[9] E.P. Herrero, M.J. Alonso, N. Csaba, Polymer-based oral peptide nanomedicines, Ther. Deliv. 3 (2012) 657–668. doi:10.4155/tde.12.40.

[10] K.B. Ryan, S. Maher, D.J. Brayden, C.M. O'Driscoll, Nanostructures overcoming the intestinal barrier: drug delivery strategies, in: M.J. Alonso, N. Csaba (Eds.), Nanostructured Biomater. Overcoming Biol. Barriers, Royal Society of Chemistry, 2012: pp. 63–91.

[11] I. Santalices, A. Gonella, D. Torres, M.J. Alonso, Advances on the formulation of proteins using nanotechnologies, J. Drug Deliv. Sci. Technol. 42 (2017) 155–180. doi:10.1016/j.jddst.2017.06.018.

[12] M.J. Alonso, Nanomedicines for overcoming biological barriers, Biomed. Pharmacother. 58 (2004) 168–172. doi:10.1016/j.biopha.2004.01.007.

[13] Z. Niu, I. Conejos-Sánchez, B.T. Griffin, C.M. O'Driscoll, M.J. Alonso, Lipid-based nanocarriers for oral peptide delivery, Adv. Drug Deliv. Rev. 106 (2016) 337–354. doi:10.1016/j.addr.2016.04.001.

[14] W. Suchaoin, A. Bernkop-Schnürch, Nanocarriers protecting toward an intestinal pre-uptake metabolism, Nanomedicine. 12 (2017) 255–269. doi:10.2217/nnm-2016-0331.

[15] T.A.S. Aguirre, D. Teijeiro-Osorio, M. Rosa, I.S. Coulter, M.J. Alonso, D.J. Brayden, Current status of selected oral peptide technologies in advanced preclinical development and in clinical trials, Adv. Drug Deliv. Rev. 106 (2016) 223–241. doi:10.1016/j.addr.2016.02.004.

[16] C. Liu, Y. Kou, X. Zhang, H. Cheng, X. Chen, S. Mao, Strategies and industrial perspectives to improve oral absorption of biological macromolecules, Expert Opin. Drug Deliv. 15 (2018) 223–233.

doi:10.1080/17425247.2017.1395853.

[17] H.R. Lakkireddy, M. Urmann, M. Besenius, U. Werner, T. Haack, P. Brun, J. Alié, B. Illel, L. Hortala, R. Vogel, D. Bazile, Oral delivery of diabetes peptides — Comparing standard formulations incorporating functional excipients and nanotechnologies in the translational context, Adv. Drug Deliv. Rev. 106 (2016) 196–222. doi:10.1016/j.addr.2016.02.011.

[18] L. Rosenmayr-Templeton, The oral delivery of peptides and proteins: established versus recently patented approaches, Pharm. Pat. Anal. 2 (2013) 125–145. doi:10.4155/ppa.12.75.

[19] R. Devraj, H.D. Williams, D.B. Warren, A. Mullertz, C.J.H. Porter, C.W. Pouton, In vitro digestion testing of lipid-based delivery systems: calcium ions combine with fatty acids liberated from triglyceride rich lipid solutions to form soaps and reduce the solubilization capacity of colloidal digestion products, Int. J. Pharm. 441 (2013) 323–333. doi:10.1016/j.ijpharm.2012.11.024.

[20] M. Wulff-Pérez, M.J. Gálvez-Ruíz, J. de Vicente, A. Martín-Rodríguez, Delaying lipid digestion through steric surfactant Pluronic F68: a novel in vitro approach, Food Res. Int. 43 (2010) 1629–1633. doi:10.1016/j.foodres.2010.05.006.

[21] M. Wulff-Pérez, J. de Vicente, A. Martín-Rodríguez, M.J. Gálvez-Ruiz, Controlling lipolysis through steric surfactants: new insights on the controlled degradation of submicron emulsions after oral and intravenous administration, Int. J. Pharm. 423 (2012) 161–166. doi:10.1016/j.ijpharm.2011.12.025.

[22] L. Serra, J. Doménech, N.A. Peppas, Engineering design and molecular dynamics of mucoadhesive drug delivery systems as targeting agents, Eur. J. Pharm. Biopharm. 71 (2009) 519–528. doi:10.1016/j.ejpb.2008.09.022.

[23] F.J.O. Varum, F. Veiga, J.S. Sousa, A.W. Basit, An investigation into the role of mucus thickness on mucoadhesion in the gastrointestinal tract of pig, Eur. J. Pharm. Sci. 40 (2010) 335–341. doi:10.1016/j.ejps.2010.04.007.

[24] Y.-Y. Wang, S.K. Lai, C. So, C. Schneider, R. Cone, J. Hanes, Mucoadhesive nanoparticles may disrupt the protective human mucus barrier by altering its microstructure, PLoS One. 6 (2011) e21547. doi:10.1371/journal.pone.0021547.

[25] C. Atuma, V. Strugala, A. Allen, L. Holm, The adherent gastrointestinal mucus gel layer: thickness and physical state in vivo, Am. J. Physiol. Gastrointest. Liver Physiol. 280 (2001) G922–G929. http://www.ncbi.nlm.nih.gov/pubmed/11292601.

[26] L.M. Ensign, R. Cone, J. Hanes, Oral drug delivery with polymeric nanoparticles: the gastrointestinal mucus barriers, Adv. Drug Deliv. Rev. 64 (2012) 557–570. doi:10.1016/j.addr.2011.12.009.

[27] S.K. Lai, Y.-Y. Wang, D. Wirtz, J. Hanes, Micro- and macrorheology of mucus, Adv. Drug Deliv. Rev. 61 (2009) 86–100. doi:10.1016/j.addr.2008.09.012.

[28] H. Takeuchi, Y. Matsui, H. Yamamoto, Y. Kawashima, Mucoadhesive properties of carbopol or chitosan-coated liposomes and their effectiveness in the oral administration of calcitonin to rats, J. Control. Release. 86 (2003) 235–242. doi:10.1016/S0168-3659(02)00411-X.

[29] J.D. Smart, The basics and underlying mechanisms of mucoadhesion, Adv. Drug Deliv. Rev. 57 (2005) 1556–1568. doi:10.1016/j.addr.2005.07.001.

[30] S.E. Harding, Trends in muco-adhesive analysis, Trends Food Sci. Technol. 17 (2006) 255–262.

doi:10.1016/j.tifs.2005.12.007.

[31] S.K. Lai, Y.-Y. Wang, J. Hanes, Mucus-penetrating nanoparticles for drug and gene delivery to mucosal tissues, Adv. Drug Deliv. Rev. 61 (2009) 158–171. doi:10.1016/j.addr.2008.11.002.

[32] M. Yang, S.K. Lai, Y.-Y. Wang, W. Zhong, C. Happe, M. Zhang, J. Fu, J. Hanes, Biodegradable nanoparticles composed entirely of safe materials that rapidly penetrate human mucus, Angew. Chemie - Int. Ed. 50 (2011) 2597–2600. doi:10.1002/anie.201006849.

[33] C. Prego, D. Torres, E. Fernandez-Megia, R. Novoa-Carballal, E. Quiñoá, M.J. Alonso, Chitosan-PEG nanocapsules as new carriers for oral peptide delivery: effect of chitosan pegylation degree, J. Control. Release. 111 (2006) 299–308. doi:10.1016/j.jconrel.2005.12.015.

[34] C. Prego, D. Torres, M.J. Alonso, Chitosan nanocapsules as carriers for oral peptide delivery: effect of chitosan molecular weight and type of salt on the in vitro behaviour and in vivo effectiveness, J. Nanosci. Nanotechnol. 6 (2006) 2921–2928. doi:10.1166/jnn.2006.429.

[35] C. Prego, M. Fabre, D. Torres, M.J. Alonso, Efficacy and mechanism of action of chitosan nanocapsules for oral peptide delivery, Pharm. Res. 23 (2006) 549–556. doi:10.1007/s11095-006-9570-8.

[36] Z. Niu, E. Tedesco, F. Benetti, A. Mabondzo, I.M. Montagner, I. Marigo, D. Gonzalez-Touceda, S. Tovar, C. Diéguez, M.J. Santander-Ortega, M.J. Alonso, Rational design of polyarginine nanocapsules intended to help peptides overcoming intestinal barriers, J. Control. Release. 263 (2016) 4–17. doi:10.1016/j.jconrel.2017.02.024.

[37] P. Calvo, C. Remuñán-López, J.L. Vila-Jato, M.J. Alonso, Development of positively charged colloidal drug carriers: chitosan-coated polyester nanocapsules and submicron-emulsions, Colloid Polym. Sci. 275 (1997) 46–53. doi:10.1007/s003960050050.

[38] C. Prego, D. Torres, M.J. Alonso, The potential of chitosan for the oral administration of peptides, Expert Opin. Drug Deliv. 2 (2005) 843–854. doi:10.1517/17425247.2.5.843.

[39] M. V. Lozano, G. Lollo, M. Alonso-Nocelo, J. Brea, A. Vidal, D. Torres, M.J. Alonso, Polyarginine nanocapsules: a new platform for intracellular drug delivery, J. Nanoparticle Res. 15 (2013) 15:1515. doi:10.1007/s11051-013-1515-7.

[40] J. das Neves, M.F. Bahia, M.M. Amiji, B. Sarmento, Mucoadhesive nanomedicines: characterization and modulation of mucoadhesion at the nanoscale, Expert Opin. Drug Deliv. 8 (2011) 1085–1104. doi:10.1517/17425247.2011.586334.

[41] C. Prego, M. García, D. Torres, M.J. Alonso, Transmucosal macromolecular drug delivery, J. Control. Release. 101 (2005) 151–162. doi:10.1016/j.jconrel.2004.07.030.

[42] P. Hervella, G. Lollo, F. Oyarzñun-Ampuero, G. Rivera, D. Torres, M.J. Alonso, Nanocapsules as carriers for the transport and targeted delivery of bioactive molecules, Pan Stanford Publishing Pte. Ltd., 2011. doi:10.1201/b11035-4.

[43] F.M. Goycoolea, A. Valle-Gallego, R. Stefani, B. Menchicchi, L. David, C. Rochas, M.J. Santander-Ortega, M.J. Alonso, Chitosan-based nanocapsules: physical characterization, stability in biological media and capsaicin encapsulation, Colloid Polym. Sci. 290 (2012) 1423–1434. doi:10.1007/s00396-012-2669-z.

[44] M.J. Santander-Ortega, M. Plaza-Oliver, V. Rodríguez-Robledo, L. Castro-Vázquez, N. Villaseca-González, J. González-Fuentes, E.L. Cano, P. Marcos, M. V. Lozano, M.M. Arroyo-Jiménez, PEGylated nanoemulsions for oral delivery: role of the inner core on the final fate of the formulation, Langmuir. 33 (2017) 4269–4279. doi:10.1021/acs.langmuir.7b00351.

[45] W. Sajomsang, P. Gonil, U.R. Ruktanonchai, N. Pimpha, I. Sramala, O. Nuchuchua, S. Saesoo, S. Chaleawlert-umpon, S. Puttipipatkhachorn, Self-aggregates formation and mucoadhesive property of water-soluble β-cyclodextrin grafted with chitosan, Int. J. Biol. Macromol. 48 (2011) 589–595. doi:10.1016/j.ijbiomac.2011.01.028.

[46] A. Tachaprutinun, P. Pan-In, S. Wanichwecharungruang, Mucosa-plate for direct evaluation of mucoadhesion of drug carriers, Int. J. Pharm. 441 (2013) 801–808. doi:10.1016/j.ijpharm.2012.12.028.

[47] V. V. Khutoryanskiy, Advances in mucoadhesion and mucoadhesive polymers, Macromol. Biosci. 11 (2011) 748–764. doi:10.1002/mabi.201000388.

[48] M. Garcia-Fuentes, M.J. Alonso, Chitosan-based drug nanocarriers: where do we stand?, J. Control. Release. 161 (2012) 496–504. doi:10.1016/j.jconrel.2012.03.017.

[49] S. Roy, K. Pal, A. Anis, K. Pramanik, B. Prabhakar, Polymers in mucoadhesive drug-delivery systems: a brief note, Des. Monomers Polym. 12 (2009) 483–495. doi:10.1163/138577209X12478283327236.

[50] E. Zagato, K. Forier, T. Martens, K. Neyts, J. Demeester, S. De Smedt, K. Remaut, K. Braeckmans, Single-particle tracking for studying nanomaterial dynamics: applications and fundamentals in drug delivery, Nanomedicine. 9 (2014) 913–927. doi:10.2217/nnm.14.43.

[51] B.S. Schuster, L.M. Ensign, D.B. Allan, J.S. Suk, J. Hanes, Particle tracking in drug and gene delivery research: state-of-the-art applications and methods, Adv. Drug Deliv. Rev. 91 (2015) 70–91. doi:10.1016/j.addr.2015.03.017.

[52] J. Suh, M. Dawson, J. Hanes, Real-time multiple-particle tracking: Applications to drug and gene delivery, Adv. Drug Deliv. Rev. 57 (2005) 63–78. doi:10.1016/j.addr.2004.06.001.

[53] J. Kirch, A. Schneider, B. Abou, A. Hopf, U.F. Schaefer, M. Schneider, C. Schall, C. Wagner, C.-M. Lehr, Optical tweezers reveal relationship between microstructure and nanoparticle penetration of pulmonary mucus, Proc. Natl. Acad. Sci. 109 (2012) 18355–18360. doi:10.1073/pnas.1214066109.

[54] M. Kaipel, A. Wagner, E. Wassermann, K. Vorauer-Uhl, R. Kellner, H. Redl, H. Katinger, R. Ullrich, Increased biological half-life of aerosolized liposomal recombinant human Cu/Zn superoxide dismutase in pigs, J. Aerosol Med. Pulm. Drug Deliv. 21 (2008) 281–290. doi:10.1089/jamp.2007.0667.

[55] M.J. Santander-Ortega, M. V. Lozano-López, D. Bastos-González, J.M. Peula-García, J.L. Ortega-Vinuesa, Novel core-shell lipid-chitosan and lipid-poloxamer nanocapsules: Stability by hydration forces, Colloid Polym. Sci. 288 (2010) 159–172. doi:10.1007/s00396-009-2132-y.

[56] M.J. Santander-Ortega, J.M. Peula-García, F.M. Goycoolea, J.L. Ortega-Vinuesa, Chitosan nanocapsules: effect of chitosan molecular weight and acetylation degree on electrokinetic behaviour and colloidal stability, Colloids Surfaces B Biointerfaces. 82 (2011) 571–580. doi:10.1016/j.colsurfb.2010.10.019.

[57] D. Torrecilla, M. V. Lozano, E. Lallana, J.I. Neissa, R. Novoa-Carballal, A. Vidal, E. Fernandez-Megia, D. Torres, R. Riguera, M.J. Alonso, F. Dominguez, Anti-tumor efficacy of chitosan-g-poly(ethylene glycol) nanocapsules containing docetaxel: anti-TMEFF-2 functionalized nanocapsules vs. non-functionalized nanocapsules, Eur. J. Pharm. Biopharm. 83 (2013) 330–337. doi:10.1016/j.ejpb.2012.10.017.

[58] M.J. Santander-Ortega, A.B. Jódar-Reyes, N. Csaba, D. Bastos-González, J.L. Ortega-Vinuesa, Colloidal stability of Pluronic F68-coated PLGA nanoparticles: a variety of stabilisation mechanisms, J. Colloid Interface Sci. 302 (2006) 522–529. doi:10.1016/j.jcis.2006.07.031.

[59] A. Torcello-Gómez, J. Maldonado-Valderrama, J. de Vicente, M.A. Cabrerizo-Vílchez, M.J. Gálvez-Ruiz, A. Martín-Rodríguez, Investigating the effect of surfactants on lipase interfacial behaviour in the presence of bile salts, Food Hydrocoll. 25 (2011) 809–816. doi:10.1016/j.foodhyd.2010.09.007.

[60] M. Plaza-Oliver, J. Fernández Sainz de Baranda, V. Rodríguez Robledo, L. Castro-Vázquez, J. Gonzalez-Fuentes, P. Marcos, M. V. Lozano, M.J. Santander-Ortega, M.M. Arroyo-Jimenez, Design of the interface of edible nanoemulsions to modulate the bioaccessibility of neuroprotective antioxidants, Int. J. Pharm. 490 (2015) 209–218. doi:10.1016/j.ijpharm.2015.05.031.

[61] Y.-Y. Wang, S.K. Lai, J.S. Suk, A. Pace, R. Cone, J. Hanes, Addressing the PEG mucoadhesivity paradox to engineer nanoparticles that “slip” through the human mucus barrier, Angew. Chemie - Int. Ed. 47 (2008) 9726–9729. doi:10.1002/anie.200803526.

[62] M. Tobío, A. Sánchez, A. Vila, I. Soriano, C. Evora, J.. J. Vila-Jato, M.. M. Alonso, The role of PEG on the stability in digestive fluids and in vivo fate of PEG-PLA nanoparticles following oral administration, Colloids Surfaces B Biointerfaces. 18 (2000) 315–323. doi:10.1016/S0927-7765(99)00157-5.

[63] M. García-Fuentes, D. Torres, M.J. Alonso, Design of lipid nanoparticles for the oral delivery of hydrophilic macromolecules, Colloids Surfaces B Biointerfaces. 27 (2002) 159–168. doi:10.1016/S0927-7765(02)00053-X.

[64] M. Tirado-Miranda, A. Schmitt, J. Callejas-Fernández, A. Fernández-Barbero, The aggregation behaviour of protein-coated particles: a light scattering study, Eur. Biophys. J. 32 (2003) 128–36. doi:10.1007/s00249-002-0275-6.

[65] J.A. Bernate, Vector chromatography of suspendedparticles in 1D-periodic systems, ProQuest LLC, 2012.

[66] M.J. Santander-Ortega, N. Csaba, M.J. Alonso, J.L. Ortega-Vinuesa, D. Bastos-González, Stability and physicochemical characteristics of PLGA, PLGA: poloxamer and PLGA: poloxamine blend nanoparticles: a comparative study, Colloids Surfaces A Physicochem. Eng. Asp. 296 (2007) 132–140. doi:10.1016/j.colsurfa.2006.09.036.

[67] C. Olbrich, R.H. Müller, Enzymatic degradation of SLN-effect of surfactant and surfactant mixtures, Int. J. Pharm. 180 (1999) 31–39. doi:10.1016/S0378-5173(98)00404-9.

[68] F.B. Landry, D. V. Bazile, G. Spenlehauer, M. Veillard, J. Kreuter, Degradation of poly (D,L-lactic acid) nanoparticles coated with albumin in model digestive fluids (USP XXII), Biomaterials. 17 (1996) 715–723. doi:10.1016/0142-9612(96)86742-1.

[69] O. Etienne, A. Schneider, C. Taddei, L. Richert, P. Schaaf, J.-C. Voegel, C. Egles, C. Picart, Degradability

of polysaccharides multilayer films in the oral environment: an in vitro and in vivo study, Biomacromolecules. 6 (2005) 726–733. doi:10.1021/bm049425u.

[70] R.A.A. Muzzarelli, Human enzymatic activities related to the therapeutic administration of chitin derivatives, Cell. Mol. Life Sci. 53 (1997) 131–140. doi:10.1007/PL00000584.

[71] H. Zhang, Y. Du, X. Yu, M. Mitsutomi, S. Aiba, Preparation of chitooligosaccharides from chitosan by a complex enzyme, Carbohydr. Res. 320 (1999) 257–260. doi:10.1016/S0008-6215(99)00154-8.

[72] M.J. Santander-Ortega, D. Bastos-González, J.L. Ortega-Vinuesa, M.J. Alonso, Insulin-loaded PLGA nanoparticles for oral administration: an in vitro physico-chemical characterization, J. Biomed. Nanotechnol. 5 (2009) 45–53. doi:10.1166/jbn.2009.022.

[73] A. Torcello-Gómez, J. Maldonado-Valderrama, A.B. Jódar-Reyes, T.J. Foster, Interactions between Pluronics (F127 and F68) and bile salts (NaTDC) in the aqueous phase and the interface of oil-in-water emulsions, Langmuir. 29 (2013) 2520–2529. doi:10.1021/la3044335.

[74] C. Prego, D. Torres, M.J. Alonso, Chitosan nanocapsules: a new carrier for nasal peptide delivery, J. Drug Deliv. Sci. Technol. 16 (2006) 331–337. doi:10.1016/S1773-2247(06)50061-9.

[75] A.C. Groo, F. Lagarce, Mucus models to evaluate nanomedicines for diffusion, Drug Discov. Today. 19 (2014) 1097–1108. doi:10.1016/j.drudis.2014.01.011.

[76] Q. Xu, L.M. Ensign, N.J. Boylan, A. Schön, X. Gong, J.C. Yang, N.W. Lamb, S. Cai, T. Yu, E. Freire, J. Hanes, Impact of surface polyethylene glycol (PEG) density on biodegradable nanoparticle transport in mucus ex vivo and distribution in vivo, ACS Nano. 9 (2015) 9217–9227. doi:10.1021/acsnano.5b03876.

UNIVERSIDADE DE SANTIAGO DE COMPOSTELA

# Chapter 4

## A nanoemulsion/micelles mixed nanosystem for the oral administration of hydrophobically modified insulin

USC
UNIVERSIDADE
DE SANTIAGO
DE COMPOSTELA

# Chapter 4

## A nanoemulsion/micelles mixed nanosystem for the oral administration of hydrophobically modified insulin

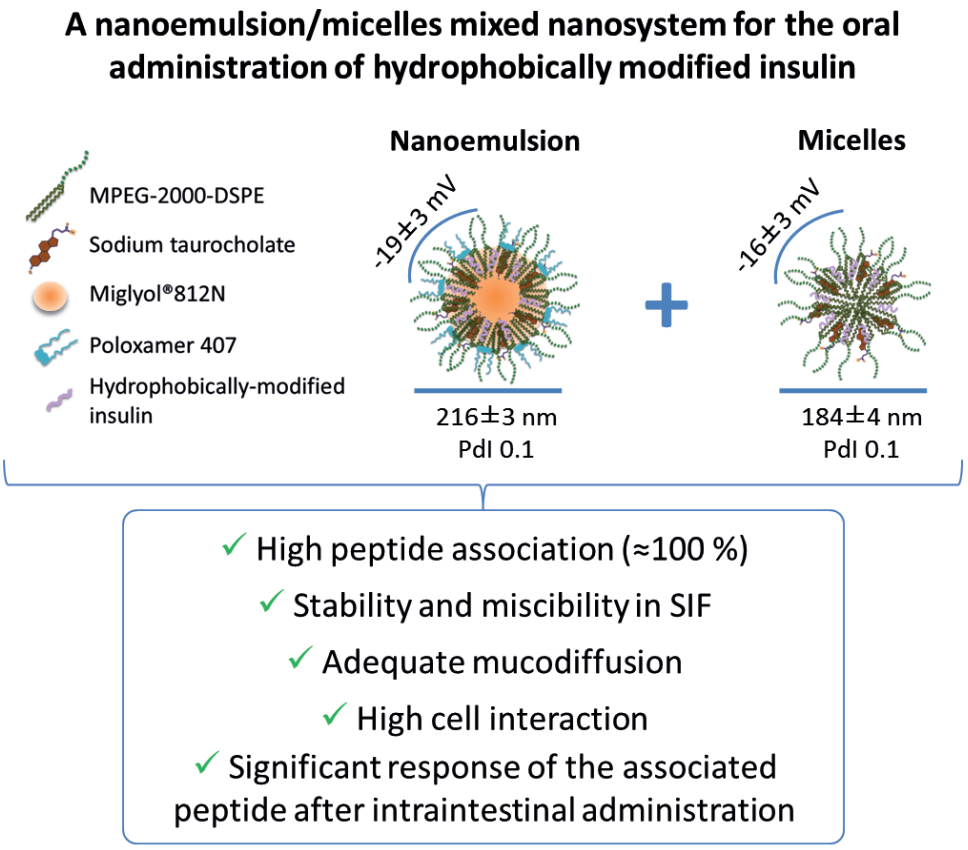
*This work was done in collaboration with: the Departament of Physical Chemistry and the Department of Physiology at the Universidade de Santigo de Compostela (Spain), Universidad de Castilla-La Mancha (Spain), Universidade de Porto (Portugal), Université Catholique de Louvain (Belgium), European Center for the Sustainable Impact of Nanotechnology (Italy) and Veneto Institute of Oncology (Italy).*


### Abstract

The potential of nanoemulsions for the oral administration of peptides is still in its early stage. The aim of the present work was to rationally design, develop and fully characterize a new nanoemulsion (NE) intended for the oral administration of hydrophobically modified insulin (HM-insulin). The components of the NE were carefully selected attending to their intrinsic properties: *i)* Miglyol® 812N, used to entrap the peptide and known for its permeation enhancing properties; *ii)* a PEGylated phospholipid (MPEG-2000-DSPE) and poloxamer 407, intended to stabilize the nanoemulsion and to provide it with a PEG shell, which is expected to increase the stability of the NE in the intestinal fluids and its mucodiffusion; *iii)* sodium taurocholate, a penetration enhancer used to enhance the encapsulation of the peptide based on the formation of ionic pairing. The results showed that the NE co-existed with a population of micelles (mixed system) and exhibited a 100 % of insulin association efficiency. The mixed nanosystem showed good stability and miscibility in different bio-relevant media and displayed an acceptable mucodiffusive behavior in porcine mucus. Cell culture studies performed in both, mono-cultures (Caco−2 and C2BBe1 human colon carcinoma Caco−2 clone cells) and co-culture (C2BBe1 human colon carcinoma Caco−2 clone/HT29−MTX cells), resulted in 100 % of positive cells. Additionally, an internalization of the mixed nanosystem was observed in Caco−2 monolayers using confocal microscopy. *In vivo* fluorescence biodistribution studies showed an accumulation of the formulation at the intestinal level. Finally, the promising behavior of the nanosystem in terms of overcoming the biological barriers of the intestinal tract was translated into a moderate, although significant, hypoglycemic response (≈ 20−30 %) following intestinal administration to rats. Overall, this information underlines the crucial steps to address when designing peptide-based nanoformulations to successfully overcome gastrointestinal barriers.

USC
UNIVERSIDADE
DE SANTIAGO
DE COMPOSTELA

## Graphical abstract



USC
UNIVERSIDADE
DE SANTIAGO
DE COMPOSTELA

## Table of contents

**1. Introduction**

**2. Materials and Methods**

2.1. Materials

2.2. Preparation of hydrophobically modified insulin (HM-insulin)-loaded mixed nanosystem (NE + micelles) and its separate species

2.3. Physicochemical and morphological properties of HM-insulin-loaded mixed nanosystem (NE + micelles) and its separate species (DLS, TEM, MALS, AFM, NTA)

2.4. Association efficiency (AE %) of HM-insulin and loading capacity of the mixed nanosystem (LC %)

2.5. Stability of HM-insulin formulated in the mixed nanosystem during storage

2.6. Interaction of HM-insulin formulated in the mixed nanosystem with bio-relevant media: colloidal stability, HM-insulin release and miscibility

2.7. Assessment of the mucodiffusive behavior of the HM-insulin formulated in the mixed nanosystem (NE + micelles) and its separate species (MTA)

2.8. *In vitro* cell culture studies of HM-insulin formulated in the mixed nanosystem

2.8.1. Colloidal stability and HM-insulin release in cell culture media

2.8.2. Cell Culture

2.8.3. Cytotoxicity studies of both, blank and HM-insulin-loaded nanosystem, in Caco−2, C2BBe1 and HT29−MTX cells (ATP, NRU, LDH and MTT)

2.8.4. Interaction of FITC-HM-insulin-loaded mixed nanosystem with Caco−2 and C2BBe1 cell mono-cultures and with C2BBe1/HT29−MTX co-culture

2.8.5. Bioactivity of HM-insulin formulated in the mixed nanosystem

2.9. *In vivo* evaluation of HM-insulin formulated in the mixed nanosystem

2.9.1. Animals

2.9.2. Biodistribution studies (confocal and *in vivo* imaging)

2.9.3. Hypoglycemic response

2.9.3.1. Healthy rats

2.9.3.1.1. HM-insulin dose-response and bioactivity after its inclusion in the nanosystem following subcutaneous (SC) administration

2.9.3.1.2. Effect on blood glucose levels following intrajejunal (IJ) administration of 100 IU/kg of HM-insulin-loaded mixed nanosystem to healthy rats

2.9.3.2. Diabetic rats

2.9.3.2.1. Effect on blood glucose levels following intraduodenal (ID) administration of 100 IU/kg of HM-insulin-loaded mixed nanosystem to diabetic rats

2.10. Statistical analysis

**3. Results and discussion**

3.1. Physicochemical and morphological properties of HM-insulin-loaded mixed nanosystem (NE + micelles) and its separate species (DLS, TEM, MALS, AFM, NTA)

3.2. Association efficiency (AE %) of HM-insulin and loading capacity of the mixed nanosystem (LC %)

3.3. Stability of HM-insulin formulated in the mixed nanosystem during storage

3.4. Interaction of HM-insulin formulated in the mixed nanosystem with bio-relevant media: colloidal stability, HM-insulin release and miscibility

3.5. Assessment of the mucodiffusive behavior of the HM-insulin formulated in the mixed nanosystem (NE + micelles) and its separate species (MTA)

3.6. *In vitro* cell culture studies of HM-insulin formulated in the mixed nanosystem

3.6.1. Colloidal stability and HM-insulin release in cell culture media

3.6.2. Cytotoxicity studies of both, blank and HM-insulin-loaded nanosystem, in Caco−2, C2BBe1 and HT29−MTX cells (ATP, NRU, LDH and MTT)

3.6.3. Interaction of FITC-HM-insulin-loaded mixed nanosystem with Caco−2 and C2BBe1 cell mono-cultures and with C2BBe1/HT29−MTX co-culture

3.6.4. Bioactivity of HM-insulin formulated in the mixed nanosystem

3.7. *In vivo* evaluation of HM-insulin formulated in the mixed nanosystem

3.7.1. Biodistribution studies (confocal and *in vivo* imaging)

3.7.2. Hypoglycemic response

3.7.2.1. Healthy rats

3.7.2.1.1. HM-insulin dose-response and bioactivity after its inclusion in the nanosystem following subcutaneous (SC) administration

3.7.2.1.2. Effect on blood glucose levels following intrajejunal (IJ) administration of 100 IU/kg of HM-insulin-loaded mixed nanosystem to healthy rats

3.7.2.2. Diabetic rats

3.7.2.2.1. Effect on blood glucose levels following intraduodenal (ID) administration of 100 IU/kg of HM-insulin-loaded mixed nanosystem to diabetic rats

**4. Conclusions**

USC
UNIVERSIDADE
DE SANTIAGO
DE COMPOSTELA

## 1. Introduction

Therapeutic proteins and peptides have gained increasing attention in the pharmaceutical field. Indeed, around 240 therapeutic peptides and proteins have already been approved by the FDA during the last decades [1,2]. The attractiveness of these macromolecular drugs, which have opened up doors to many new and powerful therapies, relies on their specificity and potency. Despite of this, these macromolecules exhibit severe biopharmaceutical limitations, i.e., instability, short half-life and limited bioavailability) [3,4], which limit their efficient clinical exploitation. As a consequence, most of these drugs need to be administered by injection, a fact that is associated to a limited patient compliance, especially in chronic treatments [5]. Due to the indicated limitations, the search for an alternative and non-invasive administration route for these molecules has become an attractive goal in the biopharmaceutical field [6,7]. The oral route is usually the preferred choice in the case of chronic treatments, being also particularly valuable for the treatment of some specific diseases. For example, in the case of diabetes, the oral administration of insulin would mimic the physiological pathway of the endogenously secreted insulin by directly entering its target organ, the liver, through the portal circulation, avoiding its unwanted systemic distribution [8]. However, the oral administration is specially complicated by the fact that peptides are susceptible to pre-systemic degradation by intestinal peptidases [9]. Additionally, the high hydrosolubility and molecular weight usually inherent to peptides, such as insulin (Mw ≈ 5.8 kDa), lead to its insufficient mucosal diffusion and its low membrane permeability [5,10,11], thus reducing their possibility of being absorbed through either transcellular (passive diffusion) [12] or paracellular transport [13,14].

Recently, nanotechnology has gained increasing attention as a valuable strategy to improve the oral bioavailability of peptides and proteins. The inclusion of these macromolecules in a variety of nanovehicles produced with biodegradable and biocompatible biomaterials allows peptide protection and its modulated delivery [15–19]. Among them, lipid-based nanocarriers have been outlined as promising oral drug delivery carriers based on their biocompatibility and also in the inherent stabilizing and absorption enhancing properties of their lipid constituents [20,21]. Within this frame, our group has dedicated a great deal of effort into this challenging goal by designing a wide variety of lipid-based nanocarriers (i.e., nanoparticles [22,23] and nanocapsules [24–32]). In particular, nanocapsules with a polymer shell of chitosan [24–27], polyarginine [27–30] and protamine [31,32] have shown a valuable potential for oral peptide delivery.

On the other hand, the interest around nanoemulsions as peptide delivery vehicles has also increased [19,21]. A number of emulsification techniques including double emulsification, reverse micellization, hydrophobic ion paring or peptide-lipid/surfactant interactions have been described for the loading hydrophilic macromolecules [33–36]. However, despite the good association efficiencies achieved in these systems, their reported peptide loading capacity is usually lower than 1 % [37,38], a fact that limits their utility for oral administration.

Considering this background information and based on the formulation screenings detailed in *Chapters 2* and 3, the aim of this work was to rationally design, develop and fully characterize a novel lipid-based nanosystem with the capacity to overcome the barriers associated to the oral modality of administration. For this purpose, a hydrophobically modified insulin (HM-insulin) was selected to be associated to the nanosystem. This peptide modification, which ended up in a hydrophobized insulin (GRAVY ≈ −0.0333) with 8 positively-ionizable aminoacids, was intended to enhance its penetration through the intestinal epithelium. A medium chain caprylic/capric triglyceride (Miglyol® 812N) was selected to constitute the lipid core of the nanosystem both because of its peptide protective and permeation enhancer properties [39,40]. A PEGylated phospholipid (MPEG-2000-DSPE) and poloxamer 407 were selected as surfactants, with the idea that their PEG moieties would enhance the stability of the nanosystem in intestinal fluids [24,27,41,42], as well as promote its mucodiffusion [27,43–46]. Additionally, sodium taurocholate (STC) was selected as co-surfactant due to its penetration enhancing properties [47,48]. Finally, apart from the previously mentioned properties of MPEG-2000-DSPE and sodium taurocholate (STC), they are both negatively charged, which was expected to favor the retention of the HM-insulin in the lipid core, thus improving its association efficiency through the formation of hydrophobic ionic pairs [49–52]. As an outcome of this rational design, a mixed nanosystem consisting of nanoemulsion and clusters of micelles was developed and its potential as oral delivery system was extensively evaluated. Namely, the mixed nanosystem was characterized in terms of *i)* stability and miscibility in simulated intestinal fluids with and without enzymes, *ii)* mucodiffusive properties, *iii)* ability to interact with the intestinal cells, *iv)* biodistribution following oral administration and *v)* potential to be used for the oral delivery of insulin in both healthy and diabetic rats.

## 2. Materials and Methods

### 2.1. Materials

Hydrophobically modified insulin, named as HM-insulin (Mw 6256.23 Da), was kindly provided by Sanofi (Paris, France). Pharmaceutical grade poloxamer 407 (Kolliphor® P 407), sodium taurocholate (STC) and N-(carbonyl-methoxypolyethylene glycol-2000)-1,2-distearoyl-sn-glycero-3-phosphoethanolamine sodium salt (LIPOID PE 18:0/18:0-PEG 2000 (MPEG-2000-DSPE)), were purchased from BASF (Ludwigshafen, Germany), New Zealand Pharmaceuticals (Palmerston North, New Zealand) and Lipoid GmbH (Ludwigshafen, Germany) respectively. Caprylic/capric triglyceride (Miglyol® 812N) was purchased from Cremer, Oleo Division (Witten, Germany). The fluorescent dyes 1,10-dioctadecyl-3,3,30,30-tetramethylindodicarbocyanine perchlorate fluorescent dye (DiD oil, $\lambda_{Ex}$ = 663 nm, $\lambda_{Em}$ = 644 nm) and 2-(6-hydroxy-3-oxo-(3H)-xanthen-9-yl)-5-isothiocyanatobenzoic acid (5−FITC, $\lambda_{Ex}$ = 494 nm, $\lambda_{Em}$ = 519 nm) were purchased from Life Technologies (Eugene, USA) and EMP GmbH Biotech (Berlin, Germany) respectively. Sodium glycocholate of pharmaceutical grade was purchased from New Zealand Pharmaceuticals (Palmerston North, New Zealand) for miscibility studies. Triton™ X−100 for molecular biology was obtained from Sigma Aldrich (St. Louis, USA). Pancreatin (8 × USP) was purchased from Biozym (Hamburg, Germany). Organic solvents used were of HPLC grade and all other products used were of high purity or reagent grade.

Human colorectal adenocarcinoma Caco−2 cells were purchased from American Type Culture Collection (Manassas, VA, USA) and used at passages 20–30. C2BBe1 human colon carcinoma Caco−2 clone, mucus secreting HT29−MTX and Human Burkitt's lymphoma Raji B cell lines were purchased from the American Type Culture Collection (ATCC) and used at passages 53–64, 42–55 and X+15–X+20, respectively. The Hep G2 cell line was obtained from ECACC (UK, distributed by Sigma) and used at passages 9–12. Dulbecco's Modified Eagle Medium (DMEM), fetal bovine serum (FBS), L-glutamine, non-essential amino acids, 100 U/mL penicillin and 100 mg/mL streptomycin, trypsin–EDTA, Hank's Balanced Salt Solution (HBSS) were obtained from Gibco (Invitrogen Corporation, Life Technologies, UK). Eagle's Minimum Essential Medium (EMEM) (1 g glucose/L) was purchased from Sigma Aldrich (St. Louis, USA), while phosphate-buffered saline (PBS), Dulbecco's phosphate-buffered saline with calcium and magnesium (DPBS) were purchased from Lonza (Basel, Switzerland). Reagents for cytotoxicity assays were ATPLite™ (Perkin Elmer, Massachusetts, MA, USA), Neutral Red based In Vitro Toxicology

Assay Kit, LDH cytotoxicity detection kit plus (Roche, Mannheim, Germany) and MTT reagent (Sigma Aldrich, St. Louis, USA). For confocal studies, Transwell® polycarbonate inserts (6 wells, pore diameter of 3 µm polycarbonate, 4.67 $cm^2$) were purchase from Corning (Madrid, Spain).

## 2.2. Preparation of HM-insulin-loaded mixed nanosystem (NE + micelles) and its separate species

Insulin-loaded mixed system (nanoemulsion together with micelles) was prepared by the solvent displacement technique, as previously described our group [53]. Briefly, MPEG-2000-DSPE (15 mg) and Miglyol® 812N (59 mg) were dissolved in 4.875 mL ethanol. Twenty-five µL of an aqueous solution of sodium taurocholate (100 mg/mL) were then added to this lipidic phase followed by the addition of 1.5 mg insulin dissolved in 100 µL 0.01 M HCl. This organic phase was vortexed (VELP Scientifica, Usmate, Italy) and then immediately poured over 10 mL of an aqueous solution of poloxamer 407 (0.25 % w/v) under magnetic stirring at 900 rpm, causing the instantaneous diffusion of the ethanol towards the aqueous phase, leading to the rapid formation of the nanoemulsion (NE). At the same time the MPEG-2000-DSPE forms micelles with insulin. Finally, ethanol was removed and the formulation, which is a mixture of oily droplets (NE) and micelles, was concentrated up to a final volume of 5 mL by evaporation under vacuum (Rotavapor Heidolph Hei−VAP Advantage, Schwabach, Germany). The blank nanosystem, used as control, was prepared by the same method without incorporating the insulin. To separately obtain the nanoemulsion and the micelles, the system was isolated by ultracentrifugation (Avanti® J−E, Ultracentrifuge, rotor 70.1.Ti, Beckman Coulter, USA) at 11,2202.7 g for 1 h at 15 °C.

In order to better understand the system, HM-insulin-loaded micelles consisting of pegylated phospholipids and sodium taurocholate were formulated and analyzed separately. For this purpose, non-loaded and HM-insulin-loaded micelles were obtained under magnetic stirring by the physical mixture of pegylated phospholipids and STC dissolved in water with the addition of HM-insulin dissolved in HCl 0.01 M in the case of the loaded ones, to obtain a final concentration of 15 mg/mL, 2.5 mg/mL and 1.5 mg/mL respectively.

For cell studies, fluorescent covalently linked FITC-insulin was prepared. Briefly, insulin was dissolved in 0.1 M sodium bicarbonate buffer (pH 9.5) at 5 mg/mL and 5−FITC in EtOH

at 10 mg/mL. For each mL of insulin solution, 50 µL of 5−FITC solution were dropwise added under magnetic stirring (900 rpm). After 1 h incubation at room temperature protected from light, the free 5−FITC was removed passing the mixture through 5 kDa Centri Pure P10 columns (Zetadex Gel Filtration columns - Centri Pure P10, EMP GmbH Biotech, Berlin, Germany). The pH of the obtained FITC-HM-insulin conjugated was then adjusted to 6.8 (HM-insulin isoelectric point) with HCl 1 M to precipitate the conjugate. Then, after removing the bicarbonate buffer through centrifugation (5430 R Eppendorf Centrifuge, rotor F−35−6−30, Eppendorf AG, Germany) at 7,197 g during 1 h at 4 °C, the precipitated FITC-insulin conjugated was dissolved in HCl 0.05 M to obtain a final insulin concentration of 15 mg/mL. This solution was used to formulate the FITC-insulin-loaded system exactly as was previously described but adding 100 µL of FITC-insulin dissolved in HCl 0.05 M instead of non-labeled insulin. For mucodiffusion and *in vivo* biodistribution studies, fluorescently DiD-labeled mixed nanosystem was produced as above-described with the addition of 80 µL of a 2.5 mg/mL ethanolic solution of DiD to the organic phase.

## 2.3. Physicochemical and morphological properties of HM-insulin-loaded mixed nanosystem (NE + micelles) and its separate species (DLS, TEM, MALS, AFM, NTA)

The mean particle size and polydispersity index (PdI) of the nanocarriers were measured by dynamic light scattering using a Zetasizer® (NanoZS, ZEN 3600, Malvern Instruments, Worcestershire, UK) after diluting the samples with ultrapure water 33 times in the case of the mixed system and isolated nanoemulsion and directly in the case of the isolated micelles. Additionally, in order to get a more accurate size characterization, the light scattering ALV SP−86 goniometer (ALV 5000 Multi-tau correlator and a Coherent Sapphire optically pumped semiconductor laser operating at λ = 488 nm and 200 mW power) and the NanoSight NS3000 (laser operating at λ = 488 nm, Malvern Instruments, Worcestershire, UK) were also used to characterized the formulation through multi-angle light scattering (MALS) and nanoparticle tracking analysis (NTA) respectively. MALS measurements were performed at 25 °C (fixed temperature) and angles between 30 and 150 ° with increments of 15 [54]. NTA measurements were also performed at 25 °C (fixed temperature) by diluting the NE and the micelles in ultrapure water 10,000 and 100 times respectively. This last technique was also used to quantify the concentration of NE and micelles in the mixed nanosystem. The ζ−potential was measured by laser-Doppler anemometry after diluting 33 times all the samples in 1 mM KCl (Zetasizer®, NanoZS, ZEN 3600, Malvern Instruments, Worcestershire, UK).

The transmission electron microscopy (TEM CM 12, Philips, Netherlands) was used to analyze the shape of the separate species that define the mixed system (nanoemulsion and micelles). For TEM analysis samples were diluted with ultrapure water 1:50 and deposited on copper grids and stained with 2 % (w/v) phosphotungstic acid (Sigma-Aldrich, St. Louis, USA) solution, allowed to dry and then viewed under the TEM.

Atomic force microscopy (AFM) was used to analyze under normal ambient conditions the topography of the mixed nanosystem and its separate species (nanoemulsion and micelles). For AFM analysis samples were diluted with ultrapure water 1:1000, deposited onto a mica substrate (SPI Supplies, Grade V−1 Muscovite), allowed to dry and then, viewed using a XE−100 instrument (Park Systems, Korea) with a non-contact silicon cantilever probe with high resonant frequency (325 kHz) and backside aluminum reflex coating (ACTA, supplied by Park Systems) [55].

## 2.4. Association efficiency (AE %) of HM-insulin and loading capacity of the mixed nanosystem (LC %)

The percentage of insulin associated to the nanosystem was directly determined after extracting the insulin from both the NE and the micelles present in the mixed nanosystem by their complete disruption. For digestion, the insulin-loaded mixed nanosystem was vortexed together with a combination of acetonitrile, Triton™ X−100 and 0.05 % formic acid using a 2:1:1:16 proportion until obtaining a clear solution. To distinguish the amount of insulin associated either to the NE or to the micelles, the same treatment was carried out after the separation of both species present in the mixed nanosystem by ultracentrifugation. For that purpose, 1 mL of the mixed nanosystem was ultracentrifuged at 112,202.7 g for 1 h at 15 °C (Beckman Coulter, Optima L−90K, 70.1 Ti rotor, Brea, USA) obtaining a cream consisting of the isolated NE and an undernatant containing the micelles. Then, both fractions were collected and diluted with ultrapure water up to 1 mL to maintain the same concentrations as before, and then, they were disrupted using the treatment above-explained. Ultra performance liquid chromatography (Acquity UPLC, Waters, Spain) with a C18 column as stationary phase (Acquity UPLC BEH C18 300 Å, 1.7 µm 2.1 × 50 mm, Waters, Spain) at 40 °C, coupled with a UV detector set at 215 nm was used for the insulin analysis. For this purpose, 5 µL of each sample at 10 °C were injected in duplicate and the flow rate was set to 0.5 mL/min. The gradient was obtained, as showed in *Table 1*, by mixing two mobile phases: 0.05 % formic acid in ultrapure water (phase A) and 0.035 % formic acid in acetonitrile (phase B).

***Table 1.*** *UPLC analytical method*

| Time (min) | Phase A (%) | Phase B (%) |
|---|---|---|
| 0.00 | 85 | 15 |
| 0.20 | 85 | 15 |
| 3.54 | 50 | 50 |
| 3.78 | 10 | 90 |
| 4.49 | 10 | 90 |
| 4.53 | 85 | 15 |
| 5.43 | 85 | 15 |

The AE (%) of insulin was calculated according to the following equation (*Eq. 1*):

$$AE(\%) = \frac{Insulin\ in\ the\ disrupted\ nanocarrier}{Total\ insulin}\ X\ 100$$

Where *Insulin in the disrupted* nanocarrier is the insulin concentration determined by UPLC after treating the nanosystem for its disruption, and *Total insulin* is the theoretical total insulin concentration in the formulation. Analysis was done at least in triplicate.

The LC (%) was calculated as follows (*Eq. 2*):

$$LC\ (\%)\ = \frac{Total\ insulin\ X\ AE}{Total\ weight\ of\ nanocarrier}\ X\ 100$$

Where *Total insulin* is the theoretical total insulin concentration in the formulation, *AE is the insulin association efficiency* and *Total weight of nanocarrier* is the weight of the nanocarrier calculated using its yield. For calculating the total weight of both the mixed nanosystem and its separate species, they were separately lyophilized in microtubes. Then, by the difference of the weight before and after the freeze-drying process the yield of the process was determined. Analysis was done in triplicate.

## 2.5. Stability of HM-insulin formulated in the mixed nanosystem during storage

The colloidal stability of the HM-insulin-loaded mixed nanosystem was evaluated under three different storage conditions (4 °C, room temperature ≈25 °C and 40 °C). For that purpose, the particle size, PdI and ζ–potential of the formulation were monitored up to 6 months (0.5, 1, 2, 3 and 6 months) to check its potential colloidal destabilization. The

amount of insulin that remained associated to the nanosystem after 3 months storage was also determined. Analysis was done in triplicate.

## 2.6. Interaction of HM-insulin formulated in the mixed nanosystem with bio-relevant media: colloidal stability, HM-insulin release and miscibility

The colloidal stability of the HM-insulin-loaded nanosystem was evaluated by analyzing its particle size by DLS (Zetasizer® NanoZS, ZEN 3600, Malvern Instruments, Worcestershire, UK) during 4 hours incubation under moderate horizontal shaking (300 rpm, Heidolph Instruments GmbH & Co. KG, Schwabach, Germany) at 37 °C with different gastrointestinal media (dilution 33.33), whose composition is detailed in *Table 2* [56,57]. To evaluate the effect of the intestinal enzymes, SIF supplemented with 1 % pancreatin (8 × USP) was also prepared and centrifuged at 5,000 g for 5 minutes at 5 °C (5430 R Eppendorf Centrifuge, rotor F−35−6−30, Eppendorf AG, Germany) to remove pancreatin aggregates before its incubation with the nanosystem [28,31]. PdI, and derived count rate were also monitored (data not shown). To verify that the effect of each media was not interfering in the analysis, blank controls of each medium alone were also carried out. This study was done at least in three different batches in triplicate.

***Table 2.*** *FaSSGF, SIF, FaSSIF−V2 and FeSSIF−V2 without enzymes media composition. Adapted with permission from* [28,58].

| Composition | FaSSGF without enzymes | SIF | FaSSIF−V2 | FeSSIF−V2 without enzymes |
|---|---|---|---|---|
| Sodium hydroxide | | 15.4 mM | 34.8 mM | 81.65 mM |
| Monobasic potassium phosphate | | 50 mM | | |
| Sodium taurocholate | 0.08 mM | | 3 mM | 10 mM |
| Lecithin | 0.02 mM | | 0.2 mM | 2 mM |
| Maleic acid | | | 19.12 mM | 55.02 mM |
| Glyceryl monooleate | | | | 5 mM |
| Sodium oleate | | | | 0.8 mM |
| Sodium chloride | 34.2 mM | | 68.62 mM | 125.5 mM |
| Calcium chloride | | | | 5 mM |
| pH | 1.6 / 4 | 6.8 | 6.5 | 5.8 |

The amount of HM-insulin released from the mixed nanosystem upon their contact with SIF was also evaluated. For this purpose, the mixed nanosystem was diluted three times in this medium and samples were immediately ultracentrifuged at 18,001 g for 1 h at 15 °C (Beckman Coulter, Optima L−90K, 70.1 Ti rotor, Brea, USA). The insulin present in the fractions obtained (cream, undernatant and precipitate) was determined by HPLC as described in *Section 2.4*.. This study was done at least in three different batches in triplicate.

Additionally, the miscibility of the system with SIF was also evaluated to predict if once in the intestine, the system is going to be able to mix well with the intestinal fluids being homogenously distributed along the gastrointestinal tract. For this purpose, and mimicking the *in vivo* dilution in rats when orally administered [59], 300 µL of the nanosystem were slowly added over 3.2 mL of SIF (water content in the gastrointestinal tract of fasted rats) and the way of mixture was monitored. This experiment was also performed by adding a 5 % (w/v) of sodium glycocholate to the system solution to evaluate the effect of extra permeation enhancers on the miscibility.

## 2.7. Assessment of the mucodiffusive behavior of the HM-insulin formulated in the mixed nanosystem (NE + micelles) and its separate species (MTA)

Mucodiffusion of this prototype was assessed by multiple particle tracking analysis (MTA) using fresh porcine intestinal mucus, which was obtained from the local slaughterhouse, as model of the human intestinal mucosa. In this study we evaluated the mucodiffusive behavior of the mixed nanosystem (NE + micelles) as well as the mucodiffusion of both separate species. For that purpose, the lipophilic tracer DiD was incorporated either to the oil core in the case of the NE or to the inner hydrophobic cavity the in the case of the micelles during the formulation process as described in *Section 2.2*. Briefly, 5 µL of the DiD-loaded nanosystem previously diluted in water (1/20) were mixed with 100 µL of mucus. Volumes of 10 µL of each sample were placed between a microscope slide and a cover glass in a chamber created by the placement of a 120 µm thick, double-sided adhesive sticker between slide and cover (Sigma). The Nikon microscope (Izasa Scientific, Spain) equipped with an Andor Zyla 4.2 camera and a PLAN APO 100X 1.4 oil-immersion objective was always focused at 12−16 µm above the cover glass. For each sample, more than 20 movies of 800 frames were recorded at a frame rate of 100 fps, obtaining more than 100 trajectories per movie. The diffusion coefficient of each particle was obtained

off-line from the fitting of the mean square displacement ⟨MSD⟩ as a function of the time according to the following equation: (*Eq. 3*): $\langle MSD \rangle = 4D_e\tau^{\alpha}$, where $D_e$ is the effective diffusion coefficient, α the anomalous exponent that gives information about the nature of the diffusion mode of the nanoparticle in mucus (active transport ($\alpha \approx 2$); super diffusion ($0.9 \leq \alpha < 2$); subdiffusion ($0.4 \leq \alpha < 0.9$); hindered diffusion ($0.2 \leq \alpha < 0.4$); immobilization ($0.2 < \alpha$)) and τ, the time scale, which is the time over which particles are allow to move before calculating their displacement trajectories. The time scale was fixed at 1 second for these experiments (100 frames/s) [27,60–63].

Both mucoadhesive (polystyrene nanoparticles) and mucodiffusive (poloxamer 407-coated polystyrene nanoparticles) nanoparticles were used as controls. Additionally, the same procedure was performed using an aqueous solution of DiD (same concentration as in the nanoemulsion) to ensure that the signal observed did not originated from the released DiD.

## 2.8. *In vitro* cell culture studies of HM-insulin formulated in the mixed nanosystem

### 2.8.1. Colloidal stability and insulin release in cell culture media

On the one hand, since cytotoxicity (*Section 2.8.3.*) and bioactivity (*Section 2.8.5.*) cell studies were performed using supplemented-DMEM (high glucose w L–Glutamine, containing 10 % (v/v) heat-inactivated fetal bovine serum (FBS), 1 % (v/v) non-essential amino acids and 1 % (v/v) penicillin and streptomycin (100 U/mL and 100 µg/mL respectively)) and supplemented-EMEM (1 g glucose/L, 0.5 % (v/v) heat-inactivated FBS, 1 % (v/v) non-essential aminoacids, 2 mM L–Glutamine, 2 mM Metformin and 1 % (v/v) penicillin and streptomycin (100 U/mL and 100 µg/mL respectively)), the colloidal stability of the mixed nanosystem during 24 hours contact with these cell media was evaluated following the same procedure described in *Section 2.6*.. Additionally, HM-insulin released from the mixed nanosystem upon 20 hours contact with supplemented-EMEM (maximum time used in these cell assays) was quantified (n = 3) as follows. The HM-insulin-loaded mixed nanosystem was incubated in supplemented-EMEM at 45 µg/mL of final HM-insulin concentration for 20 hours at 37 °C under constant and moderate horizontal shaking (300 rpm, Heidolph Instruments GmbH & Co. KG, Schwabach, Germany). The same procedure was done with free insulin as control. Thereafter, samples were ultracentrifuged at 112,202.7 g for 1 h at 15 °C (Beckman Coulter, Optima L–90K, 70.1 Ti

rotor, Brea, USA) and the separated fractions were analyzed as follows. Free insulin presented in the undernatant was directly quantified by UPLC (method previously described in *Section 2.4.*), while insulin associated to the system in the different fractions was quantified after disrupting NE and micelles by treating them as explained in *Section 2.4.*. These studies were done in triplicate.

On the other hand, since confocal and FACS (*Section 2.8.4.*) *in vitro* cell studies were performed in HBSS, the colloidal stability of the mixed nanosystem after contact with this medium was evaluated as described in *Section 2.6.* and the HM-insulin released from the mixed nanosystem upon 4 hours contact with this cell culture medium (maximum time used in these cell assays) was quantified (n = 3). For this latest purpose, the HM-insulin-loaded mixed nanosystem was incubated in HBSS at 45 µg/mL of final HM-insulin concentration for 4 hours at 37 °C under constant and moderate horizontal shaking (300 rpm, Heidolph Instruments GmbH & Co. KG, Schwabach, Germany). The same procedure was done with free insulin as control. Thereafter, samples were ultracentrifuged at 112,202.7 g for 1 h at 15 °C (Beckman Coulter, Optima L−90K, 70.1 Ti rotor, Brea, USA) and the separated fractions were analyzed as follows. Free insulin presented in the undernatant was directly quantified by UPLC (method previously described in *Section 2.4.*), while the quantification of the free precipitated insulin required its previous solubilization in 500 µL of 0.05 % (v/v) formic acid (mobile phase A of the UPLC quantification method). Insulin associated to the system in the different fractions was quantified after disrupting NE and micelles by treating them as explained in *Section 2.4.*. These studies were done in triplicate.

### 2.8.2. Cell Culture

Caco−2 cells, C2BBe1 human colon carcinoma Caco−2 clone cells, mucus producing HT29−MTX cells and Human Burkitt's lymphoma Raji B cells were separately cultured in flasks containing Dulbecco's Modified Eagle Medium (DMEM) high glucose w L−Glutamine cell culture medium (CCM) containing 10 % (v/v) heat-inactivated fetal bovine serum (FBS), 1 % (v/v) non-essential amino acids and 1 % (v/v) penicillin and streptomycin (100 U/mL and 100 µg/mL respectively). Cells were maintained at 37 °C in a humidified incubator (Binder, Germany) under a controlled atmosphere with 95 % of relative humidity and 5 % $CO_2$. CCM was renewed every 2−3 days and cells were passaged when 70 – 80 % confluence was achieved by trypsinization. Hep G2 cells were grown in EMEM (1 g glucose/L) supplemented with 10 % FBS, 1 % non-essential aminoacids, 2 mM

L–Glutamine, 1 % penicillin (100 U/mL) streptomycin (100 µg/mL) at 37 °C, 95 % of relative humidity and 5 % $CO_2$ and passaged by trypsinization weekly.

### 2.8.3. Cytotoxicity studies of both, blank and HM-insulin-loaded nanosystem, in Caco–2, C2BBe1 and HT29–MTX cells (ATP, NRU, LDH and MTT)

**Cell culture seeding.** Cell cultures are maintained in supplemented DMEM high glucose w L–Glutamine cell culture medium (CCM) containing 10 % heat inactivated fetal bovine serum (FBS), 1 % non-essential amino acids and 1 % penicillin (100 U/mL) streptomycin (100 µg/mL) at 37 °C, 95 % of relative humidity and 5 % $CO_2$. The collection of the cells involves first their trypsinization with 2 mL of trypsin (5 min incubation at 37 °C, 95 % of relative humidity and 5 % $CO_2$) followed by the addition of the same amount of CCM in order to inactivate the trypsin. Subsequently, cells were counted using a Neubauer chamber after their staining with trypan blue, centrifuged at 4 °C, 400 g during 5 min (5810 R Eppendorf centrifuge, A–4–44 oscillation rotor, Eppendorf AG, Germany) in order to remove trypsin and cell rests, and then resuspended in CCM for being seeded at a density of $1 \times 10^4$ viable cells/well for ATP, NRU and LDH assays and $2 \times 10^4$ viable cells/well in the case of MTT studies. For samples, positive and negative control wells 200 µL of cell suspension was then transferred into each single well of the flat-bottom 96–well plate, while for blank control wells just 200 µL of CCM was transferred. Plates were incubated for 24 h in a humidified incubator at 37 °C with 95 % of relative humidity and 5 % $CO_2$ to allow cell attachment prior the cytotoxicity studies. All assays were done at least in triplicate and ECs50 values were calculated using the GraphPad Prism 7 program (California, USA).

**ATP cell viability assay in Caco–2 cells.** Adenosine Triphosphate (ATP) is a marker of cell viability because it is present in all metabolically active cells and its concentration decreases rapidly when the cells undergo necrosis or apoptosis. ATPLite™ is a luminescence-based method to measure intracellular ATP, based on the firefly (Photinus pyralis) luciferase. This assay, whose major advantages are rapidity, very high sensitivity, excellent linearity and simplicity, is based on the production of light caused by the reaction of ATP with added luciferase and D–luciferin. 24 h after cell seeding (96–well format), CCM was replaced with 200 µ of *i)* different dilutions of nanosystem suspension in CCM (8, 6, 4, 2, 1, 0.5 and 0.25 mg/mL of particles, which correspond to 117, 87, 58, 29, 15, 7 and 4 µg/mL of insulin), *ii)* water as control of the nanosystem vehicle, *iii)* 1 µM staurosporine solution from Streptomyces in CCM to death positive control wells, *iv)* CCM

for untreated controls. Then, after 2 and 24 h incubation at 37 °C, 5 % $CO_2$ and 90−95 % humidity, supernatants were removed and cells were washed with 100 µL of PBS without Ca/Mg per well. Straightaway, 100 µL of new PBS without Ca/Mg and 50 µL of mammalian cell lysis solution were added per well and the plate was shaken for 5 minutes on an orbital shaker at 700 rpm. For the measurement, 150 µL of cell lysates were transferred into a white flat-bottom 96−well plate. For the standards, 10 µL of each concentration 90 µL of PBS without Ca/Mg and 50 µL mammalian cell lysis solution were added in the respective wells. For blank wells, 100 µL PBS without Ca/Mg and 50 µL of mammalian cell lysis solution were added per well. Finally, 50 µL of substrate solution were added to all the wells and microplates were shaken for 5 minutes (700 rpm, orbital shaker). All steps were performed in the dark and measurements were performed at 22 °C in a luminometer Synergy 4 microplate reader (BioTek Instruments, Inc., Winooski, USA).

**Neutral Red Uptake (NRU) in Caco−2 cells.** This simple, accurate and reproducible assay, measures living cells via the uptake of the vital dye neutral red. Viable cells will take up the vital dye, neutral red (Basic Red 5, Toluylene Red) by active transport and incorporate it into lysosomes, whereas non-viable cells will not take up the dye. 24 h after cell seeding, CCM was replaced with 200 µL of *i)* different dilutions of nanosystem suspension in CCM (8, 6, 4, 2, 1, 0.5 and 0.25 mg/mL of particles, which correspond to 117, 87, 58, 29, 15, 7 and 4 µg/mL of insulin), *ii)* water as control of the nanosystem vehicle, *iii)* 100 µg/mL of SDS in CCM to death positive control wells, *iv)* CCM for untreated controls. Then, after 2 and 24 h incubation at 37 °C, 5 % $CO_2$ and 90−95 % humidity, supernatants were removed and cells were washed with 100 µL of PBS with Ca/Mg per well. 100 µL of a solution containing 10 % of a 0.33 % Neutral Red Solution in PBS with Ca/Mg and 90 % CCM were added and plates were incubated for 3 h at 37 °C. Then, the medium was removed and cells were washed twice with 100 µL of PBS with Ca/Mg and 100 µL of Neutral Red Assay Solubilization Solution were added to solubilize the incorporated dye. Plates were then shaken at 300 rpm during 45 min at room temperature (orbital shaker), and the absorbance was measured at $\lambda = 540$ nm using a Synergy 4 microplate reader (BioTek Instruments, Inc., Winooski, USA). The background absorbance at $\lambda = 690$ nm was subtracted from the measurements [28,31].

**Lactate dehydrogenase (LDH) in Caco−2 cells.** Plasma membrane damage was quantified by the measurement of cytoplasmic LDH activity released (colorimetric cytotoxicity detection kit plus LDH), which is directly correlated to the proportion of lysed cells through a coupled enzymatic reaction. 24 h after cell seeding, CCM was replaced with

200 µL of *i)* different dilutions of nanosystem suspension in CCM (8, 6, 4, 2, 1, 0.5 and 0.25 mg/mL of particles, which correspond to 117, 87, 58, 29, 15, 7 and 4 µg/mL of insulin), *ii)* water as control of the nanosystem vehicle, *iii)* CCM to LDH positive control wells, *iv)* CCM for untreated controls. Then, 15 min before the end of the incubation (2 and 24 h at 37 °C, 5 % $CO_2$ and 90−95 % humidity), 10 µL of LDH lysis solution were added into the positive control wells. After the incubation time, plates were centrifuged 5 min at 300 g (5810 R Eppendorf centrifuge, Eppendorf swing-bucket A-4-81 rotor with HL026 adapter, Eppendorf AG, Germany. Then, 50 µL of supernatant from all wells were transferred into another 96−well plate that was incubated 20 min at room temperature in the dark after the addition of 50 µL of working reagent for LDH detection to all the wells. Finally, 25 µL of LDH stop solution were added per well and plates were shaken 30 seconds (700 rpm, orbital shaker) before reading the absorbance at λ = 500 nm with reference at λ = 750 nm using a Synergy 4 microplate reader (BioTek Instruments, Inc., Winooski, USA) [28,31].

**MTT cell viability assay in C2BBe1 and HT29−MTX cells.** The MTT (3-(4,5-dimethylthiazol-2-yl)-2,5-diphenyltetrazolium bromide) tetrazolium reduction assay was performed to determine if both HM-insulin-loaded and blank nanosystem showed direct cytotoxicity in both C2BBe1 human colon carcinoma Caco−2 clone and HT29−MTX cells, that lead to cell death through decreasing the metabolic capacity of viable cells. Since MTT reagent consists of a positively charged tetrazolium compound able to easily penetrate viable eukaryotic cells that will convert the substrate to a colored purple formazan (die cells rapidly lose this capability), this color signal will be proportional to the number of viable cells with active metabolism [64]. 24 h after cell seeding, CCM was replaced with 200 µL of *i)* different dilutions of nanosystem suspension in CCM (20.6, 6.86, 3.43, 1.72, 0.85 and 0.43 mg/mL of particles, which correspond to 300, 100, 50, 25, 12.5 and 6.25 µg/mL of insulin), *ii)* water as control of the nanosystem vehicle, *iii)* Triton™ X−100 1 % (v/v) in CCM to negative control wells, *iv)* CCM for untreated controls. After 3 and 24 h of incubation at 37 °C, 5 % $CO_2$ and 90−95 % humidity, the medium was removed and cells were washed once with 200 µL of PBS and 200 µL of 0.5 mg/mL of MTT solution in CCM were added per well. Plates were incubated for 4 hours at 37 °C protected from light. Then, the excess solution was removed from the wells leading the formazan product accumulated as an insoluble purple colored precipitate inside cells as well as near the cell surface. Finally, formazan was solubilized in DMSO (200 µL per well) during 20 min at room temperature in the dark with horizontal shaking (500 rpm) in order to record absorbance readings. The absorbance signal emitted by the solubilized formazan was

measured at a wavelength of 590 nm using a Synergy™ Mx Monochromator-Based Multi-Mode Microplate Reader (BioTek®, Winooski, Vermont, USA) taking as reference the absorbance measured at a wavelength of 630 nm [65].

### 2.8.4. Interaction of FITC-HM-insulin-loaded mixed nanosystem with Caco−2 and C2BBe1 cell mono-cultures and with C2BBe1/HT29−MTX co-culture

After confirming the colloidal stability of the nanosystem and its negligible release of insulin after 4 hours contact at 37 °C with the cell culture medium used for these studies (HBSS), the interaction of the FITC− HM-insulin -loaded nanosystem ($\lambda_{Ex}$ = 494 nm, $\lambda_{Em}$ = 519 nm) with the intestinal cells was both quantitatively and qualitatively studied using flow cytometry (BD FACSVerse™ flow cytometer, Becton Dickinson Biosciences, San Jose, CA, US) and confocal microscopy (Cell Observer Spinning Disk, Zeiss, Germany) respectively.

FACS analysis was performed in Caco−2 and C2BBe1 human colon carcinoma Caco−2 cell monoculters, as well as in C2BBe1 human colon carcinoma Caco−2 clone/HT29−MTX co-cultures. For this purpose, Caco−2, C2BBe1 human colon carcinoma Caco−2 clone, and C2BBe1 human colon carcinoma Caco−2 clone/HT29−MTX (9:1) cells were seeded in 6−well cell culture plates at a density of $3 \times 10^5$ cells/well and incubated at 37 °C with 95 % of relative humidity and 5 % $CO_2$. After 48 h incubation, cells were washed twice with pre-warmed HBSS buffer, and 0.5 mL of the fluorescently labeled nanosystem at 0.3 mg/mL, which correspond to 45 µg/mL of FITC-HM-insulin, were added to each well. Additionally, control wells were prepared by adding either 45 µg/mL of free FITC-HM-insulin or just HBSS. Plates were then incubated for 3 h at 37 °C. Afterward, the cells were washed with HBSS buffer, and detached from the wells by trypsinization. Cell suspensions were then centrifuged 5 min at 4 °C at 400 g (5810 R Eppendorf centrifuge, A−4−44 oscillation rotor, Eppendorf AG, Germany), and the supernatant was discarded. Cells were re-suspended in 500 µL of HBSS, and analyzed using flow cytometry. The fluorescence corresponding to the nanosystem and free FITC-HM-insulin was measured at 519 nm. For each sample, 10,000 events were collected and FlowJo (TreeStar, USA) software was used for analyzing the samples.

For confocal microscopy, which was performed for the qualitative visualization of the cell−nanosystem interaction, Caco−2 monolayers were cultured by seeding $5 \times 10^5$ cells/well in 12−well cell culture inserts (Transwell®, Corning, USA) and replacing

the CCM on alternate days until 21 days. Then, monocultures were washed twice with HBSS buffer and the integrity of the cell monolayers was confirmed by measuring the transepithelial electrical resistance values (TEER) both before and after the incubation of the cells with the nanosystems using an EVOM epithelial voltammeter equipped with "chopstick" electrodes (World Precision Instruments, Sarasota, FL, USA). 400 µL of 0.3 mg/mL FITC-HM-insulin-loaded mixed nanosystem, which correspond to 45 µg/mL of FITC-HM-insulin, were added to the apical side of the Transwells®, and fresh pre-warmed HBSS buffer was added to the basolateral chamber. After 2 h of incubation at 37 °C, cell inserts were washed twice with HBSS, fixed with 4 % paraformaldehyde and stored at 4 °C. Afterwards, the fixed cell culture inserts were gently washed in PBS and the actin filaments were stained by adding 200 µL of a rhodamine–phalloidin solution (1.3 µL of phalloidin in 1 mL of 0.5 % (v/v) Triton™ X−100 in PBS) to the apical chamber and incubating for 20 min in the dark at room temperature to reveal cell borders. Subsequently, the Transwell® membranes with the fixed cell monolayers were removed from the inserts and mounted on the glass slide. Then, to stain the cell nuclei, one drop of a solution of DAPi in Mowiol (1:5000) was added, and coverslips were placed over the monolayers avoiding any bubbles. Mowiol® was then allowed to polymerize for 24 h at room temperature in dark [66]. Finally, monolayers were visualized under a Zeiss™ confocal microscope (LSM 150). Data were analyzed by the Axio Vision software (version 4.8) to obtain y–z, x–z, x–y and z-stack views of the cell monolayers.

### 2.8.5. Bioactivity of HM-insulin formulated in the mixed nanosystem

After confirming the colloidal stability of the nanosystem and the amount of insulin released from the nanosystem upon 20 hours contact at 37 °C with the cell culture medium used for these studies (cell deprivation medium), the preservation of the bioactivity of HM-insulin after its association to the nanosystem was evaluated using an insulin activity based on promoter assay. For this purpose, Hep G2 cells, originated from a human liver carcinoma and enriched in insulin receptor expression [67], were grown in EMEM (1 g glucose/L) supplemented with 10 % FBS, 1 % non-essential aminoacids, 2 mM L−Glutamine, 1 % penicillin (100 U/mL) streptomycin (100 µg/mL) at 37 °C, 95 % of relative humidity and 5 % $CO_2$. For transfection, Viafect (Promega, Madison, USA) and Turbofect (Thermo Fisher Scientific, USA) were compared by measuring the transfection efficiency of a commercial plasmid preparation of pMAXGFP (Lonza, Köhln, Germany) following the standard recommended protocols. Efficiency was calculated by measuring the number of

GFP fluorescent cells respect to the total number of cells stained with Hoescht 33258 (Sigma, Israel). Apoptosis was measured as condensed Hoescht positive cells and discarded for efficiency. Since the obtained Viafect transfection efficiency was > 95 % (Turbofect ≈ 65 %) was selected to perform this experiment. In this insulin activity based on promoter assay two different DNA plasmids were used.

*i)* pSynSRE-T-luc (Addgene, Cambridge, USA). pSynSRE-T-luc contains the −324 to −225 bp fragment of the hamster HMG−CoA synthase promoter with the SRE elements upstream of the minimal HMG−CoA synthase TATA box (−28 to +39) [68,69]. This plasmid was chosen because it has been already proved that insulin regulates HMG−CoA synthase expression through those SRE sites in human cells [70].

*ii)* pRSV-βgal (Promega, Madison, USA), which was used as transfection control.

Firstly, the transfection mixture containing 3.4 µg/mL of the corresponding promoter plasmid (pSynSRE-T-luc), 1.4 µg/mL of pRSV-βgal plasmid, 60 µL/mL of Viafect transfection reagent and 940 µL/mL of non-supplemented EMEM (serum free) was prepared. Secondly, MW48 multiwell plates (Costar, Thermo Fisher Scientific, USA) were coated with 40 µL/well of freshly prepared Type I collagen solution (100 µg/mL) in PBS (stock solution of 4 mg/mL, Sigma, St Louis, MO, USA) and washed three times with PBS (Sigma, St Louis, MO, USA). Hep G2 were trypsinized, resuspended in growth medium (supplemented-EMEM), seeded at a density of $2.5 \times 10^4$ cells/well and allowed to grow for one full day at 37 °C, 95 % of relative humidity and 5 % $CO_2$. 25 µL of the previously prepared transfection mixture were drop by drop added per well. After 6 hours incubation, plates were washed three times with warmed PBS and 400 µL of culture deprivation medium, which is the same as the growth medium but with only 0.5 % FBS and supplemented with 2 mM Metformin (helps to reduce the basal luciferase expression while the cells were under transfection) (Sigma, Steinheim, Germany), were added per well and plates were incubated for 4 hours. 100 µL of the sample and the corresponding controls (HM-insulin solution, HM-insulin-loaded mixed nanosystem, blank mixed nanosystem and blank nanosystem later spiked with HM-insulin) appropriately diluted in culture deprivation medium to obtain 10, 100, 200 and 400 µIU/mL as insulin final concentration were then added to each well (each condition was tested in six−eight replicates) and incubated for 20 hours. Thereafter, plates were washed three times with PBS and 40 µL of PassiveLysis Buffer 1X (Promega, Madison, USA) were added per well. Finally, in order to perform two different analyses, the lysate was divided as follows [71]:

*i)* 20 µL were transferred to a 96−well flat-bottom white plate (Costar, Thermo Fisher Scientific, USA) for luciferase assay and 40 µL of Luciferase Assay Buffer (*Table 3*) were added per well. Meanwhile, a positive control (mix of previous excellent transfections) and a blank (just buffer) were included in the plate. A Luciferin solution (*Table 3*) was prepared as substrate and set at the injector. The luminescence reader program was set to add 35 µL/well of luciferin solution and read 5 seconds/well using a luminometer Mithras microplate reader (LB940, Berthold, Bad Wildbad, Germany).

*ii)* 20 µL were transferred to a 96 well plasticware (Costar, Thermo Fisher Scientific, USA) for the β-galactosidase assay and 40 µL of Buffer ONPG (*Table 3*) together with 180 µL Buffer Z (*Table 3*) were added per well. Plates were incubated at 37 °C until the mixture turned yellow (from nothing to 10 minutes) being then added 75 µL/well of Buffer Stop ($Na_2CO_3$ 1 M). Plates were read in a colorimetric Mithras microplate reader (LB940, Berthold, Bad Wildbad, Germany) at 490 nm.

Experiments were performed in triplicate. To obtain final data, vehicle media was considered as 1, being all wells expressed as increments respect to this value.

***Table 3.*** *Luciferase Assay Buffer, Luciferin solution, Buffer Z and Buffer ONPG media composition* [71].

| Composition | Luciferase Assay Buffer | Luciferin solution | Buffer Z | Buffer ONPG |
|---|---|---|---|---|
| Glycylglycine (pH 7.8) | 25 mM | 25 mM | | |
| $K_2PO_4$ | 15 mM | | | |
| $Mg_2SO_4$ | 15 mM | | 1 mM | |
| Ethyleneglycoltetraacetic acid (EGTA) | 4 mM | | | |
| ATP | 2 mM | | | |
| Dithiothreitol (DTT) | 1 mM | | | |
| D−Luciferin | | 140 µM | | |
| $Na_2HPO_4$ | | | 60 mM | 577 mM |
| $Na_2H_2PO_4$ | | | 40 mM | 423 mM |
| KCl | | | 10 mM | |
| β−mercaptoethanol (pH 7.5) | | | 50 mM | |
| Orthonitrophenolgalactopyranoside (ONPG) | | | | 13.3 mM |

## 2.9. *In vivo* evaluation of HM-insulin formulated in the mixed nanosystem

### 2.9.1. Animals

Biodistribution animal experiments (Chapter 4) were done in Padova and approved by Ministero della Salute Italiano ID: CEASA 24A (Italian Legislative Decree 240/2012B, of October 10$^{th}$) and were executed in accordance with governing Italian law and European Directives and Guidelines for the use of animals in animal studies; performed therefore in compliance with the Directive 2010/63/EU of the European Parliament and Council of 22$^{nd}$ September 2010 on the protection of animals used for scientific purposes. Female BALB/c mice of 8 weeks (about 21 g of weight) were obtained from Charles River Laboratories (Italy), monitored daily and euthanized when displaying excessive discomfort.

For bioactivity and efficacy studies (Chapter 4) all animal experiments were reviewed and approved by the ethics committee at the University of Santiago de Compostela ID: 1500AE/12/FUN01/FIS02/CDG3 (Spanish Royal Decree 1201/2005, of October 10$^{th}$) and ID: 15010/17/17002 (Spanish Royal Decree 53/2013, of February 1$^{st}$) and were executed in accordance with governing Spanish law and European Directives and Guidelines for the use of animals in animal studies; performed therefore in compliance with the Directive 2010/63/EU of the European Parliament and Council of 22$^{nd}$ September 2010 on the protection of animals used for scientific purposes and under the Spanish Royal Decree 53/2013 February 1$^{st}$ on the protection of animals used for experimental and other scientific purposes, including teaching. For these studies male healthy Sprague-Dawley rats were obtained from the Central Animals House of the University of Santiago de Compostela (Spain) and kept under 12 h light / 12 h dark cycles and were fed a standard laboratory rodent diet (Panlab A04, Panlab laboratories).

### 2.9.2. Biodistribution studies (confocal and *in vivo* imaging)

The biodistribution of DiD- HM-insulin-loaded mixed nanosystem (NE + micelles) was evaluated using free DiD and untreated mice as controls. One week before the treatment, BALB/c female mice of 8 weeks (about 21 g weight) were placed on a low manganese diet to reduce auto-fluorescence from normal mouse chow. Then, after 24 h fasting, both prototype (n = 4) and control (n = 2) were orally administrated (200 µL volume) by gavage to the mice at a dose of 100 IU/kg, which corresponded to 62.5 µg/mL of DiD.

To investigate the *in vivo* biodistribution, the abdominal fur was removed by depilation and isoflurane/oxygen anesthetized mice were analyzed by total body scanning at different time points (0, 1, 2, 3, 6, and 24 h) using the IVIS Lumina II Imaging System (PerkinElmer, Zaventem, Belgium). Biodistribution kinetics of the compounds were assessed by fluorescence optical imaging with 640 nm ex./670 nm em. filter set, and laser power was automatically adjusted for each scan session. Finally, a constant region of interest (ROI) was manually selected around the abdomen of animals and the signal intensity was measured as radiance (photons/sec/cm$^2$/sr) using the LivingImage software 3.2 (PerkinElmer, Zaventem, Belgium).

Confocal microscopy was performed to further evaluate the interaction of the DiD-HM-insulin-loaded mixed nanosystem with the intestinal epithelium along different regions of the intestine. The mice's intestines were dissected at different time points (1, 3, 6, and 24 h) after the oral administration of the formulation and control (free DiD), washed with PBS and fixed in 4 % paraformaldehyde for 4 h at 4 °C to evaluate the fluorescence of the tissues. Afterwards, they were treated and stored at −80 °C for cryostate processing. Samples were cut into 7 or 10 µm thick cryoslices using a Leica CM 1850 CM cryostat and transferred to slides (SuperFrost Plus, Thermo Fisher Scientific, USA). Confocal images were acquired with a resolution of 1024 × 1024 pixel, equivalent to 775 × 775 µm for 20X dry objective using a Leica TCS SP5 II microscope. Autofluorescence and DiD fluorescence were acquired using the same acquisition parameters, using cryoslices autofluorescence at 514 nm as a reference. For each observed field, a z−stack (from 10 to 12 µm) was performed with a step size comprised between 0.4 to 0.5 µm. Final images are the sum of the intensities along z−axis (maximum projection) of the acquired volume. Images brightness and contrast were further processed using ImageJ® software, keeping identical setting between images.

### 2.9.3. Hypoglycemic response

#### 2.9.3.1. Healthy rats

##### 2.9.3.1.1. HM-insulin dose-response and bioactivity after its inclusion in the mixed nanosystem following subcutaneous (SC) administration

Male healthy Sprague-Dawley rats (average weight 313 ± 27 g) kept under 12 h light/12 h dark cycles and fed on a standard laboratory rodent diet (Panlab A04, Panlab laboratories)

were fasted for 4 h prior to the experiments, which were carried out without anesthesia, with free access to water. Two different doses of HM-insulin-loaded mixed nanosystem and HM-insulin solution, 1 and 2 IU/kg (n = 8 and n = 13 respectively), were administered subcutaneously (SC) in a ratio of 1 µL/1 g rat. Blood samples were withdrawn from the tail vein 30 min prior to the subcutaneous administration and measured using a hand-held glucometer (Glucocard™ G+ meter, Arkray Factory, Japan) to establish the baseline blood glucose level. Only those rats with initial glucose level ≥ 70 mg/dL were chosen for the study (average initial glucose level 92 ± 10 mg/dL) and randomly grouped for the different treatments. Blood samples were collected at the following time points: 0.5, 1, 1.5, 2, 3, 4, 5, 6, 7, and 8 h after administration, in order to monitor the blood glucose levels following the administration of both treatments. Additionally, the area above the curves (AAC) representing the hypoglycemic were calculated (GraphPad Prism 7 program) to estimate the overall response obtained.

#### 2.9.3.1.2. Effect on blood glucose levels following intrajejunal (IJ) administration of 100 IU/kg of HM-insulin-loaded mixed nanosystem to healthy rats

Male healthy Sprague-Dawley rats (average weight 298 ± 19 g) kept under 12 h light/12 h dark cycles and fed on a standard laboratory rodent diet (Panlab A04, Panlab laboratories) were fasted for 4 h prior to the experiments, which were carried out without anesthesia, with free access to water. HM-insulin-loaded mixed nanosystem was intrajejunally (IJ) administered to the rats through a cannula that was surgically implanted into the jejunum of each rat. In the surgery, the proximal ends of the catheters were subcutaneously addressed to the back of the neck, and rats were daily weighed and monitored during 1 week to ensure their complete recovery. The HM-insulin-loaded mixed nanosystem was administered in a maximum volume of 0.3 mL at an insulin dose of 100 IU/kg body weight (n = 8). The same dose of blank nanosystem was administered as control following the same procedure (n = 6). Additionally, 2 IU/kg body weight of an insulin solution in saline were subcutaneously administered to a different control group (n = 6). Blood samples were withdrawn from the tail vein 30 min prior to the treatment administration and measured using a hand-held glucometer (Glucocard™ G+ meter, Arkray Factory, Japan) to establish the baseline blood glucose levels. Only those rats with initial glucose level ≥ 70 mg/dL were chosen for the study (average initial glucose level 92 ± 9 mg/dL) and randomly grouped for the different treatments. Blood samples were collected at the following time points: 0.5, 1, 1.5, 2, 3, 4, 5, 6, 7, and 8 h after administration, in order to

monitor the blood glucose levels following the treatments administration. As in the previous section, the area above the curves (AAC) representing the hypoglycemic effect were calculated (GraphPad Prism 7 program) to estimate the overall response.

### 2.9.3.2. Diabetic rats

#### 2.9.3.2.1. Effect on blood glucose levels following intraduodenal (ID) administration of 100 IU/kg of HM-insulin-loaded mixed nanosystem to diabetic rats

After 12 hours fasting with free access to water, a single intraperitoneal Streptozocin injection in 50 mM sodium citrate buffer at pH 4.5 was administered to male healthy Sprague-Dawley rats (average weight 223 ± 81 g) at a dose of 60 mg/kg body weight to render them diabetic. After this procedure, animals were kept under 12 h light/12 h dark cycles and fed on a standard laboratory rodent diet (Panlab A04, Panlab laboratories), while their blood glucose levels were daily monitored. Afterwards, 1 IU/kg body weight of insulin was subcutaneously administered to rats with blood glucose > 500 mg/dL and a second intraperitoneal Streptozocin injection was administered to rats with blood glucose < 250 mg/dL (still non-diabetic). After one week recovery, rats were fasted for 12 h prior to the experiments, with free access to water, and blood samples were withdrawn from the tail vein 30 min prior to the treatment administration and measured using a hand-held glucometer (Glucocard™ G+ meter, Arkray Factory, Japan) to establish the baseline blood glucose levels. Only those rats with initial glucose level ≥ 250 mg/dL were chosen for the study (average initial glucose level 382 ± 114 mg/dL) and randomly grouped for the different treatments. Animals were then anesthetized in an induction box using 1 g/g body weight of isoflurane liquid for inhalation (Iso−Vet, Piramal Healthcare, UK) at a flow rate of 4−5 L/min together with 0.5−1 L/min of $O_2$ and a midline laparotomy was performed to expose their jejunum for the following treatment administration. The HM-insulin-loaded mixed nanosystem (n = 8) at an insulin dose of 100 IU/kg body weight and the same dose of blank nanosystem (n = 7) were intraduodenally administered in a maximum volume of 0.3 mL using a 25G needle. Rats were then allowed to completely recover and kept conscious, with free access to water, for the duration of the experiment. Additionally, 2 IU/kg body weight of an insulin solution in saline were subcutaneously administered to a different control group (n = 6). Blood samples were collected at the following time points: 0.5, 1, 1.5, 2, 3, 4, 5, 6, 7, and 8 h after administration, in order to monitor the blood

glucose levels following the treatments administration. As in the previous sections, the area above the curves (AAC) representing the hypoglycemic effect were calculated (GraphPad Prism 7 program) to estimate the overall response.

### 2.10. Statistical analysis

GraphPad Prism 7 program (California, USA) was used to perform the statistical analysis. Where applicable, data were compared using either the one-way or two-way ANOVA followed by a Fisher's LSD test, considering p-values lower than 0.05 as statistically significant.

## 3. Results and discussion

The goal of this work was the rational design, development and characterization of a nanometric delivery system with the capacity to efficiently load peptides and confront the physiological barriers associated to the oral modality of administration. For that purpose, and taking into account our previous experience designing lipid-based nanocarriers [24,26,28,72,73] and the formulation screenings detailed in *Chapters 2 and 3*, we engineered a nanoemulsion that fulfills the main requirements for an efficient oral peptide administration. The design of this lipid-based nanocarrier was based on the following criteria *i)* possibility of producing a mono-dispersed population of carrier with nanometric size in a reproducible way, *ii)* efficient insulin loading, *iii)* colloidal stability in simulated intestinal fluids and appropriate miscibility with them, *iv)* mucodiffusive properties, *v)* ability to interact with the intestinal cells without causing cytotoxic effects and *vi)* ability to lead an adequate pharmacological response once administered *in vivo*.

Interestingly, when we fully characterized the prototype, we observed a population of oily nanodroplets and a population of micelles, both containing the HM-insulin, that were characterized in detail.

### 3.1. Physicochemical and morphological properties of HM-insulin-loaded mixed nanosystem (NE + micelles) and its separate species (DLS, TEM, MALS, AFM, NTA)

A schematic representation of the organization of the rationally selected components, leading to different nanostructures is illustrated in *Figure 3*. Miglyol® 812N, a medium

chain caprylic/capric triglyceride was selected as the lipid core of the NE not only because of its permeation enhancing properties, but also because its potential contribution to the protection of the loaded peptide against the degradation [39,40]. MPEG-2000-DSPE sodium salt and poloxamer 407 were selected as surfactants to disperse the oily phase into the external aqueous phase because of their colloidal stabilizing properties as well as their capacity to prevent the attachment of degrading enzymes onto the nanosystem [24,27,41,42,74]. On the other hand, the presence of PEG molecules on the surface of the nanostructure was expected to promote its mucodiffusion [27,43–46]. Additionally, sodium taurocholate (STC) was selected as an additional surfactant due to its penetration enhancing properties [47,48]. Apart from the previously mentioned properties of MPEG-2000-DSPE and sodium taurocholate (STC), they are both negatively charged (*Figure 1*), which was supposed to favor the retention of the HM-insulin in the lipid core, thus improving its association efficiency through the formation of hydrophobic ionic pairs [49–52]. Finally, using the HM-insulin we expected that its hydrophobic domains (GRAVY ≈ −0.0333) together with its 8 positively-ionizable aminoacids would favor its entrapment within the nanoemulsion.

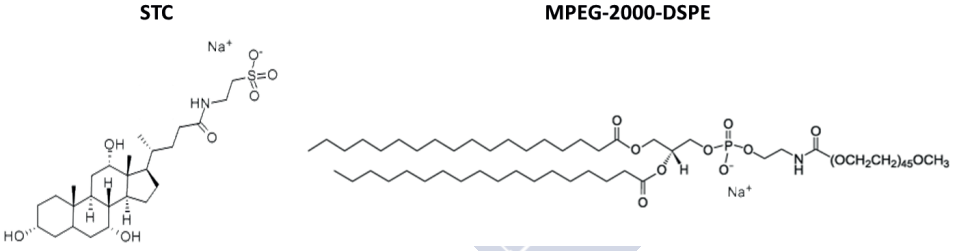



***Figure 1.*** *Chemical structure of STC and MPEG-2000-DSPE.*

The physicochemical characterization of the selected prototype, which consists of a mixture of NE and micelles, as well as that of their separate species, is presented in *Table 4*. The results indicate that it was possible to obtain a mixed nanosystem containing NE and micelles, loaded with HM-insulin, with a hydrodynamic mean size of 219 ± 7 nm, low polidispersity index (0.1) and negative ζ−Potential of −20 ± 1 mV. The negative surface charge of the system, which is attributed to the negatively charged lipids, and the presence of PEG on its surface, are expected to contribute to stabilize the formulation in the intestinal fluids [27,75], and to facilitate its mucodiffusion [27,43].

The results in *Table 4* also indicate that the size, PdI and ζ–potential were not affected by the encapsulation of HM-insulin as such or chemically linked to FITC or by the co-encapsulation of the lipophilic dye DiD. The loading of these fluorescent markers was necessary for subsequent *in vitro*/*in vivo* characterization studies. Additionally, NMR analysis illustrated in *Figure 2* of free FITC and HM-insulin and fluorescently labeled FITC-HM-insulin proved that FITC was covalently linked to HM-insulin.

***Table 4.*** *Physicochemical properties and association efficiency (AE %) of the mixed nanosystem and its separate species (nanoemulsion and micelles), loaded or not with HM-insulin and DiD or 5–FITC fluorescent dyes* (mean ± SD, n ≥ 3).

| System | Loaded molecule(s) | Size (nm) | PdI | ζ–Potential (mV) | AE (%) |
|---|---|---|---|---|---|
| **Mixed system (NE + micelles)** | – | 233 ± 11 | 0.1 | −25 ± 1 | n.a. |
| | HM-insulin | 219 ± 7 | 0.1 | −20 ± 1 | ≈ 100 |
| | DiD / HM-insulin | 217 ± 7 | 0.1 | −17 ± 1 | ≈ 100 |
| | FITC-HM-insulin | 214 ± 10 | 0.1 | −19 ± 1 | ≈ 100 |
| **NE** | – | 230 ± 13 | 0.1 | −26 ± 1 | n.a. |
| | HM-insulin | 216 ± 3 | 0.1 | −19 ± 3 | 47 ± 11 |
| | DiD / HM-insulin | 215 ± 12 | 0.1 | −15 ± 1 | 53 ± 1 |
| | FITC-HM-insulin | 216 ± 13 | 0.1 | −22 ± 1 | 48 ± 5 |
| **Micelles** | – | 200 ± 17 | 0.1 | −18 ± 5 | n.a. |
| | HM-insulin | 184 ± 4 | 0.1 | −16 ± 3 | 56 ± 8 |
| | DiD / HM-insulin | 181 ± 32 | 0.2 | −17 ± 2 | 60 ± 2 |
| | FITC-HM-insulin | 179 ± 18 | 0.1 | −15 ± 1 | 67 ± 1 |

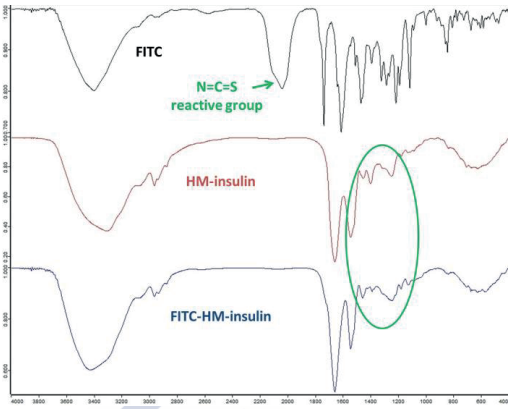



***Figure 2.*** *NMR spectra of FITC, HM-insulin and FITC-HM-insulin.*

In order to rigorously characterize the mixed nanosystem the particle size of its separate species was also measured using multi-angle light scattering (MALS) and nanoparticle tracking analysis (NTA) (*Figure 3*). MALS measurements showed a single population around 150 nm in the case of the NE (*left*) while the main population of the non-loaded pegylated phospholipid micelles (*right*) was detected around 2 nm. Interestingly, MALS characterization of the HM-insulin-loaded micelles (*middle*), showed two differentiated populations, one that would correspond to the non-loaded phospholipid micelles (population on the left) and other corresponding to clusters of HM-insulin-loaded micelles (population on the right). From these data we can conclude that the interaction between peptide and phospholipids is strong enough to change the structural configuration of the micelles leading to the formation of clusters. Although the different species showed similar size, their different nature was also proved by their different ability to scatter the light (represented along the intensity axe on the NTA 3D plot, *Figure 3*), thus confirming their different refractive index [76]. In addition, NTA analysis gave us the concentration of the two species in the mixed nanosystem, these being $2.81 \times 10^{12} \pm 1.84 \times 10^{11}$ and $6.64 \times 10^{10} \pm 4.45 \times 10^{9}$ particles/mL for the NE and micelles respectively (*Figure 3*).

The size and shape of the separate species of the mixed nanosystem was further confirmed by TEM and AFM analysis (*Figure 3*). Results from both techniques, which should be cautiously considered as the different species have probably shrunk during the drying process, illustrate the spherical shape and different appearance of both species (NE and micelles). Additionally, the analyses performed for blank micelles further supported that the structure of the micelles changes drastically after the inclusion of the insulin in the system forming a homogeneous population of clusters of HM-insulin-loaded micelles.

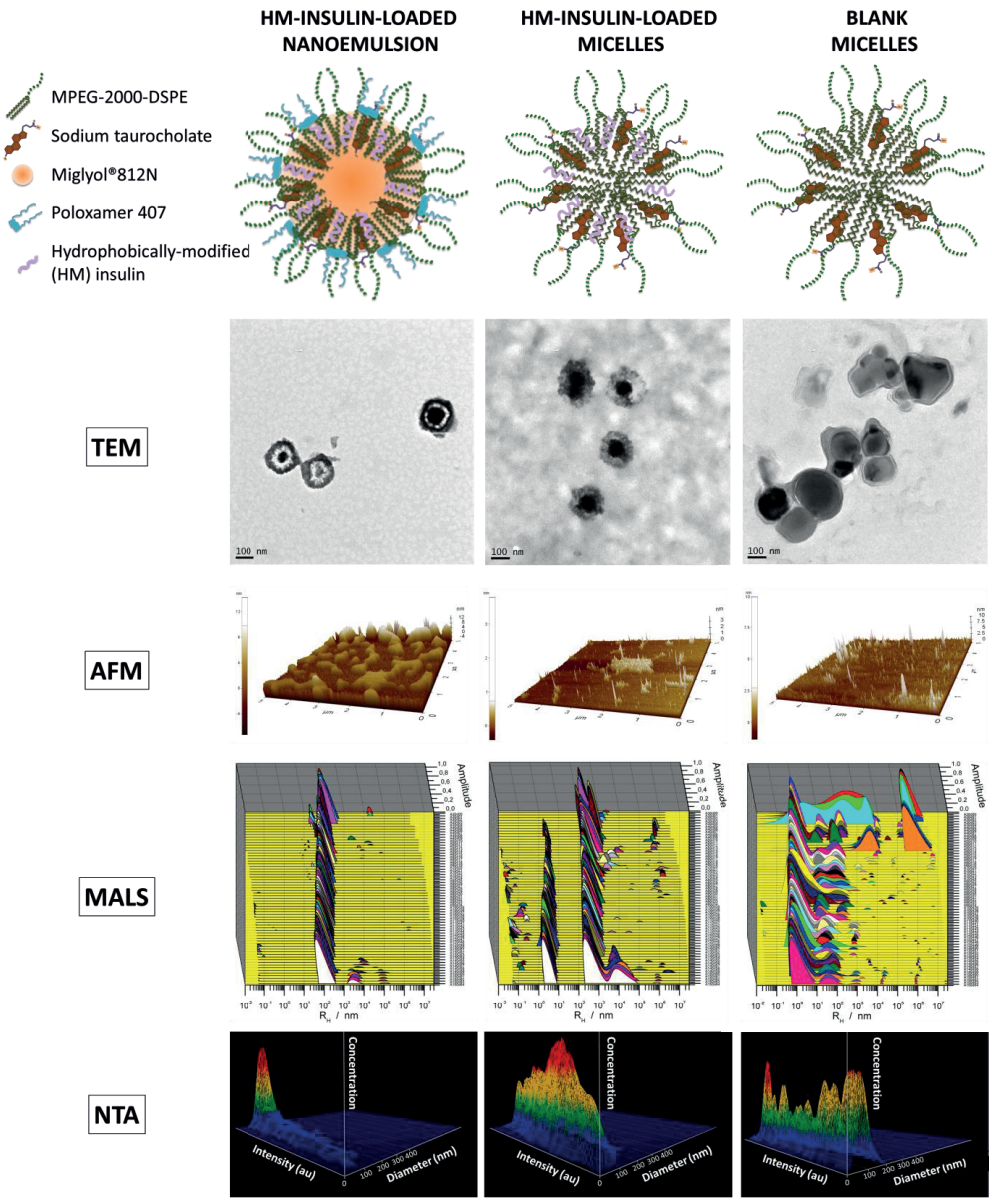



***Figure 3.*** *Schematic representation, TEM, AFM, MALS and NTA characterization of the separated species of the mixed nanosystem: HM-insulin-loaded NE (left), HM-insulin-loaded micelles (middle) and also blank micelles (right) as a comparative control*

## 3.2. Association efficiency (AE %) of HM-insulin and loading capacity of the mixed nanosystem (LC %)

As indicated, the type of insulin used in this work is a polypeptide hydropobically-modified (GRAVY value of −0.033333) from human insulin with 6.249 kDa of molecular weight, 8 positively-ionizable aminoacids and an isoelectric point ≈ 6.78. Our strategy to entrap insulin within the oily core of the nanosystem was based on its increased hydrophobicity (hydrophobic modifications illustrated in *Figure 4*) and on tuning its ionization towards a positive charge (dissolved in HCl 0.01 N, pH ≈ 2) in order to facilitate its electrostatic interaction with the negatively charged lipids and surfactants [73]. Additionally, the final pH of the formulation (pH ≈ 6.5 ± 0.2), which was close to the insulin isoelectric point (IP = 6.78), should facilitate the hydrophobic interactions among the hydrophobic domains of the insulin with the different components of the lipidic nanosystem [28,77]. As showed in *Table 4*, 100 % AE is attained in the mixed system, which corresponds with a final loading capacity (LC) of 1.65 ± 0.3 % (w/w), being around 45 % of the insulin associated to the NE (LC = 1.13 ± 0.4 %) and 55 % associated to clusters of micelles (LC = 2.11 ± 0.4 %). In addition, when micelles were formulated separately, ≈ 8 % LC and 100 % of HM-insulin AE can be achieved.

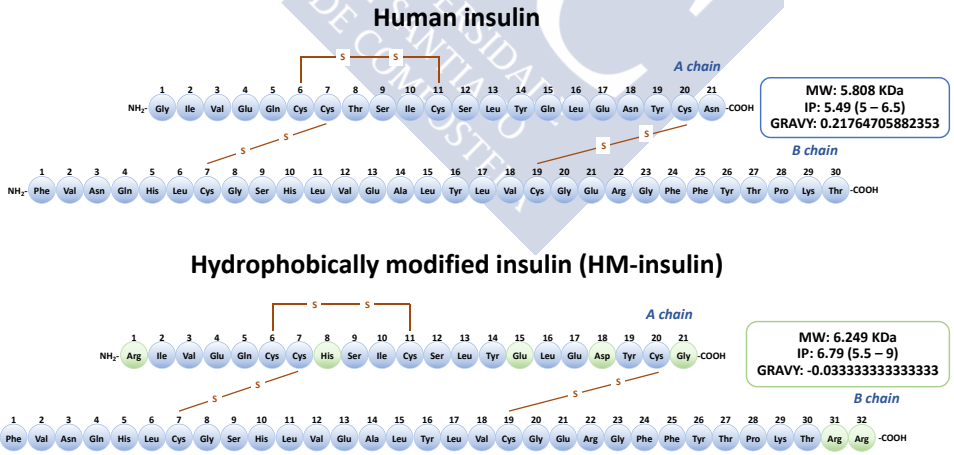



***Figure 4.*** *Amino acid sequence of human insulin and HM-insulin, with the hydrophobic modifications represented in green.*

### 3.3. Stability of HM-insulin formulated in the mixed nanosystem during storage

The results of the colloidal stability studies during storage indicated that the system was stable for, at least, 6 months at 4 °C, room temperature (RT ≈ 25 °C) and 40 °C (*Figure 5*). Size, PdI and ζ−potential were monitored and found to be constant during this period. Furthermore, the insulin content in the system was maintained after 3 months storage at 4 °C.

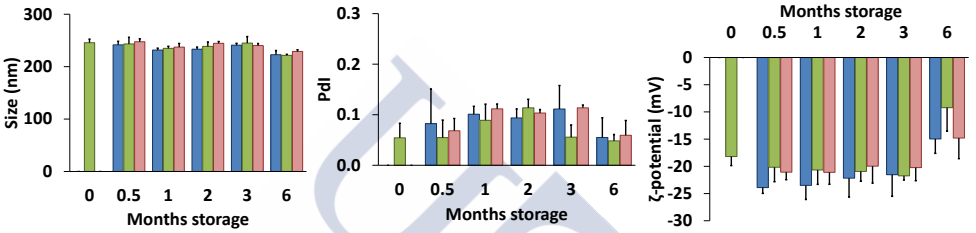



***Figure 5.*** *Colloidal stability studies during storage of the HM-insulin-loaded mixed nanosystem (NE + micelles) at three different conditions: 4 °C (blue), RT ≈ 25 °C (green) and 40 °C (red).* Mean ± SD, n ≥ 3.

### 3.4. Interaction of HM-insulin formulated in the mixed nanosystem with bio-relevant media: colloidal stability, HM-insulin release and miscibility

The ability of the nanosystem to maintain its physicochemical properties upon exposure to the intestinal fluids was thought to be critical to assess its capacity to overcome biological barriers. The colloidal stability of the HM-insulin-loaded mixed nanosystem during 4 hours contact with simulated gastric and intestinal fluids at 37 °C was monitored by DLS (size, PdI and derived count rate). The fluids selected were: FaSSGF, SIF with and without 1 % pancreatin, FaSSIF−V2 and FeSSIF−V2 without enzymes (composition detailed in *Table 2*). As depicted in *Figure 6*, the system remained colloidally stable for, at least, 4 hours in all the biologically relevant media tested, independently of their composition. Due to the moderate nanosystem surface charge (≈ −20 mV), its favorable stability in the different media cannot be result of the repulsive electrostatic potential of the nanosystem (DLVO theory) [78]. However, it could be mainly attributed to the protective steric layer conferred by the combination of MPEG−2000−DSPE and poloxamer 407 onto the oil/water interphase [27,42,75,79,80]. On the other hand, the presence of two saturated 18−carbon acyl chains in the MPEG−2000−DSPE molecules might have driven the self-assembling process and the formation of micelles through strong hydrophobic forces (low critical micelle concentration ≈ $1 \times 10^{-6}$ M) [81].

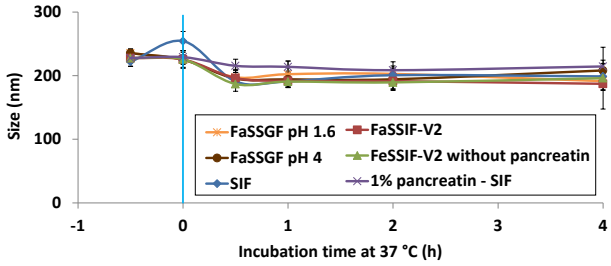



***Figure 6.*** *Colloidal stability profile of the HM-insulin-loaded mixed nanosystem (NE + micelles) after its incubation in different simulated bio-relevant media (SGF, SIF, FaSSIF−v2, FeSSIF−v2 without pancreatin and 1 % pancreatin supplemented-SIF) at 37 °C.* Mean ± SD, n ≥ 3.

On the other hand, the ultracentrifugation process involved in the methodology to determine *in vitro* the release of HM-insulin in SIF, together with the high ionic strength of this medium, caused the precipitation of part of the system containing around the 80 % of the HM-insulin. However, the fact that if the insulin presents in the precipitate was free or still associated to the system remains to be elucidated.

Miscibility studies were also performed mimicking the *in vivo* conditions [59] by carefully mixing (drop by drop) the HM-insulin-loaded mixed nanosystem with SIF. Our group has previously shown the possibility of modulate the miscibility of a lipid-based nanosystem with SIF by adding an extra amount of surfactant to the formulation [28]. Hence, we added 5 % (w/v) of sodium glycocholate (SGC) in the formulation suspension. As shown in *Figure 7*, the nanosystem was able to mix well with SIF without needing extra surfactant, however, it was faster dispersed when was co-administered with 5 % extra of SGC. These slight different miscibilities can be attributed to the already known emulsifying properties of SGC [82–84].

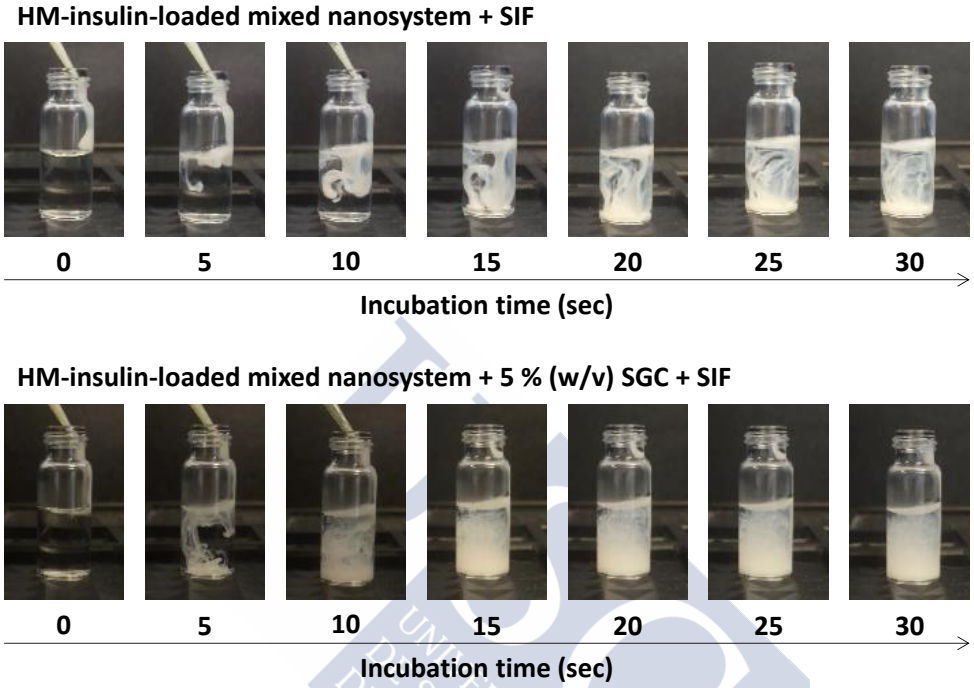



***Figure 7.*** *Miscibility of the HM-insulin-loaded mixed nanosystem (NE + micelles) after its incubation in SIF and of the HM-insulin-loaded mixed nanosystem (NE + micelles) together with a 5 % (w/v) of extra sodium glycocholate (SGC).*

## 3.5. Assessment of the mucodiffusive behavior of the HM-insulin formulated in the mixed nanosystem (NE + micelles) and its separate species (MTA)

Once the nanosystem reaches the intestine, its proper diffusion through the intestinal mucus blanket is a crucial step before achieving its internalization into the epithelium. For this purpose, the mucodiffusion capacity of the HM-insulin-loaded mixed nanosystem was evaluated by multiple particle tracking analysis using intestinal porcine mucus as mucus model [85]. This technique allows the estimation of the effective diffusion coefficient ($D_e$) of each individual particle of the formulation by correlating its mean square displacement ⟨MDS⟩ with the time, according to the following equation (*Eq. 3*):

$$\langle MSD \rangle = 4D_e\tau^{\alpha}$$

Where $\alpha$ gives information about the nature of the diffusion mode of the nanoparticle in mucus, $\tau$ is the space of time used for calculating their displacement trajectories in mucus and $D_e$ is the effective diffusion coefficient [27,60–62].

Polystyrene nanoparticles and poloxamer 407-coated polystyrene nanoparticles were used as mucoadhesive and mucodiffusive controls. The diffusion capacities ($D_m/D_w$), calculated by dividing the mean effective diffusion coefficient of the particles in mucus ($D_m$) vs the same in water ($D_w$) at a 1 second time scale ($\tau$) are represented in *Figure 8, left*. Overall, the results showed that both, the mixed nanosystem and its separated species present an acceptable diffusion in mucus. The $D_m/D_w$ obtained were $\approx 4.2 \times 10^{-2}$, $1.0 \times 10^{-1}$ and $1.2 \times 10^{-1}$ for the mixed nanosystem (NE + micelles), the isolated NE and the isolated micelles respectively. The fact that HM-insulin-loaded mixed nanosystem displayed the lowest $D_m/D_w$ ratio ($\approx 4.2 \times 10^{-2}$) could be attributed to a higher concentration of particles in suspension due to the coexistence of both species. In the same line, the mean α values were in the 0.47 – 0.58 range, which is an indicative of a close to free diffusion mode of these nanostructures in mucus. In this regard, in order to deeply characterize the diffusion mode of these nanostructures in mucus, the distributions of the α parameter were analyzed in detail (*Figure 8, right*). For this purpose, four different α populations were set as follows: $\alpha \geq 0.9$ (diffusive particles), $0.4 \leq \alpha < 0.9$ (subdiffusive particles), $0.2 \leq \alpha < 0.4$ (hindered subdiffusive particles) and $0.2 < \alpha$ (immobile particles) [60,62,63]. The results show that mucoadhesive control nanoparticles were immobile or displayed hindered diffusion, whereas the mucodiffusive control showed a subdiffusive/diffusive behavior. Similar diffusion was observed for both, the mixed nanosystem and the individual NE or micelles, showing around 30-40 % of immobile/hindered species while 60-70 % of particles displayed diffusive or subdiffusive behaviour. These results suggest that, despite the fact that the hydrophobic character of the NE and micelles could promote their retention into the mucus matrix [75,86], the presence of PEG derivatives with a PEG−Mw below 10 kDa on the surface was enough to enhance their mucodiffusion capacity [27,45,86].

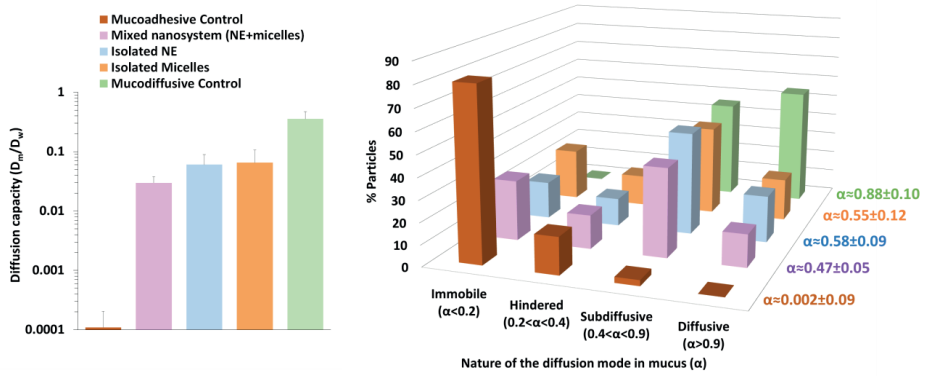



***Figure 8.*** *Diffusion capacity of the HM-insulin-loaded mixed nanosystem and its separate species calculated as mean effective diffusion coefficient in porcine mucus/mean effective diffusion coefficient in water ($D_m/D_w$) (left) and percentage of particles showing different α values (gives information about the nature of the diffusion mode in the corresponding matrix) (right).* Mean ± SD; *Number of batches analyzed n = 3; n ≥ 1000 nanoparticles.*

## 3.6. *In vitro* cell culture studies of HM-insulin formulated in the mixed *nanosystem*

### 3.6.1. Colloidal stability and insulin release in cell culture media

The colloidal stability of the HM-insulin-loaded mixed nanosystem upon incubation in cell culture media (HBSS, supplemented-DMEM and supplemented-EMEM - composition detailed in *Section 2.8.1.* for the cell deprivation medium) for up to 24 h was monitored by DLS (size, PdI and derived count rate). As depicted in *Figure 9*, the system remained colloidally stable for, at least, 24 hours in all cellular media tested, independently of their composition. The potential release of HM-insulin in the cell culture medium (HBSS and supplemented-EMEM) was also quantified. The results showed negligible insulin release after 4 h incubation with HBSS (n = 3), whereas 86 ± 1 % of the HM-insulin was released from the mixed nanosystem (n = 3) after 20 h contact with supplemented-DMEM.

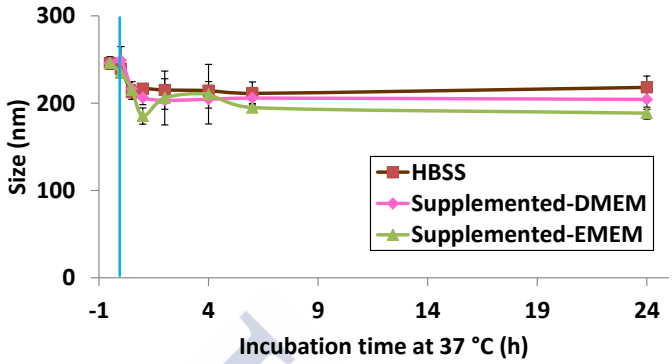



***Figure 9.*** *Colloidal stability profile of the HM-insulin -loaded mixed nanosystem (NE + micelles) after its incubation in different cellular media (HBSS, supplemented-DMEM and supplemented EMEM) at 37 °C. Mean ± SD, n ≥ 3.*

### 3.6.2. Cytotoxicity studies of both, blank and HM-insulin-loaded nanosystem, in Caco−2, C2BBe1 and HT29−MTX cells (ATP, NRU, LDH and MTT)

The Caco−2 cell line is widely accepted as an *in vitro* model to study the interaction of the formulations with the enterocytes because it resembles some crucial characteristics of the human intestine structure, such as the formation of tight junctions between the enterocytes and the presence of microvilli in their surface [65,87,88]. Despite these interesting properties, some important characteristics, such as the presence of mucus secreting goblet cells (second major cell population in human intestine) with the subsequent mucus secretion [89], are normally absent in this cellular model. Additionally, it has been reported that the permeability through the paracellular pathway in this monolayer is lower than the one observed in the human small intestine due to the high presence of tight junctions [65,90,91]. For these reasons, the potential cytotoxicity of the nanosystem was first evaluated in Caco−2 cells and then in both, the C2BBe1 human colon carcinoma Caco−2 clone (more morphologically homogeneous than Caco−2 cells, with the micriovilliar brush border exclusively localized in the apical side) and mucus secreting HT29−MTX (smaller microvilli, and softer tight junctions than Caco−2 cells) by MTT [31,87,91,92].

Firstly, the cytotoxicity of the blank and HM-insulin-loaded mixed nanosystem was assessed in Caco−2 cells using three different techniques (ATP, NRU and LDH). Different concentrations of the formulation were tested after 2 and 24 h (intestinal transit time range) incubation with the cell line in order to estimate the adequate concentration for subsequent cellular studies. While non-important cytotoxic effects were found after a-2 h incubation time, for concentrations as high as 8 mg/mL by the ATP and NRU assays, a noticeable dose-dependent LDH release was observed (*Figure 10, upper panel*). Interestingly, at concentrations > 1 mg/mL, the LDH release of cells exposed to HM-insulin-loaded mixed nanosystem was lower than the one observed for the cells treated with the blank nanosystem. This could be attributed to the ability of insulin to activate both phosphofructokinase and pyruvate dehydrogenase enzymes [93,94]. This stimulated enzymatic activity, will increase the amount of $NADH^+$ and pyruvate in the medium and thus it will hamper the first limiting reaction of the LDH assay (lactate + $NAD^+$ → pyruvate + $NADH^+$ + $H^+$) by displacing the equilibrium to the lactate production[95–97]. On the other hand, the slightly higher cell viability observed after treating the cells with the HM-insulin-loaded mixed nanosystem (ATP and NRU assays), could be related to the cell proliferation properties of insulin [95–97]. These results are in the same line than those reported for similar lipid-based nanosystems [24,31,72].

After a 24 h incubation time, a clear dose-dependent cytotoxic profile, probably attributable to the penetration enhancer properties of the formulation components and their interaction with the enterocytes [39,40,47,83,98], was found with the three assays (*Figure 10, lower panel*). ECs50 ranged from ≈ 2.2 to 2.6 mg/mL were estimated for both, the blank and the HM-insulin-loaded nanosystem using the ATP and NRU techniques, and an EC50 value of ≈ 6.5 mg/mL was found for the HM-insulin-loaded nanosystem when using the LDH release technique.

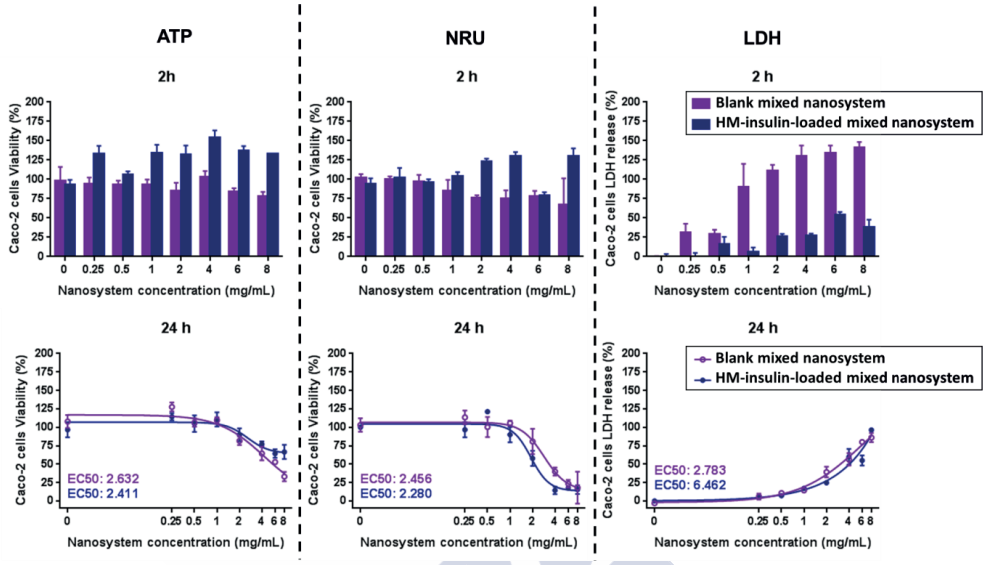



***Figure 10.*** *% Caco−2 cell viability (ATP and NUR) and plasma membrane damage (% LDH release) after 2 (top) and 24 h (bottom) incubation with different concentration of blank and HM-insulin-loaded mixed nanosystem.* Mean ± SD, n = 3.

Additionally, the cytotoxicity was assessed in C2BBe1 human colon carcinoma Caco−2 clone and mucus secreting HT29−MTX after 3 and 24 hours incubation. The results were in the same line than those obtained from the first screening performed in Caco−2 cells, confirming that non-cytotoxic effects were caused after 3 h incubation in both C2BBe1 human colon carcinoma Caco−2 clone and HT29−MTX cells for both blank and HM-insulin-loaded mixed nanosystem (*Figure 11, upper panel*), whereas a dose-dependent cytotoxic effect was observed after 24 h incubation with estimated ECs50 ranged from 2.0 to 2.3 mg/mL of system concentration (*Figure 11, lower panel*).

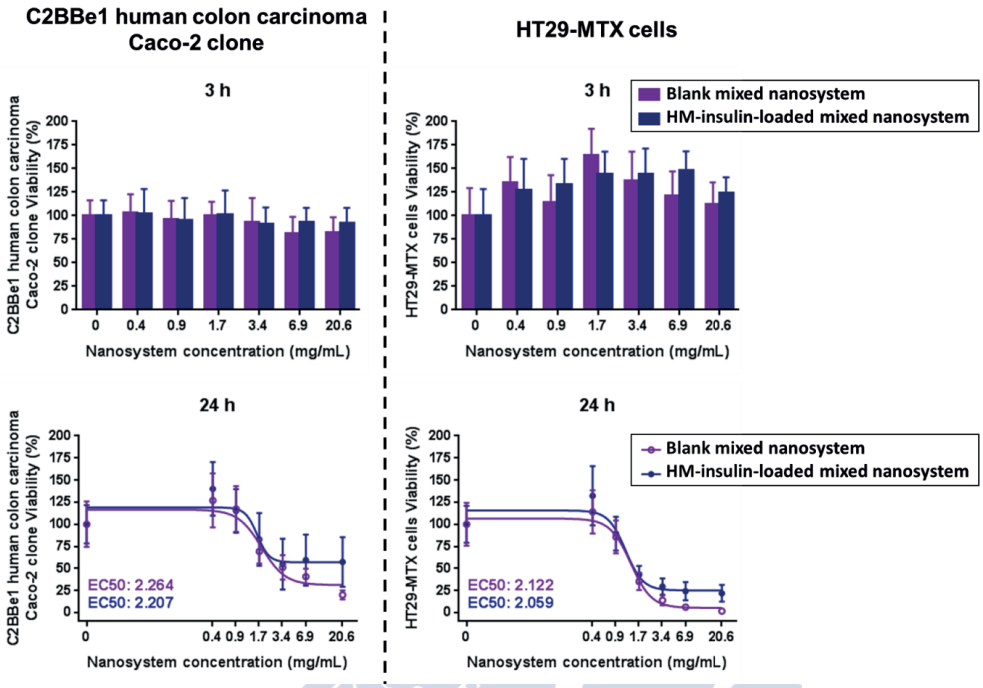



***Figure 11.*** *% Cell viability (MTT) of C2BBe1 human colon carcinoma Caco−2 clone and HT29−MTX cells after 3 (top) and 24 h (bottom) incubation with different concentrations of blank and HM-insulin-loaded mixed nanosystem. Mean ± SD, n ≥ 3.*

### 3.6.3. Interaction of FITC-HM-insulin-loaded mixed nanosystem with Caco−2 and C2BBe1 cell mono-cultures and with C2BBe1/HT29−MTX co-culture

The interaction of both free FITC-HM-insulin and FITC-HM-insulin-loaded mixed nanosystem (NE + micelles) with Caco−2 and C2BBe1 human colon carcinoma Caco−2 clone monocultures, as well as with C2BBe1 human colon carcinoma Caco−2 clone:HT29−MTX (9:1) co-culture was quantitatively analyzed using flow cytometry (FACS). Untreated cells were used as controls. Measurements were done after 3 h incubation for a FITC-HM-insulin concentration of 45 µg/mL, corresponding to 3 mg/mL of nanosystem (non-cytotoxic dose, see *Section 3.6.2.*). FACS showed significant differences ($p \leq 0.0001$) between the non-treated cells and those treated with free FITC-HM-insulin and FITC-HM-insulin-loaded mixed nanosystem, which were 100 % fluorescence positive irrespective of

the cell line (*Figure 12*). These results indicate that both, free FITC-HM-insulin and FITC-HM-insulin-loaded mixed nanosystem had the capacity to interact with the intestinal cells (≈ 100 % of FITC-positive cells). The possibility for FITC-HM-insulin to be released from the nanosystem during the incubation process was excluded, as reported in *Section 3.6.1.*

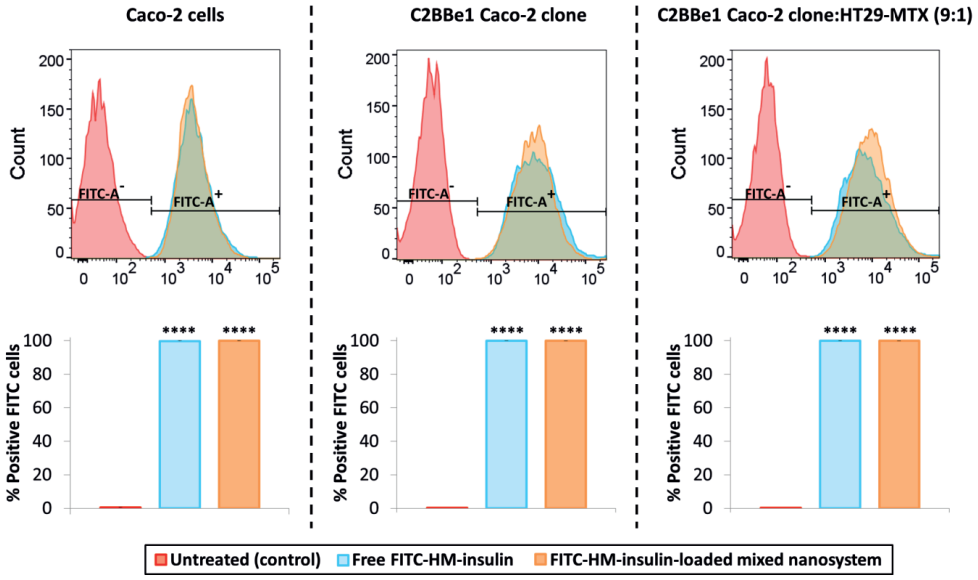



***Figure 12. Top:*** *Flow cytometry profile showing the interaction of free FITC-HM-insulin (blue) and FITC-HM-insulin-loaded mixed system (NE and micelles) (orange) with Caco−2 (**left**) and C2BBe1 human colon carcinoma Caco−2 clone (**middle**) monocultures, as well as with C2BBe1 human colon carcinoma Caco−2 clone:HT29−MTX (9:1) co-culture (**right**) compared to the non-treated control cells (red).* ***Bottom:*** *Percentage of FITC-positive cells calculated based on parent cells in Caco−2 (**left**) and C2BBe1 human colon carcinoma Caco−2 clone (**middle**) monocultures, as well as with C2BBe1 human colon carcinoma Caco−2 clone:HT29−MTX (9:1) co-culture (***right***).* Mean ± SD, n ≥ 3 *(Two-way ANOVA followed by a Fisher's LSD test were applied for the statistical analysis; significance level comparing to the control ****p ≤ 0.001).*

The interaction of the nanosystems with the monolayers was also analyzed using confocal laser scanning microscopy. For this purpose, since no differences were found in FACS for the different cell types, confocal images were taken in Caco−2 monolayers after 2 h incubation with both free FITC-HM-insulin and FITC-HM-insulin-loaded mixed nanosystem at the same concentration used for FACS. Images of untreated monolayers were taken as a control. Interestingly, as shown in *Figure 13*, the confocal studies showed differences regarding the type of interactions displayed by the free FITC-HM-insulin and FITC-HM-

insulin-loaded mixed nanosystem. While almost all free FITC-HM-insulin was found on the surface of the monolayer, FITC-HM-insulin-loaded mixed nanosystem appeared also located inside the cells. This internalization could be attributed to the permeation enhancing properties of some components of the formulation, i.e., oil, and surfactants. On the other hand, TEER analysis performed before and 2 hours after the experiment, confirmed that neither free FITC-HM-insulin nor FITC-HM-insulin-loaded mixed nanosystem caused a significant effect in the TEER values respect to the control (untreated cells) (*Figure 14*). These results indicate that the tight junctions were not affected by either treatment, thus discarding the possibility of paracellular FITC-HM-insulin transport.

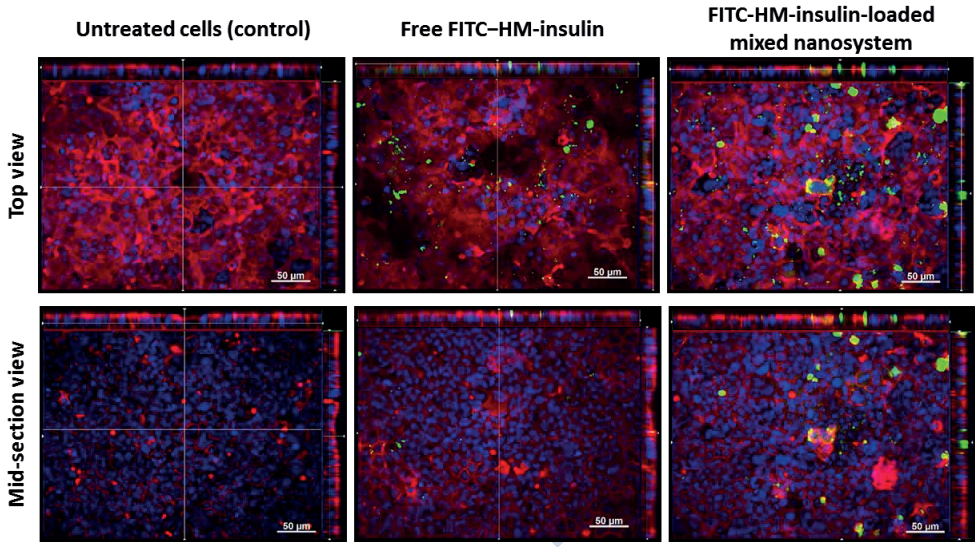



***Figure 13.*** *Confocal images in Caco–2 monolayers (top and mid-section views at 25X) representing the y–z, x–z and x–y view of Caco–2 monolayers after 2 h incubation with free FITC-HM-insulin (**middle**) and FITC-HM-insulin-loaded mixed nanosystem (NE + micelles) (**right**). Untreated monolayers were used as control (**left**). Cell membranes (rhodamine–phalloidin), cell nuclei (DAPI) and HM-insulin (FITC) are visualized in red, blue and green respectively.*

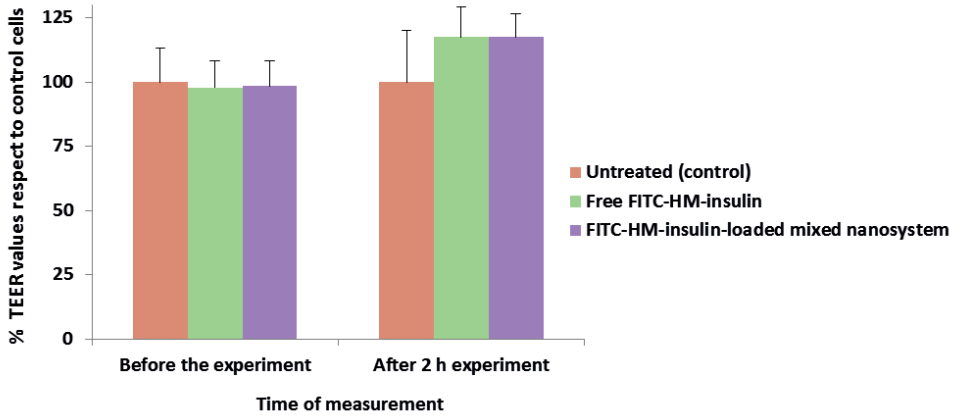



***Figure 14.*** *Caco−2 cells TEER values normalized respect to control cells (red) before and after 2 hours incubation with either free FITC-HM-insulin (green) or FITC-HM-insulin-loaded nanosystem (NE + micelles) (purple)* Mean ± SD, n ≥ 3 *(Two-way ANOVA followed by a Fisher's LSD test were applied for the statistical analysis).*

### 3.6.4. Bioactivity of HM-insulin formulated in the mixed nanosystem

Since it is well-known that peptides are labile macromolecules that may result inactivated as consequence of the formulation process [99], the preservation of the HM-insulin bioactivity after its inclusion in the nanosystem was first studied *in vitro*. The assay involved testing different concentrations of the HM-insulin-loaded nanosystem, using blank mixed nanosystem and HM-insulin solutions as negative and positive controls respectively. Additionally, different concentrations of the blank mixed nanosystem supplemented with HM-insulin were included in the study to discard any potential interference of the formulation components with the assay. The results (*Figure 15*), which were normalized respect to the negative control (blank mixed nanosystem), indicated that the HM-insulin associated to the mixed nanosystem and consequently released from it in the course of the experiment (*Section 3.6.1*.) exhibited the same activity than both, free HM-insulin alone and blank mixed nanosystem later spiked with HM-insulin (no significant differences at any of the concentrations tested). Therefore, it can be concluded that the bioactivity of HM-insulin was preserved following its incorporation into the mixed nanosystem and its subsequent release.

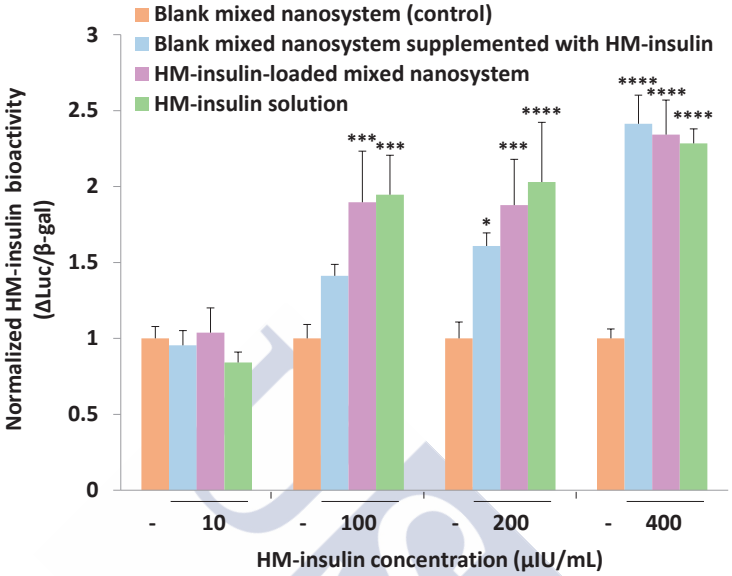



***Figure 15.*** *Insulin activity based on promoter assay.* Normalized HM-insulin bioactivity (ΔLuc/β−gal) obtained after HEP G2 incubation with different insulin concentrations (from 10 to 400 μIU/mL) in form of blank *mixed nanosystem supplemented with HM-insulin (blue), HM-insulin-loaded mixed nanosystem (purple) and HM-insulin solution (green).* Blank *mixed nanosystem was used as negative control (orange).* Mean ± SD, n = 5 *(Two-way ANOVA followed by a Fisher's LSD test were applied for the statistical analysis; significance levels comparing to the control *p ≤ 0.05; ***p ≤ 0.001, ****p ≤ 0.001).*

## 3.7. *In vivo* evaluation of HM-insulin formulated in the mixed nanosystem

### 3.7.1. Biodistribution studies (confocal and *in vivo* imaging)

The interaction of the mixed nanosystem with the intestinal tract was evaluated *in vivo* by scanning of the total body of mice at different time points (0, 1, 2, 3, 6 and 24 h) after the administration by oral gavage of 200 μL of DiD-HM-insulin-loaded mixed nanosystem at an insulin dose of 100 IU/kg (62.5 μg/mL of DiD). *Figure 16* shows the tracking of the fluorescent marker in both, the study and control (62.5 μg/mL of free DiD) groups. The bioluminescent images profile (*Figure 16, left*) recorded for free DiD and DiD-HM-insulin-loaded mixed system for up to 24 h were similar. The histograms (*Figure 16, right*) built from the mean of total photons emitted per second inside the gastrointestinal tract were not statistically different for the free DiD and the DiD-HM-insulin loaded nanosystem. The signal coming from the free DiD could be associated to its affinity for the cellular

membranes due to its amphiphilic character. The association of the nanosystem with the intestinal mucosa would be in agreement with its mucopermeating properties (*Section 3.5.*) and its capacity to interact with the epithelial intestinal cells (*Section 3.6.3.*). Nevertheless, this study, as such, does not allow us to conclude about a significant retention given the similar patters observed for the nanosystem and the free dye.

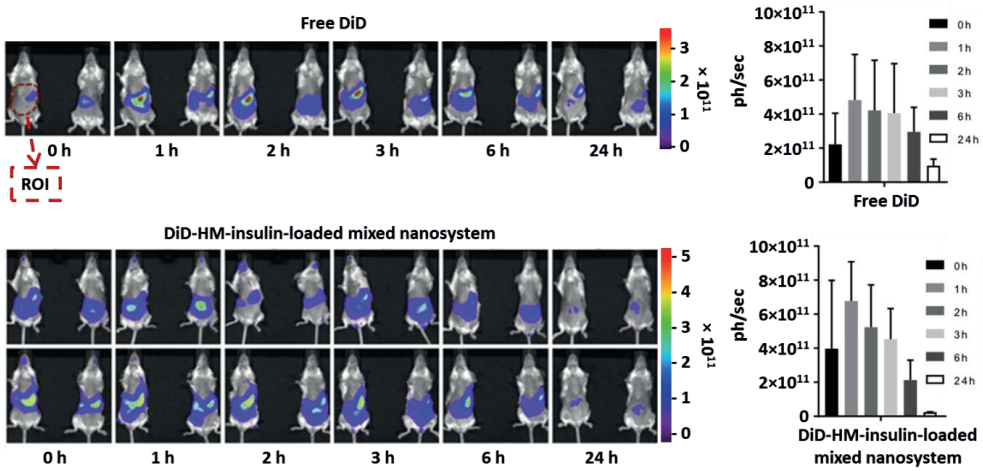



***Figure 16.*** *Scanning in vivo images of n = 2 mice treated with free DiD in solution (top, left) and n = 4 mice treated with DiD-HM-insulin-loaded mixed nanosystem (bottom, left) administrated by oral gavages at different time points (0, 1, 2, 3, 6 and 24 h). On the right, intensity of fluorescence as mean of total photons emitted per second ± SD for the treated mice at each time point inside the ROI (regions of interest – gastrointestinal tract).*

In order to have a more precise estimation of the fate of the mixed nanosystem along the gastrointestinal tract (either duodenum, small and large intestine) over the time, a more detailed analysis of the dissected mice intestines was performed at 1, 3, 6 and 24 hours post-administration [28,100]. As shown in *Figure 17*, the system displayed a defined spatial- and temporal-distribution. At 1 hour post-administration non-detectable signal was found in the duodenum, however an intense signal surrounding the cells was captured in the rest of the small and large intestine. This signal was maintained for at least 6 hours. The signal of DiD-HM-insulin-loaded mixed nanosystem-treated mice was higher and more prolonged compared to the one of free DiD-treated mice. In addition, the signal coming from the nanosystem was mainly localized at the surface of the intestinal borders, while the one from free-DiD was detected inside the cells.

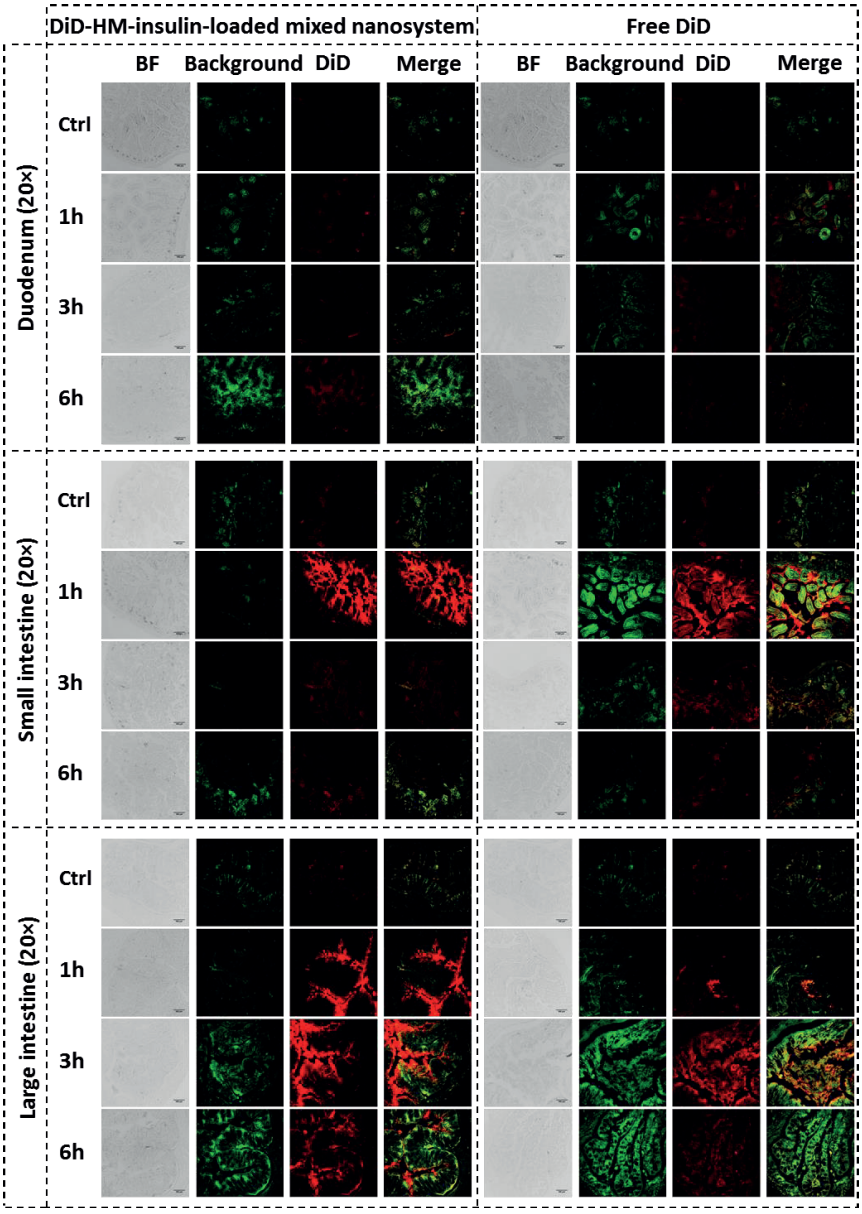



***Figure 17.*** *Confocal images showing the interaction of DiD-HM-insulin-loaded mixed nanosystem (left) and free DiD (right) with different segments of mice gastrointestinal tract (duodenum – top, small intestine – middle and large intestine – top) at 1, 3, and 6 h after oral gavage (20X magnification, dry objective) (Ctrl = untreated mice).*

### 3.7.2. Hypoglycemic response

The evaluation of the hypoglycemic response of HM-insulin-loaded formulations has been performed in healthy [48,101] and diabetic [28,31,48,102] animal models, both of them with pros and cons. In normoglycemic rats, the exogenous insulin may decrease the secretion of the endogenous one by the β−cells and its effect might be hindered by the autoregulation phenomenon [103,104]. However, the commonly used streptozocin (STZ) model leads to different degrees of β−cell deficiency and, hence, very variable glycemic responses [28,31]. On the other hand, in the diabetic rat model, the lack of auto-regulation phenomenon suppressing the secretion of endogenous insulin and the β−cell deficiency makes these animals more insulin-sensitive [103,104]. Bearing these differences in mind, the efficacy of the formulation was evaluated in both, healthy and diabetic rat models.

#### 3.7.2.1. Healthy rats

##### 3.7.2.1.1. HM-insulin dose-response and bioactivity after its inclusion in the nanosystem following subcutaneous (SC) administration

We first conducted a dose-response study (1 and 2 IU/kg body weight) following subcutaneous administration (SC) of HM-insulin in the free form or associated to the nanosystem to fasted healthy rats. *Figure 18* shows the glucose values normalized respect to the glucose baseline level (measured 30 min prior to the treatments administration), which was considered as 100 %.

The results indicate that the overall hypoglycemic response measured by the area above the curve (AAC) was similar for the free and encapsulated HM-insulin, however it was significantly influenced by the dose (*Figure 18, right*). Beyond these similar global values, the profiles observed for the low HM-insulin dose (1 IU/kg) were different (*Figure 18, left*). In the case of the HM-insulin-loaded nanosystems a slow release could be responsible for a low and prolonged hypoglycemic response. The reason why this delayed response was not observed for the high insulin dose remains to be elucidated. Irrespective of this, these results corroborated that HM-insulin preserves its bioactivity *in vivo* after its inclusion in the formulation.

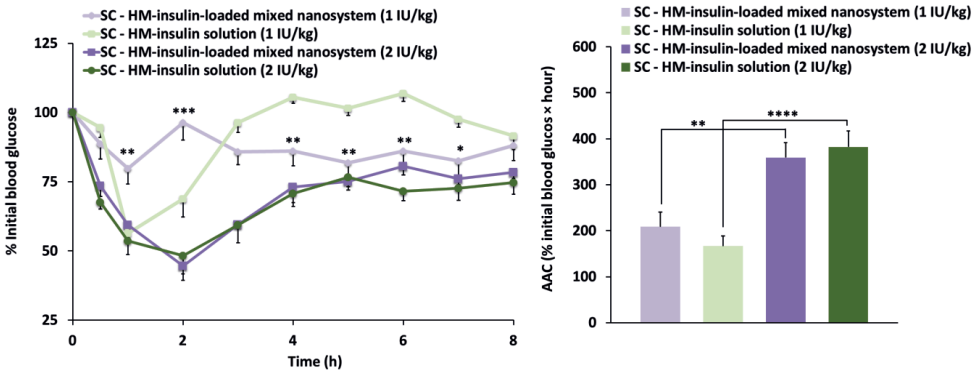



***Figure 18. Left:*** *Normalized hypoglycemic effect (blood glucose % of the initial) following subcutaneous (SC) administration of a saline HM-insulin solution and HM-insulin-loaded mixed nanosystem (NE + micelles) at both 1 (n = 8) and 2 IU/kg body weight (n = 13) to healthy rats (Mean ± SEM) (Two-way ANOVA followed by a Fisher's LSD test were applied for the statistical analysis; significance levels comparing to the HM-insulin solution at the same concentration *p ≤ 0.05; **p ≤ 0.01; ***p ≤ 0.005).* ***Right:*** *Area above the curve at time = 8 h calculated by establishing 120 % as upper limit (% initial blood glucose × hour) (Mean ± SEM) (One-way ANOVA followed by a Fisher's LSD test were applied for the statistical analysis; significance levels **p ≤ 0.01; ****p ≤ 0.0001).*

### 3.7.2.1.2. Effect on blood glucose levels following intrajejunal (IJ) administration of 100 IU/kg of HM-insulin-loaded mixed nanosystem to healthy rats

Firstly, we performed a preliminary *in vivo* study aimed at exploring the influence of the site of administration, intraduodenal vs. intrajejunal on the hypoglycemic effect. As expected [31], the results indicated that there were no differences in the glucose levels following both modalities of administration (data not shown).

Based on these preliminary results and the dose-response effect previously observed in *Section 3.7.2.1.1.*, the HM-insulin-loaded mixed nanosystem was intrajejunally administered (IJ) (100 IU/kg body weight) to healthy rats, using the blank mixed nanosystem (IJ) and a saline HM-insulin solution (SC) (2 IU/kg body weight) as negative and positive controls respectively. *Figure 19* shows the blood glucose levels monitored for up to 8 hours post-administration and normalized respect to the glucose baseline level (measured 30 min prior to the treatments administration). A slight hypoglycemic effect, which was significant different ($p \leq 0.05$) respect to the control (≈ 20 %), was observed at 1 and 4 hours post-administration (*Figure 19, left*), although, no significant differences were found in the overall response, represented as AAC after 8 hours (*Figure 19, right*).

These results are comparable to those previously reported and performed under similar conditions [28,31,48,102], although higher hypoglycemic responses have also been reported for non-modified insulin under different experimental conditions (i.e., intraileal administration, long fasting period, anesthesia, glucose exogenously overload) [103–107]. The conclusion from this study was that the experimental conditions may significantly affect the intensity of the hypoglycemic response and, hence, a second study was planned to further investigate the response to the developed formulation.

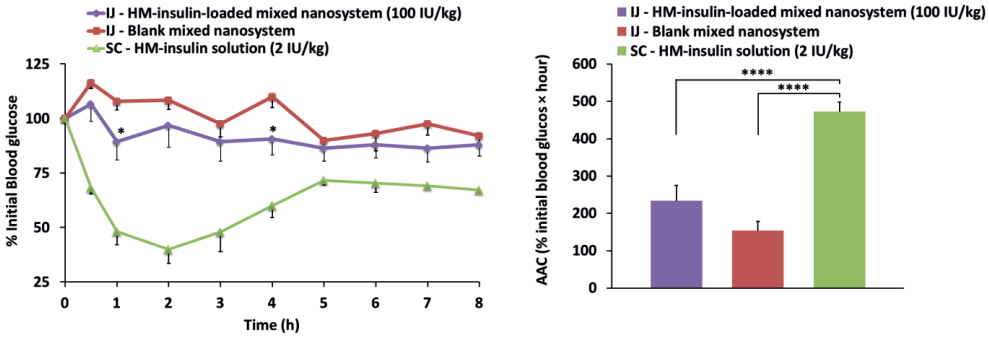



***Figure 19. Left:*** *Normalized hypoglycemic effect (blood glucose % of the initial) following intrajejunal (IJ) administration of HM-insulin-loaded mixed nanosystem (n = 8) at 100 IU/kg, blank mixed nanosystem (n = 6) and subcutaneous (SC) administration of a saline HM-insulin solution (n = 6) at 2 IU/kg to healthy rats (Mean ± SEM) (Two-way ANOVA followed by a Fisher's LSD test were applied for the statistical analysis; significance levels *p ≤ 0.05);* ***Right:*** *Area above the curve at time = 8 h calculated by establishing 120 % as upper limit (% initial blood glucose × hour) (Mean ± SEM) (One-way ANOVA followed by a Fisher's LSD test were applied for the statistical analysis; significance levels ****p ≤ 0.0001).*

### 3.7.2.2. Diabetic rats

#### 3.7.2.2.1. Effect on blood glucose levels following intraduodenal (ID) administration of 100 IU/kg of HM-insulin-loaded mixed nanosystem to diabetic rats

The efficacy of the formulation was also evaluated in a diabetic rat model. For this purpose, the HM-insulin-loaded mixed nanosystem was intraduodenally administered (ID) (100 IU/kg body weight) to diabetic rats, using the blank mixed nanosystem (ID) and a saline HM-insulin solution (SC) (2 IU/kg body weight) as negative and positive controls respectively. Blood glucose levels were monitored up to 8 hours post-administration and

values were normalized respect to the glucose baseline level (measured 30 min prior to the treatments administration) considered as 100 %.

The results presented in *Figure 20* indicate that the intraduodenal administration of the HM-insulin-loaded mixed nanosystem triggered a significant hypoglycemic response (≈ 30 %) compared to the control (intradudenally administered blank mixed nanosystem) at 1 ($p \leq 0.05$), 2, 4 and 5 ($p \leq 0.01$) hours post-administration. Statistically significant differences ($p \leq 0.01$) were also found in the overall response, represented as AAC after 8 hours (*Figure 20, right*), between the HM-insulin-loaded mixed nanosystem (ID) and the blank mixed nanosystem (ID), which further substantiates the hypothesis claiming that the lack of auto-regulation phenomenon suppressing the secretion of endogenous insulin and the β−cell deficiency become these animals much more insulin-sensitive [103,104] and correlates with the fact that the majority of positive hypoglycemic responses reported up to now have been achieved using either anesthetized or diabetic rats [48,101].

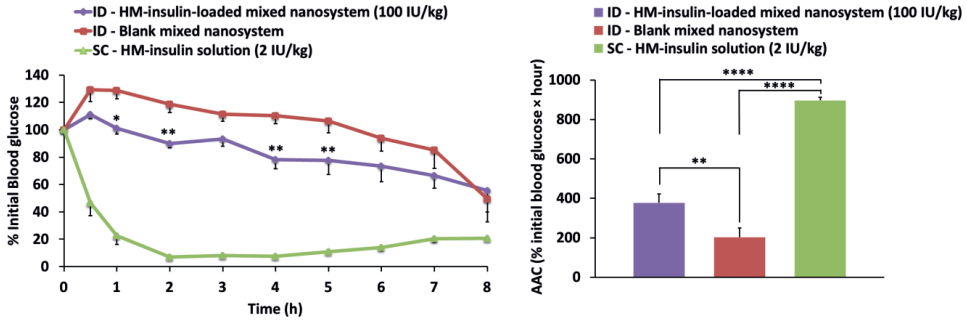



***Figure 20. Left:*** *Normalized hypoglycemic effect (blood glucose % of the initial) following intraduodenal (ID) administration of HM-insulin-loaded mixed nanosystem (n = 8) at 100 IU/kg, blank mixed nanosystem (n = 7) and subcutaneous (SC) administration of a HM-insulin solution (n = 6) at 2 IU/kg to diabetic rats. (Mean ± SEM) (Two-way ANOVA followed by a Fisher's LSD test were applied for the statistical analysis; significance levels *p ≤ 0.05; **p ≤ 0.01);* ***Right:*** *Area above the curve at time = 8 h calculated by establishing 130 % as upper limit (% initial blood glucose × hour) (Mean ± SEM) (One-way ANOVA followed by a Fisher's LSD test were applied for the statistical analysis; significance levels **p ≤ 0.01; ****p ≤ 0.0001).*

Overall, the results suggest that the mixed nanosystem was able to protect a portion of the HM-insulin intraduodenally administered from the degradation and allowed its intestinal absorption, triggering, subsequently, a significant hypoglycemic response ($p \leq 0.01$). However, bearing in mind the rational design of this formulation, and its favorable properties displayed *in vitro*, we must admit that its performance was lower

than expected, a result that brings the difficult *in vitro–in vivo* correlation to light. In this regard, we hypothesize that the *in vivo* conditions are slightly harsher and wanted to emphasize the importance of standardizing experimental protocols to obtain more predictive values *in vitro* and facilitate the comparison among different formulations.

## 4. Conclusions

Herein, a new formulation consisting of a mixture of nanoemulsion and micelles was designed, developed and fully characterized, by rationally selecting biomaterials with stabilizing, penetration and mucodiffusive properties. A hydrophobically modified insulin was used as model peptide to assess the ability of the nanosystem to successfully deliver peptides orally. The HM-loaded mixed nanosystem exhibited *in vitro* appropriate properties, such as good stability, mucodiffusion, cell interaction and uptake without cytotoxic effects, which reinforced the interest of its further *in vivo* evaluation. *In vivo* biodistribution showed the potential of this formulation to interact with the intestinal epithelium. Following its intraduodenal administration, a significant, but moderate hypoglycemic response was observed *in vivo*. Overall, despite the promising properties displayed by the formulation here disclosed and the significant effect observed *in vivo*, the *in vitro–in vivo* correlation when referring to the rational design of oral peptide delivery formulations remains still a challenge.

## References

[1] S.S. Usmani, G. Bedi, J.S. Samuel, S. Singh, S. Kalra, P. Kumar, A.A. Ahuja, M. Sharma, A. Gautam, G.P.S. Raghava, THPdb: Database of FDA-approved peptide and protein therapeutics, PLoS One. 12 (2017). doi:10.1371/journal.pone.0181748.

[2] S.S. Kulkarni, J. Sayers, B. Premdjee, R.J. Payne, Rapid and efficient protein synthesis through expansion of the native chemical ligation concept, Nat. Rev. Chem. 2 (2018) 0122. doi:10.1038/s41570-018-0122.

[3] T.A.S. Aguirre, D. Teijeiro-Osorio, M. Rosa, I.S. Coulter, M.J. Alonso, D.J. Brayden, Current status of selected oral peptide technologies in advanced preclinical development and in clinical trials, Adv. Drug Deliv. Rev. 106 (2016) 223–241. doi:10.1016/j.addr.2016.02.004.

[4] C. Liu, Y. Kou, X. Zhang, H. Cheng, X. Chen, S. Mao, Strategies and industrial perspectives to improve oral absorption of biological macromolecules, Expert Opin. Drug Deliv. 15 (2018) 223–233. doi:10.1080/17425247.2017.1395853.

[5] S. Mitragotri, P.A. Burke, R. Langer, Overcoming the challenges in administering biopharmaceuticals: formulation and delivery strategies, Nat Rev Drug Discov. 13 (2014) 655–672. doi:10.1038/nrd4363.

[6] M. Berger, Oral insulin 1922–1992: the history of continuous ambition and failure, in: B. M, G. FA (Eds.), Front. Insul. Pharmacol., Germany: Thieme Publishing Group, 1993: pp. 144–148.

[7] L. Heinemann, Y. Jacques, Oral Insulin and Buccal Insulin: A Critical Reappraisal, J. Diabetes Sci. Technol. 3 (2009) 568–584. doi:10.1177/193229680900300323.

[8] E. Arbit, The physiological rationale for oral insulin administration, Diabetes Technol. Ther. 6 (2004) 510–517. doi:10.1089/1520915041705929.

[9] A. Sood, R. Panchagnula, Peroral route: An opportunity for protein and peptide drug delivery, Chem. Rev. 101 (2001) 3275–3303. doi:10.1021/cr000700m.

[10] J. Wang, V. Yadav, A.L. Smart, S. Tajiri, A.W. Basit, Toward oral delivery of biopharmaceuticals: An assessment of the gastrointestinal stability of 17 peptide drugs, Mol. Pharm. 12 (2015) 966–973. doi:10.1021/mp500809f.

[11] M. Morishita, N.A. Peppas, Is the oral route possible for peptide and protein drug delivery?, Drug Discov. Today. 11 (2006) 905–910. doi:10.1016/j.drudis.2006.08.005.

[12] G. Camenisch, J. Alsenz, H. Van De Waterbeemd, G. Folkers, Estimation of permeability by passive diffusion through Caco-2 cell monolayers using the drugs' lipophilicity and molecular weight, Eur. J. Pharm. Sci. 6 (1998) 313–319. doi:10.1016/S0928-0987(97)10019-7.

[13] W. Rubas, M.E.M. Cromwell, Z. Shahrokh, J. Villagran, T.N. Nguyen, M. Wellton, T.H. Nguyen, R.J. Mrsny, Flux measurements across Caco-2 monolayers may predict transport in human large intestinal tissue, J. Pharm. Sci. 85 (1996) 165–169. doi:10.1021/js950267+.

[14] M. Bendayan, E. Ziv, D. Gingras, R. Ben-Sasson, H. Bar-On, M. Kidron, Biochemical and morpho-cytochemical evidence for the intestinal absorption of insulin in control and diabetic rats. Comparison between the effectiveness of duodenal and colon mucosa, Diabetologia. 37 (1994) 119–126. doi:10.1007/s001250050081.

[15] D.S. Pisal, M.P. Kosloski, S. V. Balu-Iyler, Delivery of therapeutic proteins, J. Pharm. Sci. 99 (2010) 2557–2575. doi:10.1002/jps.22054.

[16] C.F. Van Der Walle, O. Olejnik, An overview of the field of peptide and protein delivery, in: C.F. Van Der Walle (Ed.), Pept. Protein Deliv., First, Academic Press, 2011: pp. 1–22. doi:10.1016/b978-0-12-384935-9.10001-x.

[17] B.J. Bruno, G.D. Miller, C.S. Lim, Basics and recent advances in peptide and protein drug delivery, Ther. Deliv. 4 (2013) 1443–1467. doi:10.4155/tde.13.104.

[18] K. Mg, Krenn V, F. Huebner, W. Wagner, Resch R, History and possible uses of nanomedicine based on nanoparticles and nanotechnological progress, J Nanomed Nanotechnol. 64172 (2015) 3362157–7439. doi:10.4172/2157-7439.1000336.

[19] I. Santalices, A. Gonella, D. Torres, M.J. Alonso, Advances on the formulation of proteins using nanotechnologies, J. Drug Deliv. Sci. Technol. 42 (2017) 155–180. doi:10.1016/j.jddst.2017.06.018.

[20] T. Karamanidou, V. Bourganis, O. Kammona, C. Kiparissides, Lipid-based nanocarriers for the oral administration of biopharmaceutics, Nanomedicine. 11 (2016) 3009–3032. doi:10.2217/nnm-2016-0265.

[21] Z. Niu, I. Conejos-Sánchez, B.T. Griffin, C.M. O'Driscoll, M.J. Alonso, Lipid-based nanocarriers for oral peptide delivery, Adv. Drug Deliv. Rev. 106 (2016) 337–354. doi:10.1016/j.addr.2016.04.001.

[22] M. Garcia-Fuentes, D. Torres, M.J. Alonso, New surface-modified lipid nanoparticles as delivery vehicles for salmon calcitonin, Int. J. Pharm. 296 (2005) 122–132. doi:10.1016/j.ijpharm.2004.12.030.

[23] M. Garcia-Fuentes, C. Prego, D. Torres, M.J. Alonso, A comparative study of the potential of solid triglyceride nanostructures coated with chitosan or poly(ethylene glycol) as carriers for oral calcitonin delivery, Eur. J. Pharm. Sci. 25 (2005) 133–143. doi:10.1016/j.ejps.2005.02.008.

[24] C. Prego, D. Torres, E. Fernandez-Megia, R. Novoa-Carballal, E. Quiñoá, M.J. Alonso, Chitosan-PEG nanocapsules as new carriers for oral peptide delivery: effect of chitosan pegylation degree, J. Control. Release. 111 (2006) 299–308. doi:10.1016/j.jconrel.2005.12.015.

[25] C. Prego, D. Torres, M.J. Alonso, Chitosan nanocapsules as carriers for oral peptide delivery: effect of chitosan molecular weight and type of salt on the in vitro behaviour and in vivo effectiveness, J. Nanosci. Nanotechnol. 6 (2006) 2921–2928. doi:10.1166/jnn.2006.429.

[26] C. Prego, M. Fabre, D. Torres, M.J. Alonso, Efficacy and mechanism of action of chitosan nanocapsules for oral peptide delivery, Pharm. Res. 23 (2006) 549–556. doi:10.1007/s11095-006-9570-8.

[27] I. Santalices, D. Torres, M.V. Lozano, M.M. Arroyo-Jiménez, M.J. Alonso, M.J. Santander-Ortega, Influence of the surface properties of nanocapsules on their interaction with intestinal barriers, Submitt. to Eur. J. Pharm. Biopharm. (2018).

[28] Z. Niu, E. Tedesco, F. Benetti, A. Mabondzo, I.M. Montagner, I. Marigo, D. Gonzalez-Touceda, S. Tovar, C. Diéguez, M.J. Santander-Ortega, M.J. Alonso, Rational design of polyarginine nanocapsules intended to help peptides overcoming intestinal barriers, J. Control. Release. 263 (2016) 4–17. doi:10.1016/j.jconrel.2017.02.024.

[29] G. Lollo, A. Gonzalez-Paredes, M. Garcia-Fuentes, P. Calvo, D. Torres, M.J. Alonso, Polyarginine nanocapsules as a potential oral peptide delivery carrier, J. Pharm. Sci. 106 (2017) 611–618. doi:10.1016/j.xphs.2016.09.029.

[30] A. Gonzalez-Paredes, D. Torres, M.J. Alonso, Polyarginine nanocapsules: A versatile nanocarrier with potential in transmucosal drug delivery, Int. J. Pharm. 529 (2017) 474–485. doi:10.1016/j.ijpharm.2017.07.001.

[31] L.N. Thwala, A. Beloqui, N.S. Csaba, D. González-Touceda, S. Tovar, C. Dieguez, M.J. Alonso, V. Préat, The interaction of protamine nanocapsules with the intestinal epithelium: a mechanistic approach, J. Control. Release. 243 (2016) 109–120. doi:10.1016/j.jconrel.2016.10.002.

[32] P. Jakubiak, L.N. Thwala, A. Cadete-Pires, V. Préat, M.J. Alonso, A. Beloqui, N. Csaba, Solvent-free protamine nanocapsules as carriers for mucosal delivery of therapeutics, Eur. Polym. J. In Press (2017). doi:10.1016/j.eurpolymj.2017.03.049.

[33] G. Sharma, K. Wilson, C.F. van der Walle, N. Sattar, J.R. Petrie, M.N.V. Ravi Kumar, Microemulsions for oral delivery of insulin: design, development and evaluation in streptozotocin induced diabetic rats, Eur. J. Pharm. Biopharm. 76 (2010) 159–169. doi:10.1016/j.ejpb.2010.07.002.

[34] E. Ma, H. Ma, Z. Liu, C. Zheng, M. Duan, In vitro and in vivo evaluation of a novel oral insulin formulation, Acta Pharmacol. Sin. 27 (2006) 1382–1388. doi:10.1111/j.1745-7245.2006.00424.x.

[35] A. Silva-Cunha, J.L. Grossiord, F. Puisieux, M. Seiller, W/O/W multiple emulsions of insulin containing a protease inhibitor and an absorption enhancer: preparation, characterization and determination of stability towards proteases in vitro, Int. J. Pharm. 158 (1997) 79–89. doi:10.1016/S0378-5173(97)00249-4.

[36] A. Elsayed, M. Al Remawi, N. Qinna, A. Farouk, A. Badwan, Formulation and characterization of an oily-based system for oral delivery of insulin, Eur. J. Pharm. Biopharm. 73 (2009) 269–279. doi:10.1016/j.ejpb.2009.06.004.

[37] T. Karamanidou, K. Karidi, V. Bourganis, K. Kontonikola, O. Kammona, C. Kiparissides, Effective incorporation of insulin in mucus permeating self-nanoemulsifying drug delivery systems, Eur. J. Pharm. Biopharm. 97 (2015) 223–229. doi:10.1016/j.ejpb.2015.04.013.

[38] F. Hintzen, G. Perera, S. Hauptstein, C. Müller, F. Laffleur, A. Bernkop-Schnürch, In vivo evaluation of an oral self-microemulsifying drug delivery system (SMEDDS) for leuprorelin, Int. J. Pharm. 472 (2014) 20–26. doi:10.1016/j.ijpharm.2014.05.047.

[39] K.A. Traul, A. Driedger, D.L. Ingle, D. Nakhasi, Review of the toxicologic properties of medium-chain triglycerides, Food Chem. Toxicol. 38 (2000) 79–98. doi:10.1016/S0278-6915(99)00106-4.

[40] B. Marten, M. Pfeuffer, J. Schrezenmeir, Medium-chain triglycerides, Int. Dairy J. 16 (2006) 1374–1382. doi:10.1016/j.idairyj.2006.06.015.

[41] M. Tobío, A. Sánchez, A. Vila, I. Soriano, C. Evora, J.. J. Vila-Jato, M.. M. Alonso, The role of PEG on the stability in digestive fluids and in vivo fate of PEG-PLA nanoparticles following oral administration, Colloids Surfaces B Biointerfaces. 18 (2000) 315–323. doi:10.1016/S0927-7765(99)00157-5.

[42] M. Wulff-Pérez, J. de Vicente, A. Martín-Rodríguez, M.J. Gálvez-Ruiz, Controlling lipolysis through

steric surfactants: new insights on the controlled degradation of submicron emulsions after oral and intravenous administration, Int. J. Pharm. 423 (2012) 161–166. doi:10.1016/j.ijpharm.2011.12.025.

[43] L.M. Ensign, R. Cone, J. Hanes, Oral drug delivery with polymeric nanoparticles: the gastrointestinal mucus barriers, Adv. Drug Deliv. Rev. 64 (2012) 557–570. doi:10.1016/j.addr.2011.12.009.

[44] A. Vila, H. Gill, O. McCallion, M.J. Alonso, Transport of PLA-PEG particles across the nasal mucosa: Effect of particle size and PEG coating density, J. Control. Release. 98 (2004) 231–244. doi:10.1016/j.jconrel.2004.04.026.

[45] Q. Xu, L.M. Ensign, N.J. Boylan, A. Schön, X. Gong, J.C. Yang, N.W. Lamb, S. Cai, T. Yu, E. Freire, J. Hanes, Impact of surface polyethylene glycol (PEG) density on biodegradable nanoparticle transport in mucus ex vivo and distribution in vivo, ACS Nano. 9 (2015) 9217–9227. doi:10.1021/acsnano.5b03876.

[46] D. Chen, D. Xia, X. Li, Q. Zhu, H. Yu, C. Zhu, Y. Gan, Comparative study of Pluronic® F127-modified liposomes and chitosan-modified liposomes for mucus penetration and oral absorption of cyclosporine A in rats, Int. J. Pharm. 449 (2013) 1–9. doi:10.1016/j.ijpharm.2013.04.002.

[47] M. Niu, Y. Tan, P. Guan, L. Hovgaard, Y. Lu, J. Qi, R. Lian, X. Li, W. Wu, Enhanced oral absorption of insulin-loaded liposomes containing bile salts: A mechanistic study, Int. J. Pharm. 460 (2014) 119–130. doi:10.1016/j.ijpharm.2013.11.028.

[48] M. Niu, Y. Lu, L. Hovgaard, P. Guan, Y. Tan, R. Lian, J. Qi, W. Wu, Hypoglycemic activity and oral bioavailability of insulin-loaded liposomes containing bile salts in rats: The effect of cholate type, particle size and administered dose, Eur. J. Pharm. Biopharm. 81 (2012) 265–272. doi:10.1016/j.ejpb.2012.02.009.

[49] C. Chen, T. Fan, Y. Jin, Z. Zhou, Y. Yang, X. Zhu, Z. Zhang, Q. Zhang, Y. Huang, Orally delivered salmon calcitonin-loaded solid lipid nanoparticles prepared by micelle–double emulsion method via the combined use of different solid lipids, Nanomedicine. 8 (2013) 1085–1100. doi:10.2217/nnm.12.141.

[50] J. Liu, T. Gong, C. Wang, Z. Zhong, Z. Zhang, Solid lipid nanoparticles loaded with insulin by sodium cholate-phosphatidylcholine-based mixed micelles: preparation and characterization, Int. J. Pharm. 340 (2007) 153–162. doi:10.1016/j.ijpharm.2007.03.009.

[51] S. Sun, N. Liang, H. Piao, H. Yamamoto, Y. Kawashima, F. Cui, Insulin-S.O (sodium oleate) complex-loaded PLGA nanoparticles: Formulation, characterization and *in vivo* evaluation, J. Microencapsul. 27 (2010) 471–478. doi:10.3109/02652040903515490.

[52] S. Hu, M. Niu, F. Hu, Y. Lu, J. Qi, Z. Yin, W. Wu, Integrity and stability of oral liposomes containing bile salts studied in simulated and ex vivo gastrointestinal media, Int. J. Pharm. 441 (2013) 693–700. doi:10.1016/j.ijpharm.2012.10.025.

[53] P. Calvo, C. Remuñán-López, J.L. Vila-Jato, M.J. Alonso, Development of positively charged colloidal drug carriers: chitosan-coated polyester nanocapsules and submicron-emulsions, Colloid Polym. Sci. 275 (1997) 46–53. doi:10.1007/s003960050050.

[54] V. Francisco, N. Basilio, L. Garcia-Rio, J.R. Leis, E.F. Marques, C. Vázquez-Vázquez, Novel catanionic vesicles from calixarene and single-chain surfactant, Chem. Commun. 46 (2010) 6551. doi:10.1039/c0cc01806f.

[55] Y.A. Attia, C. Vázquez-Vázquez, M.C. Blanco, D. Buceta, M.A. López-Quintela, Gold nanorod synthesis catalysed by Au clusters, Faraday Discuss. 191 (2016) 205–213. doi:10.1039/C6FD00015K.

[56] E. Jantratid, N. Janssen, C. Reppas, J.B. Dressman, Dissolution media simulating conditions in the proximal human gastrointestinal tract: An update, Pharm. Res. 25 (2008) 1663–1676. doi:10.1007/s11095-008-9569-4.

[57] E. Roger, F. Lagarce, J.P. Benoit, The gastrointestinal stability of lipid nanocapsules, Int. J. Pharm. 379 (2009) 260–265. doi:10.1016/j.ijpharm.2009.05.069.

[58] S. Klein, The use of biorelevant dissolution media to forecast the in vivo performance of a drug, AAPS J. 12 (2010) 397–406. doi:10.1208/s12248-010-9203-3.

[59] E.L. McConnell, A.W. Basit, S. Murdan, Measurements of rat and mouse gastrointestinal pH, fluid and lymphoid tissue, and implications for in-vivo experiments, J. Pharm. Pharmacol. 60 (2008) 63–70. doi:10.1211/jpp.60.1.0008.

[60] E. Zagato, K. Forier, T. Martens, K. Neyts, J. Demeester, S. De Smedt, K. Remaut, K. Braeckmans, Single-particle tracking for studying nanomaterial dynamics: applications and fundamentals in drug delivery, Nanomedicine. 9 (2014) 913–927. doi:10.2217/nnm.14.43.

[61] B.S. Schuster, L.M. Ensign, D.B. Allan, J.S. Suk, J. Hanes, Particle tracking in drug and gene delivery research: state-of-the-art applications and methods, Adv. Drug Deliv. Rev. 91 (2015) 70–91. doi:10.1016/j.addr.2015.03.017.

[62] J. Suh, M. Dawson, J. Hanes, Real-time multiple-particle tracking: Applications to drug and gene delivery, Adv. Drug Deliv. Rev. 57 (2005) 63–78. doi:10.1016/j.addr.2004.06.001.

[63] R. Metzler, J. Klafter, The random walk's guide to anomalous diffusion: A fractional dynamics approach, Phys. Rep. 339 (2000) 1–77. doi:10.1016/S0370-1573(00)00070-3.

[64] T. Riss, R. Moravec, A. Niles, S. Duellman, H. Benink, T. Worzella, L. Minor, Cell Viability Assays, in: Assay Guid. Man. [Internet], Bethesda (MD): Eli Lilly & Company and the National Center for Advancing Translational Sciences, n.d.

[65] F. Antunes, F. Andrade, F. Araújo, D. Ferreira, B. Sarmento, Establishment of a triple co-culture in vitro cell models to study intestinal absorption of peptide drugs, Eur. J. Pharm. Biopharm. 83 (2013) 427–435. doi:10.1016/j.ejpb.2012.10.003.

[66] A. des Rieux, V. Fievez, I. Théate, J. Mast, V. Préat, Y.J. Schneider, An improved in vitro model of human intestinal follicle-associated epithelium to study nanoparticle transport by M cells, Eur. J. Pharm. Sci. 30 (2007) 380–391. doi:10.1016/j.ejps.2006.12.006.

[67] The human protein atlas, (n.d.). https://www.proteinatlas.org/ENSG00000171105-INSR/cell (accessed February 27, 2017).

[68] K.A. Dooley, S. Millinder, T.F. Osborne, Sterol regulation of 3-hydroxy-3-methylglutaryl-coenzyme A synthase gene through a direct interaction between sterol regulatory element binding protein and the trimeric CCAAT-binding factor/nuclear factor Y, J. Biol. Chem. 273 (1998) 1349–1356. doi:10.1074/jbc.273.3.1349.

[69] J.R. Smith, T.F. Osborne, M.S. Brown, J.L. Goldstein, G. Gil, Multiple sterol regulatory elements in promoter for hamster 3-hydroxy-3-methylglutaryl-coenzyme A synthase, J. Biol. Chem. 263 (1988)

18480–18487.

[70] I.R. Harris, H. Höppner, W. Siefken, A.M. Farrell, K.P. Wittern, Regulation of HMG-CoA synthase and HMG-CoA reductase by insulin and epidermal growth factor in HaCaT keratinocytes, J. Invest. Dermatol. 114 (2000) 83–87. doi:10.1046/j.1523-1747.2000.00822.x.

[71] S.B. Bravo, M.E.R. Garcia-Rendueles, S. Perez-Romero, J. Cameselle Teijeiro, J.S. Rodrigues, F. Barreiro, C. V. Alvarez, Expression of exogenous proteins and short hairpin RNAs in human primary thyrocytes, Anal. Biochem. 400 (2010) 219–228. doi:10.1016/j.ab.2010.01.034.

[72] C. Prego, M. García, D. Torres, M.J. Alonso, Transmucosal macromolecular drug delivery, J. Control. Release. 101 (2005) 151–162. doi:10.1016/j.jconrel.2004.07.030.

[73] L.N. Thwala, Protamine nanocapsules as carriers for oral peptide delivery, University of Santiagode de Compostela; University Catholique de Louvain, 2016.

[74] M. Tobío, R. Gref, A. Sanchez, R. Langer, M.J. Alonso, Stealth PLA-PEG nanoparticles as protein carriers for nasal administration, Pharm. Res. 15 (1998) 270–275. doi:10.1023/A:1011922819926.

[75] M. Plaza-Oliver, J. Fernández Sainz de Baranda, V. Rodríguez Robledo, L. Castro-Vázquez, J. Gonzalez-Fuentes, P. Marcos, M. V. Lozano, M.J. Santander-Ortega, M.M. Arroyo-Jimenez, Design of the interface of edible nanoemulsions to modulate the bioaccessibility of neuroprotective antioxidants, Int. J. Pharm. 490 (2015) 209–218. doi:10.1016/j.ijpharm.2015.05.031.

[76] E. Van Der Pol, F.A.W. Coumans, A. Sturk, R. Nieuwland, T.G. Van Leeuwen, Refractive index determination of nanoparticles in suspension using nanoparticle tracking analysis, Nano Lett. 14 (2014) 6195–6201. doi:10.1021/nl503371p.

[77] Z. Sezgin, N. Yüksel, T. Baykara, Preparation and characterization of polymeric micelles for solubilization of poorly soluble anticancer drugs, Eur. J. Pharm. Biopharm. 64 (2006) 261–268. doi:10.1016/j.ejpb.2006.06.003.

[78] J.A. Bernate, Vector chromatography of suspendedparticles in 1D-periodic systems, ProQuest LLC, 2012.

[79] L. Vukovic, F.A. Khatib, S.P. Drake, A. Madriaga, K.S. Brandenburg, P. Král, H. Onyuksel, Structure and Dynamics of Highly PEG-ylated Sterically Stabilized Micelles in Aqueous Media Petr Kr, J. Am. Chem. Soc. 133 (2011) 13481–13488. doi:10.1021/ja204043b.

[80] A. Torcello-Gómez, J. Maldonado-Valderrama, J. de Vicente, M.A. Cabrerizo-Vílchez, M.J. Gálvez-Ruiz, A. Martín-Rodríguez, Investigating the effect of surfactants on lipase interfacial behaviour in the presence of bile salts, Food Hydrocoll. 25 (2011) 809–816. doi:10.1016/j.foodhyd.2010.09.007.

[81] M. Kastantin, B. Ananthanarayanan, P. Karmali, E. Ruoslahti, M. Tirrell, Effect of the lipid chain melting transition on the stability of DSPE- PEG(2000) micelles, Langmuir. 25 (2009) 7279–7286. doi:10.1021/la900310k.

[82] H. Takeuchi, Y. Matsui, H. Sugihara, H. Yamamoto, Y. Kawashima, Effectiveness of submicron-sized, chitosan-coated liposomes in oral administration of peptide drugs, Int. J. Pharm. 303 (2005) 160–170. doi:10.1016/j.ijpharm.2005.06.028.

[83] R. Holm, A. Mu̎llertz, H. Mu, Bile salts and their importance for drug absorption, Int. J. Pharm. 453 (2013) 44–55. doi:10.1016/j.ijpharm.2013.04.003.

[84] T.S. Wiedmann, W. Liang, L. Kamel, Solubilization of drugs by physiological mixtures of bile salts, Pharm. Res. 19 (2002) 1203–1208. doi:10.1023/A:1019858428449.

[85] A.C. Groo, F. Lagarce, Mucus models to evaluate nanomedicines for diffusion, Drug Discov. Today. 19 (2014) 1097–1108. doi:10.1016/j.drudis.2014.01.011.

[86] M.J. Santander-Ortega, M. Plaza-Oliver, V. Rodríguez-Robledo, L. Castro-Vázquez, N. Villaseca-González, J. González-Fuentes, E.L. Cano, P. Marcos, M. V. Lozano, M.M. Arroyo-Jiménez, PEGylated nanoemulsions for oral delivery: role of the inner core on the final fate of the formulation, Langmuir. 33 (2017) 4269–4279. doi:10.1021/acs.langmuir.7b00351.

[87] F. Araújo, B. Sarmento, Towards the characterization of an in vitro triple co-culture intestine cell model for permeability studies, Int. J. Pharm. 458 (2013) 128–134. doi:10.1016/j.ijpharm.2013.10.003.

[88] F. Araújo, C. Pereira, J. Costa, C. Barrias, P.L. Granja, B. Sarmento, In vitro M-like cells genesis through a tissue-engineered triple-culture intestinal model, J. Biomed. Mater. Res. - Part B Appl. Biomater. 104 (2016) 782–788. doi:10.1002/jbm.b.33508.

[89] D. Yang, D. Liu, M. Qin, B. Chen, S. Song, W. Dai, H. Zhang, X. Wang, Y. Wang, B. He, X. Tang, Q. Zhang, Intestinal mucin induces more endocytosis but less transcytosis of nanoparticles across enterocytes by triggering nano-clustering and strengthening the retrograde pathway, ACS Appl. Mater. Interfaces. (2018) acsami.7b19153. doi:10.1021/acsami.7b19153.

[90] C. Hilgendorf, H. Spahn-langguth, C.G. Regårdh, E. Lipka, Caco-2 versus Caco-2/HT29-MTX co-cultured cell lines: permeabilities via diffusion, inside- and outside-directed carrier-mediated transport, J. Pharm. Sci. 89 (2000) 63–75.

[91] I. Behrens, P. Stenberg, P. Artursson, T. Kissel, Transport of lipophilic drug molecules in a new mucus secreting cell culture model based on Ht-29 MTX cells, Pharm. Res. 18 (2001) 1138–1145.

[92] T. Lesuffleur, A. Barbat, E. Dussaulx, A. Zweibaum, Growth Adaptation to Methotrexate of HT-29 Human Colon Carcinoma Cells Is Associated with Their Ability to Differentiate into Columnar Absorptive and Mucus-secreting Cells, Cancer Res. 50 (1990) 6334–6343.

[93] F. Berhane, A. Fite, N. Daboul, W. Al-Janabi, Z. Msallaty, M. Caruso, M.K. Lewis, Z. Yi, M.P. Diamond, A.B. Abou-Samra, B. Seyoum, Plasma lactate levels increase during hperinsulinemic euglycemic clamp and oral glucose tolerance test, Diabetes Res. Clin. Pract. 2015 (2015) Article ID 102054. doi:10.1016/S0168-8227(14)70028-2.

[94] R.A. DeFronzo, Insulin resistance, lipotoxicity, type 2 diabetes and atherosclerosis: The missing links. The Claude Bernard Lecture 2009, Diabetologia. 53 (2010) 1270–1287. doi:10.1007/s00125-010-1684-1.

[95] R.A. Goodlad, C.Y. Lee, S.G. Gilbey, M.A. Ghatei, S.R. Bloom, Insulin and intestinal epithelial cell proliferation, Exp Physiol. 78 (1993) 697–705.

[96] E.E. Wheeler, D.N. Challacombe, The trophic action of growth hormone , insulin- like growth factor-I , and insulin on human duodenal mucosa cultured in vitro, Transplantation. 40 (1997) 57–60. doi:10.1136/gut.40.1.57.

[97] W.H. Hartl, D.H. Alpers, The trophic effects of substrate, insulin, and the route of administration on

protein synthesis and the preservation of small bowel mucosal mass in large mammals, Clin. Nutr. 30 (2011) 20–27. doi:10.1016/j.clnu.2010.03.002.

[98] D.J. Brayden, J. Gleeson, E.G. Walsh, A head-to-head multi-parametric high content analysis of a series of medium chain fatty acid intestinal permeation enhancers in Caco-2 cells, Eur. J. Pharm. Biopharm. 88 (2014) 830–839. doi:10.1016/j.ejpb.2014.10.008.

[99] M.C. Manning, G.J. Evans, R.W. Payne, Protein stability during bioprocessing, in: F. Jameel, S. Hershenson (Eds.), Formul. Process Dev. Strateg. Manuf. Biopharm., John Wiley & Sons, Inc., 2010: pp. 605–624. doi:10.1002/9780470595886.

[100] L. Inchaurraga, N. Martín-Arbella, V. Zabaleta, G. Quincoces, I. Peñuelas, J.M. Irache, In vivo study of the mucus-permeating properties of PEG-coated nanoparticles following oral administration, Eur. J. Pharm. Biopharm. 97 (2015) 280–289. doi:10.1016/j.ejpb.2014.12.021.

[101] N. Reix, A. Parat, E. Seyfritz, R. Van Der Werf, V. Epure, N. Ebel, L. Danicher, E. Marchioni, N. Jeandidier, M. Pinget, Y. Frère, S. Sigrist, In vitro uptake evaluation in Caco-2 cells and in vivo results in diabetic rats of insulin-loaded PLGA nanoparticles, Int. J. Pharm. 437 (2012) 213–220. doi:10.1016/j.ijpharm.2012.08.024.

[102] Z. Niu, E. Samaridou, E. Jaumain, J. Coëne, G. Ullio, N. Shrestha, J. Garcia, M. Durán-Lobato, S. Tovar, M.J. Santander-Ortega, M.V. Lozano, M.M. Arroyo-Jimenez, R. Ramos-Membrive, I. Peñuelas, A. Mabondzo, V. Préat, M. Teixidó, E. Giralt, M.J. Alonso, PEG-PGA enveloped octaarginine-peptide nanocomplexes: an oral peptide delivery strategy, J. Control. Release. 276 (2018) 125–139. doi:10.1016/j.jconrel.2018.03.004.

[103] C. Damge, C. Michel, M. Aprahamian, P. Couvreur, New approach for oral administration of insulin with polyalkylcyanoacrylate nanocapsules as drug carrier, Diabetes. 37 (1988) 246–251. doi:10.2337/diab.37.2.246.

[104] C. Damge, C. Michel, M. Aprahamian, P. Couvreur, J.P. Devissaguet, Nanocapsules as carriers for oral peptide delivery, J. Control. Release. 13 (1990) 233–239. doi:10.1016/0168-3659(90)90013-J.

[105] L. Yin, J. Ding, C. He, L. Cui, C. Tang, C. Yin, Drug permeability and mucoadhesion properties of thiolated trimethyl chitosan nanoparticles in oral insulin delivery, Biomaterials. 30 (2009) 5691–5700. doi:10.1016/j.biomaterials.2009.06.055.

[106] C. Michel, M. Aprahamian, L. Defontaine, P. Couvreur, C. Damgé, The effect of site of administration in the gastrointestinal tract on the absorption of insulin from nanocapsules in diabetic rats, J. Pharm. Pharmacol. 43 (1991) 1–5. doi:10.1111/j.2042-7158.1991.tb05437.x.

[107] M. Morishita, T. Goto, K. Nakamura, A.M. Lowman, K. Takayama, N.A. Peppas, Novel oral insulin delivery systems based on complexation polymer hydrogels: Single and multiple administration studies in type 1 and 2 diabetic rats, J. Control. Release. 110 (2006) 587–594. doi:10.1016/j.jconrel.2005.10.029.




# Overall discussion

USC
UNIVERSIDADE
DE SANTIAGO
DE COMPOSTELA

Despite the increasing number of therapeutic proteins and peptides, justified by their well-known advantages in terms of potency and selectivity, their efficient exploitation is being limited by their instability, restricted bioavailability and, in some cases, intrinsic immunogenicity [1]. In addition to these drawbacks, the limited patient compliance associated to the parenteral routes, which are nowadays the most commonly used for these drug products [2], and the fast body clearance of these macromolecules have stimulated the research in the area of drug delivery [3–5]. Among all the explored alternative routes, the oral route has attracted a great deal of attention since it is the most preferred by patients, especially for chronic treatments [6]. However, the oral administration is specially complex for peptides and proteins, since they are susceptible to degradation along the gastrointestinal tract (pH, ionic strength, enzymes) [7]. Additionally, the high hydrophilicity and large molecular weight inherent to peptidic molecules, limit their permeability across the intestinal mucosa [2,8,9]. In this line, the formulation of these macromolecules in a variety of nanovehicles made of biodegradable and biocompatible biomaterials has emerged as a valuable strategy to improve their bioavailability and allow their protection and modulated delivery [10–15]. Among them, lipid-based nanocarriers have been outlined as promising oral drug delivery carriers based on their biocompatibility and, also, on the stabilizing and absorption enhancing properties of their lipid constituents [16,17]. However, despite all the progress achieved in this field, the use of these nanosystems for the oral administration of peptides and proteins remains a challenge [17,18]. According to our view, research on the effect of the physicochemical properties and composition of the nanocarriers in their interaction with the intestinal tract, is still needed in order to understand the key properties driving the nanocarriers' performance after their oral administration.

Within this frame, the main objectives of this thesis have been to study how the composition and surface properties of a lipid-based nanocarrier can influence its potential to be used as oral peptide delivery platform (e.g., loading capacity, final fate and interaction with the gastrointestinal tract) and to rationally design and develop a new lipid-based nanosystem intended to the efficient oral delivery of peptides, using insulin as a model peptide drug. Starting from the basis that the efficient exploitation of lipid-based nanosystems as peptide delivery platforms is highly limited by the restricted liposolubility of these macromolecules, usually with strong hydrophilic character, a systematic study aimed at identifying the key factors affecting their physicochemical properties and ability to associate peptides was performed in a first step. For this purpose, chitosan nanocapsules (CS NCs) and insulin glulisine were respectively selected as model starting point lipid-based nanosystem and hydrophilic peptide, to investigate the effect of several

formulation parameters, such as the type and concentration of different components (e.g., oil, surfactants and polymers), on the final characteristics of the system.

Bearing in mind the influence of the nanocarriers' surface properties on their interaction with the surrounding medium, in a second part of this work, iwe selected specific compositions of NCs made of CS and polyarginine (PARG), previously developed by our research group, and the corresponding uncoated nanoemulsions (NEs), to systematically evaluate the effect of their surface composition on their capacity to overcome specific intestinal barriers. Namely, we evaluated nine different nanosystems for *i)* their stability, both colloidal and chemical, in simulated intestinal fluid and *ii)* their interaction (adhesion and diffusion) with mucus, while mimicking the physiological conditions.

As a last step, and taking advantage of the information generated from the previous studies, a novel lipid-based nanosystem intended to oral peptide delivery was rationally engineered through the selection and combination of lipids with different materials (e.g., surfactants, bile salts…) with stabilizing, mucodiffusive and permeation enhancing properties. As an outcome of this rational design, a mixed nanosystem consisting of a nanoemulsion and clusters of micelles was developed and its potential as oral insulin delivery system was extensively evaluated. Particularly, the mixed nanosystem was characterized in terms of *i)* stability and miscibility in simulated intestinal fluids with and without enzymes, *ii)* mucodiffusive properties, *iii)* ability to interact with the intestinal cells, *iv)* biodistribution following oral administration and *v)* potential to be used for the oral delivery of insulin in both healthy and diabetic rats.

## 1. Identification of the key factors affecting the physicochemical properties of lipid-based nanosystems and their ability to associate peptides

As commented above, the efficient exploitation of lipid-based nanosystems as peptide delivery platforms is highly limited by the restricted solubility of these macromolecules in this kind of vehicles. For this reason, we designed a systematic study aimed at identifying the key factors affecting the physicochemical properties and ability of CS NCs to associate peptides. For this purpose and bearing in mind the previous work developed by our group, we selected the main core components of previously reported protamine NCs [10] and CS as polymeric shell [19] to constitute the starting point CS NCs. A schematic representation of the organization of the initially selected components of these CS NCs is illustrated in *Figure 1 (upper panel)*. Insulin glulisine differs from human insulin in the amino acids present at the positions 3 and 29 of its B chain (asparagine and lysine were respectively

replaced by lysine and glutamic acid). This change in the amino acid composition, which was not supposed to significantly affect its association to the nanocarrier, has been found to facilitate the dissociation of insulin hexamers into dimers and monomers, thereby eliciting a fast action upon injection. Miglyol®812N, a medium chain caprylic/capric triglyceride was selected because of its permeation enhancing properties, and its expected role in terms of protecting the peptide cargo against enzymatic degradation [20,21]. PEGst40 was selected as a surfactant under the premise that its PEG moieties would be oriented towards the external aqueous phase, thereby enhancing the stability of the nanosystem against the enzymatic degradation [22–26] and promoting its mucodiffusion [25,27–30]. Sodium cholate (NaCh) was selected as co-surfactant because, apart from its penetration enhancing properties [31,32], it was expected to form hydrophobic ionic pairs with insulin [33–36], thereby enhancing its retention in the lipid core. Finally, CS was selected as a polymeric shell due to its biocompatibility and well-known mucoadhesive properties [37–40].

The physicochemical properties and insulin association efficiency of the resulting CS NCs are presented in *Figure 1 (lower panel)*. Despite the appropriate physicochemical properties (hydrodynamic mean size of 346 ± 13 nm, low polydispersity index (0.2) and positive ζ–potential of +34 ± 2 mV) of CS NCs, the insulin association efficiency (28 ± 6 %) was much lower than expected. Indeed, protamine NCs prepared under the same conditions exhibited an association efficiency of 62 ± 16 % [10]. These results, brought to light the importance of the type of polymer coating on this characteristic and the need of optimizing each nanosystem for the cargo it is intended to.

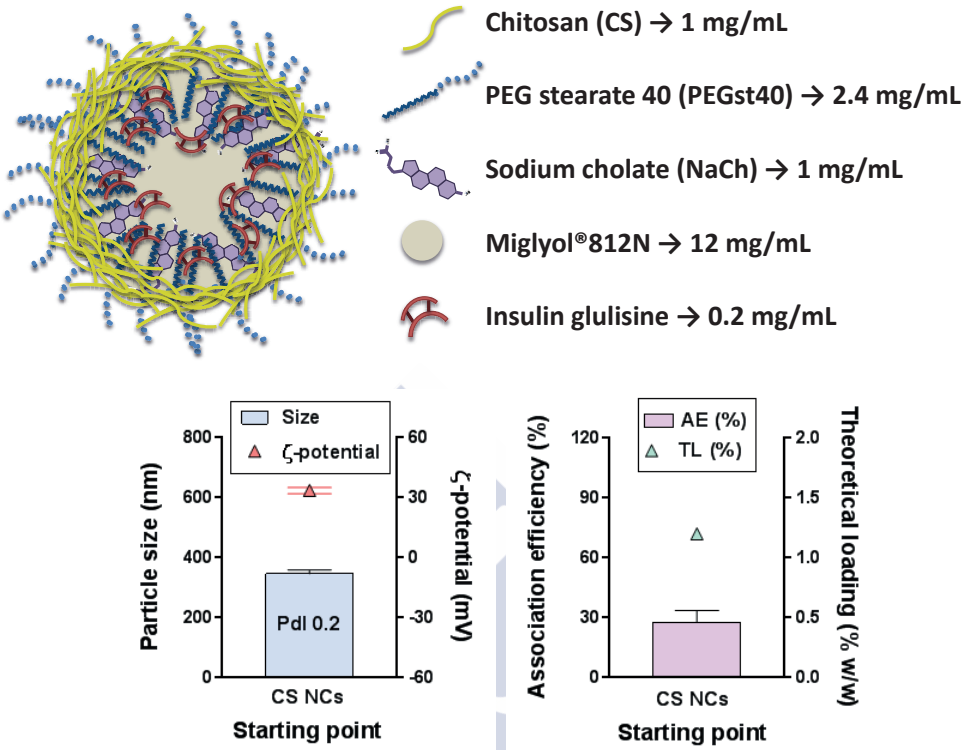



***Figure 1. Top:*** *Schematic representation and composition of the CS NCs used as screening starting point;* ***Bottom:*** *Physicochemical characterization (size, PdI and ζ-potential), insulin association efficiency (% AE) and theoretical loading (% TL) of these CS NCs (Mean ± SD, n ≥ 3).*

Accordingly, several formulation parameters, such as the type and concentration of different components (e.g., oil, main surfactant, bile salt and polymer), as well as the presence of an extra coating, were modified in a systematic way to study their influence on the physicochemical properties and insulin association efficiency of the selected prototype. *Figure 2* summarizes the modifications carried out on the nanosystem to finally end up in optimized CS NCs with appropriate physicochemical properties and insulin association efficiency (*Figure 2, lower panel*).

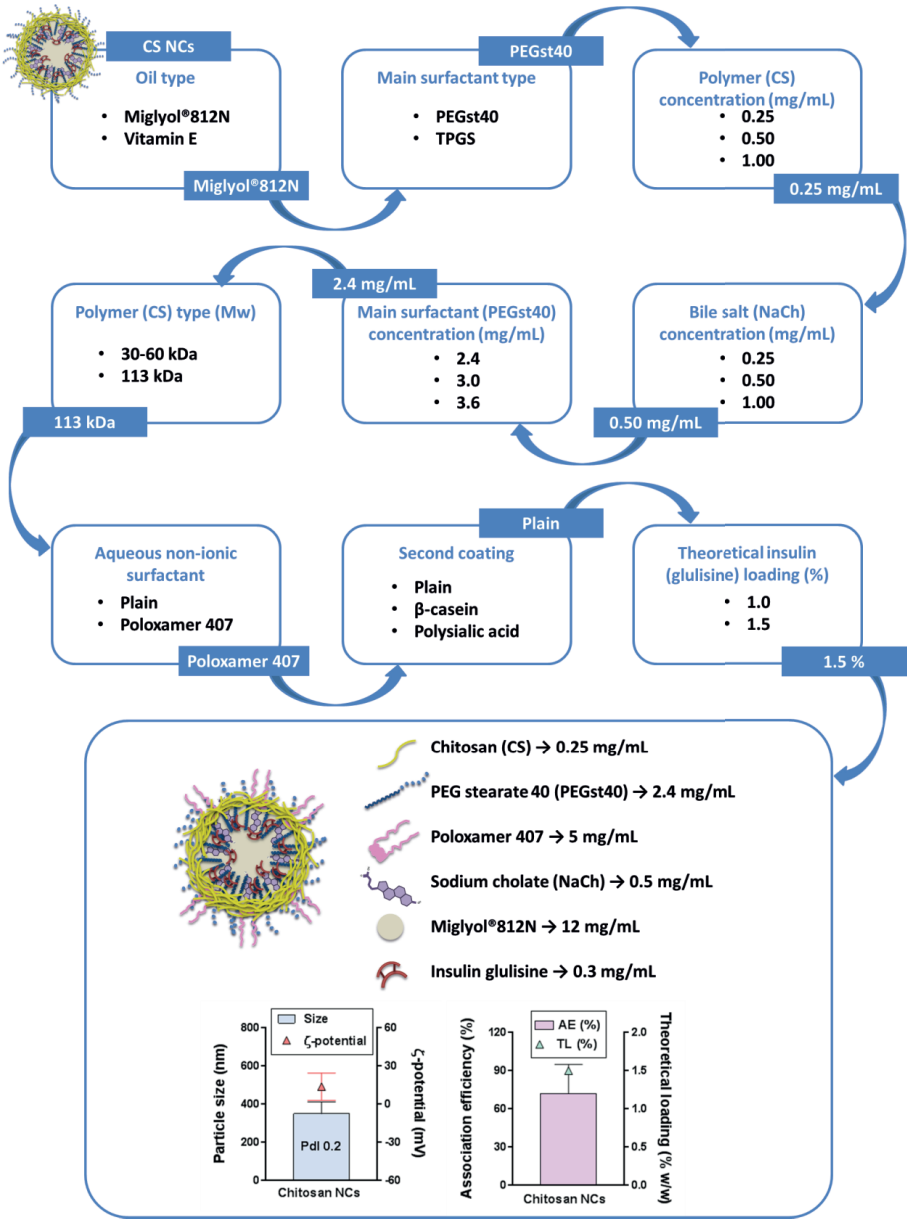



***Figure 2. Top:*** *Schematic representation of the systematic study carried out in the CS NCs selected prototype, to identify the critical factors affecting their physicochemical properties and insulin association efficiency;* ***Bottom:*** *Schematic representation, composition, physicochemical characterization (size, PdI and ζ-potential), insulin association efficiency (% AE) and theoretical loading (% TL) of the optimized CS NCs (Mean ± SD, n ≥ 3).*

*Table 1* summarizes, in a qualitative way, the results that can be extracted from this screening. While some of the studied variables, such as the type of the main surfactant or the inclusion of an extra non-ionic surfactant in the formulation, had minor effects on both, the physicochemical properties and insulin association, others, e.g., the composition of the polymer shell, had a drastic effect. Among the latest, it should be pointed out the negative effect of both, the increase of the concentration of polymer and the presence of a second coating shell on the ability of the CS NCs to associate insulin.

***Table 1.*** *Effect of the different factors under study on the size, PdI, ζ–potential (ζ–Pot.) and insulin association efficiency (AE %) of the CS NCs used as starting point. Symbols show in a qualitative way the magnitude of the corresponding effect: increment (↑), reduction (↓) and almost constant (≈).*

| Factor under study | Size | PdI | ζ–Pot. | AE % |
|---|---|---|---|---|
| **Oil type:** change from Miglyol®812N to DL–α–tocopherol | ↑↑ | ≈ | ↑ | ≈ |
| **Main surfactant type:** change from PEGst40 to TPGS | ≈ | ≈ | ≈ | ↓ |
| **Polymer concentration:** increasing CS concentration (0.25, 0.5 and 1 mg/mL) | ≈ | ≈ | ≈ | ↓↓ |
| **Bile salt concentration:** increasing NaCh concentration (0.25, 0.5 and 1 mg/mL) | ↓↓ | ↓ | ≈ | ≈ |
| **Main surfactant concentration:** increasing PEGst40 concentration (2.4, 3.0 and 3.6 mg/mL) | ↑↑ | ↑↑ | ↓ | ↑↑ |
| **Polymer type:** increasing CS Mw from 30–60 to 113 kDa | ↓ | ≈ | ↑↑ | ≈ |
| **Extra non-ionic surfactant:** inclusion of poloxamer 407 | ≈ | ≈ | ↓ | ≈ |
| **Extra second coating:** inclusion of β–casein/polysialic acid as second polymer coating | ↑↑/≈ | ↑↑/↓ | ↓↓ | ↓↓ |
| **Peptide theoretical loading:** increasing theoretical insulin loading from 1 to 1.5 % | ≈ | ≈ | ≈ | ≈ |

Overall, the formulation that was found to exhibit the best characteristics is the one composed of 0.25 mg/mL of CS, 12 mg/mL of Miglyol®812N, 2.4 mg/mL of PEGst40, 0.5 mg/mL of NaCh, 5 mg/mL of poloxamer 407 and 0.3 mg/mL of insulin glulisine (1.5 % theoretical loading). Unfortunately, when the stability of these optimized CS NCs was tested upon exposure to simulated intestinal fluids (SIF and FaSSIF–V2), their size decreased drastically (≈ 150 nm) and around the 70-80 % of the associated insulin glulisine

was immediately released from the NCs, thus hampering their potential to be used as oral delivery carriers. Consequently, the results of this work highlight the difficulties for defining an oily-based nanocarrier with the adequate properties for oral peptide delivery.

To complement this information, in a separate set of studies, our goal was to investigate the influence of the surface properties of nanocapsules on their interaction with the intestinal barriers.

## 2. Influence of the surface properties of nanocapsules on their interaction with the intestinal barriers

The versatility of the core-shell polymeric NCs relies on the possibility to adapt the composition of their oily core to the nature of the cargo, and that of the polymeric shell to the administration route or target tissue [41–45]. In this line, as previously shown, different formulation strategies can be successfully applied to improve the restricted liposolubility of peptides and proteins and increase their association to lipid-based nanosystems. Besides, following oral administration, the nanosystems should be able to protect their cargo and overcome the intestinal barriers that limit the oral bioavailability of these macromolecules. In this regard, the nanosystems' surface properties play a key role on their interaction with the surrounding medium. Bearing this in mind, we selected specific compositions of NCs made of CS and PARG, developed by our research group [19,37,46], and their corresponding NEs as controls, to systematically evaluate the effect of their surface composition on their capacity to overcome specific intestinal barriers. Overall, nine different formulations in the form of NEs or NCs (*Figure 3, lower panel*), were prepared according to the two steps procedure previously described by our group (*Figure 3, upper panel*) [47]. All the nanosystems had the same oily core (Miglyol®812N and Epikuron®145V lecithin) and their shells were made of cationic polymers (CS and PARG), surfactants (poloxamer 188 (P188) and poloxamer 407 (P407) and a combination of them. In total, 3 different NEs and 6 different NCs were analyzed in terms of *i)* their stability, both colloidal and chemical, in simulated intestinal fluid and *ii)* their interaction (adhesion and diffusion) with mucus, while mimicking the physiological conditions [48,49].

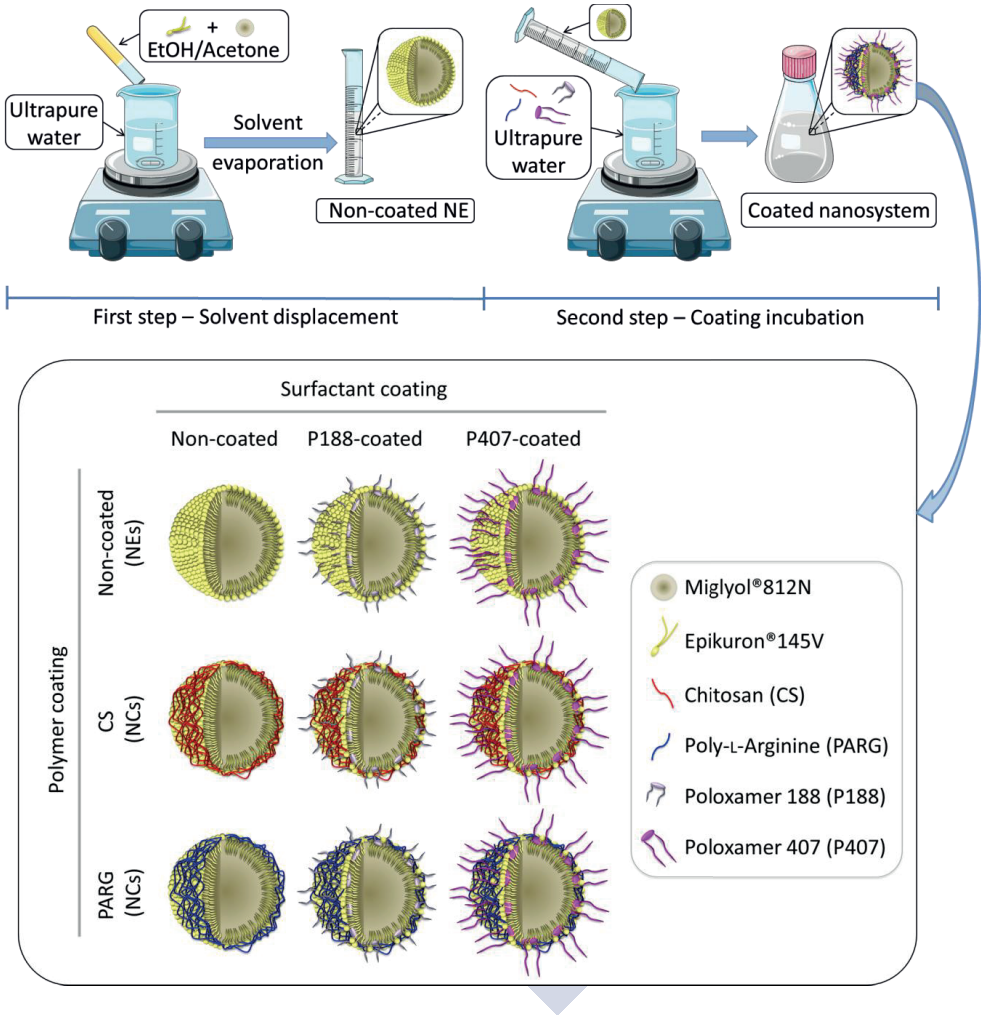



***Figure 3.*** *Schematic representation of the formulation procedure (upper panel) and the nanosystems tested (lower panel). Laboratory material and equipment (https://creativecommons.org/licenses/by/3.0/) have been modified from the original work provided by Servier Medical Art (http://smart.servier.com/).*

The results shown in *Table 2* indicate the efficient formation of a polymeric shell after the incubation of the NE with either polymer (charge inversion), most probably due to the attractive electrostatic interaction between the cationic polymer (either CS or PARG) and the negatively charged NE [41,43]. In the same line, the efficient adsorption of the non-ionic surfactants on the nanosystems surface should lead to a reduction on their ζ–potential magnitude due to the displacement of the shear plane (where the ζ–potential is defined) towards the aqueous phase [50]. In this regard, the results suggested a low

incorporation of P188 to the nanostructure based on their similar stability, lipolysis and interaction with mucin (*Table 2*) [43,51]. In contrast, the stability and mucointeraction results shown in *Table 2* suggest a better incorporation of P407 onto the oily core of the nanosystems, probably due to its higher lipophilicity.

Regarding the colloidal stability of the nanosystems in SIF, while all the NEs were stable in this medium, CS and PARG NCs formulated without surfactants or with P188 showed an immediate aggregation. In contrast, they were more stable with P407, being this effect more noticeable in the case of PARG NCs. The stability of both NE and P188-coated NE could be attributed to the repulsive electrostatic forces (ζ−potential in SIF ≈ −60 mV), whereas the improved stability of the P407-coated nanosystems is probably driven by the steric stabilization of the systems [26,52,53]. A common behaviour was observed for all the systems upon incubation in SIF with pancreatin. Although none of the nanosystems suffered aggregation, their surface charge became similar (≈ −15 ± 5 mV), probably due to the formation of an stabilizing coating of the particles by the enzymes present in the medium [54,55]. On the other hand, the most resistant systems against enzymatic degradation were those formulated with P407. Afterwards, a preliminary analysis (DLS) of the role of the surface properties of our prototypes on their interaction with mucin [48] (*Table 2*) reveled a certain interaction of all the NEs with this protein (absence of aggregation but decrease in ζ−potential magnitudes) As expected, CS and PARG NCs showed a mucin-concentration dependent aggregation. In the same line, although the incorporation of P407 cannot totally prevent the colloidal system from interacting with the mucin fibers (decrease in ζ−potential magnitudes), this interaction did not translate into their aggregation.

***Table 2.*** *Physicochemical and stability properties of nanoemulsions (NEs), chitosan (CS) and polyarginine (PARG) nanocapsules (NCs). All systems share the same Miglyol®812N/lecithin core (n ≥ 3).*

| Polymeric Coating | Surfactant Coating | Size (nm) | PdI | ζ–Potential (mV) | Colloidal stability in SIF (4 h) | Lipolysis (% degradation at 2 h in 1%-pancreatin-SIF | Mucin interaction (DLS) |
|---|---|---|---|---|---|---|---|
| -------- (NE) | ----- | 179 ± 15 | 0.1 | −54 ± 1 | ✓ | 98 ± 2 | Mucin coating / No aggregation |
| | **P188** | 172 ± 02 | 0.1 | −54 ± 3 | ✓ | 84 ± 1 | Mucin coating / No aggregation |
| | **P407** | 174 ± 04 | 0.1 | −30 ± 3[b] | ✓ | 18 ± 2 | Mucin coating / No aggregation |
| **CS (NCs)** | ----- | 380 ± 19 | 0.3 | +47 ± 3 | × | 82 ± 3 | Aggregation mucin- concentration-dependent |
| | **P188** | 383 ± 18 | 0.3 | +49 ± 1 | × | 76 ± 7 | Aggregation mucin- concentration-dependent |
| | **P407** | 327 ± 12[a] | 0.3 | +42 ± 2[c] | × | 56 ± 4 | Mucin coating / No aggregation |
| **PARG (NCs)** | ----- | 188 ± 05 | 0.1 | +43 ± 1 | × | 86 ± 3 | Aggregation mucin- concentration-dependent |
| | **P188** | 185 ± 03 | 0.1 | +45 ± 1 | × | 78 ± 6 | Aggregation mucin- concentration-dependent |
| | **P407** | 183 ± 04 | 0.1 | +27 ± 2[b] | ✓ | 22 ± 6 | Mucin coating / No aggregation |

*Two-way ANOVA followed by a Fisher's LSD test were applied for the statistical analysis. [a]Significantly different compared to the formulation without non-ionic surfactant ($p \leq 0.0001$) and to the formulation with P188 ($p \leq 0.0001$); [b]Significantly different compared to both the formulation without non-ionic surfactant and the formulation with P188 ($p \leq 0.0001$); [c]Significantly different compared to the formulation without non-ionic surfactant ($p \leq 0.01$) and to the formulation with P188 ($p \leq 0.001$).*

In order to better understand the effect that the shell composition of the systems has on their interaction with the intestinal mucosa, we *i)* semi-quantitatively studied the interaction of the nanosystems with a film of mucin immobilized on a glass bottom dish (*Figure 4, left*) [56]; and *ii)* evaluated the diffusion coefficient of the prototypes in intestinal mucus using particle tracking analysis (*Figure 4, right*) [57–59].

Although a distinct interaction with mucin was observed for the different polymeric shells (*Figure 4, left*), upon incubation in porcine mucus, all the non-surfactant coated formulations (NE and NCs) were highly retained in the mucus matrix (*Figure 4, right*). The hampered mucodiffusion could be attributed to the hydrophobic character of the NE and the positive surface charge of CS and PARG, being both characteristics expected to promote the interaction of the formulation with the mucin fibers present in the intestinal porcine mucus [24,60,61]. In line with the previous results, non-significant effect was found on both the mucoadhesive and mucodiffusive properties of the three nanosystems after the addition of P188 ($p \leq 0.05$). This suggests that the coating with PEG derivatives with a PEG−Mw in the 5−10 kDa range, which normally results in an enhancement of the mucodiffusion properties [58], is not thick enough to facilitate their mucodiffusion [29,61]. Finally, despite the fact that P407 significantly decreased the mucoadhesive properties in both NCs ($p \leq 0.05$) (*Figure 4, left*), this decrease was not reflected in their mucodiffusion capacity in porcine mucus (*Figure 4, right*). This might be due to the interference of CS and PARG in the formation of a dense and homogeneous P407 coating [29,61]. On the contrary, in the absence of the polymer shell (NE), P407 could efficiently attach to the oily nanodroplets leading to an improved mucodiffusive behavior [29,60–62].

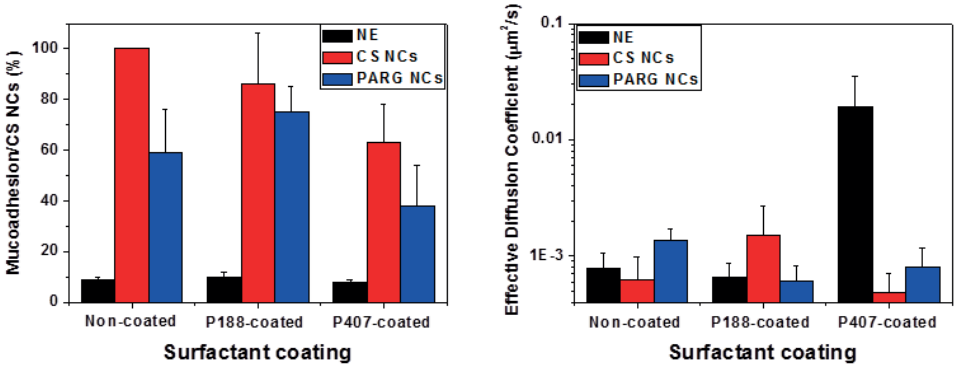



***Figure 4. Left:*** *Mucoadhesion assessed by fluorescence microscopy. Adhesion percentage upon incubation of the NEs (black), CS NCs (red) and PARG NCs (blue) with a mucin film, compared to the non-coated CS NCs (set as 100 %) (Mean ± SD, n ≥ 3).* ***Right:*** *Mucodiffusion assessed by multiple particle tracking analysis. Mean effective diffusion coefficient of the non-coated, P188-coated, and P407-coated NEs (black), CS NCs (red) and PARG NCs (blue) calculated from their trajectories in porcine intestinal mucus at 37 °C at a time scale of 1 second (Mean ± SD; number of batches analyzed n = 3; n ≥ 1000 nanoparticles).*

Overall, our results indicate that the interaction of these nanosystems with biological barriers is strongly dependent on their surface composition, being the contribution of each component susceptible to be affected by the presence of other components. The use of P407 may be a strategy to improve the capacity of a nanosystem to overcome the multiple barriers associated to the oral modality of administration, i.e. colloidal stability, resistance against enzymatic degradation and intestinal mucus interaction/diffusion. However, when using this approach, one must take into account that the incorporation of this surfactant onto the surface of the nanosystems may interfere with other constituents present in the nanosystems shell (its use in the presence of CS or PARG had a limited effect on the formulation performance).

## 3. Rational design, development and characterization of a novel lipid-based nanosystem for oral peptide delivery

The ultimate objective of this thesis was to develop a novel oily-based nanosystem for the oral administration of peptides. Taking advantage of our previous work, where CS and PARG NCs´ coatings negatively affected the potential of the formulations to overcome several intestinal barriers, we focused our efforts on designing a NE containing poloxamer 407. We selected for this final development a hydrophobically-modified insulin (HM-insulin), whose hydrophobic domains (GRAVY ≈ −0.0333) together with its 8 positively-ionizable aminoacids are expected to favor its entrapment within lipidic cores. The system was designed to meet the following criteria *i)* simple and reproducible preparation technique leading to the formation of a mono-dispersed population, *ii)* high insulin efficiency, *iii)* colloidal stability and miscibility in simulated intestinal fluids, *iv)* mucodiffusive properties, *v)* ability to interact with the intestinal cells without causing cytotoxic effects and *vi)* ability to lead to an adequate pharmacological response once administered *in vivo*. Miglyol® 812N was selected as oily core (peptide protective and permeation enhancer properties) [20,21] and a pegylated phospholipid sodium salt (MPEG-2000-DSPE) and poloxamer 407 as main surfactants (stability enhancers and mucodiffusion promoters) [23–30]. Additionally, sodium taurocholate (STC) was selected as a penetration enhancer [31,32] with the capacity to form ionic pairs with the insulin molecules [33–36]. Interestingly, a strong interaction found between the MPEG-2000-DSPE and the HM-insulin, ended up in a prototype consisting of a mixture of HM-insulin-loaded NE and micelles, whose schematic organization and deep characterization are illustrated in *Figure 5*.

*Table 3* summarizes the physicochemical properties, insulin association efficiency and mucodiffusion capacity of the resultant mixed nanosystem (NE and micelles), as well as those of their separate species. The results indicated that it was possible to obtain a mixed nanosystem containing NE and micelles, loading 100 % of the HM-insulin, with a hydrodynamic mean size of 219 ± 7 nm, low polydispersity index (0.1) and ζ−potential of −20 ± 1 mV, which also displayed acceptable mucodiffusive properties in porcine mucus (diffusion capacity $D_m/D_w \approx 4.2 \times 10^{-2}$). Our strategy to get a high insulin association was based on both, *i)* increasing its hydrophobicity (hydrophobic modifications and final pH ≈ 6.5 ± 0.2 close to the insulin isoelectric point (IP = 6.78)) to facilitate the hydrophobic interactions among the hydrophobic domains of the insulin with the different components of the lipidic nanosystem [15,63]; and *ii)* adjusting its ionization degree to facilitate its electrostatic interaction with the negatively charged STC bile salt and MPEG-2000-DSPE sodium salt surfactant [64]. On the other hand, the system remained colloidally stable at least for 4 hours in contact with different simulated intestinal media (FaSSIF, SIF with and without 1 % pancreatin, FaSSIF−V2 and FeSSIF−V2 without enzymes). In this regard, the negative surface charge of the system together with the presence of PEG derivatives with a PEG−Mw below 10 kDa on the surface (P407 and MPEG-2000-DSPE), were the reasons behind the stabilization of the formulation upon its contact with intestinal enzymes and lipids [25,60] and its facilitated mucodiffusion in porcine mucus [25,27].

***Table 3.*** *Physicochemical properties, association efficiency (AE %) and diffusion capacity (Dm/Dw)* in porcine mucus of the HM-insulin-loaded mixed nanosystem and its separate species: nanoemulsion (NE) and micelles (Mean ± SD, n ≥ 3).*

| HM-insulin-loaded system | Size (nm) | PdI | ζ−Potential (mV) | AE (%) | Diffusion capacity ($D_m/D_w$) |
|---|---|---|---|---|---|
| **Mixed system (NE + micelles)** | 219 ± 7 | 0.1 | −20 ± 1 | ≈ 100 | $4.2 \times 10^{-2}$ |
| **NE** | 216 ± 3 | 0.1 | −19 ± 3 | 47 ± 11 | $1.0 \times 10^{-1}$ |
| **Micelles** | 184 ± 4 | 0.1 | −16 ± 3 | 56 ± 8 | $1.2 \times 10^{-1}$ |

**$D_m/D_w$ was calculated by dividing the mean effective diffusion coefficient of the particles in mucus ($D_m$) vs the same in water ($D_w$).*

In order to go deeper into the characterization of the mixed nanosystem, the particle size and shape of its separate species were also evaluated using transmission electron microscopy (TEM), atomic force microscopy (AFM), multi-angle light scattering (MALS) and nanoparticle tracking analysis (NTA) (*Figure 5). Results* showed that the interaction between HM-insulin and phospholipids was strong enough to change the structural configuration of the blank micelles leading to the formation of a homogeneous population of clusters of HM-insulin-loaded micelles.

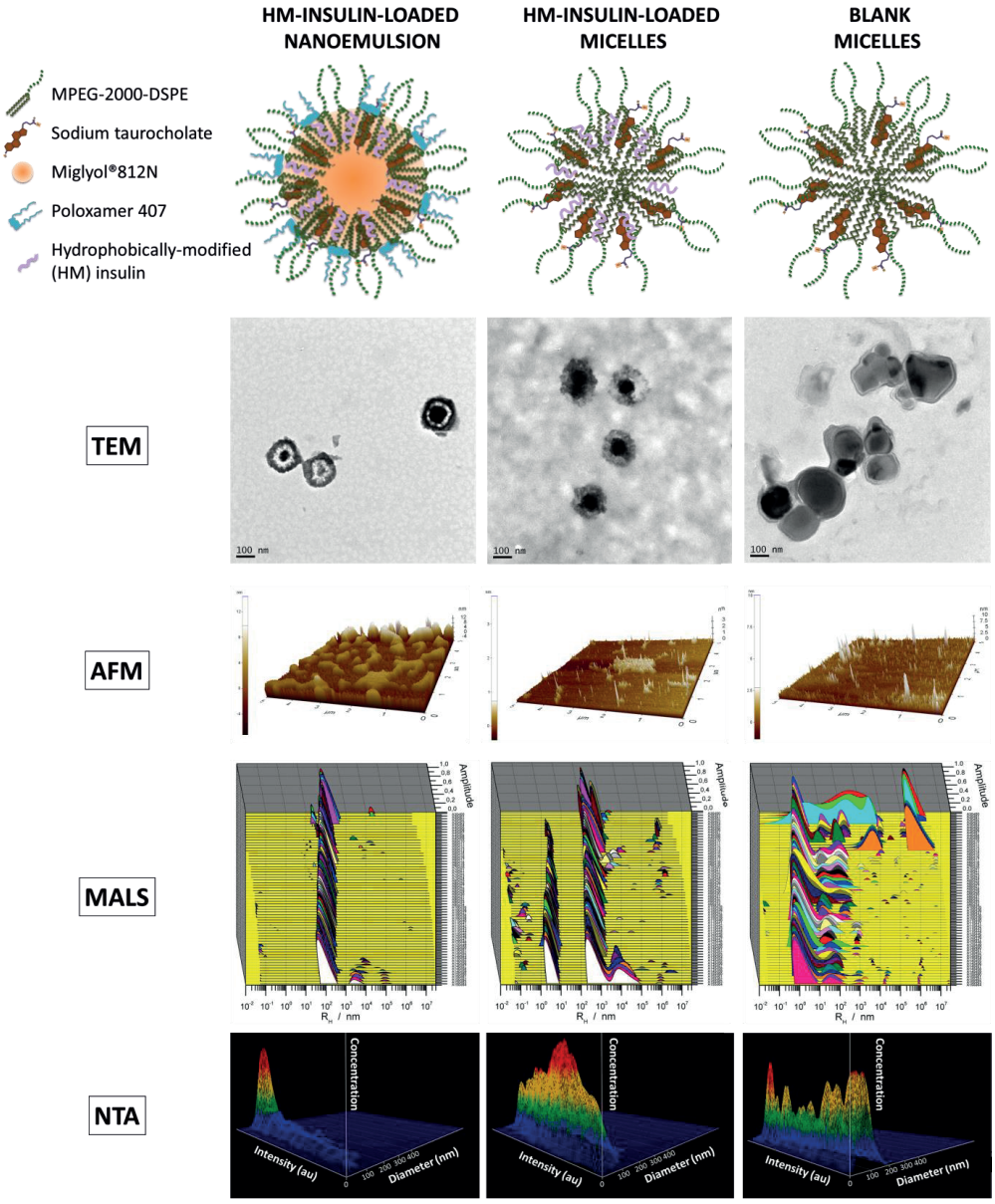



***Figure 5.*** *Schematic representation, TEM, AFM, MALS and NTA characterization of the separated species of the mixed nanosystem: HM-insulin-loaded NE (left), HM-insulin-loaded micelles (middle) and also blank micelles (right) as a comparative control.*

In a next step, the interaction of HM-insulin-loaded mixed nanosystem (NE and micelles) with intestinal cells was evaluated in different cell lines: Caco−2, C2BBe1 human colon carcinoma Caco−2 clone and mucus secreting HT29−MTX. Despite the capacity of Caco−2 cell line to grow in monolayers resembling the human intestine structure (i.e.: tight junctions and surface microvilli) [65–67], it is known to have a more restricted paracellular permeability than the human small intestine (higher presence of tight junctions) [65,68,69] and it lacks of mucus secreting goblet cells [70]. For these reasons the interaction of the mixed nanosystem with the C2BBe1 human colon carcinoma Caco−2 clone (more morphologically homogeneous than Caco−2 cells, with the microvilliar brush border exclusively localized in the apical side) and mucus secreting HT29−MTX (mucus layer, smaller microvilli, and softer tight junctions than Caco−2 cells) was also tested [10,66,69,71].

Firstly, after checking that the system remained stable in HBSS without releasing the associated insulin, the cytotoxicity of the blank and HM-insulin-loaded mixed nanosystem in the three cell lines was evaluated through different techniques (MTT, ATP, NRU and LDH). The results showed no cytotoxic effects after 2 h incubation in any of the cell lines tested, whereas a dose-dependent cytotoxic effect was observed after 24 h incubation. The estimated ECs50 ranged from 2.0 to 2.3 mg/mL, values that are low as compared to other nanometric systems.

Secondly, the interaction of the HM-insulin-loaded mixed nanosystem with Caco−2 and C2BBe1 human colon carcinoma Caco−2 clone monocultures, as well as with C2BBe1 human colon carcinoma Caco−2 clone:HT29−MTX (9:1) co-culture was quantitatively analyzed using flow cytometry (FACS). For this purpose, the HM-insulin was covalently labeled with FITC and the behaviour of both, the free HM-insulin and the one loaded in the nanosystem was analyzed. FACS showed 100 % of FITC-positive cells after 3 h incubation in all the cultures tested for both, free HM-insulin and HM-insulin-loaded mixed nanosystem, being this high interaction significantly different respect to the control (non-treated cells).

Finally, the interaction of both, the free FITC-HM-insulin and FITC-HM-insulin-loaded mixed nanosystem with Caco−2 monolayers after 2 h incubation was also qualitatively analyzed using confocal laser scanning microscopy. Interestingly, while free FITC-HM-insulin remained associated to the surface of the cells, the FITC-HM-insulin-loaded mixed nanosystem was identified inside the cells (*Figure 6*). Since TEER values were not significantly affected after confocal experiments, it can be discarded that the improved internalization was due to an increased transport through the paracellular pathway. These findings suggested that the negatively charged and pegylated shell surface of the mixed

nanosystem, which may reduce the potential interactions with the cell culture medium proteins, along with the permeation enhancing properties of its components, were able to enhance its internalization into the Caco−2 monolayer compared to the free HM-insulin.

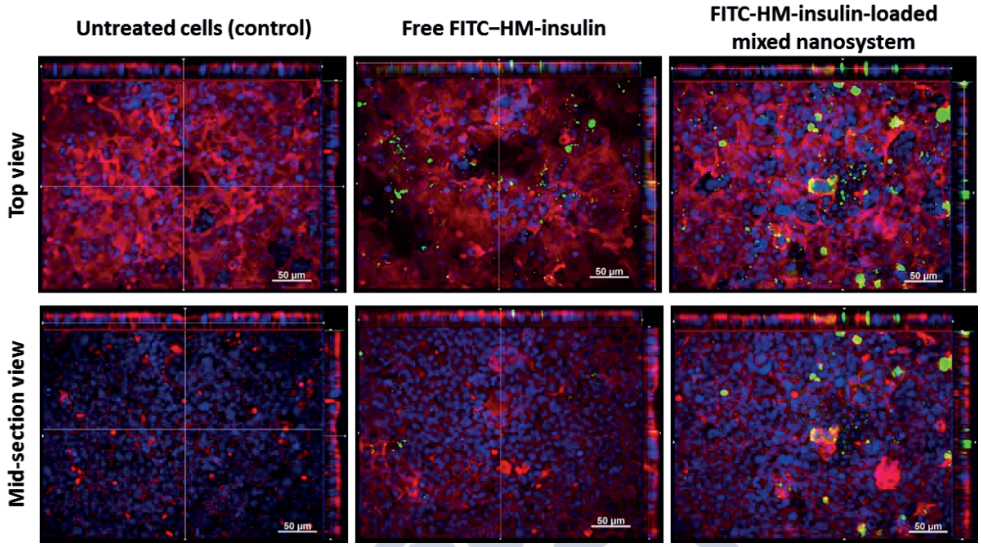



***Figure 6.*** *Confocal images in Caco−2 monolayers (top and mid-section views at 25X) representing the y−z, x−z and x−y view of Caco−2 monolayers after 2 h incubation with free FITC-HM-insulin (**middle**) and FITC-HM-insulin-loaded mixed nanosystem (NE + micelles) (**right**). Untreated monolayers were used as control (**left**). Cell membranes (rhodamine–phalloidin), cell nuclei (DAPI) and HM-insulin (FITC) are visualized in red, blue and green, respectively.*

Following the positive *in vitro* characterization results, the *in vivo* efficacy of the formulation was evaluated in healthy [32,72] and diabetic [10,11,15,32]) rats.

First of all, since it is well-known that peptides are labile macromolecules susceptible to result inactivated as consequence of the formulation process [73], we checked *i)* the dose-response effect of the HM-insulin (non-marketed); and *ii)* if its bioactivity, once entrapped into the mixed nanosystem, was maintained under *in vivo* conditions in healthy rats. Hypoglycemic responses following subcutaneous (SC) administration of the HM-insulin-loaded mixed nanosystem were comparable to those obtained with the equivalent dose of a saline solution of HM-insulin (non-significant differences in terms of total glucose decrease, quantified as area above the curve (AAC) after 8 hours) (*Figure 7, right*). Beyond these similar global values, the profiles observed for the low HM-insulin dose (1 IU/kg) were different (*Figure 7, left*). In the case of the HM-insulin-loaded nanosystems a slow release could be responsible for a low and prolonged hypoglycemic response. The reason

why this delayed response was not observed for the high insulin dose remains to be elucidated. Irrespective of this, these results confirmed that the stability and bioactivity of the peptide were not compromised by the formulation process. Regarding the dose-response evaluation, a more prolonged and statistically higher effect was observed with the higher dose tested (2 IU/kg) for both, the free insulin and the one entrapped into the mixed nanosystem.

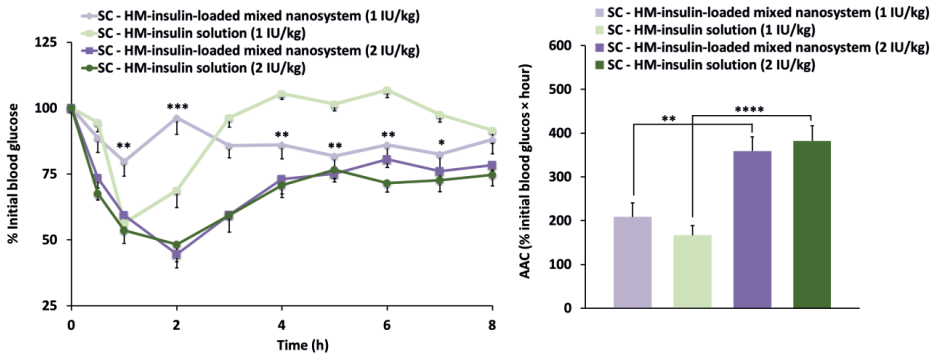



***Figure 7. Left:*** *Normalized hypoglycemic effect (blood glucose % of the initial) following subcutaneous (SC) administration of a saline HM-insulin solution and HM-insulin-loaded mixed nanosystem (NE + micelles) at both 1 (n = 8) and 2 IU/kg body weight (n = 13) to healthy rats (Mean ± SEM) (Two-way ANOVA followed by a Fisher's LSD test were applied for the statistical analysis; significance levels comparing the HM-insulin-loaded mixed nanosystem to the HM-insulin solution at the same concentration *p ≤ 0.05; **p ≤ 0.01; ***p ≤ 0.005).* ***Right:*** *Area above the curve at time = 8 h calculated by establishing 120 % as upper limit (% initial blood glucose × hour) (Mean ± SEM) (One-way ANOVA followed by a Fisher's LSD test were applied for the statistical analysis; significance levels **p ≤ 0.01; ****p ≤ 0.0001).*

Regarding the intrajejunal (IJ) *in vivo* efficacy of this formulation (100 IU/kg body weight) in healthy rats, a slight, but significantly different hypoglycemic effect ($p \leq 0.05$) was observed at 1 and 4 hours post-administration, when compared to the blank mixed nanosystem (≈ 20 %) (*Figure 8, left*). However, non-significant differences were found in the overall response, represented as AAC after 8 hours (*Figure 8, right*).

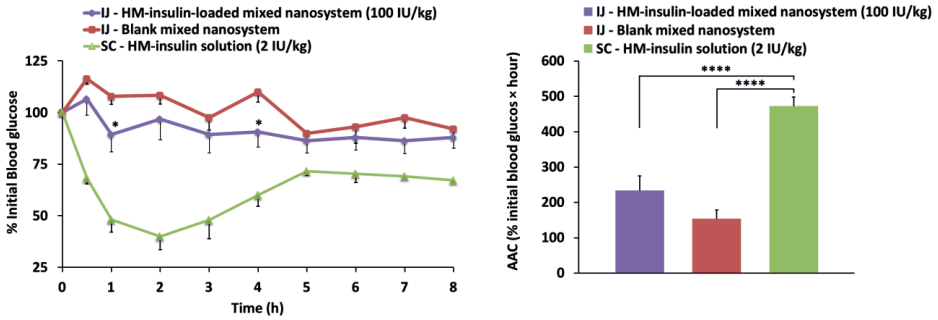



***Figure 8. Left:*** *Normalized hypoglycemic effect (blood glucose % of the initial) following intrajejunal (IJ) administration of HM-insulin-loaded mixed nanosystem (n = 8) at 100 IU/kg, blank mixed nanosystem (n = 6) and subcutaneous (SC) administration of a saline HM-insulin solution (n = 6) at 2 IU/kg to healthy rats (Mean ± SEM) (Two-way ANOVA followed by a Fisher's LSD test were applied for the statistical analysis; significance levels *p ≤ 0.05);* ***Right:*** *Area above the curve at time = 8 h calculated by establishing 120 % as upper limit (% initial blood glucose × hour) (Mean ± SEM) (One-way ANOVA followed by a Fisher's LSD test were applied for the statistical analysis; significance levels ****p ≤ 0.0001).*

Interestingly, when the efficacy of the formulation (100 IU/kg body weight) intraduodenally administered (ID) was evaluated in a diabetic rat model, in addition to a higher significant hypoglycemic response (≈ 30 %) compared to the blank mixed nanosystem at 1 ($p \leq 0.05$), 2, 4 and 5 ($p \leq 0.01$) hours post-administration (*Figure 9, left*), significant differences ($p \leq 0.01$) were also found in the overall response, represented as AAC after 8 hours, between both groups (*Figure 9, right*).

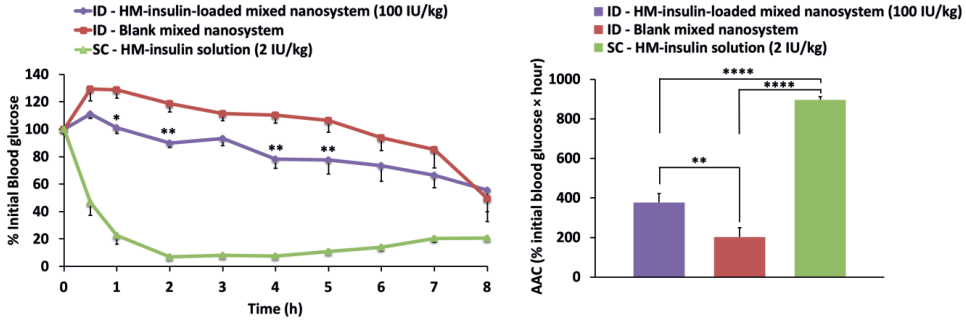



***Figure 9. Left:*** *Normalized hypoglycemic effect (blood glucose % of the initial) following intraduodenal (ID) administration of HM-insulin-loaded mixed nanosystem (n = 8) at 100 IU/kg, blank mixed nanosystem (n = 7) and subcutaneous (SC) administration of a HM-insulin solution (n = 6) at 2 IU/kg to diabetic rats. (Mean ± SEM) (Two-way ANOVA followed by a Fisher's LSD test were applied for the statistical analysis; significance levels *p ≤ 0.05; **p ≤ 0.01);* ***Right:*** *Area above the curve at time = 8 h calculated by establishing 130 % as upper limit (% initial blood glucose × hour) (Mean ± SEM) (One-way ANOVA followed by a Fisher's LSD test were applied for the statistical analysis; significance levels **p ≤ 0.01; ****p ≤ 0.0001).*

The different efficacy results found depending on the animal model used, evidence the importance of reaching a consensus in this regard among the scientific community to be able to compare this parameter in a global manner. When using normoglycemic rats it is possible to avoid the potential alteration of the absorption process caused by the anesthesia and also the hyperglycemia variability among rats caused by the administration of streptozocin to render the rats diabetic, which leads different degrees of β−cell deficiency intrinsically dependent on the animal [10,15]. Nevertheless, despite the fact that the effect of the exogenous insulin might be hindered by the autoregulation phenomenon (braking secretion of the endogenous insulin by the β−cells) [74,75] in normoglycemic rats, higher responses can be found in literature when using different experimental protocols (i.e., intraileal administration, long fasting period, anesthesia, glucose exogenously overload) [74–78]. Interestingly, similar results were reported when the administration was intraduodenal/intrajejunal (high enzymatic activity and M−cells presence), the fasting time was shorter and the anesthesia was avoided [10,11,15,32]. On the other hand, the diabetic rat model mimics better the physiological conditions to evaluate the hypoglycemic responses because it presents β−cell deficiency and lacks of the auto-regulation phenomenon. These characteristics, which make these animals more insulin-sensitive [74,75], support the higher efficacy we found in the diabetic model, and correlate with the fact that the majority of positive hypoglycemic responses reported up to now have been achieved using either anesthetized or diabetic rats [32,72].

Irrespective of the positive value of the *in vivo* data, taking into account the favorable *in vitro* properties of the system (i.e., insulin bioactivity preservation, good stability and miscibility in simulated intestinal media, mucodiffusive properties, high cell interaction with no cytotoxic effects promoting the insulin cellular uptake and the interaction with the intestinal epithelium), one could expect a more robust *in vivo* response. We hypothesized that the moderate *in vivo* efficacy obtained can be attributable to the harsher nature of the *in vivo* conditions that probably led to a restricted transport of the insulin to the blood stream. These results, which bring the difficult *in vitro–in vivo* correlation to light, lead us to emphasize the importance of standardizing experimental protocols to obtain more predictive results *in vitro* and facilitate the comparison among different formulations.

## References


[1] T.A.S. Aguirre, D. Teijeiro-Osorio, M. Rosa, I.S. Coulter, M.J. Alonso, D.J. Brayden, Current status of selected oral peptide technologies in advanced preclinical development and in clinical trials, Adv. Drug Deliv. Rev. 106 (2016) 223–241. doi:10.1016/j.addr.2016.02.004.

[2] S. Mitragotri, P.A. Burke, R. Langer, Overcoming the challenges in administering biopharmaceuticals: formulation and delivery strategies, Nat Rev Drug Discov. 13 (2014) 655–672. doi:10.1038/nrd4363.

[3] D.S. Pisal, M.P. Kosloski, S. V. Balu-Iyler, Delivery of therapeutic proteins, J. Pharm. Sci. 99 (2010) 2557–2575. doi:10.1002/jps.22054.

[4] C.F. Van Der Walle, O. Olejnik, An overview of the field of peptide and protein delivery, in: C.F. Van Der Walle (Ed.), Pept. Protein Deliv., First, Academic Press, 2011: pp. 1–22. doi:10.1016/b978-0-12-384935-9.10001-x.

[5] B.J. Bruno, G.D. Miller, C.S. Lim, Basics and recent advances in peptide and protein drug delivery, Ther. Deliv. 4 (2013) 1443–1467. doi:10.4155/tde.13.104.

[6] E. Arbit, The physiological rationale for oral insulin administration, Diabetes Technol. Ther. 6 (2004) 510–517. doi:10.1089/1520915041705929.

[7] A. Sood, R. Panchagnula, Peroral route: An opportunity for protein and peptide drug delivery, Chem. Rev. 101 (2001) 3275–3303. doi:10.1021/cr000700m.

[8] J. Wang, V. Yadav, A.L. Smart, S. Tajiri, A.W. Basit, Toward oral delivery of biopharmaceuticals: An assessment of the gastrointestinal stability of 17 peptide drugs, Mol. Pharm. 12 (2015) 966–973. doi:10.1021/mp500809f.

[9] M. Morishita, N.A. Peppas, Is the oral route possible for peptide and protein drug delivery?, Drug Discov. Today. 11 (2006) 905–910. doi:10.1016/j.drudis.2006.08.005.

[10] L.N. Thwala, A. Beloqui, N.S. Csaba, D. González-Touceda, S. Tovar, C. Dieguez, M.J. Alonso, V. Préat, The interaction of protamine nanocapsules with the intestinal epithelium: a mechanistic approach, J. Control. Release. 243 (2016) 109–120. doi:10.1016/j.jconrel.2016.10.002.

[11] Z. Niu, E. Samaridou, E. Jaumain, J. Coëne, G. Ullio, N. Shrestha, J. Garcia, M. Durán-Lobato, S. Tovar, M.J. Santander-Ortega, M.V. Lozano, M.M. Arroyo-Jimenez, R. Ramos-Membrive, I. Peñuelas, A. Mabondzo, V. Préat, M. Teixidó, E. Giralt, M.J. Alonso, PEG-PGA enveloped octaarginine-peptide nanocomplexes: an oral peptide delivery strategy, J. Control. Release. 276 (2018) 125–139. doi:10.1016/j.jconrel.2018.03.004.

[12] X. Li, S. Guo, C. Zhu, Q. Zhu, Y. Gan, J. Rantanen, U.L. Rahbek, L. Hovgaard, M. Yang, Intestinal mucosa permeability following oral insulin delivery using core shell corona nanolipoparticles, Biomaterials. 34 (2013) 9678–9687. doi:10.1016/j.biomaterials.2013.08.048.

[13] L. Inchaurraga, N. Martín-Arbella, V. Zabaleta, G. Quincoces, I. Peñuelas, J.M. Irache, In vivo study of the mucus-permeating properties of PEG-coated nanoparticles following oral administration, Eur. J. Pharm. Biopharm. 97 (2015) 280–289. doi:10.1016/j.ejpb.2014.12.021.

[14] W. Shan, X. Zhu, M. Liu, L. Li, J. Zhong, W. Sun, Z. Zhang, Y. Huang, Overcoming the diffusion barrier of mucus and absorption barrier of epithelium by self-Assembled nanoparticles for oral delivery of insulin, ACS Nano. 9 (2015) 2345–2356. doi:10.1021/acsnano.5b00028.

[15] Z. Niu, E. Tedesco, F. Benetti, A. Mabondzo, I.M. Montagner, I. Marigo, D. Gonzalez-Touceda, S.

Tovar, C. Diéguez, M.J. Santander-Ortega, M.J. Alonso, Rational design of polyarginine nanocapsules intended to help peptides overcoming intestinal barriers, J. Control. Release. 263 (2016) 4–17. doi:10.1016/j.jconrel.2017.02.024.

[16] T. Karamanidou, V. Bourganis, O. Kammona, C. Kiparissides, Lipid-based nanocarriers for the oral administration of biopharmaceutics, Nanomedicine. 11 (2016) 3009–3032. doi:10.2217/nnm-2016-0265.

[17] Z. Niu, I. Conejos-Sánchez, B.T. Griffin, C.M. O'Driscoll, M.J. Alonso, Lipid-based nanocarriers for oral peptide delivery, Adv. Drug Deliv. Rev. 106 (2016) 337–354. doi:10.1016/j.addr.2016.04.001.

[18] L. Rosenmayr-Templeton, The oral delivery of peptides and proteins: established versus recently patented approaches, Pharm. Pat. Anal. 2 (2013) 125–145. doi:10.4155/ppa.12.75.

[19] P. Calvo, C. Remuñán-López, J.L. Vila-Jato, M.J. Alonso, Development of positively charged colloidal drug carriers: chitosan-coated polyester nanocapsules and submicron-emulsions, Colloid Polym. Sci. 275 (1997) 46–53. doi:10.1007/s003960050050.

[20] K.A. Traul, A. Driedger, D.L. Ingle, D. Nakhasi, Review of the toxicologic properties of medium-chain triglycerides, Food Chem. Toxicol. 38 (2000) 79–98. doi:10.1016/S0278-6915(99)00106-4.

[21] B. Marten, M. Pfeuffer, J. Schrezenmeir, Medium-chain triglycerides, Int. Dairy J. 16 (2006) 1374–1382. doi:10.1016/j.idairyj.2006.06.015.

[22] M. Tobío, R. Gref, A. Sanchez, R. Langer, M.J. Alonso, Stealth PLA-PEG nanoparticles as protein carriers for nasal administration, Pharm. Res. 15 (1998) 270–275. doi:10.1023/A:1011922819926.

[23] M. Tobío, A. Sánchez, A. Vila, I. Soriano, C. Evora, J.. J. Vila-Jato, M.. M. Alonso, The role of PEG on the stability in digestive fluids and in vivo fate of PEG-PLA nanoparticles following oral administration, Colloids Surfaces B Biointerfaces. 18 (2000) 315–323. doi:10.1016/S0927-7765(99)00157-5.

[24] C. Prego, D. Torres, E. Fernandez-Megia, R. Novoa-Carballal, E. Quiñoá, M.J. Alonso, Chitosan-PEG nanocapsules as new carriers for oral peptide delivery: effect of chitosan pegylation degree, J. Control. Release. 111 (2006) 299–308. doi:10.1016/j.jconrel.2005.12.015.

[25] I. Santalices, D. Torres, M.V. Lozano, M.M. Arroyo-Jiménez, M.J. Alonso, M.J. Santander-Ortega, Influence of the surface properties of nanocapsules on their interaction with intestinal barriers, Submitt. to Eur. J. Pharm. Biopharm. (2018).

[26] M. Wulff-Pérez, J. de Vicente, A. Martín-Rodríguez, M.J. Gálvez-Ruiz, Controlling lipolysis through steric surfactants: new insights on the controlled degradation of submicron emulsions after oral and intravenous administration, Int. J. Pharm. 423 (2012) 161–166. doi:10.1016/j.ijpharm.2011.12.025.

[27] L.M. Ensign, R. Cone, J. Hanes, Oral drug delivery with polymeric nanoparticles: the gastrointestinal mucus barriers, Adv. Drug Deliv. Rev. 64 (2012) 557–570. doi:10.1016/j.addr.2011.12.009.

[28] A. Vila, H. Gill, O. McCallion, M.J. Alonso, Transport of PLA-PEG particles across the nasal mucosa: Effect of particle size and PEG coating density, J. Control. Release. 98 (2004) 231–244. doi:10.1016/j.jconrel.2004.04.026.

[29] Q. Xu, L.M. Ensign, N.J. Boylan, A. Schön, X. Gong, J.C. Yang, N.W. Lamb, S. Cai, T. Yu, E. Freire, J. Hanes, Impact of surface polyethylene glycol (PEG) density on biodegradable nanoparticle transport in mucus ex vivo and distribution in vivo, ACS Nano. 9 (2015) 9217–9227. doi:10.1021/acsnano.5b03876.

[30] D. Chen, D. Xia, X. Li, Q. Zhu, H. Yu, C. Zhu, Y. Gan, Comparative study of Pluronic® F127-modified liposomes and chitosan-modified liposomes for mucus penetration and oral absorption of cyclosporine A in rats, Int. J. Pharm. 449 (2013) 1–9. doi:10.1016/j.ijpharm.2013.04.002.

[31] M. Niu, Y. Tan, P. Guan, L. Hovgaard, Y. Lu, J. Qi, R. Lian, X. Li, W. Wu, Enhanced oral absorption of insulin-loaded liposomes containing bile salts: A mechanistic study, Int. J. Pharm. 460 (2014) 119–130. doi:10.1016/j.ijpharm.2013.11.028.

[32] M. Niu, Y. Lu, L. Hovgaard, P. Guan, Y. Tan, R. Lian, J. Qi, W. Wu, Hypoglycemic activity and oral bioavailability of insulin-loaded liposomes containing bile salts in rats: The effect of cholate type, particle size and administered dose, Eur. J. Pharm. Biopharm. 81 (2012) 265–272. doi:10.1016/j.ejpb.2012.02.009.

[33] C. Chen, T. Fan, Y. Jin, Z. Zhou, Y. Yang, X. Zhu, Z. Zhang, Q. Zhang, Y. Huang, Orally delivered salmon calcitonin-loaded solid lipid nanoparticles prepared by micelle–double emulsion method via the combined use of different solid lipids, Nanomedicine. 8 (2013) 1085–1100. doi:10.2217/nnm.12.141.

[34] J. Liu, T. Gong, C. Wang, Z. Zhong, Z. Zhang, Solid lipid nanoparticles loaded with insulin by sodium cholate-phosphatidylcholine-based mixed micelles: preparation and characterization, Int. J. Pharm. 340 (2007) 153–162. doi:10.1016/j.ijpharm.2007.03.009.

[35] S. Sun, N. Liang, H. Piao, H. Yamamoto, Y. Kawashima, F. Cui, Insulin-S.O (sodium oleate) complex-loaded PLGA nanoparticles: Formulation, characterization and *in vivo* evaluation, J. Microencapsul. 27 (2010) 471–478. doi:10.3109/02652040903515490.

[36] S. Hu, M. Niu, F. Hu, Y. Lu, J. Qi, Z. Yin, W. Wu, Integrity and stability of oral liposomes containing bile salts studied in simulated and ex vivo gastrointestinal media, Int. J. Pharm. 441 (2013) 693–700. doi:10.1016/j.ijpharm.2012.10.025.

[37] C. Prego, D. Torres, M.J. Alonso, The potential of chitosan for the oral administration of peptides, Expert Opin. Drug Deliv. 2 (2005) 843–854. doi:10.1517/17425247.2.5.843.

[38] V. V. Khutoryanskiy, Advances in mucoadhesion and mucoadhesive polymers, Macromol. Biosci. 11 (2011) 748–764. doi:10.1002/mabi.201000388.

[39] M. Garcia-Fuentes, M.J. Alonso, Chitosan-based drug nanocarriers: where do we stand?, J. Control. Release. 161 (2012) 496–504. doi:10.1016/j.jconrel.2012.03.017.

[40] S. Roy, K. Pal, A. Anis, K. Pramanik, B. Prabhakar, Polymers in mucoadhesive drug-delivery systems: a brief note, Des. Monomers Polym. 12 (2009) 483–495. doi:10.1163/138577209X12478283327236.

[41] C. Prego, M. Fabre, D. Torres, M.J. Alonso, Efficacy and mechanism of action of chitosan nanocapsules for oral peptide delivery, Pharm. Res. 23 (2006) 549–556. doi:10.1007/s11095-006-9570-8.

[42] F.M. Goycoolea, A. Valle-Gallego, R. Stefani, B. Menchicchi, L. David, C. Rochas, M.J. Santander-Ortega, M.J. Alonso, Chitosan-based nanocapsules: physical characterization, stability in biological media and capsaicin encapsulation, Colloid Polym. Sci. 290 (2012) 1423–1434. doi:10.1007/s00396-012-2669-z.

[43] M.J. Santander-Ortega, M. V. Lozano-López, D. Bastos-González, J.M. Peula-García, J.L. Ortega-Vinuesa, Novel core-shell lipid-chitosan and lipid-poloxamer nanocapsules: Stability by hydration forces, Colloid Polym. Sci. 288 (2010) 159–172. doi:10.1007/s00396-009-2132-y.

[44] M.J. Santander-Ortega, J.M. Peula-García, F.M. Goycoolea, J.L. Ortega-Vinuesa, Chitosan

nanocapsules: effect of chitosan molecular weight and acetylation degree on electrokinetic behaviour and colloidal stability, Colloids Surfaces B Biointerfaces. 82 (2011) 571–580. doi:10.1016/j.colsurfb.2010.10.019.

[45] D. Torrecilla, M. V. Lozano, E. Lallana, J.I. Neissa, R. Novoa-Carballal, A. Vidal, E. Fernandez-Megia, D. Torres, R. Riguera, M.J. Alonso, F. Dominguez, Anti-tumor efficacy of chitosan-g-poly(ethylene glycol) nanocapsules containing docetaxel: anti-TMEFF-2 functionalized nanocapsules vs. non-functionalized nanocapsules, Eur. J. Pharm. Biopharm. 83 (2013) 330–337. doi:10.1016/j.ejpb.2012.10.017.

[46] M. V. Lozano, G. Lollo, M. Alonso-Nocelo, J. Brea, A. Vidal, D. Torres, M.J. Alonso, Polyarginine nanocapsules: a new platform for intracellular drug delivery, J. Nanoparticle Res. 15 (2013) 15:1515. doi:10.1007/s11051-013-1515-7.

[47] C. Prego, M. García, D. Torres, M.J. Alonso, Transmucosal macromolecular drug delivery, J. Control. Release. 101 (2005) 151–162. doi:10.1016/j.jconrel.2004.07.030.

[48] S.K. Lai, Y.-Y. Wang, D. Wirtz, J. Hanes, Micro- and macrorheology of mucus, Adv. Drug Deliv. Rev. 61 (2009) 86–100. doi:10.1016/j.addr.2008.09.012.

[49] J. das Neves, M.F. Bahia, M.M. Amiji, B. Sarmento, Mucoadhesive nanomedicines: characterization and modulation of mucoadhesion at the nanoscale, Expert Opin. Drug Deliv. 8 (2011) 1085–1104. doi:10.1517/17425247.2011.586334.

[50] M.J. Santander-Ortega, A.B. Jódar-Reyes, N. Csaba, D. Bastos-González, J.L. Ortega-Vinuesa, Colloidal stability of Pluronic F68-coated PLGA nanoparticles: a variety of stabilisation mechanisms, J. Colloid Interface Sci. 302 (2006) 522–529. doi:10.1016/j.jcis.2006.07.031.

[51] L. Zhang, J.M. Chan, F.X. Gu, J.W. Rhee, A.Z. Wang, A.F. Radovic-Moreno, F. Alexis, R. Langer, O.C. Farokhzad, Self-assembled lipid-polymer hybrid nanoparticles: A robust drug delivery platform, ACS Nano. 2 (2008) 1696–1702. doi:10.1021/nn800275r.

[52] M.J. Santander-Ortega, N. Csaba, M.J. Alonso, J.L. Ortega-Vinuesa, D. Bastos-González, Stability and physicochemical characteristics of PLGA, PLGA: poloxamer and PLGA: poloxamine blend nanoparticles: a comparative study, Colloids Surfaces A Physicochem. Eng. Asp. 296 (2007) 132–140. doi:10.1016/j.colsurfa.2006.09.036.

[53] C. Olbrich, R.H. Müller, Enzymatic degradation of SLN-effect of surfactant and surfactant mixtures, Int. J. Pharm. 180 (1999) 31–39. doi:10.1016/S0378-5173(98)00404-9.

[54] M. García-Fuentes, D. Torres, M.J. Alonso, Design of lipid nanoparticles for the oral delivery of hydrophilic macromolecules, Colloids Surfaces B Biointerfaces. 27 (2002) 159–168. doi:10.1016/S0927-7765(02)00053-X.

[55] M. Tirado-Miranda, A. Schmitt, J. Callejas-Fernández, A. Fernández-Barbero, The aggregation behaviour of protein-coated particles: a light scattering study, Eur. Biophys. J. 32 (2003) 128–36. doi:10.1007/s00249-002-0275-6.

[56] A. Tachaprutinun, P. Pan-In, S. Wanichwecharungruang, Mucosa-plate for direct evaluation of mucoadhesion of drug carriers, Int. J. Pharm. 441 (2013) 801–808. doi:10.1016/j.ijpharm.2012.12.028.

[57] E. Zagato, K. Forier, T. Martens, K. Neyts, J. Demeester, S. De Smedt, K. Remaut, K. Braeckmans, Single-particle tracking for studying nanomaterial dynamics: applications and fundamentals in drug

delivery, Nanomedicine. 9 (2014) 913–927. doi:10.2217/nnm.14.43.

[58] B.S. Schuster, L.M. Ensign, D.B. Allan, J.S. Suk, J. Hanes, Particle tracking in drug and gene delivery research: state-of-the-art applications and methods, Adv. Drug Deliv. Rev. 91 (2015) 70–91. doi:10.1016/j.addr.2015.03.017.

[59] J. Suh, M. Dawson, J. Hanes, Real-time multiple-particle tracking: Applications to drug and gene delivery, Adv. Drug Deliv. Rev. 57 (2005) 63–78. doi:10.1016/j.addr.2004.06.001.

[60] M. Plaza-Oliver, J. Fernández Sainz de Baranda, V. Rodríguez Robledo, L. Castro-Vázquez, J. Gonzalez-Fuentes, P. Marcos, M. V. Lozano, M.J. Santander-Ortega, M.M. Arroyo-Jimenez, Design of the interface of edible nanoemulsions to modulate the bioaccessibility of neuroprotective antioxidants, Int. J. Pharm. 490 (2015) 209–218. doi:10.1016/j.ijpharm.2015.05.031.

[61] M.J. Santander-Ortega, M. Plaza-Oliver, V. Rodríguez-Robledo, L. Castro-Vázquez, N. Villaseca-González, J. González-Fuentes, E.L. Cano, P. Marcos, M. V. Lozano, M.M. Arroyo-Jiménez, PEGylated nanoemulsions for oral delivery: role of the inner core on the final fate of the formulation, Langmuir. 33 (2017) 4269–4279. doi:10.1021/acs.langmuir.7b00351.

[62] Y.-Y. Wang, S.K. Lai, J.S. Suk, A. Pace, R. Cone, J. Hanes, Addressing the PEG mucoadhesivity paradox to engineer nanoparticles that “slip” through the human mucus barrier, Angew. Chemie - Int. Ed. 47 (2008) 9726–9729. doi:10.1002/anie.200803526.

[63] Z. Sezgin, N. Yüksel, T. Baykara, Preparation and characterization of polymeric micelles for solubilization of poorly soluble anticancer drugs, Eur. J. Pharm. Biopharm. 64 (2006) 261–268. doi:10.1016/j.ejpb.2006.06.003.

[64] L.N. Thwala, Protamine nanocapsules as carriers for oral peptide delivery, University of Santiagode de Compostela; University Catholique de Louvain, 2016.

[65] F. Antunes, F. Andrade, F. Araújo, D. Ferreira, B. Sarmento, Establishment of a triple co-culture in vitro cell models to study intestinal absorption of peptide drugs, Eur. J. Pharm. Biopharm. 83 (2013) 427–435. doi:10.1016/j.ejpb.2012.10.003.

[66] F. Araújo, B. Sarmento, Towards the characterization of an in vitro triple co-culture intestine cell model for permeability studies, Int. J. Pharm. 458 (2013) 128–134. doi:10.1016/j.ijpharm.2013.10.003.

[67] F. Araújo, C. Pereira, J. Costa, C. Barrias, P.L. Granja, B. Sarmento, In vitro M-like cells genesis through a tissue-engineered triple-culture intestinal model, J. Biomed. Mater. Res. - Part B Appl. Biomater. 104 (2016) 782–788. doi:10.1002/jbm.b.33508.

[68] C. Hilgendorf, H. Spahn-langguth, C.G. Regårdh, E. Lipka, Caco-2 versus Caco-2/HT29-MTX co-cultured cell lines: permeabilities via diffusion, inside- and outside-directed carrier-mediated transport, J. Pharm. Sci. 89 (2000) 63–75.

[69] I. Behrens, P. Stenberg, P. Artursson, T. Kissel, Transport of lipophilic drug molecules in a new mucus secreting cell culture model based on Ht-29 MTX cells, Pharm. Res. 18 (2001) 1138–1145.

[70] D. Yang, D. Liu, M. Qin, B. Chen, S. Song, W. Dai, H. Zhang, X. Wang, Y. Wang, B. He, X. Tang, Q. Zhang, Intestinal mucin induces more endocytosis but less transcytosis of nanoparticles across enterocytes by triggering nano-clustering and strengthening the retrograde pathway, ACS Appl. Mater. Interfaces. (2018) acsami.7b19153. doi:10.1021/acsami.7b19153.

[71] T. Lesuffleur, A. Barbat, E. Dussaulx, A. Zweibaum, Growth Adaptation to Methotrexate of HT-29

Human Colon Carcinoma Cells Is Associated with Their Ability to Differentiate into Columnar Absorptive and Mucus-secreting Cells, Cancer Res. 50 (1990) 6334–6343.

[72] N. Reix, A. Parat, E. Seyfritz, R. Van Der Werf, V. Epure, N. Ebel, L. Danicher, E. Marchioni, N. Jeandidier, M. Pinget, Y. Frère, S. Sigrist, In vitro uptake evaluation in Caco-2 cells and in vivo results in diabetic rats of insulin-loaded PLGA nanoparticles, Int. J. Pharm. 437 (2012) 213–220. doi:10.1016/j.ijpharm.2012.08.024.

[73] M.C. Manning, G.J. Evans, R.W. Payne, Protein stability during bioprocessing, in: F. Jameel, S. Hershenson (Eds.), Formul. Process Dev. Strateg. Manuf. Biopharm., John Wiley & Sons, Inc., 2010: pp. 605–624. doi:10.1002/9780470595886.

[74] C. Damge, C. Michel, M. Aprahamian, P. Couvreur, New approach for oral administration of insulin with polyalkylcyanoacrylate nanocapsules as drug carrier, Diabetes. 37 (1988) 246–251. doi:10.2337/diab.37.2.246.

[75] C. Damge, C. Michel, M. Aprahamian, P. Couvreur, J.P. Devissaguet, Nanocapsules as carriers for oral peptide delivery, J. Control. Release. 13 (1990) 233–239. doi:10.1016/0168-3659(90)90013-J.

[76] L. Yin, J. Ding, C. He, L. Cui, C. Tang, C. Yin, Drug permeability and mucoadhesion properties of thiolated trimethyl chitosan nanoparticles in oral insulin delivery, Biomaterials. 30 (2009) 5691–5700. doi:10.1016/j.biomaterials.2009.06.055.

[77] C. Michel, M. Aprahamian, L. Defontaine, P. Couvreur, C. Damgé, The effect of site of administration in the gastrointestinal tract on the absorption of insulin from nanocapsules in diabetic rats, J. Pharm. Pharmacol. 43 (1991) 1–5. doi:10.1111/j.2042-7158.1991.tb05437.x.

[78] M. Morishita, T. Goto, K. Nakamura, A.M. Lowman, K. Takayama, N.A. Peppas, Novel oral insulin delivery systems based on complexation polymer hydrogels: Single and multiple administration studies in type 1 and 2 diabetic rats, J. Control. Release. 110 (2006) 587–594. doi:10.1016/j.jconrel.2005.10.029.

UNIVERSIDADE DE SANTIAGO DE COMPOSTELA

USC
UNIVERSIDADE
DE SANTIAGO
DE COMPOSTELA




# Conclusions

USC
UNIVERSIDADE
DE SANTIAGO
DE COMPOSTELA

The overall objective of this PhD thesis was to study how the composition and surface properties of oily-based nanocarriers influence their potential for oral peptide delivery. The physicochemical properties, the peptide loading capacity and the interaction of the nanocarriers with the gastrointestinal barriers were selected as critical parameters in their rational design and screening process. The results obtained from the experimental work here detailed led us to state the following conclusions:

1. The limited solubility of peptides and proteins in lipid-based nanosystems, as well as their physicochemical properties can be optimized by modifying different formulation parameters. Particularly, in the development of peptide-loaded chitosan nanocapsules, we observed that while the type of non-ionic surfactants had minor effects on both, the physicochemical properties and insulin association, others factors, such as the increase of the concentration of polymer and the presence of a second coating shell were found to have a negative effect on the peptide loading of the nanocapsules.

2. The interaction of oily-based nanosystems with multiple barriers associated to the oral modality of administration is strongly dependent on their surface composition. Specifically, we have shown that while the incorporation of the non-ionic surfactant, poloxamer 188, into the colloidal systems (nanoemulsion, chitosan and polyarginine nanocapsules) had no effect on their performance, the inclusion of poloxamer 407 had a very positive effect in their colloidal stability in simulated intestinal fluids and their resistance to enzymatic degradation. Additionally, this surfactant was also critical for improving the mucodiffusion properties of the nanoemulsions, whereas this effect could not be observed in the case of the polymeric nanocapsules. This was attributed to the different entanglement of the surfactant to the different colloidal systems.

3. A new lipid-based nanocarrier consisting of a nanoemulsion co-existing with a population of micelles (mixed nanosystem) intended to the oral administration of peptides was fully developed and characterized using as peptide drug a hydrophobically-modified insulin. This novel nanosystem showed adequate physicochemical properties (size ≈ 219 ± 7 nm; PdI ≈ 0.1; ζ–potential ≈ −20 ± 1 mV) and exhibited a 100 % of insulin association efficiency preserving its bioactivity after the formulation process. In addition:

**3.1.** The insulin-loaded mixed nanosystem exhibited *in vitro* appropriate properties, such as good miscibility and stability in simulated intestinal fluids, an acceptable mucodiffusion in porcine mucus and a significant interaction/uptake with various model cell lines, without relevant cytotoxic effects. Furthermore, the mixed nanosystem suspensions were proved to be stable for at least 3 months upon storage.

**3.2.** The *in vivo* biodistribution of the insulin-loaded mixed nanosystem revealed its potential to interact with the intestinal epithelium. Finally, following its intraduodenal administration, a moderate but significant hypoglycemic response was observed in diabetic rats.

Overall, this work highlights the importance of the rational design of the nanocarriers in order for them to fulfill the adequate requirements for their performance as oral drug delivery vehicles. It also points out the value of properly characterizing the nanocarriers in line with their expected biological behavior. Ultimately, these results underline the difficulties for identifying *in vitro–in vivo* correlation parameters and the importance of standardizing experimental protocols for achieving more predictive *in vitro* results.

USC UNIVERSIDADE DE SANTIAGO DE COMPOSTELA




# List of abbreviations

USC
UNIVERSIDADE
DE SANTIAGO
DE COMPOSTELA

**A:** basal normalized fluorescence

**AAC:** area above the curve

**AE:** association efficiency

**AFM:** atomic force microscopy

**ATP:** adenosine triphosphate

**BA:** bioavailability

**BSA:** bovine serum albumin

**CCM:** high glucose w L–glutamine cell culture medium

**CH:** cholesterol

**CPP:** cell penetrating peptides

**CS:** chitosan

**CyA:** cyclosporine A

**$D_e$:** effective diffusion coefficient

**DiD:** DiIC18(5) oil (1,1'–dioctadecyl-3,3,3',3'–tetramethylindodicarbocyanine perchlorate)

**DLS:** dynamic light scattering

**DLVO:** Derjaguin, Landau, Verwey, and Overbeek theory

**D-Lys6-GnRH:** agonist gonadotropin releasing hormone

**$D_m$:** diffusion coefficient of the particles in mucus

**DMEN:** Dulbecco's modified Eagle medium

**DMSO:** dimethyl sulfoxide

**DNA:** deoxyribonucleic acid

**DPBS:** Dulbecco's phosphate-buffered saline

**DSPE-PEG:** 1,2-distearoyl-sn-glycero-3-phosphoethanol- amine-N-methoxy(polyethylene glycol)-2000

**$D_w$:** diffusion coefficient of the particles in water

**EC:** ethyl cellulose

**EC50:** median effective concentration

**EMEM:** Eagle's minimum essential medium

**EtOH:** ethanol

**FA:** formic acid

**FACS:** fluorescence-activated cell sorting (flow cytometry)

**FaSSIF-V2:** fasted state simulated intestinal fluid – version 2

**FBS:** fetal bovine serum

**FDA:** US Food and Drug Administration

**FeSSIF-V2:** fed state simulated intestinal fluid – version 2

**FITC:** 2-(6-hydroxy-3-oxo-(3H)-xanthen-9-yl)-5-isothiocyanatobenzoic acid

**GF:** growth factor

**GFP:** green fluorescent protein

**GRAS:** generally recognized as safe

**GRAVY:** average hydrophobicity and hydrophilicity

**HBSS:** Hank's balanced salt solution

**HLB:** hydrophilia-lipophilia balance

**HMG–CoA:** 3-hydroxy-3-methyl-glutaryl-coenzyme A reductase

**HM-insulin:** hydrophobically modified insulin

**HPH:** high pressure homogenization;

**HPLC:** high-performance liquid chromatography

**HPV:** human papilloma virus

**$I_0$:** fluorescence at mucus/nanosystems interface

**ID:** intraduodenal

**$I_F$:** normalized fluorescence

**IJ:** intrajejunal

**IP:** isoelectric point

**IU:** international units

**k:** decay constant

**LC:** loading capacity

**LDH:** lactate dehydrogenase assays

**MALS:** multi-angle light scattering

**ME:** microemulsion

**MP:** melting point

**MPEG-2000-DSPE:** N-(carbonyl-methoxypolyethylene glycol-2000)-1,2-distearoyl-sn-glycero-3 phosphoethanolamine sodium salt

**MPs:** microparticles

**MSD:** mean square displacement

**MTA:** multiple particle tracking analysis

**MTT:** 3-(4,5-dimethylthiazol-2-yl)-2,5-diphenyltetrazolium bromide

**Mw:** molecular weight

**n.a.:** not applicable

**NaCh:** sodium cholate

**NC:** nanocapsule

**NE:** nanoemulsion

**NMR:** nuclear magnetic resonance

**NP:** nanoparticles

**NRU:** neutral red uptake

**NTA:** nanoparticle tracking analysis

**O/W:** oil in water

**OGTT:** oral glucose tolerance test;

**OVA:** ovalbumin

**P188:** poloxamer 188

**P407:** poloxamer 407

**PA:** pharmacological availability

**PAH:** poly(allyl amine) hydrochloride

**PARG:** polyarginine

**PBS:** phosphate buffered saline

**$p_c$:** critical pressure

**PC:** phosphatidylcholine

**PD:** pharmacodynamics

**PdI:** polidispersity index

**PEG:** polyethylene glycol

**PEGst40:** polyethylene glycol stearate 40

**PEO:** polyethylene oxide

**PF127:** Pluronic®F127

**PF68:** Pluronic®F68

**PGA:** polyglutamic acid

**pHPMA:** N-(2-hydroxypropyl) methacrylamide copolymer

**PK:** pharmacokinectics

**PLA:** poly(lactic acid)

**PLGA:** poly(lactic-co-glycolic acid)

**PPO:** propylene oxide

**PSA:** polysialic acid

**PVA:** polyvinyl alcohol

**rHBsAg:** recombinant hepatitis B surface antigen

**rh-GH:** recombinant human growth hormone

**rhPTH1-34:** recombinant 1-34 N-terminal fragment of endogenous human parathyroid hormone

**RT:** room temperature

**s:** second

**SC:** subcutaneous

**SCF:** supercritical fluid

**SCMC:** sodium carboxymethylcellulose

**sCT:** salmon calcitonin

**SD:** standard deviation

**SDS-PAGE:** sodium dodecyl sulfate–polyacrylamide gel electrophoresis

**SEDDS:** self-emulsified drug delivery system

**SEM:** standard error of the mean

**SGC:** sodium glycocholate

**SIF:** simulated intestinal fluid

**SLN:** solid lipid nanoparticles

**SMEDDS:** self-microemulsified drug delivery system

**SNEDDS:** self-nanoemulsifying drug delivery systems

**SPC:** soybean phosphatidylcholine

**STC:** sodium taurocholate

**STZ:** streptozocin

**T:** temperature

**TAMRA:** tetramethylrhodamine

**TAT:** HIV transactivator of transcription

**$T_c$:** critical temperature

**TEER:** transepithelial electrical resistance values

**TEM:** transmission electron microscopy

**TFA:** trifluoroacetic acid

**Theor:** theoretical

**TL:** theoretical loading

**TMCS:** trimethyl chitosan

**TPGS:** d-α-tocopherol poly(ethylene glycol) 1000 succinate

**TPP:** tripolyphosphate;

**UPLC:** ultra-performance liquid chromatography

**USP:** United States Pharmacopeia

**UV:** ultra violet

**$V_A$:** attractive potential of interaction due to the Van der Waals forces

**$V_R$:** repulsive electrostatic potential

**$V_T$:** total potential of interaction between two approaching particles

**W/O/W:** water in oil in water

**W/O:** water in oil

**w/v:** weight/volume

**w/w:** weight/weight

**X:** distance from the mucus/nanoparticles interface towards the mucus

**$X_{1/2}$:** mean penetration capacity

**α:** anomalous exponent

**λ:** wavelength

**$\lambda_{em}$:** emission wavelength

**$\lambda_{ex}$:** excitation wavelength

**τ:** time scale

**[D-Trp-6] LHRH:** agonist triptorelin - luteinizing hormone-releasing hormone

USC UNIVERSIDADE DE SANTIAGO DE COMPOSTELA




# Ethical considerations

USC
UNIVERSIDADE
DE SANTIAGO
DE COMPOSTELA

## Animal studies

Biodistribution animal experiments (Chapter 4) were done in Padova and approved by Ministero della Salute Italiano ID: CEASA 24A (Italian Legislative Decree 240/2012B, of October 10th) and were executed in accordance with governing Italian law and European Directives and Guidelines for the use of animals in animal studies; performed therefore in compliance with the Directive 2010/63/EU of the European Parliament and Council of 22nd September 2010 on the protection of animals used for scientific purposes

For bioactivity and efficacy studies (Chapter 4) all animal experiments were reviewed and approved by the ethics committee at the University of Santiago de Compostela ID: 1500AE/12/FUN01/FIS02/CDG3 (Spanish Royal Decree 1201/2005, of October 10th) and ID: 15010/17/17002 (Spanish Royal Decree 53/2013, of February 1st) and were executed in accordance with governing Spanish law and European Directives and Guidelines for the use of animals in animal studies; performed therefore in compliance with the Directive 2010/63/EU of the European Parliament and Council of 22nd September 2010 on the protection of animals used for scientific purposes and under the Spanish Royal Decree 53/2013 February 1st on the protection of animals used for experimental and other scientific purposes, including teaching.

USC
UNIVERSIDADE
DE SANTIAGO
DE COMPOSTELA

USC
UNIVERSIDADE
DE SANTIAGO
DE COMPOSTELA